UNIVERSITAT DE BARCELONA

Technical and economic evaluation of anaerobic membrane bioreactors for municipal wastewater treatment

Sergi Vinardell Cruañas

UNIVERSITAT DE BARCELONA

Programa de doctorat d'Enginyeria i Ciències Aplicades

Technical and economic evaluation of anaerobic membrane bioreactors for municipal wastewater treatment

Tesi Doctoral

Sergi Vinardell Cruañas

Directors:

Dr. Joan Mata Álvarez

Dr. Joan Dosta Parras

Tutor

Dr. Joan Dosta Parras

Departament d'Enginyeria Química i Química Analítica

El Dr. Joan Mata Álvarez, Professor Emèrit del Departament d'Enginyeria Química i Química Analítica de la Universitat de Barcelona, i el Dr. Joan Dosta Parras, Professor Agregat del mateix departament:

CERTIFIQUEN QUE:

El treball de recerca titulat "*Technical and economic evaluation of anaerobic membrane bioreactors for municipal wastewater treatment*" constitueix la memòria que presenta el Sr. Sergi Vinardell Cruañas per a aspirar al grau de Doctor per la Universitat de Barcelona. Aquesta tesi doctoral ha estat realitzada dins del programa doctoral "Enginyeria i Ciències Aplicades", en el Departament d'Enginyeria Química i Química Analítica de la Universitat de Barcelona.

I per a que així consti als efectes oportuns, signen el present certificat.

Barcelona, febrer de 2022

Dr. Joan Mata Álvarez — *Director de la tesi doctoral*

Dr. Joan Dosta Parras — *Director i tutor de la tesi doctoral*

"*Success is not final; failure is not fatal: it is the courage to continue that counts*"

Winston Churchill (1874-1965)

Acknowledgments

En primer lloc, m'agradaria donar el meu sincer agraïment als meus directors de tesi, el Dr. Joan Mata i Dr. Joan Dosta. Gràcies als dos per guiar-me i ajudar-me durant aquest trajecte. Tanmateix, us agraeixo l'oportunitat que em vau donar fa quatre anys de formar part del grup de recerca de Biotecnologia Ambiental, on he pogut descobrir el meu entusiasme per la ciència. Gràcies per tot!

Al Dr. Sergi Astals, per ensenyar-me tant i tan bé. T'agraeixo molt tots els coneixements que m'has transmès i tot el suport que m'has donat durant aquests anys. Gràcies per la teva immensa dedicació en la correcció dels articles i per haver-me ajudat a ser millor dia rere dia. Aquesta tesi no hauria estat el mateix sense tu!

També m'agradaria donar les gràcies a l'Agència de Gestió d'Ajuts Universitaris i de Recerca de la Generalitat de Catalunya per la beca FI que em van concedir (2019 FI_B 00394) i que ha fet possible la realització d'aquesta tesi doctoral.

Als meus companys de laboratori amb qui he tingut el plaer de compartir aquests últims anys. Carme, Noemí, Keong, David, Andreu, Peña, Verónica, Cristopher... Gràcies per fer del laboratori un lloc tan agradable. M'ha encantat coincidir amb vosaltres! Per suposat, vull fer una menció especial als estudiants que m'han ajudat de forma

inestimable a operar l'AnMBR en el transcurs de la tesi. Miquel, Marta, Silvia, Camilo, Miguel i Lyzeth; sense vosaltres tot hauria estat molt més difícil. Us estic molt agraït!

A totes aquelles persones que m'han ajudat i acompanyat durant la realització de la tesi. A la Dra. Alicia Cardete, per ensenyar-me amb tanta dedicació com fer una bona enginyeria de detall. A la Dra. Miriam Peces, per ensenyar-me a fer uns bons gràfics i pels seus consells respecte l'operació de l'AnMBR. Al Dr. Gaetan Blandin i Dr. Federico Ferrari, amb qui he col·laborat i espero seguir col·laborant en un futur. A la Laura Abad, per haver-me dissenyat la fantàstica portada d'aquesta tesi. També m'agradaria fer menció als companys d'altres grups de recerca que he tingut la sort de conèixer durant aquests anys. Alberto, Núria, Oriol, Sina... Ha estat un plaer!

I would like to express my gratitude to Dr. Geoffroy Lesage and Dr. Marc Heran for the opportunity to join the Institut Européen des Membranes of the University of Montpellier. It was a great pleasure to spend six months with you in your research group. I am also grateful to all the people I met in Montpellier. Vincent, Lucie, Zineb, Morgane, Qazi, Azhan, Remy, Wen and Carla; thank you to welcome me and for your invaluable help!

I would also like to thank Dr. Konrad Koch to welcome me one month at the Chair of Urban Water Systems Engineering of the Technical University of Munich. I really enjoyed our meetings and I am grateful for all the wise advice you gave to me. It was a great experience for me and I hope to come back again in the future!

Als meus amics i família que m'han acompanyat i ajudat en aquest trajecte. A l'Èric, per estar sempre disposat a ajudar-me. A la Marta i l'Axel, per la seva inestimable ajuda durant l'estada a França. A mi familia Guadalajareña y Leonesa, por haberme abierto las puertas de su casa y por haberme dado tantísimo. I per suposat, als meus pares, la Isabel i en Carles. No hi ha paraules que puguin descriure l'agraïment i admiració que us tinc. Gràcies per ajudar-me i suportar-me en els meus moments difícils. Us estimo molt.

I finalment a tu, Maria. Perquè has estat la persona més important per recórrer aquest trajecte amb èxit. T'estic immensament agraït per tot el que has fet i fas per mi. Gràcies per abraçar-me, escoltar-me, suportar-me i estimar-me. I com bé diu aquella cançó dels Beatles que tan bé defineix el que sento: "To lead a better life, I need my love to be here. Here, making each day of the year. **Here, there and everywhere**". T'estimo molt.

Table of contents

Summary

Anaerobic membrane bioreactor (AnMBR), which is a combination of membrane separation and anaerobic digestion, is an emerging biotechnology for municipal sewage treatment. The application of AnMBRs in the mainline of wastewater treatment plants (WWTPs) can provide several advantages compared with conventional activated sludge processes, such as no aeration requirements, biogas production and reduction in the sludge management costs. However, despite these advantages, mainstream AnMBR application still presents challenges, whose resolution requires considering both technical and economic aspects.

The goal of this thesis is to evaluate the technical and economic implications of implementing AnMBRs for municipal sewage treatment. Specifically, the thesis covered the techno-economic implications of two main topics: (i) forward osmosis (FO) pre-concentration before AnMBR, and (ii) plant-wide impact of AnMBR implementation in a WWTP.

In the first part of this thesis, the techno-economic effects of combining FO and AnMBR technologies have been evaluated. First, a lab-scale mesophilic AnMBR operated at pre-

concentration factors of 1, 2, 5 and 10 achieved chemical oxygen demand (COD) removal efficiencies above 90% for all the conditions. The differences between the soluble COD concentration of the permeate and digester suggested that membrane biofilm contributed to COD removal efficiency. Second, the techno-economic analysis of combining FO, reverse osmosis (RO) and AnMBR was conducted. The results showed that the wastewater treatment cost of the FO-RO+AnMBR system ranged between 0.80 and 1.40 € per m^3 of wastewater treated. A sensitivity analysis illustrated that FO fluxes above 10 L m^{-2} h^{-1} (LMH) would improve the economic competitiveness of the FO-RO+AnMBR system. Finally, the impact of the draw solute and FO membrane material on the economic balance of this system was evaluated. The membrane material had a high impact on the economic balance since thin film composite (TFC) membranes substantially reduced the net cost when compared with cellulose triacetate (CTA) membranes. Conversely, the draw solute featured a moderate impact on the net cost. CH_3COONa and $CaCl_2$ were the most economically favourable draw solutes for CTA membrane, whereas $MgCl_2$ was the most economically favourable draw solute for TFC membrane.

In the second part of this thesis, the plant-wide impact of implementing AnMBRs in WWTPs has been evaluated. First, the effect of specific gas demand (SGD) and flux on membrane performance and process economics of granular AnMBRs was analysed. SGD and membrane flux impacted membrane fouling, but they did not impact organic matter rejection. The economic evaluation of granular AnMBRs showed that the most competitive strategy for fouling control relied on operating the membrane at normalised fluxes and SGDs of 7.8 LMH and 0.5 m^3 m^{-2} h^{-1}, respectively. Second, the economic feasibility of implementing mainstream AnMBR in a WWTP was evaluated for five different WWTP layouts. The results showed that the net treatment cost ranged between 0.33 and 0.43 € m^{-3} (100-1200 mg COD L^{-1}) for WWTP layouts combining AnMBR, degassing membrane, primary settler and anaerobic digester. However, when partial nitritation-anammox and chemical phosphorus precipitation were included for nutrients removal, the net treatment cost increased from 0.33-0.43 to 0.51-0.56 € m^{-3}. Finally, the techno-economic implications of co-digesting food waste with sewage sludge in the sidestream anaerobic digester of an AnMBR-WWTP were analysed. Co-digestion reduced the net cost of the sludge line when the nutrients backload was treated in the

mainstream. However, when the nutrients backload was treated in the sidestream with partial nitritation-anammox and struvite crystallisation, the electricity revenue did not offset the additional costs of these two processes. The results also indicated that biosolids disposal cost represented the highest cost contributor in the sludge line of an AnMBR-WWTP.

Resumen

El biorreactor anaeróbico de membranas (AnMBR, por sus siglas en inglés) es una tecnología emergente para el tratamiento de aguas residuales municipales. El AnMBR no requiere de aeración, produce biogás y reduce la producción de fangos en comparación con los procesos convencionales de lodos activos. Sin embargo, la aplicación del AnMBR en estaciones depuradoras de aguas residuales (EDAR) es muy limitada ya que la tecnología aún debe superar algunas barreras técnicas y económicas antes de una implementación generalizada.

El objetivo de esta tesis es evaluar las implicaciones técnicas y económicas de implementar el AnMBR para el tratamiento de aguas residuales municipales. En concreto, la tesis incluye las implicaciones tecno-económicas de dos temáticas relacionadas con el AnMBR: (i) preconcentración del agua residual municipal mediante osmosis directa (FO, por sus siglas en inglés) e (ii) impacto global de la implementación del AnMBR en una EDAR.

En la primera parte de esta tesis se ha evaluado la combinación de las tecnologías de FO y AnMBR. En primer lugar, se ha operado un AnMBR a escala de laboratorio bajo cuatro

condiciones de preconcentración. El AnMBR alcanzó eliminaciones de demanda química de oxígeno (DQO) por encima del 90% para todos los factores de preconcentración. La diferencia entre la concentración de DQO soluble del permeado y el digestor sugieren que el biofilm de la membrana tuvo un impacto en la eliminación global de DQO. En segundo lugar, se ha llevado a cabo un análisis tecno-económico sobre la combinación de la FO, osmosis inversa (RO, por sus siglas en inglés) y AnMBR para el tratamiento de aguas residuales municipales. Los resultados obtenidos mostraron que el coste de tratamiento del sistema FO-RO+AnMBR osciló entre 0,80 y 1,40 € por m^3 de agua residual tratada. Un análisis de sensibilidad mostró que obtener flujos en las membranas de FO por encima de 10 L m^{-2} h^{-1} (LMH) mejoraría el balance económico del sistema. Por último, se ha evaluado el impacto del soluto extractor y el material de la membrana de FO sobre el balance económico del sistema. El material de la membrana de FO tuvo un gran impacto en el balance económico ya que el uso de membranas compuestas de película fina (TFC, por sus siglas en inglés) redujeron sustancialmente el coste en comparación con el uso de membranas de triacetato de celulosa (CTA, por sus siglas en inglés). Por otro lado, el soluto extractor tuvo un impacto moderado en el coste. El CH_3COONa y $CaCl_2$ fueron los solutos más favorables para la membrana de CTA, mientras que el $MgCl_2$ fue el soluto más favorable para la membrana de TFC.

En la segunda parte de esta tesis se ha evaluado el impacto global del AnMBR en una EDAR. En primer lugar, se ha estudiado el impacto de la demanda específica de gas (SGD, por sus siglas en inglés) y flujo de permeado en el balance económico de un sistema AnMBR con fango granular. El SGD y flujo de permeado afectaron el ensuciamiento de la membrana, pero no afectaron la retención de materia orgánica por parte de la membrana. La evaluación económica demostró que la estrategia más competitiva para controlar el ensuciamiento de la membrana en sistemas granulares AnMBR recae en operar la membrana con flujos normalizados (J_{20}) y SGD de 7,8 LMH y 0,5 m^3 m^{-2} h^{-1}, respectivamente. En segundo lugar, la viabilidad económica de implementar un AnMBR en una EDAR se ha evaluado considerando cinco configuraciones diferentes. Los resultados mostraron que el coste de tratamiento osciló entre 0,33 y 0,43 € m^{-3} (100-1200 mg DQO L^{-1}) para configuraciones que combinaron AnMBR, membrana de desgasificación, sedimentador primario y digestor anaeróbico en la línea de fangos. Sin embargo, el coste de tratamiento se incrementó de 0.33-0.43 a

0,51-0,56 € m^{-3} cuando se incluyeron tecnologías para eliminar los nutrientes. Por último, se han evaluado las implicaciones tecno-económicas de codigerir residuos alimenticios y fango combinado en la línea de fangos de una EDAR. La codigestión permitió reducir el coste neto de tratamiento de la línea de fangos en el escenario en que la carga de nutrientes de la fracción líquida se trató en la línea de aguas. Los resultados también indicaron que el coste de disposición de los fangos representó la mayor fracción de los costes en la línea de fangos de una EDAR utilizando AnMBR para el tratamiento de las aguas residuales.

Resum

El bioreactor anaeròbic de membrana (AnMBR, per les seves sigles en anglès) és una tecnologia emergent pel tractament d'aigües residuals municipals. L'AnMBR no requereix d'aeració, produeix biogàs i redueix la producció de fangs en comparació amb els processos convencionals de fangs actius. No obstant, l'aplicació de l'AnMBR en estacions depuradores d'aigües residuals (EDAR) és molt limitada, ja que la tecnologia necessita superar algunes barreres tècniques i econòmiques abans d'una implementació generalitzada.

L'objectiu d'aquesta tesi és avaluar les implicacions tècniques i econòmiques respecte la implementació de l'AnMBR pel tractament d'aigües residuals municipals. En concret, la tesi inclou les implicacions tecno-econòmiques de dos temàtiques relacionades amb l'AnMBR: (i) preconcentració de l'aigua residual municipal mitjançant osmosis directe (FO, per les seves sigles en anglès) i (ii) l'impacte global de la implementació de l'AnMBR en una EDAR.

En la primera part d'aquesta tesi s'ha avaluat la combinació de las tecnologies de FO i AnMBR. En primer lloc, s'ha operat un AnMBR a escala laboratori sota quatre condicions de preconcentració. L'AnMBR va assolir eliminacions de demanda química

d'oxigen (DQO) majors al 90% per totes les condicions de preconcentració. La diferència entre la concentració de DQO soluble del permeat i el digestor suggereixen que el biofilm de la membrana va contribuir a l'eliminació global de DQO. En segon lloc, s'ha dut a terme un anàlisis tecno-econòmic sobre la combinació de la FO, osmosis inversa (RO, per les seves sigles en anglès) i AnMBR pel tractament d'aigües residuals municipals. Els resultats van mostrar que el cost de tractament del sistema FO-RO+AnMBR va oscil·lar entre 0,80 i 1,40 € per m^3 d'aigua residual tractada. Un anàlisi de sensibilitat va mostrar que assolir fluxos en les membranes de FO per sobre els 10 L m^{-2} h^{-1} (LMH) suposaria una millora en el balanç econòmic del sistema. Finalment, s'ha avaluat l'impacte del solut extractor i del material de la membrana de FO sobre el balanç econòmic del sistema. El material de la membrana de FO va tenir un gran impacte sobre el balanç econòmic, ja que la utilització de membranes compostes de pel·lícula fina (TFC, per les seves sigles en anglès) va reduir substancialment el cost en comparació amb la utilització de membranes de triacetat de cel·lulosa (CTA, per les seves sigles en anglès). Per altra banda, el solut extractor va tenir un impacte moderat sobre el cost. El CH_3COONa i $CaCl_2$ van ser els soluts més favorables per la membrana de CTA, mentre que el $MgCl_2$ va ser el solut més favorable per la membrana de TFC.

En la segona part d'aquesta tesi s'ha avaluat l'impacte global de l'AnMBR en una EDAR. En primer lloc, s'ha analitzat l'impacte de la demanda específica de gas (SGD, per les seves sigles en anglès) i el flux de permeat sobre el balanç econòmic d'un sistema AnMBR utilitzant fang granular. El SGD i flux de permeat van tenir un impacte sobre l'embrutiment de la membrana, però no van tenir un impacte sobre la retenció de la matèria orgànica per part de la membrana. L'avaluació econòmica va mostrar que l'estratègia més competitiva per controlar l'embrutiment de sistemes AnMBR amb fang granular recau en operar la membrana sota fluxos normalitzats (J_{20}) i SGD de 7,8 LMH i 0,5 m^3 m^{-2} h^{-1}, respectivament. En segon lloc, la viabilitat econòmica d'implementar un AnMBR en una EDAR s'ha avaluat per cinc configuracions diferents. Els resultats van mostrar que el cost del tractament va oscil·lar entre 0,33 i 0,43 € m^{-3} (100-1200 mg DQO L^{-1}) per configuracions que combinaven AnMBR, membrana de desgasificació, sedimentador primari i digestor anaeròbic a la línia de fangs. No obstant, el cost del tractament es va incrementar de 0.33-0.43 a 0,51-0,56 € m^{-3} després d'incloure tecnologies per eliminar els nutrients. Finalment, s'han analitzat les implicacions tecno-

econòmiques de codigerir residus alimentaris i fang combinat a la línia de fangs d'una EDAR. La codigestió va permetre reduir el cost net de tractament de la línia de fangs en l'escenari en què la càrrega de nutrients de la fracció líquida es va tractar a la línia d'aigües. Els resultats també van indicar que el cost de disposició dels fangs representava la major fracció dels costos a la línia de fangs d'una EDAR utilitzant AnMBR pel tractament de les aigües residuals.

Acronyms and abbreviations

AD	Anaerobic digestion
AeMBR	Aerobic membrane bioreactor
AFBR	Anaerobic fluidised bed reactor
AFMBR	Anaerobic fluidised membrane bed reactor
AnMBR	Anaerobic membrane bioreactor
AnDMBR	Anaerobic dynamic membrane bioreactor
AnMF-OMBR	Anaerobic osmotic membrane bioreactor coupled with microfiltration
AnOMBR	Anaerobic osmotic membrane bioreactor
BSA	Bovine serum albumin
CAS	Conventional activated sludge
CFV	Cross-flow velocity

CG	Centrifuge
CHP	Combined heat and power
CTA	Cellulose triacetate
COD	Chemical oxygen demand
CSTR	Continuous stirred tank reactor
DAMO	Denitrifying anaerobic methane oxidation
DCOM	Dissolved and colloidal organic matter
DLC	Discounted lifetime cost
DLVO,	Derjaguin-Landau-Verwey-Overbeek
DM	Degassing membrane
EGSB	Expanded granular sludge bed
EPS	Extracellular polymeric substances
ERD	Energy recovery device
FO	Forward osmosis
GAC	Granular activated carbon
Gl-AnMBR	Gas-lift anaerobic membrane bioreactor
HRT	Hydraulic retention time
LMH	Liters per square meter per hour
MF	Microfiltration
MLSS	Mixed liquor suspended solids
NC	Net cost
NPV	Net present value
OLR	Organic loading rate
PAC	Powdered activated carbon
PET	Polyethylene terephthalate
PN-Anammox	Partial nitritation-Anammox
PS	Primary settler
PT	Preliminary treatment

PV	Present value
PVDF	Polyvinylidene fluoride
RO	Reverse osmosis
ROSA	Reverse osmosis system analysis
RSF	Reverse solute flux
RSFS	Reverse solute flux selectivity
SGD	Specific gas demand
SMP	Soluble microbial products
SRB	Sulphate-reducing bacteria
SRT	Solids retention time
SWRO	Seawater reverse osmosis
TFC	Thin film composite
TK	Thickener
TMP	Transmembrane pressure
TAN	Total ammonium nitrogen
TS	Total solids
TSS	Total suspended solids
UASB	Upflow anaerobic sludge blanket
UF	Ultrafiltration
VFA	Volatile fatty acids
VS	Volatile solids
VSS	Volatile suspended solids
WW	Wastewater
WWTP	Wastewater treatment plant
3DEEM	Threedimensional excitation-emission matrix fluorescence

Objectives and thesis structure

Objectives

The main objective of this thesis is to evaluate the technical and economic implications of implementing anaerobic membrane bioreactors (AnMBRs) for municipal sewage treatment. Specifically, the thesis covered the techno-economic implications of two main topics: (i) forward osmosis (FO) pre-concentration before an AnMBR; and (ii) plant-wide impact of AnMBR implementation in a wastewater treatment plant (WWTP). The specific objectives of this thesis are:

- To identify the key challenges of mainstream AnMBR application.
- To evaluate the performance of an AnMBR treating pre-concentrated sewage by FO operated under different pre-concentration factors.
- To analyse the economic feasibility of combining FO for municipal sewage pre-concentration, reverse osmosis (RO) for water production from the diluted draw solution, and AnMBR for pre-concentrated sewage treatment.

- To analyse the impact of draw solute and FO membrane material on the economics of combining FO pre-concentration and AnMBR.

- To evaluate the effect of gas sparging rate and permeate flux on the membrane performance and economic balance of granular AnMBR systems.

- To compare the process economics of different WWTP layouts implementing mainstream AnMBR.

- To analyse the techno-economic feasibility of implementing sidestream co-digestion in a WWTP based on mainstream AnMBR.

Thesis structure

The thesis is structured in three chapters to meet the abovementioned specific objectives:

- ***Chapter 1***, which is the introduction of the thesis, is dedicated to explaining the application of AnMBR technology for municipal sewage treatment. The implications of changing the WWTP paradigm from energy-consuming aerobic treatment to energy-harvesting anaerobic treatment are discussed, as well as the main anaerobic configurations for sewage treatment. Moreover, a state-of-the art review of AnMBR implementation for municipal sewage treatment is presented. ***Publication I*** of the thesis corresponds to this review article. The review is entitled "*Advances in anaerobic membrane bioreactor technology for municipal wastewater treatment: A 2020 updated review*" and it was published in *Renewable and Sustainable Energy Reviews (2020, 130; 109936)*. The review identifies and analyses five challenges that should be overcome for a widespread implementation of AnMBRs in WWTPs: (i) membrane fouling, (ii) AnMBR configuration, (iii) low-temperature treatment, (iv) sewage sulphate concentration and (v) low sewage organic matter concentration.

- ***Chapter 2*** deals with the impact of combining FO pre-concentration and AnMBR for municipal sewage treatment. First, an introduction is included to briefly explain the publications and research gaps covered in this chapter. Second, the experimental and techno-economic implications of combining both technologies are evaluated in Publications II, III and IV. ***Publication II*** is entitled "*Anaerobic membrane bioreactor performance at different wastewater pre-concentration factors: An experimental and*

economic study" and it was published in *Science of the Total Environment* (*2021, 750; 141625)*. In this publication, the experimental performance of a lab-scale AnMBR treating simulated pre-concentrated sewage at FO pre-concentration factors of 1, 2, 5 and 10 is evaluated. ***Publication III*** is entitled *"Techno-economic analysis of combining forward osmosis-reverse osmosis and anaerobic membrane bioreactor technologies for municipal wastewater treatment and water production"* and it was published in *Bioresource Technology (2020, 297; 122395)*. This publication analyses the economic feasibility of combining FO, RO and AnMBR technologies under different FO pre-concentration factors and draw solute management strategies. ***Publication IV*** is entitled "*Techno-economic analysis of forward osmosis pre-concentration before an anaerobic membrane bioreactor: Impact of draw solute and membrane material"* and it has been submitted for publication. This publication is focused on evaluating the impact of two FO membrane materials and eight different draw solutes on the economic balance and effluent quality of a system combining FO and AnMBR technologies. Finally, a section devoted to describing the overall results of this chapter is included.

- ***Chapter 3*** deals with the plant-wide impact of implementing mainstream AnMBR in a WWTP. First, an introduction is included to briefly explain the publications and research gaps covered in this chapter. Second, the techno-economic implications of implementing mainstream AnMBR are evaluated in Publications V, VI and VII that cover four key aspects of the technology from an economic point of view: (i) membrane fouling control strategy, (ii) sewage pre-treatments before AnMBR, (iii) sewage post-treatments after AnMBR and (iv) AnMBR waste sludge management strategy. ***Publication V*** is entitled *"Impact of permeate flux and gas sparging rate on membrane performance and process economics of granular anaerobic membrane bioreactors"* and it has been accepted for publication in *Science of the Total Environment*. This publication analyses the impact of four specific gas demands (SGD) and four membrane fluxes on membrane performance and economic balance of novel granular AnMBR systems. ***Publication VI*** is entitled *"Unravelling the economics behind mainstream anaerobic membrane bioreactor application under different plant layouts"* and it was published in *Bioresource Technology (2021, 319; 124170)*. This publication focuses on the techno-economic analysis of AnMBRs

under different plant layouts with special emphasis in the treatment train used in the water line of the WWTP. Besides AnMBR, the different WWTP layouts were a combination of primary settler, dissolved methane recovery, nitrogen and phosphorus removal, and sidestream anaerobic digestion. ***Publication VII*** is entitled "*Co-digestion of sewage sludge and food waste in a wastewater treatment plant based on mainstream anaerobic membrane bioreactor technology: A techno-economic evaluation"* and it was published in *Bioresource Technology (2021, 330; 124978)*. This publication focuses on the sludge line of a WWTP using AnMBR for municipal wastewater treatment. Specifically, the publication evaluated the techno-economic implications of co-digesting sewage sludge (primary sludge and waste AnMBR sludge) and food waste in an AnMBR-WWTP. Finally, a section devoted to describing the overall results of this chapter is included.

CHAPTER 1:

Introduction

1.1 Towards anaerobic digestion for municipal sewage treatment

1.1.1 Current context of municipal sewage treatment

It is estimated that anthropogenic activities produce 359.4×10^{9} m^3 y^{-1} of sewage around the world [1]. The treatment of this sewage has become a major issue to improve public health and reduce environmental impacts [2]. Conventional activated sludge (CAS) is the most commonly used process in wastewater treatment plants (WWTPs) to remove the biodegradable pollutants contained in sewage. However, despite this process has allowed improving worldwide sanitation for more than one century, its application does not fit with the current context of climate change and resource depletion [3]. WWTPs based on CAS process consume large amounts of energy for aeration and produce huge amounts of sludge that substantially increase treatment costs. In addition, when the organic matter is oxidised under aerobic conditions, most of the energy potential of sewage is lost and only a little fraction can be valorised by digesting the low biodegradable sludge produced in the CAS process. This approach is questionable since the easily biodegradable organic matter contained in sewage could be directly digested without requiring an aerobic process. It is thus clear that direct anaerobic digestion could be a more sustainable process than CAS, particularly considering the high internal chemical energy contained in sewage [4].

1.1.2 Anaerobic sludge bed reactors for municipal sewage treatment

Anaerobic digestion is a biotechnology able to convert the organic matter contained in sewage into methane-rich biogas. Anaerobic digestion does not require aeration and produces less sludge than CAS since the biomass yield of anaerobic microorganisms is much lower than the yield of aerobic microorganisms [5]. Accordingly, the application of anaerobic digestion for municipal sewage treatment has the potential to (i) reduce energy consumption, (ii) increase methane production and (iii) reduce sludge treatment costs. However, despite the potential advantages to apply anaerobic digestion for municipal sewage treatment, its application is still limited. Municipal sewage contains a lower organic matter concentration and represents a larger volumetric flow rate than other high-solid content wastes such as sludge. This means that the anaerobic digestion strategy used for high-solid content wastes is not extendible to municipal sewage since it is necessary to work with digester configurations able to treat the municipal sewage without requiring huge bioreactor volumes. To this end, high-rate anaerobic digesters such as upflow anaerobic sludge blanket (UASB) and expanded granular sludge bed (EGSB) reactors were developed to achieve a good decoupling of the hydraulic retention time (HRT) from the solids retention time (SRT) [6].

UASB is the most widely used configuration for municipal sewage treatment [7]. Figure 1.1 shows a schematic representation of UASB reactor. In this configuration, the sewage upflow velocity generates a selective pressure that promotes the formation of a dense sludge bed at the bottom of the reactor [6,8]. The upflow velocity, which depends on the size and height of the UASB, plays a key role in determining the mixing conditions, level of fluidisation and retention of solids in the sludge bed [9,10]. The sewage is fed at the bottom of the UASB through an influent distribution system that ensures the contact of the sewage organic matter with the anaerobic biomass [9]. A good design of the influent distribution system is crucial to achieve a good organic matter removal in the UASB [9]. After the sludge bed, the sewage passes through the gas-liquid-solid (GLS) separator located at the top of the UASB. The GLS separator separates the liquid, suspended solids and biogas phases present in the UASB. The major function of GLS separator is to reduce the amount of solids leaving the effluent and to increase the retention of anaerobic

biomass in the UASB with a direct impact on effluent quality [9]. Finally, the treated effluent and the produced biogas are collected at the top of the UASB (see Figure 1.1).

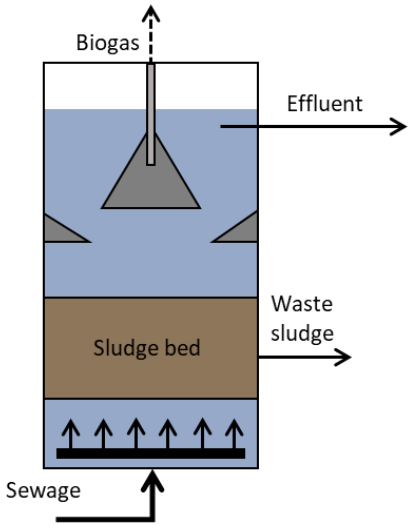

Figure 1.1. Schematic representation of an UASB reactor.

Several full-scale anaerobic sludge bed reactors for municipal sewage treatment have been implemented in warm climates [7]. However, the biochemical oxygen demand (BOD) removal efficiency has been relatively low in these full-scale experiences with average BOD removal efficiencies between 50 and 80% [7]. The application of sewage anaerobic digestion in temperate and cold climates is even more challenging than in warm climates since the low hydrolysis rate at low temperatures can lead to an accumulation of non-biomass sludge in the sludge bed with a direct impact on particulate and soluble COD removal efficiency [7,11]. Trego et al. [12] reported the first full-scale experience (Builth Wells, UK) of an anaerobic sludge bed reactor for municipal sewage treatment at low psychrophilic temperatures (<15 °C). Trego et al. [12] reached BOD removal efficiencies up to 85% when treating municipal sewage with a BOD concentration between 2 and 200 mg BOD L^{-1}. However, the authors also reported BOD removal fluctuations (40-60%) when the influent sewage BOD concentration decreased. Besides fluctuations in BOD removal efficiency, the anaerobic digester effluent could also contain relatively high concentration of suspended solids, which can affect effluent post-treatments such as nitrogen removal or dissolved methane recovery [13].

1.1.3 Anaerobic membrane bioreactors for municipal sewage treatment

Anaerobic membrane bioreactor (AnMBR) is a promising technology to overcome the limitations of anaerobic sludge bed reactors [14,15]. AnMBR, which combines anaerobic digestion with membrane separation technology, is able to convert organic matter into methane-rich biogas without requiring aeration [16]. In AnMBRs, microfiltration or ultrafiltration membranes are used to separate the biomass from the liquid fraction. This allows an excellent retention of the anaerobic biomass in the system regardless of its settling or aggregation properties [17]. Achieving a good retention of the active biomass is crucial to improve the process performance, particularly at low psychrophilic temperatures, and to reduce the amount of suspended solids present in the effluent [14].

Figure 1.2 shows the two main membrane configurations used in AnMBRs: submerged membrane configuration (Figure 1.2A) and cross-flow membrane configuration (Figure 1.2B). Submerged membrane is the most used AnMBR configuration for municipal sewage treatment [18]. In this configuration, the membrane is submerged in the mixed liquor and the permeate is obtained through the pressure difference between the mixed liquor and the permeate line. This pressure difference is called transmembrane pressure (TMP) and it is the driving force for membrane permeation in AnMBRs. A fraction of the produced biogas is typically recirculated to the AnMBR to scour the membrane and reduce long-term membrane fouling [14,19]. Gas sparging is the main energy requirement in submerged AnMBRs [18]. Regarding cross-flow membrane configuration, the mixed liquor is recirculated to the external membrane modules to generate the TMP and to produce the desired permeate flow rate. The biomass rejected by the membrane is returned back to the AnMBR. In this configuration, membrane fouling is controlled with the crossflow velocity (CFV), which can be defined as the tangential velocity of the liquor flowing through the membrane channels. The CFV allows providing turbulent conditions to reduce foulants' deposition on membrane surface [20]. Cross-flow membrane configuration is usually less attractive than submerged membrane configuration since the energy consumption required to achieve the CFV is substantially higher than the energy consumption required for gas sparging [21].

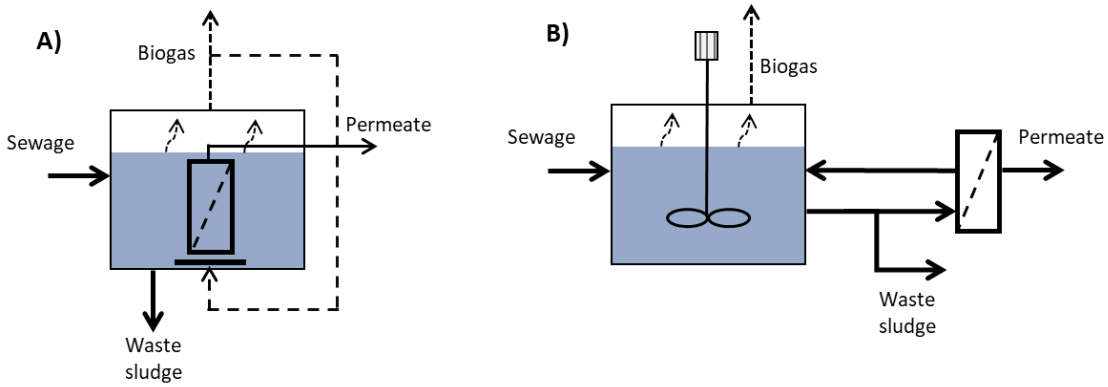

Figure 1.2. (A) Submerged AnMBR configuration and (B) cross-flow membrane configuration.

AnMBR technology has a high potential for municipal sewage treatment. Many pilot- and demonstration-scale plants have been developed during the last years to test the influence of operational conditions and membrane fouling strategies on AnMBR performance [18,22,23]. However, despite the increasing interest in the technology, its implementation is scarce since AnMBR still presents some challenges concerning mainstream application in a WWTP. In Section 1.2, a state-of-the-art review was conducted about five challenges that AnMBR technology needs to overcome before getting ready for full-scale implementation.

1.2 Publication I: *Advances in anaerobic membrane bioreactor technology for municipal wastewater treatment: A 2020 updated review*

Vinardell S, Astals S, Peces M, Cardete M.A, Fernández I, Mata-Alvarez J, Dosta J. (2020). Advances in anaerobic membrane bioreactor technology for municipal wastewater treatment: A 2020 updated review. Renew. Sustain. Energy Rev. 130, 109936. https://doi.org/10.1016/j.rser.2020.109936

Renewable and Sustainable Energy Reviews 130 (2020) 109936

Contents lists available at ScienceDirect

Renewable and Sustainable Energy Reviews

journal homepage: http://www.elsevier.com/locate/rser

Advances in anaerobic membrane bioreactor technology for municipal wastewater treatment: A 2020 updated review

S. Vinardell [a], S. Astals [a], M. Peces [b], M.A. Cardete [a], I. Fernández [c], J. Mata-Alvarez [a,d], J. Dosta [a,d,*]

[a] Department of Chemical Engineering and Analytical Chemistry, University of Barcelona, 08028, Barcelona, Spain
[b] Department of Chemistry and Bioscience, Centre for Microbial Communities, Aalborg University, 9220, Aalborg, Denmark
[c] CETIM Technological Centre, 15180, Culleredo, A Coruña, Spain
[d] Water Research Institute, University of Barcelona, 08001, Barcelona, Spain

ARTICLE INFO

Keywords:
Anaerobic digestion
Anaerobic membrane bioreactor (AnMBR)
Forward osmosis (FO)
Fouling
Water resource recovery facility (WRRF)
Municipal sewage

ABSTRACT

The application of anaerobic membrane bioreactors (AnMBR) for mainstream municipal sewage treatment is almost ready for full-scale implementation. However, some challenges still need to be addressed to make AnMBR technically and economically feasible. This article presents an updated review of five challenges that currently hinder the implementation of AnMBR technology for mainstream sewage treatment: (i) membrane fouling, (ii) process configuration, (iii) process temperature, (iv) sewage sulphate concentration, and (v) sewage low organics concentration. The gel layer appears to be the main responsible for membrane fouling and flux decline being molecules size and morphology critical properties for its formation. The review also discusses the advantages and disadvantages of five novel AnMBR configurations aiming to optimise fouling control. These include the integration of membrane technology with CSTR or upflow digesters, and the utilisation of scouring particles. Psychrophilic temperatures and high sulphate concentrations are two other limiting factors due to their impact on methane yields and membrane performance. Besides the methane dissolved in the effluent and the competition for organic matter between sulphate reducing bacteria and methanogens, the review examines the impact of temperature on microbial kinetics and community, and their combined effect on AnMBR performance. Finally, the review evaluates the possibility to pre-concentrate municipal sewage by forward osmosis. Sewage pre-concentration is an opportunity to reduce the volumetric flow rate and the dissolved methane losses. Overall, the resolution of these challenges requires a compromise solution considering membrane filtration, anaerobic digestion performance and economic feasibility.

1. Introduction

Climate change and resource depletion are pushing a paradigm shift in municipal wastewater management from end-of-pipe treatment towards integrated resource recovery [1]. New schemes consider wastewater as a source of energy, nutrients and water rather than as a source of pollution [2,3].

Anaerobic digestion represents a more sustainable technology to manage the organics contained in wastewater than the conventional activated sludge (CAS) treatment [4,5]. The CAS process is an

Abbreviations: AeMBR, aerobic membrane bioreactor; AFBR, anaerobic fluidised bed reactor; AFMBR, anaerobic fluidised membrane bed reactor; AnMBR, anaerobic membrane bioreactor; AnDMBR, anaerobic dynamic membrane bioreactor; AnMF-OMBR, anaerobic osmotic membrane bioreactor coupled with microfiltration; AnOMBR, anaerobic osmotic membrane bioreactor; BSA, bovine serum albumin; CAS, conventional activated sludge; CFV, cross-flow velocity; COD, chemical oxygen demand; CSTR, completely stirred tank reactor; DAMO, denitrifying anaerobic methane oxidation; DLVO, Derjaguin-Landau-Verwey-Overbeek; EGSB, expanded granular sludge bed; EPSs, extracellular polymeric substances; FO, forward osmosis; GAC, granular activated carbon; Gl-AnMBR, Gas-lift anaerobic membrane bioreactor; HRT, hydraulic retention time; LMH, liters per square meter per hour; MF, microfiltration; MLSS, mixed liquor suspended solids; OLR, organic loading rate; PAC, powdered activated carbon; PET, polyethylene terephthalate; PVDF, polyvinylidene fluoride; RO, reverse osmosis; SGD, specific gas demand; SMP, soluble microbial products; SRB, sulphate-reducing bacteria; SRT, solids retention time; TMP, transmembrane pressure; UASB, upflow anaerobic sludge blanket; UF, ultrafiltration; WW, wastewater; WWTP, wastewater treatment plant.

* Corresponding author. Department of Chemical Engineering and Analytical Chemistry, University of Barcelona, 08028, Barcelona, Spain.
E-mail address: jdosta@ub.edu (J. Dosta).

https://doi.org/10.1016/j.rser.2020.109936
Received 17 December 2019; Received in revised form 9 May 2020; Accepted 26 May 2020
Available online 11 June 2020
1364-0321/

energy-intensive treatment, accounting for more than 50% of the total energy consumption of a typical wastewater treatment plant (WWTP) [6,7]. Paradoxically, this energy is spent into converting organic matter into CO_2 and poorly biodegradable microbial mass [8]. Alternatively, anaerobic digestion provides several advantages such as renewable methane energy production, lower biomass production and no aeration requirements [9,10]. Anaerobic digestion is an emerging technology for municipal wastewater treatment.

Upflow anaerobic sludge blanket (UASB) and expanded granular sludge bed reactors (EGSB) are the most important anaerobic technologies for wastewater treatment [11,12]. The competitive advantage of these technologies (also known as high-rate anaerobic reactors) is due to the retention of biomass in the reactor that allows to decouple the hydraulic retention time (HRT) from the solids retention time (SRT) [11,13]. The full-scale application of UASB technology as mainstream sewage treatment has been applied in warm climates such as Brazil, India and the Middle East [14]. However, in many applications, the performance of full-scale UASB plants treating municipal sewage is suboptimal with chemical oxygen demand (COD) removal efficiencies around 60% [14–16]. This has been attributed to poor operating and maintenance procedures as well as to improper design [15]. Consequently, the UASB process can generate effluents with a high biodegradable organic matter concentration which may require aerobic post-treatment [17].

Anaerobic membrane bioreactor (AnMBR) technology overcomes the limitations of UASB technology and further improves the competitiveness and applicability of anaerobic systems as mainstream process for municipal sewage treatment [18–20]. Both ultrafiltration (UF) and microfiltration (MF) membranes enable a complete decoupling of hydraulic retention time (HRT) from solids retention time (SRT), which allows high controllability of the biomass in the digester, while obtaining a high-quality effluent free of suspended solids and pathogens [21,22]. The higher quality effluent is a competitive distinctive advantage of AnMBR over UASB technology [20,23–25]. However, a certain level of post-treatment is required since mainstream AnMBR effluents do not comply with the nutrients (i.e. N, P, S) discharge limits [26,27]. It should be noted that the concentration of nutrients in AnMBR effluents is typically higher than in their influent as a result of organic matter degradation [22].

As for 2020, several pilot-scale and demonstration plants equipped with AnMBR technology have been satisfactorily operated to treat municipal sewage [28]. Many studies have demonstrated that mainstream AnMBR application could make a WWTP energy neutral or even positive due to the potential energy production in the form of methane-rich biogas [17,29–32]. However, some technological challenges need to be addressed to make AnMBR a technically and economically competitive alternative for municipal sewage treatment.

Most of the operational and technical challenges of AnMBR technology (e.g. membrane fouling, reactor configuration, operational conditions, dissolved methane) have been previously discussed in literature reviews devoted to AnMBR technology [9,21,22,27,33–39]. However, the resolution of these challenges is complex and includes a broad range of considerations that require a compromise solution considering membrane filtration, anaerobic digestion performance and economic feasibility. In this literature review, the most important challenges associated with mainstream AnMBR technology are discussed to support its implementation now that AnMBR is getting closer for full-scale commercial application. Specifically, this review discusses the implications of membrane fouling, process configuration, temperature, influent sulphate concentration, and sewage pre-concentration on AnMBR performance and economic feasibility to clarify and simplify the decision-making process.

Membrane fouling is widely recognised as the main barrier for a widespread application of AnMBR technology [35,40]. However, despite extensive research, the mechanisms underlying this phenomenon are yet to be unfolded. Membrane fouling occurrence has been linked to several factors such as operational conditions (e.g. HRT, SRT, temperature), biomass characteristics (e.g. type of foulants, size of foulants) and membrane characteristics (e.g. material, pore size, type) [37,41–43]. The operational challenges associated with membrane fouling have resulted in the development of a wide range of physical and chemical cleaning strategies (e.g. backwashing, relaxation cycles, chemical reagents) and fouling control methods [27,44–46]. The strategy used to control membrane fouling is particularly important since it represents the main operational cost of AnMBR [28,47]. To date, gas sparging is the most used method for fouling control for submerged membranes [48–51]. However, novel AnMBR configurations are gaining attention to partially, or totally, replace gas sparging and further optimise AnMBR treatment [35,39]. This review provides a holistic updated understanding of the causes and implications of membrane fouling (Section 2) as well as an in-depth analysis of the most promising AnMBR configurations (Section 3).

Temperature is one of the most important process variables in anaerobic digestion systems due to its impact on metabolic kinetics and equilibrium constants. The application of AnMBR technology in temperate and cold climates has been identified as possible but challenging [52,53]. In these climates, the low concentration of organics in municipal sewage makes psychrophilic conditions (<20 °C) the only energetically feasible option. However, the lower process kinetics under psychrophilic conditions imply higher retention times and, therefore, higher capital costs. Moreover, the higher amount of methane dissolved in the effluent at lower temperatures is especially worrisome considering that the global warming potential of methane is 34 times higher than CO_2 [54]. Consequently, developing strategies to maximise the recovery of dissolved methane is essential to increase methane yield and reduce greenhouse gas emissions of AnMBR technology (Section 4).

The presence of sulphate in municipal sewage is another important constraint for the feasibility of AnMBR technology since sulphate-reducing bacteria (SRB) reduce sulphate to sulphide oxidising COD to CO_2 [55,56]. The lower amount of COD available for methanisation and the formation of sulphide could compromise the economic feasibility of the process [18,57]. Sulphide is a corrosive compound which has been reported to affect membrane performance by reducing its fluxes and durability. Concomitantly, the presence of hydrogen sulphide in the biogas increases the capital cost due to the need to use corrosive resistant equipment and piping as well as to implement measures for odour control. Sulphate-rich municipal sewage may require the implementation of a desulphurisation unit to reduce the biogas hydrogen sulphide concentration [58]. Therefore, the sulphate concentration of sewage is an important parameter for the design, profitability and operation of AnMBR (Section 5).

The high volumetric flow rate and the low concentration of organics in municipal sewage limit the applicability of AnMBR technology owing to the higher capital and operating expenditures, the higher amounts of dissolved methane lost through the effluent and the lower methane production per volume of wastewater treated. In this regard, municipal sewage pre-concentration by different membrane technologies has been considered to overcome these limitations, including direct membrane filtration, dynamic membrane filtration and forward osmosis (FO) [59]. In particular, FO stands as a promising technology to pre-concentrate municipal sewage with low energy inputs [60–63]. However, little attention has been given to this approach in previous AnMBR reviews. Municipal sewage pre-concentration opens new windows of opportunity for future AnMBR applications (Section 6).

This publication critically reviews five challenges that limit the applicability of AnMBR technology for municipal sewage treatment. These five challenges are: (i) membrane fouling, (ii) process configuration, (iii) process temperature, (iv) sewage sulphate concentration, and (v) sewage low organics concentration. For each challenge, novel knowledge and updated solutions proposed in the literature are critically analysed and future research needs are identified.

2. Membrane fouling mechanisms

Membrane fouling is the main cause for membrane flux decline over time. This is critical since membrane flux determines the membrane area required, which has a direct impact on both capital and operating expenditures. Additionally, membrane fouling leads to complex cleaning protocols that hinder the operability of the process due to more frequent backwash cycles and chemical cleanings. In the last years, significant advances on fouling control have been made including new AnMBR configurations [28,64], optimisation of operational conditions [29,65], gas sparging optimisation [48,49], and improvements on backwash and chemical cleaning protocols [44,66]. However, most research has focused on reducing fouling rather than on understanding the underlying fouling formation mechanisms. Studies focusing on the mechanisms leading to membrane fouling are inconclusive and, in some cases, contradictory. This situation can be attributed to several interconnected factors taking part in the complex network that comprises membrane fouling.

2.1. Extracellular polymeric substances

Extracellular polymeric substances (EPSs) have been considered the primary precursors of membrane fouling [42,67,68]. EPSs can be defined as organic macromolecules that are present outside and inside microbial aggregates mainly composed of proteins, polysaccharides and humic acids [69–71]. EPSs can be classified into (i) tightly bound EPSs (TB-EPSs), (ii) loosely bound EPSs (LB-EPSs) and (iii) soluble EPSs (sEPS) [27,72]. The latter is commonly known as soluble microbial products (SMPs) [69,73]. The adhesion forces causing the attachment of these substances on the membrane surface is challenging and remains under discussion as recently reviewed by Zhen et al. [27]. The composition of EPSs appears determinant to understand the interaction between the EPS substances and the membrane surface and, consequently, to understand the occurrence, structure and composition of membrane fouling [27,67,74].

Membrane hydrophobicity has been reported as an important factor for membrane fouling since it affects the interaction with hydrophobic and hydrophilic EPSs compounds [65,75,76]. Lin et al. [77] attributed the higher impact of protein EPSs on membrane fouling to the higher hydrophobicity of proteins compared to polysaccharides. Lin et al. [77] concluded that the EPSs protein to polysaccharide ratio was a better indicator for fouling control than the total amount of EPSs. Similarly, Arabi and Nakhla [78] reported that an EPS protein to carbohydrate ratio of 8/1 and 2/1 in the influent exhibited the highest and the lowest fouling rates, respectively. The importance of EPS proteins on membrane fouling has been reported in several publications [79–88]. However, other publications concluded that polysaccharides are the main responsible for membrane fouling [89–93]. These discrepancies can be related to multiple factors including AnMBR operational conditions, macromolecules composition, microbiome composition, influent composition, membrane configuration and properties, and the extraction and analytical methods used for EPS analysis [27]. Nonetheless, these studies did not elucidate the EPS attachment mechanisms leading to membrane fouling.

Teng et al. [94] recently published a systematic research study concluding that small size and disperse SMPs are thermodynamically favoured to adhere on the membrane and cause fouling. This was attributed to the smaller real separation between the SMP and the membrane. Teng et al. [94] also reported that SMPs morphology plays a role in membrane fouling since it controls SMP attachment to the membrane surface. This is in agreement with previous publications that indicated that membrane roughness and surface characteristics are important factors on membrane fouling [95–97]. Teng et al. [94] study is highly relevant since it shows that molecules size and morphology, rather than the composition, may control membrane fouling. However, further research is required to elucidate the relative impact of the different factors on membrane fouling.

2.2. Particle size distribution

Particle size distribution has been reported as an important factor to predict and control fouling in aerobic and anaerobic MBRs [53,65,77,80,98–101]. Particularly important appears the role of particle size distribution on back-transport mechanisms which has been highlighted as a crucial factor for foulants deposition [53,102]. Zhou et al. [103,104] demonstrated the importance of sub-visible particles (0.45–10 μm) and their associated microbial community on membrane fouling. Specifically, Zhou et al. [104] reported that micro-particles (5–10 μm) and colloidal particles (0.45–1 μm) had different microbial communities and played different roles in membrane fouling. On the one hand, micro-particles were mainly formed by filamentous microorganisms and were associated with the cake layer resistance. On the other hand, colloidal particles were mainly formed by sulphate-reducing bacteria and were linked to the initial fouling formation. However, further research is needed to better comprehend the role of particle size distribution and microbial composition on membrane fouling.

2.3. Fouling structure and composition

Different theories have been proposed to provide a reliable explanation for the role of foulants on filtration resistance. According to the literature, different fouling layers can be distinguished depending on the filtration resistance [91,105]. However, this distinction has been different for aerobic and anaerobic MBRs. In AnMBRs, it is generally accepted that pore clogging is followed by cake layer formation on the membrane surface [36,77,106], which confronts the most recent findings in aerobic membrane bioreactors (AeMBRs) [93,94]. These AeMBR studies have differentiated two distinct layers on the membrane; a gel layer and a cake layer. The gel layer is formed by the precipitation and gelation of colloidal and soluble polymeric substances (including SMPs and EPSs) on the membrane, while the cake layer is formed by the adhesion and accumulation of sludge flocs on the gel layer [105,107].

The gel layer has been reported to contain negatively charged groups such as carboxyl, hydroxyl and phosphoric. These groups have an important role in the gelling processes and filtration resistance [69,91]. Gelling properties have been mainly attributed to carboxyl groups in polysaccharides, especially in the presence of divalent or multivalent cations in the mixed liquor [67]. Cations complexation has been reported to be an important mechanism for the formation and consolidation of a three-dimensional gel matrix on the membrane surface [90,105]. In AeMBR, Teng et al. [94] reported that the specific filtration resistance of the gel layer is much higher than the cake layer. However, it has also been reported that the gel layer pores are much larger than the cake layer pores [93].

Chen et al. [108] and Zhang et al. [109] reported the decisive role of osmotic pressure on filtration resistance in both AnMBRs and AeMBRs. These two studies laid the foundations for new theories regarding the role of the chemical potential to the gel layer filtration resistance. Hong et al. [91] reported that the negatively charged functional groups of the gel layer led to high concentrations of counter-ions surrounding the membrane surface. This results in an osmotic gradient between the permeate and the gel layer that can generate a filtration resistance much higher than the cake layer [91]. However, this theory cannot provide a reliable explanation for the high filtration resistance in zones where the gel layer is nearly electro-neutral. Chen et al. [93] suggested that Flory-Huggins theory could give a response to this phenomenon, since their experimental results showed that the filtration resistance depends on the gel thickness rather than on the pH and ionic strength. Accordingly, the chemical potential variation in the gel layer could be one of the main mechanisms affecting the filtration resistance of the gel layer [93,94,110].

2.4. Future research on membrane fouling

Future research efforts on membrane fouling in anaerobic systems should focus on broadening the understanding and applicability of the aforementioned theories. Most of the AnMBR publications have not differentiated foulant layers and only a few recent publications have identified the formation of a gel layer under anaerobic conditions. This is important since (i) membrane filtration resistance appears to be governed by gel layer formation rather than the cake layer formation and (ii) it can lead to contradictory and confusing information in the literature. Further research should evaluate the implications of gel layer formation in AnMBRs performance from which researchers can conceive and develop improved configurations and operational conditions for fouling control.

3. Novel configurations for membrane fouling control

Many pilot and lab-scale AnMBR configurations have been trialled to treat municipal sewage. These AnMBR configurations can be classified in two groups (i) completely stirred tank reactor (CSTR) (Fig. 1a and b) and (ii) UASB reactors (Fig. 1c) [10,39]. In both systems, gas sparging is the most used strategy for membrane scouring and fouling control (Tables 1 and 2). However, gas sparging consumes a large amount of energy (0.21 ± 0.13 kWh m^{-3}) and, therefore, its optimisation is important to minimise energy consumption and related operating costs [28,30,57]. This section discusses the most promising new configurations proposed to replace or reduce gas sparging requirements. It is worth mentioning that anaerobic dynamic membrane bioreactors (AnDMBR) are out of the scope of the present review since AnDMBRs were recently reviewed by Hu et al. [33].

3.1. Novel configurations in AnMBR-CSTR systems

3.1.1. Rotating membranes

Rotative membrane modules have been considered as a possible alternative to gas sparging [123,124]. This configuration consists of coupling the membrane in a rotatory axis that generates shear stress (Fig. 2a). Ruigómez et al. [125] compared, in lab-scale short-term assays (~1 h), a conventional gas sparging system and a rotating system for membrane fouling control. The latter consisted of a hollow-fibre module rotating between 330 and 100 rpm to guarantee the generation of a scouring effect on the membrane surface. Ruigómez et al. [125] showed that the fouling rate (defined as dTMP/dt) decreased with the rotating velocity. However, when fouling rate reached values close to 0.01 kPa s^{-1} further improvements on fouling reduction could not be achieved by increasing the rotating velocity. Ruigómez et al. [125] attributed this phenomenon to the formation of a primary irreversible layer that could not be removed with physical methods. Regarding the gas-sparged AnMBR, Ruigómez et al. [125] reported that the membrane fouling rate decreased by increasing the specific gas demand (SGD) until the SGD reached 1.3 m^3 m^{-2} h^{-1}. Beyond this value, no fouling mitigation was achieved by increasing the SGD intensity. The authors attributed these results to the higher resistance that the membrane module offered to the gas passing through the fibres than passing through the membrane sides. Ruigómez et al. [125] concluded that membrane rotation can be more effective for fouling control than gas sparging since the power supplied by the rotating engine is more homogeneously distributed on the membrane. Ruigómez et al. [111] compared both configurations (i.e. conventional gas sparging system and a rotating system) at pilot-scale. The rotating membrane system exhibited better performance than the gas sparging confirming their lab-scale results. Specifically, the rotating system achieved critical fluxes around 20% higher than the gas sparging. In a subsequent study by the authors, a lab-scale AnMBR equipped with a rotating hollow-fibre module allowed to achieve a stable flux of 6.7 L m^{-2} h^{-1} (LMH) at 340 rpm with long term-assays (400 h) [126].

Despite the improved fouling control of the membrane rotating system, the main concern of this technology is related to energy consumption. Shin and Bae [28] estimated that the energy consumption of the Ruigómez et al. [111] pilot-scale AnMBR was 0.30 kWh m^{-3}, which was higher than the reported in other pilot-scale AnMBRs using gas sparging for fouling control. Therefore, it is required to optimise the energy consumption of AnMBRs using rotating membranes as fouling control strategy by exploring different mixing modes and intensities. Finally, the impact of high rotating velocities on process performance and stability as well as on microbial community capacity is yet to be explored. Intensive mixing has been reported particularly counterproductive during shock loads or during start-up of the digestion process [127].

3.1.2. Anaerobic osmotic membrane bioreactors (AnOMBR)

The forward osmosis (FO) process is getting attention to reduce fouling in both AnMBRs and AeMBRs due to the lower fouling and the higher rejection of dissolved pollutants than UF and MF membranes [128]. FO is driven by an osmotic gradient generated by saline draw solutions that facilitates water permeation through a semipermeable dense membrane from the region of lower osmotic pressure (mixed liquor) to the region of higher osmotic pressure (draw solution) [129]. Accordingly, FO systems do not require hydraulic pressure to achieve water permeation. The installation of FO membranes in AnMBR systems is known as anaerobic membrane bioreactor coupled with FO (AnOMBR) (Fig. 2b).

Chen et al. [112] treated synthetic municipal wastewater at 25 °C using an AnOMBR. The reactor exhibited more than 96% of organic carbon removal. However, the membrane flux decreased from 9.5 to 3.5 LMH within 22 days. This flux drop was attributed to the salinity build-up in the bioreactor which increased the conductivity from 1.0 to 20.5 mS cm^{-1}. Gu et al. [113] also reported that the flux gradually decreased due to the accumulation of ions in the AnOMBR. The accumulation of ions in the mixed liquor reduces the driving force (i.e. osmotic gradient) and exacerbates membrane fouling [130,131]. The

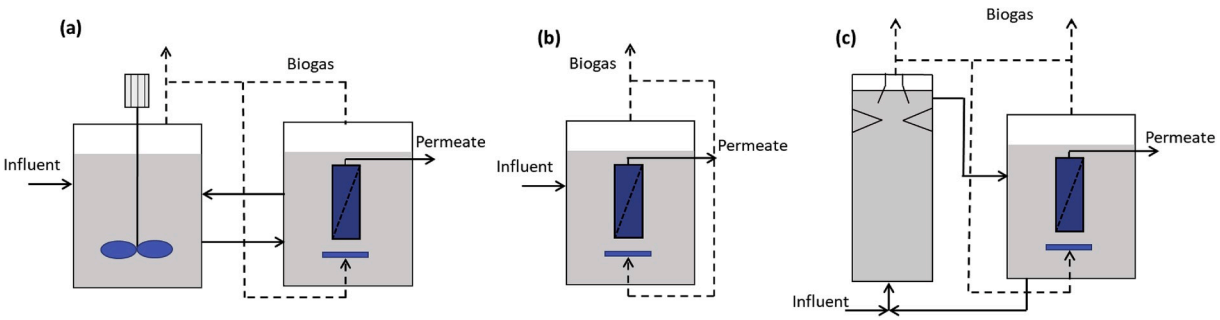

Fig. 1. AnMBR configurations for municipal sewage treatment. (a) AnMBR-CSTR with separated membrane tank; (b) AnMBR-CSTR in a single tank; (c) AnMBR-UASB with separated membrane tank.

Table 1
Membrane characteristics and performance in AnMBR-CSTR configurations for municipal wastewater treatment.

Membrane configuration	Pore size (μm)	Material	Flux (L m^{-2} h^{-1})	Filtration area (m^2)	Fouling control	Chemical cleaning	Reference
Hollow fibre	0.05 UF	–	10[a]	30	Gas sparging (0.23 m^3 m^{-2} h^{-1})	No	[18]
Hollow fibre	0.05 UF	–	9–13.3[a]	30	Gas sparging (0.23–0.33 m^3 m^{-2} h^{-1})	No	[44]
Hollow fibre	0.04 UF	PVDF	17	5.4	Gas sparging + $FeCl_3$	Yes	[46]
Hollow fibre	0.05 UF	–	9–13.3	30	Gas sparging (0.23 m^3 m^{-2} h^{-1})	No	[48]
Flat sheet	0.2 MF	Polyethersulfone	5–7	0.0387	Gas sparging (7.24 m^3 m^{-2} h^{-1})	No	[52]
Hollow fibre	0.2 MF	–	6	5.4	Gas sparging	No	[56]
Flat sheet	0.45 MF	Polyethersulfone	5.3–7.9	0.118	Gas sparging	Yes	[65]
Hollow fibre	0.04	PVDF	11.7–12.3	0.9	Rotating membrane	Yes	[111]
Flat sheet	Dense	Cellulose triacetate	3.5–9.5	0.025	Gas sparging (4.8 m^3 m^{-2} h^{-1})	–	[112]
Flat sheet	Dense	Cellulose triacetate	3–10	0.025	Gas sparging (4.8 m^3 m^{-2} h^{-1})	–	[113]
Flat sheet	Dense	Cellulose triacetate	2–6	0.025	Gas sparging (2.4 m^3 m^{-2} h^{-1})	–	[114]
Flat sheet	0.2 MF	PVDF	<6	0.025	Gas sparging (2.4 m^3 m^{-2} h^{-1})	No	[114]
Flat sheet	0.038 UF	Polyether sulfone	7	3.5	Gas sparging	No	[115]
Hollow fibre	0.03 UF	PVDF	–	0.031	CFV (0.3 m s^{-1})	No	[116]

[a] Flux normalized to 20 °C (LMH).

Table 2
Membrane characteristics and performance in AnMBR-UASB configurations for municipal wastewater treatment.

Membrane configuration	Pore size (μm)	Material	Flux (L m^{-2} h^{-1})	Filtration area (m^2)	Fouling control	Chemical cleaning	Reference
–	0.08–0.3	Alumina	6	–	Gas sparging	No	[41]
Hollow fibre	0.04 UF	PVDF	9–15	0.93	Gas sparging (0.2–2 m^3 m^{-2} h^{-1})	Yes	[50]
Hollow fibre	0.03 UF	PVDF	4.1–7.5	39.5	Granular activated carbon	No	[64]
Hollow fibre	0.045 UF	PVDF	10–14	0.93	Gas sparging (0.4–1 m^3 m^{-2} h^{-1})	Yes	[117]
Hollow fibre	0.045 UF	PVDF	8–15	0.93	Gas sparging (0.4–1 m^3 m^{-2} h^{-1})	No	[118]
Tubular	0.03 UF	PVDF	10–15	0.013	Gas lift mode (CFV of 0.3–1 m s^{-1})	Yes	[119]
Tubular	0.03 UF	PVDF	4.5	0.066	Gas lift mode (CFV of 0.12 m s^{-1})	Yes	[120]
Hollow fibre	0.1 UF	PVDF	10	0.091	Granular activated carbon	Yes	[121]
Hollow fibre	0.4 MF	–	11.3	0.19	Granular activated carbon	–	[122]

reasons leading to membrane fouling exacerbation under high salinity conditions remain under discussion. It has been hypothesised that this phenomenon could be explained using the Derjaguin-Landau-Verwey-Overbeek (DLVO) theory. Briefly, the presence of counter-ions in the mixed liquor compresses the electric double layer around the floccules, reducing the electrostatic repulsion and increasing the attractive Van Der Waals forces [132–134]. According to this theory, the interaction between foulants and membrane increases with the ionic strength. However, other studies have stated that this theory partially fails to describe membrane behaviour under specific salinity conditions [97,135,136].

Miao et al. [97] tested the influence of the ionic strength on membrane permeation by adding different NaCl concentrations in a synthetic bovine serum albumin (BSA) solution. Miao et al. [97] reported that membrane fouling increased as the NaCl concentration increased from 0 to 0.06 g L^{-1}. However, membrane fouling was significantly reduced when the NaCl concentration ranged between 0.6 and 6 g L^{-1}. Miao et al. [97] linked membrane fouling behaviour to the hydration repulsion forces. At low ionic strength, hydration forces are weak and, therefore, the variation of the electrostatic force generated by the compression of the double layer increased foulants attachment on the membrane surface. On the other hand, at high ionic strength, the hydration repulsion forces originated by the highly hydrated sodium ions surrounding negative charges of the polyvinylidene fluoride (PVDF) membrane and BSA are more relevant. From Miao et al. [97] results, it can be concluded that membrane flux is not only affected by the accumulation of salts in the solution. Thus, other factors (e.g. biologic performance, operational conditions, membrane material) have to be also taken into account. However, the relative importance of these factors on membrane fouling is yet to be unfolded. In any case, salinity and ionic strength have a well-known impact on microbial community, morphology, structure and capacity [137–139] which can affect floccules composition and particle size distribution [140–143]. Therefore, successful AnOMBR operation requires achieving a compromise solution between membrane performance and biological performance.

Wang et al. [114] proposed a new AnMBR configuration combining MF membrane and FO membrane (AnMF-OMBR) to control the accumulation of salts in the mixed liquor. This configuration allowed to keep the conductivity of the mixed liquor between 2.5 and 4.0 mS cm^{-1}. However, biofouling and inorganic scaling, that could not be removed with physical methods, were observed on the FO membrane. In this regard, Wang et al. [66] applied a chemical cleaning method to mitigate the long-term fouling on the FO membrane. The optimum chemical cleaning protocol consisted of applying a 0.5% H_2O_2 solution at 25 °C during 6 h. In a subsequent study, Wang et al. [144] proposed a new operational strategy consisting of a two-stage pattern: a first stage using a low driving force (i.e. low draw solution concentration) and a second stage using a high driving force (i.e. high draw solution concentration). Wang et al. [144] reported that this operational mode alleviated the flux drop and enhanced the filtration performance of the FO membrane.

Despite the recent advances, the implementation of AnOMBR is still challenging. The impact of salinity on the long-term feasibility of this technology requires research focused on both anaerobic digestion and membrane performance. The AnMF-OMBR system is a step forward to overcome salinity constraints. However, the necessity of using two membrane processes (i.e. FO and UF) in the bioreactor significantly hinders the technical and economic prospect of this approach (i.e. higher capital and operating costs, more complex physical and chemical cleaning procedures, and draw solution regeneration among others). Overall, the development of FO membranes able to achieve high water fluxes and low reverse solute fluxes is crucial to reduce capital and operating costs of AnOMBRs.

3.2. Novel configurations in AnMBR-UASB systems

3.2.1. Membrane coupled at the top of the AnMBR-UASB

Most common AnMBR-UASB configurations include the membrane module in an external tank [49,98,117,144,145] or at the top of the UASB reactor [77,146,147]. The former is the most reported system. However, if poorly managed, this configuration can lead to solids

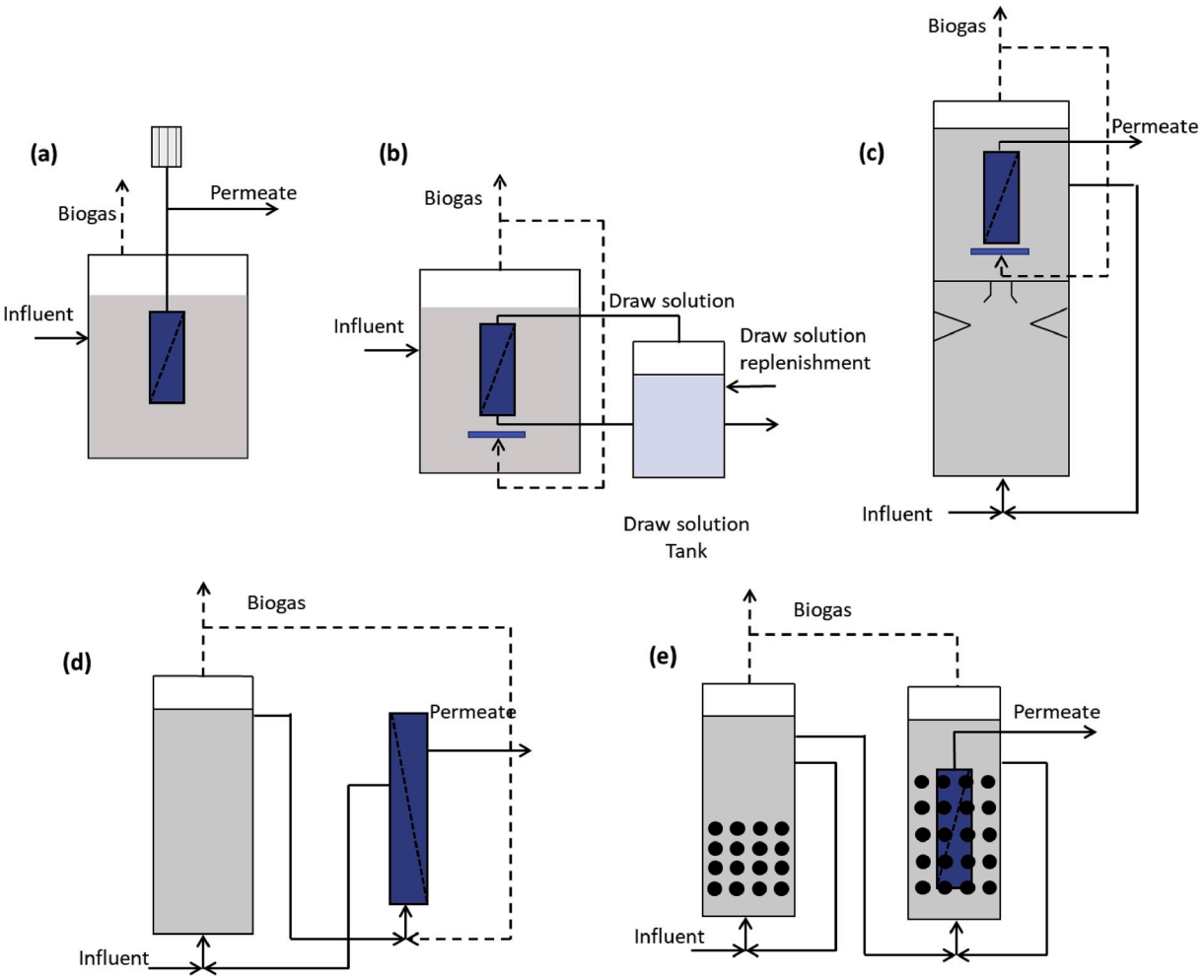

Fig. 2. Novel AnMBR configurations for municipal sewage treatment. (a) Rotating membranes (adapted from Ruigómez et al. [125]); (b) Anaerobic osmotic membrane bioreactor (adapted from Chen et al. [112] and Gu et al. [113]); (c) membrane coupled at the top of the AnMBR-UASB (adapted from Gouveia et al. [118]); (d) Gas-lift AnMBR (adapted from Prieto et al. [119]); (e) two-stage anaerobic fluidised membrane bed bioreactor (adapted from Shin et al. [64] and Kim et al. [121]).

accumulation in the membrane tank and exacerbate membrane fouling. The accumulation of fine solids in the membrane tank occurs when the recirculation flow from the membrane tank to the UASB is not high enough or the system is not properly designed. This is of special concern considering the poor settling characteristics of the suspended biomass leaving the UASB and entering the membrane tank. According to Gouveia et al. [117], these particles tend to accumulate close to the membrane module due to their lower back-transport. The design of AnMBR systems able to provide high shear conditions on the membrane surface by combining gas sparging with other fouling mitigation alternatives is necessary to reduce the accumulation of fine solids and improve membrane fouling control in AnMBR-UASB systems. Consequently, optimising the recirculation flow between the UASB and the membrane module as well as providing enough turbulence in the membrane tank are important factors for fouling control in this configuration.

Gouveia et al. [118] proposed a new pilot-plant system in which the membrane module was submerged at the top of the reactor rather than submerged in an external membrane tank (Fig. 2c). The novelty of this system was that the AnMBR-UASB consisted of two differentiated zones: (i) the biological zone, located at the bottom of the UASB, and (ii) the filtration zone, located at the top of the UASB. In the filtration zone, a high degree of mixing was achieved by (i) biogas sparging which was recirculated at the bottom of the membrane modules, (ii) the recirculation flow from the bottom of the membrane modules to the biological zone, and (iii) the use of two baffles placed between the filtration zone and the three-phase separator. Gouveia et al. [118] reported that the COD accumulation rate in the filtration zone was reduced from 239–702 mg COD L^{-1} d^{-1} to 90–119 mg COD L^{-1} d^{-1} when recirculation was turned on. These results suggested that proper mixing is needed to prevent solids accumulation and membrane fouling. Gouveia et al. [118] configuration was operated for three years with a permeate flux between 12 and 14 LMH, without requiring any physical or chemical cleaning.

Shin and Bae [28] estimated the energy consumption of the pilot-plant in Gouveia et al. [118] and reported that their configuration featured a low SGD (0.16 m^3 m^{-2} h^{-1}) and the lowest energy consumption (0.05 kW m^{-3}) among the eleven evaluated AnMBR pilot-plants. Peña et al. [24] recently used the same pilot-plant configuration to treat municipal sewage but operated without temperature control (10-28 °C). The temperature fluctuations led to a variable anaerobic digestion and membrane performance, which could be the factor behind the increased SGD requirements (0.66–0.74 m^3 m^{-2} h^{-1}) when compared to those of Gouveia et al. [118]. The impact of temperature and temperature fluctuations on SGD optimisation should be studied in more detail since it plays a notable role in the AnMBR operational costs.

3.2.2. Gas-lift AnMBR (Gl-AnMBR)

Submerged configurations are preferred over side-stream configurations for municipal sewage treatment due to their lower energy consumption [148,149]. The cross-flow velocity (CFV) required for fouling control is the main bottleneck of side-stream configurations [37]. Prieto et al. [119] proposed a hybrid gas-lift AnMBR (Gl-AnMBR), a side-stream system aiming to minimise the CFVs and the associated energy consumption. In Gl-AnMBR system, the CFV for fouling control is provided by both mixed liquor recirculation and biogas recirculation (Fig. 2d). This strategy provides a two-phase (gas-liquid) flow through the membrane, where the rising bubbles improve the turbulence on the membrane surface. Consequently, lower CFVs are required which reduce energy consumption. Prieto et al. [119] configuration sustained stable membrane fluxes ranging from 10 to 15 LMH with a CFV of 0.5 m s^{-1}, and a gas to liquid ratio of 0.1.

Dolejs et al. [120] assessed the effects that temperature shocks would have on the performance of the Gl-AnMBR system (i.e. short-term shocks of 12–48 h from 35 to 15 °C). The TMP slightly increased after the temperature shock owing to the higher water viscosity at lower temperatures. However, Dolejs et al. [120] concluded that both membrane flux and TMP remained stable during the 15 °C shocks, which is important for the robustness of the Gl-AnMBR system.

The Gl-AnMBR system is of special interest since it addressees the optimisation of a side-stream configuration, which has been rarely considered for municipal sewage treatment. However, this configuration presents critical challenges for its full-scale implementation. Although Gl-AnMBR requires lower CFVs in comparison with classic side-stream systems, this configuration could have higher capital costs due to the installation of both gas and liquid recirculation systems. Additionally, the technical implications of combining gas and liquid turbulence for membrane fouling control still needs more research. Special attention should be given to the technical challenges associated with biogas recirculation and the associated implications in membrane operability (e.g. backwash, membrane chemical clean in place and out of place). Preferably, these studies should be carried out at pilot-scale since, to the best of our knowledge, the Gl-AnMBR configuration has not been tested at pilot-scale.

3.2.3. Anaerobic fluidised membrane bed bioreactor (AFMBR)

The use of granular activated carbon (GAC) as a fouling control method is gaining attention for AnMBRs [29,149]. In this configuration, GAC particles are fluidised and used for membrane scouring. Fluidisation is energy-intensive although its energy consumption can be lower than the required for gas sparging. Shin and Bae [28] reported GAC fluidisation as one of the most competitive approaches in terms of energy consumption for fouling control (0.102 kWh m^{-3}).

In its early stages, this process consisted of two separated reactors, an anaerobic fluidised bed reactor (AFBR) and an anaerobic fluidised membrane bed reactor (AFMBR) (Fig. 2e). Both reactors were filled with GAC particles to (i) provide a carrier surface where the biomass was attached, (ii) scour the membrane, and (iii) adsorb soluble and colloidal matter surrounding membrane surface. Kim et al. [121] used the AFBR-AFMBR system for sewage treatment and biogas production. The short-term experiments showed that GAC fluidisation was an effective method for fouling reduction, while the long-term experiments showed that GAC addition was able to keep membrane fluxes at 10 LMH for 40 days with only a slight TMP increase (0.025 bar). Yoo et al. [150] operated an AFBR-AFMBR system for 192 days, and observed that the GAC scouring effect and relaxation periods were enough to prevent significant fouling and hence neither chemical nor physical cleaning were needed. The membrane reached fluxes up to 9 LMH during the first period of operation (160 days). However, when the membrane flux was increased up to 12 LMH an important TMP increase (0.2 bar) was observed.

As the technology evolved, some studies considered the possibility to use a single-stage system (i.e. AFMBR only) rather than a two-stage system (AFBR-AFMBR). Bae et al. [151] compared both systems under similar operating conditions and concluded that both systems exhibited similar COD removal efficiencies (93–96%) and TMPs (0.1 bar). Similarly, Wu et al. [152] reported COD removal efficiencies above 97% for both configurations. Therefore, according to Bae et al. [151] and Wu et al. [152] the first-stage AFBR could be avoided. However, the performance of the single-staged AFMBR needs to be tested at pilot-scale.

Alternative materials have been used for fouling control [149]. Hu & Stuckey [153] compared GAC and powdered activated carbon (PAC) and concluded that PAC could be a better material for fouling control than GAC. However, Yang et al. [154] reported that both materials were able to reduce cake layer formation, although GAC was slightly superior than PAC. The addition of polyethylene terephthalate (PET) or PVDF as scouring materials has also been tested [155–158]. Aslam et al. [156] reported that SGDs were reduced by 67% when gas sparging was combined with PET particles.

The durability of the membranes in constant contact with the scouring particles is important for the application of AFMBR technology. Shin et al. [159] operated an AFBR-AFMBR pilot-scale for two years and reported that the membrane was severely damaged due to the continuous contact with fluidised GAC. Shin et al. [159] observed that the middle and bottom of the membrane was significantly damaged due to the contact with more densely-packed particles. Larger particles are more damaging than smaller ones for the membrane but are better for fouling control. Accordingly, the selection of a suitable particle size is critical for membrane performance and integrity [160,161].

Ceramic membranes have recently gained attention due to their higher resistance to abrasion [162,163]. Additionally, these membranes characteristically achieve excellent membrane flux performance. Aslam et al. [163] used a single-stage AFMBR equipped with a ceramic membrane composed of aluminium oxide (Al_2O_3) and achieved high COD removals (~90%) and net fluxes of 17 LMH in long-term operation (395 days). In a subsequent study, Aslam et al. [164] reached higher membrane fluxes (~22 LMH) when using a ceramic membrane in an AFBR-AFMBR system. However, further studies are required to better understand the membrane performance differences between the AFMBR and the AFBR-AFMBR systems.

The long-term effects of the scouring particles on membrane integrity is a primary barrier for the implementation of AFMBR. The use of alternative membrane materials (e.g. ceramic membranes) is a research direction which should be further explored to overcome this limitation. Evans et al. [29] recently compared two pilot-scales using gas sparging and AFBR-AFMBR for fouling control. The AFBR-AFMBR, which used GAC as scouring material, allowed to work at shorter HRTs than the gas-sparged AnMBR. This improvement was attributed to the higher resilience of the biomass attached to the GAC particles. However, the gas sparging provided a more flexible operation due to the possibility to (i) adjust the gas sparging rate, (ii) avoid the damaging effect of GAC and (iii) keep the membrane permeability constant with higher concentrations of suspended solids and colloids in the mixed liquor. Evans et al. [29] concluded that a hybrid system combining a GAC-fluidised bioreactor and gas-sparged membranes would benefit from the capacities of both fouling control methods while improving the technical feasibility of GAC-fluidised AnMBR. However, the combination of these two energy-intensive alternatives (i.e. gas sparging and GAC fluidisation) could compromise the economic feasibility of the AnMBR system, despite their combination could improve membrane fouling control and biological performance.

4. Temperature

4.1. Temperature influence on anaerobic digestion performance

The diluted origin of municipal sewage makes unfeasible to heat the digester content and, therefore, AnMBRs are typically operated at ambient uncontrolled temperature conditions [165]. Psychrophilic

conditions (<20 °C) have been used for AnMBR at lab-scale [52,53,62,65,114] and at pilot-scale [24,48,64,111,117,165] (Tables 3 and 4).

Temperature fluctuations and temperatures below 10 °C are two important challenges for AnMBR technology. Ferrari et al. [62] evaluated the influence of seasonal temperature variations and monitored COD removal efficiencies above 87% for temperatures between 23 and 34 °C. However, when the temperature decreased to 15 and 17 °C, the COD removal efficiency decreased to around 70%. Similarly, Peña et al. [24] operated an AnMBR without temperature control (10–28 °C) and reported higher COD concentrations in the effluent when the temperature was 10 °C. These results are in agreement with other publications studying AnMBR performance at psychrophilic conditions [106,120,122,165,166].

Temperature has an impact on the digesters microbial community and degradation rates [167]. Hydrolysis is typically considered the rate-limiting step in the anaerobic digestion of highly particulate waste and wastewater [168,169]. One advantage of AnMBR is that the membrane provides excellent retention of solids in the bioreactor giving more time for particles to be hydrolysed. Therefore, if the SRT is high enough, the decrease of the hydrolysis rate at lower temperatures may not be controlling the amount of methane recovered in AnMBR. Temperature changes may also affect the degradation rate of the other anaerobic digestion steps (i.e. acidogenesis, acetogenesis and methanogenesis) as well as the syntrophic relationships between microorganisms [170,171]. The slightly lower equilibrium constant and the higher H_2 solubility makes volatile fatty acids (VFA) degradation less favourable at psychrophilic temperatures [172]. If improperly managed, this can increase the VFA concentration and decrease the pH of the mixed liquor which, in turn, can partially, or totally, inhibit methanogenic activity. Besides the great adaptability of microorganisms to different environmental conditions, the lower degradation rate at lower temperatures can be compensated by increasing the amount of active biomass in the digester (higher SRT).

Acetoclastic methanogenesis and hydrogenotrophic methanogenesis are the two main pathways for methane generation [173]. Smith et al. [22] reported that hydrogenotrophic methanogenesis could be the predominant pathway in AnMBRs operated under psychrophilic conditions, which was attributed to the higher solubility of hydrogen at lower temperatures. However, in a subsequent publication, Smith et al. [52] reported that acetoclastic methanogens were more abundant than hydrogenotrophic methanogens in an AnMBR treating municipal sewage at 15 °C. Acetoclastic methanogens were also reported as the dominant methanogens in other psychrophilic AnMBR studies [53,62,106]. Ozgun et al. [53] stated that the higher hydrogen solubility under psychrophilic conditions could have promoted acetate production through the homoacetogenic pathway. However, more studies are required to understand the impact of temperature on microbial community structure, degradation rates and degradation pathways. It is worth mentioning that the microbial community, and methanogens in particular, can be affected by several factors such as pH, loading rate and presence of inhibitors (e.g. Na^+, H_2S, NH_3, heavy metals, organic acids) among others.

COD removal efficiencies around 90% have been achieved in AnMBRs working at psychrophilic temperatures [52,53,57,115,174]. These results show the great adaptability of the microbial community to perform at low temperatures. However, these results are the combination of the microbial community capacity with other factors such as membrane configuration [52,53] and operational conditions (e.g. HRT, SRT and OLR) [21,22,35]. Ozgun et al. [53] and Lim et al. [57] attributed the high COD removals at psychrophilic conditions to the membrane separation process. The membrane retains particulate and colloidal COD in the digester providing a high-quality effluent. Smith et al. [52] reported that the biofilm on the membrane surface has a role in the removal of soluble organic matter under psychrophilic conditions. Indeed, several studies have reported significant differences between the bioreactor and the permeate soluble COD [52,115,174]. Smith et al. [174] observed that, under psychrophilic conditions, *Methanosaeta* (acetoclastic methanogenic) was the most abundant methanogen in the mixed liquor while *Methanospirillum* and *Methanoregula* (hydrogenotrophic methanogens) were the most abundant in the membrane biofilm. The principal coordinates analysis in Smith et al. [174] showed a distinct microbial community structure (including both archaea and bacteria) between the suspended biomass and the biofilm. Understanding the role, structure and development of the biofilm attached to the membrane surface is paramount for AnMBR technology.

4.2. Temperature influence on membrane performance

Temperature affects fluid and sludge properties [170]. The membrane permeability decreases as the temperature decreases due to the higher viscosity of water. Foulants properties also change with temperature. Watanabe et al. [106] and Martin-Garcia et al. [165] reported that membrane fouling was exacerbated at lower temperatures due to changes in SMP characteristics. Both studies associated the fouling rate increase to the higher protein to carbohydrate ratio at lower temperatures. Robles et al. [175] also reported an increase of membrane fouling when the temperature of an AnMBR pilot-plant was changed from mesophilic to psychrophilic conditions. However, these authors observed a lower SMPs protein to carbohydrate ratio at psychrophilic conditions. Nonetheless, as discussed in Section 2, the SMP protein to

Table 3
Biological performance in AnMBR-CSTR configurations for municipal wastewater treatment.

Reactor configuration	Scale	Type WW	T (°C)	OLR (kg COD m^{-3} day^{-1})	COD removal (%)	MLSS (g TSS L^{-1})	Methane yield (m^3 CH_4 kg^{-1} COD)	HRT (h)	SRT (days)	Reference
Submerged	Pilot	Real	33	–	87	6–22[a]	0.069	6–20	70	[18]
Submerged	Pilot	Real	17–33	0.3–1.1	85	10–30[a]	–	6–26	30–70	[44]
Submerged	Pilot	Synthetic	23	–	–	11.3–21.3	–	8.5	40–100	[46]
Submerged	Pilot	Real	15–33	–	–	10–30[a]	–	5–24	40–100	[48]
Submerged	Lab	Synthetic and real	15	0.44–0.66	92 (Synthetic) 69 (Real)	6–10.6[b]	–	16–24	300	[52]
Submerged	Pilot	Real	35	3	87	4.7–20.1	0.12	2.2	60	[56]
Submerged	Lab	Synthetic	25–30	1.10–1.65	95–99	5.5–10.4	0.124–0.25	8–12	30-∞	[65]
Submerged	Pilot	Real	19	1.1	91	21.3	0.012	33	270	[111]
Submerged	Lab	Synthetic	25	–	97	3.9–4.6[b]	0.21	15–40	90	[112]
Submerged	Lab	Synthetic	35	–	>95	–	0.25–0.3	15–40	90	[113]
Submerged	Lab	Synthetic	25	–	90–96[c]	–	0.25–0.28	35–60	80	[114]
Submerged	Pilot	Real	20–35	0.5–1.1	82–90	15–21	0.27–0.23	19.2	–	[115]
Side-stream	Lab	Synthetic	35	0.8–10	97–99	16	0.088–0.393	6–12	1000	[116]

[a] TS concentration (g L^{-1}).
[b] VSS concentration (g L^{-1}).
[c] Total organic carbon removal (%).

Table 4
Biological performance in AnMBR-UASB configurations for municipal wastewater treatment.

Reactor configuration	Scale	Type WW	T (°C)	OLR (kg COD m^{-3} day^{-1})	COD removal (%)	MLSS (g TSS L^{-1})	Methane yield (m^3 CH_4 kg^{-1} COD)	HRT (h)	SRT (days)	Upflow velocity (m h^{-1})	References
Submerged	Lab	Real	25–30	–	86–89	12.8–12.9	0.1 ± 0.02	7.5	60	–	[41]
Submerged	Pilot	Real	16.3	–	83.0	0.384[a]	–	8	–	0.8–0.9	[50]
Submerged	Pilot	Real	9–30	–	81–94	–	–	4.6–6.8	6.2–36	27–75	[64]
Submerged	Pilot	Real	18	0.81–4.70	87	–	0.16–0.23	17–7	–	0.15–0.45	[117]
Submerged	Pilot	Real	18	0.6–3.18	75–90	–	0.26–0.14	9.8–20.3	–	0.12–0.34	[118]
Side-stream	Lab	Synthetic	37	0.42	93	22	–	72	60	–	[119]
Side-stream	Lab	Synthetic	15–35	0.62–0.88	94	–	0.19–0.07	30–36	–	–	[120]
Submerged	Lab	Synthetic	35	4.4–6.2	99	–	–	2.0–2.8	–	–	[121]
Submerged	Lab	Synthetic	15–35	1.21–1.44	51–74	–	0.14–0.19	6	–	–	[122]

[a] Concentration in the membrane tank.

carbohydrate ratio does not seem to be a reliable indicator to predict fouling behaviour. Instead, particle size distribution appears to be more suitable for fouling evaluation and comparison. In this regard, Robles et al. [175] observed a smaller floc size at lower temperatures attributed to the lower biomass activity under psychrophilic conditions. Ozgun et al. [53] also observed that the average particle size decreased and the SMPs production increased when the temperature was decreased from 25 to 15 °C. In both studies, the total filtration resistance significantly increased at lower temperatures. Peña et al. [24] evaluated membrane performance under annual temperature variations in a pilot-scale study. The filtration flux remained between 10 and 11 LMH at temperatures around 24 °C. However, a gradual decrease in the flux (2–3.5 LMH) was reported at lower temperatures (~15 °C). Future research should aim to improve membrane flux performance at low temperatures.

4.3. Dissolved methane

Methane solubility increases as the temperature decreases [176]. The methane solubility at 20 °C is around 30% higher than at 35 °C, hence, the methane concentration leaving the permeate is higher at psychrophilic than at mesophilic conditions [115]. The methane dissolved in the permeate has a double negative connotation: (i) it decreases the methane yield of the AnMBR and, therefore, the profitability of the technology and (ii) it is an important source of greenhouse gas emissions [177]. Smith et al. [52] found that 40–50% of the methane generated in a psychrophilic AnMBR remained dissolved in the permeate at 15 °C. The authors hypothesised that the biofilm activity on the membrane surface increased the concentration of methane in the permeate above oversaturation levels. Similarly, Lim et al. [57] found that 47% of the methane remained dissolved in the effluent between 15 and 20 °C. This is critical since fugitive methane emissions significantly compromise the environmental feasibility of AnMBRs. Accordingly, developing technologies and operational strategies to minimise or recover the methane dissolved in the effluent is crucial for the success of AnMBR technology [23,31,178,179].

Technologies dealing with the methane dissolved in the AnMBR effluents include degassing membranes, aeration, and air stripping [180–182]. Degassing membranes appear as the most suitable technology due to (i) the capacity to recover the methane instead of oxidising it to CO_2 and (ii) the relatively high recovery yields achieved [9,177,181,183–186]. Seco et al. [187] recovered 67% of the dissolved methane in the effluent of a pilot-plant AnMBR by using a hollow-fibre degassing membrane. In another pilot-scale study, Lim et al. [57] reported methane recovery efficiencies of 70 ± 5%.

Several studies analysed the economic impact of recovering the methane dissolved in the effluent of a psychrophilic AnMBR using degassing membranes. Crone et al. [181] estimated that the AnMBR technology could be operated without energy input if the dissolved methane was efficiently recovered. Pretel et al. [188] calculated that integrating a degassing membrane would allow to operate the AnMBR with a very low energy input (0.04 kWh m^{-3}) and life-cycle cost (0.135 € m^{-3}). Evans et al. [29] reported that the energy requirements of a degassing membrane system were nearly negligible (0.01 kWh m^{-3}) when compared with the environmental and energy benefits. Similarly, Lim et al. [57] reported that a membrane contactor was able to recover up to 0.052 kWh m^{-3} from the methane dissolved in the effluent with an energy consumption of 0.008 kWh m^{-3}. Sanchis-Perucho et al. [186] estimated that the payback period for degassing membranes was around 10.5 years. Accordingly, the recovery of the methane is not only necessary, but also encouraging. Nonetheless, Lim et al. [57] noted that the methane remaining in the effluent was equivalent to 0.11 kg CO_2 m^{-3} and stated that further research is needed to reach higher methane recovery efficiencies. Another alternative is to combine gas contactors with other technologies to minimise methane emissions. The utilisation of denitrifying anaerobic methane oxidation (DAMO) process is an attractive biological process for the simultaneous removal of methane and nitrogen from AnMBR effluent [189,190]. However, this technology is still under development.

5. Sulphate

The presence of sulphate in municipal sewage significantly affects the anaerobic digestion and the filtration processes [191,192]. Sulphate reducing bacteria (SRB) use organic compounds and hydrogen as electron donors to convert sulphate into sulphide. In the presence of sulphate, SRB compete with methanogens for the same substrates decreasing the substrate availability for methanogenesis. Moreover, the production of sulphide from SRB can inhibit methanogenic activity, which could further decrease methane conversion [193,194]. The presence of hydrogen sulphide in biogas also requires the utilisation of corrosive resistant instrumentation and equipment [195], whereas the dissolved hydrogen sulphide lowers the durability of the membrane [9]. Therefore, the concentration of sulphate in sewage has a direct impact on the economic feasibility of AnMBR [47].

Shin and Bae [28] reported that AnMBR pilot-plants treating sewage with high sulphate concentrations (>99 mg SO_4^{2-}-S L^{-1}) obtained poor methane yields (0.08–0.15 L CH_4 g^{-1} COD) when compared to the average methane yield of those treating sewage with low sulphate concentrations (0.22 L CH_4 g^{-1} COD). Giménez et al. [18], who studied the influence of the COD/SO_4^{2-}-S ratio on anaerobic digestion performance, reported a sharp decrease of the methane production as the influent sulphate concentration increased. The methane production nearly ceased when COD/SO_4^{2-}-S was below the stoichiometric ratio for sulphate reduction of 2.01 mg COD mg^{-1} SO_4^{2-}-S (0.67 mg COD mg^{-1} SO_4^{2-}) [18]. The latter results showed that SRB outcompete methanogens and nearly all the sulphate is converted to sulphide if enough biodegradable COD is available. Furthermore, the presence of dissolved sulphide in the permeate can affect the overall treatment efficiency since sulphide contributes to the effluent COD [196]. The removal of sulphide from AnMBR effluents has been recently addressed by using

coagulation-flocculation [57] and membrane distillation [197]. However, alternative methods such as electrochemical systems are also gaining attention due to their capacity to recover sulphide as sulphur or other oxidised sulphur species [198].

The corrosive nature of sulphide also affects membrane permeability and durability. Sulphide has been reported to damage the internal material when transported through the membrane cell, making it more susceptible to membrane fouling [9,199]. In this regard, Song et al. [191] observed that membrane fouling increased as the influent sulphate concentration increased. Specifically, the TMP sharply increased from 0.5 to 0.85 bar after the addition of more than 33 mg SO_4^{2-}-S L^{-1}. Song et al. [191] attributed these results to the larger release of EPSs under high sulphide concentrations. However, there is a little understanding of the impact of sulphide concentration on the microbial community activity, particle size distribution, EPS composition, and membrane performance and durability.

Some publications have evaluated the impact of sulphate concentration on the economic and energetic prospects of the AnMBR process [28,200,201]. Ferrer et al. [200] estimated that the treatment of low-sulphate (57 mg COD mg^{-1} SO_4^{2-}-S) municipal sewage is more favourable than the treatment of sulphate-rich (5.7 mg COD mg^{-1} SO_4^{2-}-S) municipal sewage (0.070 and 0.097 € m^{-3}, respectively). Ferrer et al. [200] also stated that methane recovery from AnMBR effluents is more economically attractive when treating low-sulphate municipal sewage due to the low methane production at high sulphate concentrations.

These results clearly illustrate that sulphate concentration in sewage has a significant impact on AnMBR performance and profitability and, therefore, it has a key role in the decision-making process. Some studies have reported that COD/SO_4^{2-}-S ratios at or above 30 (10 mg COD mg^{-1} SO_4^{2-}) could be adequate to sustain a good anaerobic digestion performance and high methane yields [9,191]. However, further studies including technical, economic and energetic challenges connected to sulphate concentration are necessary. Particularly useful would be to determine a COD/SO_4^{2-}-S ratio threshold above which the AnMBR is recommendable for the treatment of municipal sewage. However, further understanding of the implication of sulphide concentration on anaerobic digestion and membrane performance is needed before carrying out such techno-economic study.

6. Forward osmosis pre-concentration (FO + AnMBR)

The application of anaerobic digestion to low-strength municipal sewage presents some challenges, including large AnMBR facilities (e.g. membrane area, digester volume and footprint), higher amounts of dissolved methane lost with the effluent, and low methane productivities per m^3 of wastewater treated. Municipal sewage pre-concentration by FO technology represents an opportunity to tackle these challenges since it allows to pre-concentrate municipal sewage with low energy inputs [60,62,202]. The FO process is spontaneously driven by an osmotic gradient between municipal sewage and a saline draw solution, which allows to produce permeate without requiring hydraulic pressure [203,204].

6.1. Configurations to integrate FO and AnMBR technologies

The configuration used to integrate FO sewage pre-concentration and AnMBR technologies is highly dependent on the draw solution availability. In coastal areas, seawater availability makes open-loop schemes particularly advantageous if the seawater can be discharged to the environment after its utilisation. However, some pollutants and nutrients can diffuse from sewage to seawater through dense FO membranes. Particularly worrying is the diffusion of ammonium nitrogen, since low ammonium rejections (<80%) have been reported for FO membranes [205–207]. Accordingly, FO membranes future development should aim to reduce the diffusion of these compounds to prevent potential environmental impacts in coastal areas after seawater discharge. In contrast, closed-loop schemes require the re-concentration of the draw solution while producing reclaimed water. In both schemes, pre-treatment of raw wastewater is needed to prevent potential fouling in FO membranes [208].

Two main draw solution management alternatives have been conceived for open-loop schemes: (i) the draw solution is discharged after the FO step (Fig. 3a) and (ii) the draw solution is discharged after reverse osmosis (RO) stage for reclaimed water production (Fig. 3b). The latter could be more attractive since it allows to combine sewage treatment and high-quality reclaimed water production (dual barrier) in the same facility. However, this alternative incurs extra operating costs due to the high energy required to operate the RO system. The energy requirements to produce reclaimed water from diluted seawater has been estimated to be in the range of 1.6–2.0 kWh per m^3 of produced water [60]. Therefore, the implementation of RO systems for reclaimed water production should be particularly considered in coastal areas with water scarcity. Detailed information regarding the possibilities of implementing a hybrid FO-RO system is already available in several publications [203,204,209–211].

Closed-loop schemes are required when natural draw solutions are not available (Fig. 3c). In closed-loop schemes, the synthetic draw solution is regenerated after the FO stage (e.g. by RO) to re-establish the draw solution osmotic pressure. Although NaCl is the most used solute for synthetic draw solutions [212,213], this solute can present high reverse solute fluxes (i.e. solute flux from the draw solution to the sewage). Consequently, alternative solutes (e.g. organics, Mg^{2+}, Ca^{2+}) are being evaluated as potential draw solutes. Diminishing the reverse solute flux is crucial to reduce draw solution replenishment cost [60], prevent the inhibition of the AnMBR microbial community [61,214,215], and facilitate the reuse of the digestate as fertiliser or soil conditioner [216,217].

6.2. FO + AnMBR sewage pre-concentration and energy production

Pilot and lab-scale studies have pre-concentrated municipal sewage prior to AnMBR with FO water recoveries ranging between 50 and 90% leading to concentration factors of 2 and 10, respectively [61,63,206,218]. Ansari et al. [218] evaluated FO membrane and anaerobic digestion performance with ten different solutes as well as their impact on anaerobic digestion performance. Ansari et al. [218] reported that NaCl provides higher water fluxes (4.1 LMH) than other inorganic and organic solutes (e.g. NaAc and $MgSO_4$ had water fluxes <3.5 LMH). However, reverse solute fluxes were higher for NaCl (~3 g m^{-2} h^{-1}) than for other solutes such as NaAc (<1 g m^{-2} h^{-1}).

Solute selection must consider both water fluxes and reverse solute fluxes since high reverse solute fluxes highly increase the salinity of the AnMBR influent. Ansari et al. [218] reported that Na^+ inhibition is not significant for Na^+ concentrations below 3 g L^{-1}, which is in agreement with previously reported values [194,219,220]. In a subsequent study, Ansari et al. [61] also reported that NaAc (organic solute) led to higher methane yields than NaCl (inorganic solute). However, the study did not elucidate if these results are a consequence of (i) microbial inhibition as a result of the higher inhibition when using NaCl as solute, or (ii) the higher organic matter in the influent caused by the reverse solute flux of acetate when using NaAc as solute. Further studies are required to holistically evaluate the suitability of the different solutes, including FO performance, AnMBR performance, digestate management, and economic feasibility among others.

FO pre-concentration is an opportunity to make AnMBR energy self-sufficient. Wei et al. [116] conducted an energy balance for the FO + AnMBR system and showed that the biogas produced by the AnMBR could be sufficient to heat the influent to mesophilic conditions (~35 °C). However, this alternative fails to transform the energy contained in the biogas to electricity and, therefore, it makes the process energetically negative instead of energetically neutral or positive. Accordingly,

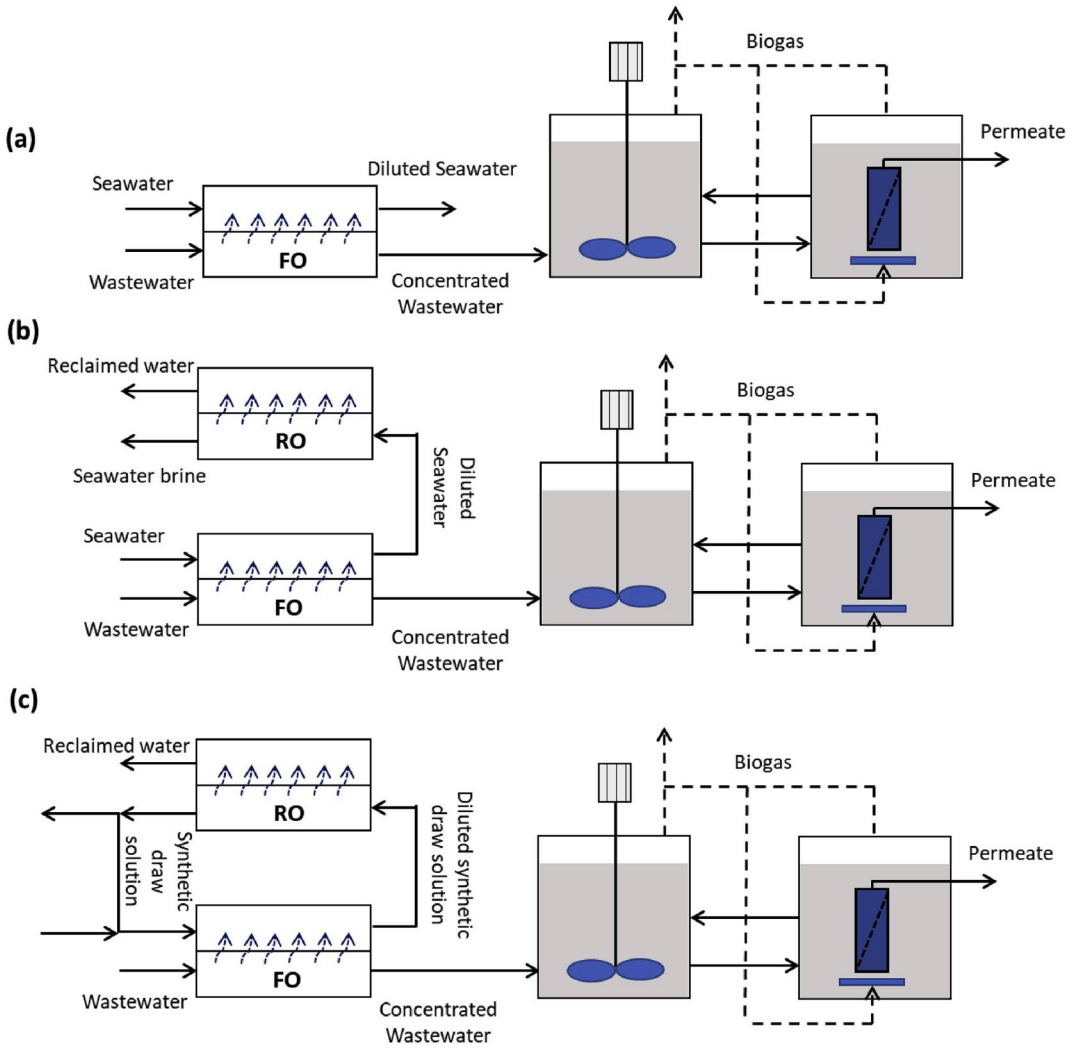

Fig. 3. Configurations to integrate FO and AnMBR technologies for municipal sewage treatment (a) Open-loop FO + AnMBR; (b) Open-loop FO-RO + AnMBR; (c) Closed-loop FO-RO + AnMBR (adapted and expanded from Vinardell et al. [60]).

other alternatives (e.g. co-generation and biogas upgrading) appear more suitable attaining the emergence of the circular biobased economy.

7. Conclusions

Anaerobic membrane bioreactor (AnMBR) is a promising technology for mainstream municipal sewage treatment due to its capacity to produce high-quality effluents and renewable methane energy. However, there are still some technical challenges that need to be addressed to make AnMBR technically and economically competitive. Membrane fouling is a primary barrier for the applicability of AnMBRs. In AnMBRs, fouling has been generally attributed to pore clogging and cake layer formation. However, recent research has shown that the gel layer could be the main responsible for membrane fouling. Further research is needed to understand the relative importance of factors controlling the formation of the gel layer, from which new and improved fouling mitigation strategies could be developed. Novel AnMBR configurations and operational conditions have also been researched to improve fouling control in CSTR and UASB reactors, bringing new opportunities for fouling control beyond gas sparging. Temperature affects metabolic kinetics, microbial community, membrane performance, particle size distribution and, most importantly, the amount of methane dissolved in the effluent. In this regard, FO pre-concentration could improve the process applicability by decreasing the AnMBR volumetric flow rate and reducing methane losses through the effluent. However, FO technology is still under development. Overall, the success of the AnMBR technology relies on improving membrane performance without hindering the biological process nor the economic feasibility of the process.

Declaration of competing interests

The authors declare that they have no known competing financial interests or personal relationships that could have appeared to influence the work reported in this paper. The authors also declare that this manuscript reflects only the authors' view and that the Executive Agency for SME/EU Commission are not responsible for any use that may be made of the information it contains.

Credit author contribution statement

Sergi Vinardell: Conceptualisation, Writing-Original Draft. Sergi Astals: Writing-Review and Editing, Supervision. Miriam Peces: Writing-Review and Editing. Maria Alicia Cardete: Writing-Review and Editing, Isaac Fernández: Writing-Review and Editing, Funding acquisition. Joan Mata-Alvarez: Supervision, Funding acquisition. Joan Dosta: Writing-Review and Editing, Supervision.

Acknowledgments

This work was supported by the European Union LIFE programme (LIFE Green Sewer project, LIFE17 ENV/ES/000341). Sergi Vinardell is grateful to the Generalitat de Catalunya for his predoctoral FI grant (2019FI_B 00394). Sergi Astals is grateful to the Spanish Ministry of Science, Innovation and Universities for his Ramon y Cajal fellowship (RYC-2017-22372).

References

[1] Sheik AR, Muller EEL, Wilmes P, Clark KB, Zhang X. A hundred years of activated sludge: time for a rethink. Froint Microbiol 2014;5:1–7.
[2] Guest JS, Skerlos SJ, Barnard JL, Beck MB, Daigger GT, Hilger H, et al. A new planning and design paradigm to achieve sustainable resource recovery from wastewater. Environ Sci Technol 2009;43:6126–30.
[3] Puyol D, Batstone DJ, Hülsen T, Astals S, Peces M, Krömer JO. Resource recovery from wastewater by biological technologies: opportunities, challenges, and prospects. Front Microbiol 2017;7.
[4] McCarty PL, Bae J, Kim J. Domestic wastewater treatment as a net energy producer - can this be achieved? Environ Sci Technol 2011;45:7100–6.
[5] Wan J, Gu J, Zhao Q, Liu Y. COD capture: a feasible option towards energy self-sufficient domestic wastewater treatment. Sci Rep 2016;6:1–10.
[6] Garrido-Baserba M, Sobhani R, Asvapathanagul P, McCarthy GW, Olson BH, Odize V, et al. Modelling the link amongst fine-pore diffuser fouling, oxygen transfer efficiency, and aeration energy intensity. Water Res 2017;111:127–39.
[7] Macintosh C, Astals S, Sembera C, Ertl A, Drewes JE, Jensen PD, et al. Successful strategies for increasing energy self-sufficiency at Grüneck wastewater treatment plant in Germany by food waste co-digestion and improved aeration. Appl Energy 2019;242:797–808.
[8] Verstraete W, Vlaeminck SE. ZeroWasteWater: short-cycling of wastewater resources for sustainable cities of the future. Int J Sustain Dev World Ecol 2011;18:253–64.
[9] Lei Z, Yang S, Li Y, Wen W, Wang XC, Chen R. Application of anaerobic membrane bioreactors to municipal wastewater treatment at ambient temperature: a review of achievements, challenges, and perspectives. Bioresour Technol 2018;267:756–68.
[10] Liao BQ, Kraemer JT, Bagley DM. Anaerobic membrane bioreactors: applications and research directions. Crit Rev Environ Sci Technol 2006;36:489–530.
[11] Van Lier JB, Van der Zee FP, Frijters CTMJ, Ersahin ME. Celebrating 40 years anaerobic sludge bed reactors for industrial wastewater treatment. Rev Environ Sci Biotechnol 2015;14:681–702.
[12] Tauseef SM, Abbasi T, Abbasi SA. Energy recovery from wastewaters with high-rate anaerobic digesters. Renew Sustain Energy Rev 2013;19:704–41.
[13] De Graaff MS, Temmink H, Zeeman G, Buisman CJN. Anaerobic treatment of concentrated black water in a UASB reactor at a short HRT. Water 2010;2:101–19.
[14] Chernicharo CAL, van Lier JB, Noyola A, Bressani Ribeiro T. Anaerobic sewage treatment: state of the art, constraints and challenges. Rev Environ Sci Biotechnol 2015;14:649–79.
[15] Heffernan B, Van Lier JB, Van Der Lubbe J. Performance review of large scale up-flow anaerobic sludge blanket sewage treatment plants. Water Sci Technol 2011;63:100–7.
[16] Van Lier JB, Vashi A, Van Der Lubbe J, Heffernan B. Anaerobic sewage treatment using UASB reactors: engineering and operational aspects. In: Fang HHP, editor. Environ. Anaerob. Technol. Appl. New dev. Imperial College Press; 2010. p. 59–89.
[17] Batstone DJ, Hülsen T, Mehta CM, Keller J. Platforms for energy and nutrient recovery from domestic wastewater: a review. Chemosphere 2015;140:2–11.
[18] Giménez JB, Robles A, Carretero L, Durán F, Ruano MV, Gatti MN, et al. Experimental study of the anaerobic urban wastewater treatment in a submerged hollow-fibre membrane bioreactor at pilot scale. Bioresour Technol 2011;102:8799–806.
[19] Foglia A, Cipolletta G, Frison N, Sabbatini S, Gorbi S, Eusebi AL, et al. Anaerobic membrane bioreactor for urban wastewater valorisation: operative strategies and fertigation reuse. Chem Eng Trans 2019;74:247–52.
[20] Ozgun H, Gimenez JB, Evren Ersahin M, Tao Y, Spanjers H, Van Lier JB. Impact of membrane addition for effluent extraction on the performance and sludge characteristics of upflow anaerobic sludge blanket reactors treating municipal wastewater. J Membr Sci 2015;479:95–104.
[21] Stuckey DC. Recent developments in anaerobic membrane reactors. Bioresour Technol 2012;122:137–48.
[22] Smith AL, Stadler LB, Love NG, Skerlos SJ, Raskin L. Perspectives on anaerobic membrane bioreactor treatment of domestic wastewater: a critical review. Bioresour Technol 2012;122:149–59.
[23] Batstone DJ, Virdis B. The role of anaerobic digestion in the emerging energy economy. Curr Opin Biotechnol 2014;27:142–9.
[24] Peña M, do Nascimento T, Gouveia J, Escudero J, Gómez A, Letona A, et al. Anaerobic submerged membrane bioreactor (AnSMBR) treating municipal wastewater at ambient temperature: operation and potential use for agricultural irrigation. Bioresour Technol 2019:285–93.
[25] Chong S, Sen TK, Kayaalp A, Ang HM. The performance enhancements of upflow anaerobic sludge blanket (UASB) reactors for domestic sludge treatment - a State-of-the-art review. Water Res 2012;46:3434–70.
[26] Foglia A, Akyol Ç, Frison N, Katsou E, Eusebi AL, Fatone F. Long-term operation of a pilot-scale anaerobic membrane bioreactor (AnMBR) treating high salinity low loaded municipal wastewater in real environment. Separ Purif Technol 2020;236:116279.
[27] Zhen G, Pan Y, Lu X, Li Y-Y, Zhang Z, Niu C, et al. Anaerobic membrane bioreactor towards biowaste biorefinery and chemical energy harvest: recent progress, membrane fouling and future perspectives. Renew Sustain Energy Rev 2019;115:109392.
[28] Shin C, Bae J. Current status of the pilot-scale anaerobic membrane bioreactor treatments of domestic wastewaters: a critical review. Bioresour Technol 2018;247:1038–46.
[29] Evans PJ, Parameswaran P, Lim K, Bae J, Shin C, Ho J, et al. A comparative pilot-scale evaluation of gas-sparged and granular activated carbon-fluidized anaerobic membrane bioreactors for domestic wastewater treatment. Bioresour Technol 2019;288:1–5.
[30] Pretel R, Shoener BD, Ferrer J, Guest JS. Navigating environmental, economic, and technological trade-offs in the design and operation of submerged anaerobic membrane bioreactors (AnMBRs). Water Res 2015;87:531–41.
[31] Smith AL, Stadler LB, Cao L, Love NG, Raskin L, Skerlos SJ. Navigating wastewater energy recovery strategies: a life cycle comparison of anaerobic membrane bioreactor and conventional treatment systems with anaerobic digestion. Environ Sci Technol 2014;48:5972–81.
[32] Cogert KI, Ziels RM, Winkler MKH. Reducing cost and environmental impact of wastewater treatment with denitrifying methanotrophs, anammox, and mainstream anaerobic treatment. Environ Sci Technol 2019;53:12935–44.
[33] Hu Y, Wang XC, Ngo HH, Sun Q, Yang Y. Anaerobic dynamic membrane bioreactor (AnDMBR) for wastewater treatment: a review. Bioresour Technol 2018;247:1107–18.
[34] Ozgun H, Dereli RK, Ersahin ME, Kinaci C, Spanjers H, Van Lier JB. A review of anaerobic membrane bioreactors for municipal wastewater treatment: integration options, limitations and expectations. Separ Purif Technol 2013;118:89–104.
[35] Maaz M, Yasin M, Aslam M, Kumar G, Atabani AE, Idrees M, et al. Anaerobic membrane bioreactors for wastewater treatment: novel configurations, fouling control and energy considerations. Bioresour Technol 2019;283:358–72.
[36] Skouteris G, Hermosilla D, López P, Negro C, Blanco Á. Anaerobic membrane bioreactors for wastewater treatment: a review. Chem Eng J 2012;198–199:138–48.
[37] Lin H, Peng W, Zhang M, Chen J, Hong H, Zhang Y. A review on anaerobic membrane bioreactors: applications, membrane fouling and future perspectives. Desalination 2013;314:169–88.
[38] Song X, Luo W, Hai FI, Price WE, Guo W, Ngo HH, et al. Resource recovery from wastewater by anaerobic membrane bioreactors: opportunities and challenges. Bioresour Technol 2018;270:669–77.
[39] Chen C, Guo W, Ngo HH, Lee DJ, Tung KL, Jin P, et al. Challenges in biogas production from anaerobic membrane bioreactors. Renew Energy 2016;98:120–34.
[40] Nguyen TT, Ngo HH, Guo W. Pilot scale study on a new membrane bioreactor hybrid system in municipal wastewater treatment. Bioresour Technol 2013;141:8–12.
[41] Yue X, Keat Y, Koh K, Ng HY. Effects of dissolved organic matters (DOMs) on membrane fouling in anaerobic ceramic membrane bioreactors (AnCMBRs) treating domestic wastewater. Water Res 2015;86:96–107.
[42] Gao DW, Zhang T, Tang CYY, Wu WM, Wong CY, Lee YH, et al. Membrane fouling in an anaerobic membrane bioreactor: differences in relative abundance of bacterial species in the membrane foulant layer and in suspension. J Membr Sci 2010;364:331–8.
[43] Grossman AD, Yang Y, Yogev U, Camarena DC, Oron G, Bernstein R. Effect of ultrafiltration membrane material on fouling dynamics in a submerged anaerobic membrane bioreactor treating domestic wastewater. Environ Sci Water Res Technol 2019;5:1145–56.
[44] Robles A, Ruano MV, García-Usach F, Ferrer J. Sub-critical filtration conditions of commercial hollow-fibre membranes in a submerged anaerobic MBR (HF-SAnMBR) system: the effect of gas sparging intensity. Bioresour Technol 2012;114:247–54.
[45] Zsirai T, Buzatu P, Aerts P, Judd S. Efficacy of relaxation, backflushing, chemical cleaning and clogging removal for an immersed hollow fibre membrane bioreactor. Water Res 2012;46:4499–507.
[46] Dong Q, Parker W, Dagnew M. Long term performance of membranes in an anaerobic membrane bioreactor treating municipal wastewater. Chemosphere 2016;144:249–56.
[47] Pretel R, Robles A, Ruano MV, Seco A, Ferrer J. The operating cost of an anaerobic membrane bioreactor (AnMBR) treating sulphate-rich urban wastewater. Separ Purif Technol 2014;126:30–8.
[48] Robles A, Ruano MV, Ribes J, Ferrer J. Factors that affect the permeability of commercial hollow-fibre membranes in a submerged anaerobic MBR (HF-SAnMBR) system. Water Res 2013;47:1277–88.
[49] Wang KM, Jefferson B, Soares A, Mcadam EJ. Sustaining membrane permeability during unsteady-state operation of anaerobic membrane bioreactors for municipal wastewater treatment following. peak-flow 2018;564:289–97.
[50] Wang KM, Cingolani D, Eusebi AL, Soares A, Jefferson B, McAdam EJ. Identification of gas sparging regimes for granular anaerobic membrane bioreactor to enable energy neutral municipal wastewater treatment. J Membr Sci 2018;555:125–33.

[51] Fox RA, Stuckey DC. The effect of sparging rate on transmembrane pressure and critical flux in an AnMBR. J Environ Manag 2015;151:280–5.
[52] Smith AL, Skerlos SJ, Raskin L. Psychrophilic anaerobic membrane bioreactor treatment of domestic wastewater. Water Res 2013;47:1655–65.
[53] Ozgun H, Tao Y, Ersahin ME, Zhou Z, Gimenez JB, Spanjers H, et al. Impact of temperature on feed-flow characteristics and filtration performance of an upflow anaerobic sludge blanket coupled ultrafiltration membrane treating municipal wastewater. Water Res 2015;83:71–83.
[54] Huete A, de los Cobos-Vasconcelos D, Gómez-Borraz T, Morgan-Sagastume JM, Noyola A. Control of dissolved CH4 in a municipal UASB reactor effluent by means of a desorption – biofiltration arrangement. J Environ Manag 2018;216:383–91.
[55] Serrano A, Peces M, Astals S, Villa-Gómez DK. Batch assays for biological sulfate-reduction: a review towards a standardized protocol. Crit Rev Environ Sci Technol 2019:1–29.
[56] Mei X, Wang Z, Miao Y, Wu Z. A pilot-scale anaerobic membrane bioreactor under short hydraulic retention time for municipal wastewater treatment: performance and microbial community identification. J Water Reuse Desalin 2018;8:58–67.
[57] Lim K, Evans PJ, Parameswaran P. Long-term performance of a pilot-scale gas-sparged anaerobic membrane bioreactor under ambient temperatures for holistic wastewater treatment. Environ Sci Technol 2019;53:7347–54.
[58] Khoshnevisan B, Tsapekos P, Alfaro N, Díaz I, Fdz-Polanco M, Rafiee S, et al. A review on prospects and challenges of biological H2S removal from biogas with focus on biotrickling filtration and microaerobic desulfurization. Biofuel Res J 2017;4:741–50.
[59] Nascimento TA, Fdz-Polanco F, Peña M. Membrane-Based technologies for the up-concentration of municipal wastewater: a review of pretreatment intensification. Separ Purif Rev 2020;49:1–19.
[60] Vinardell S, Astals S, Mata-Alvarez J, Dosta J. Techno-economic analysis of combining forward osmosis-reverse osmosis and anaerobic membrane bioreactor technologies for municipal wastewater treatment and water production. Bioresour Technol 2020;297:122395.
[61] Ansari AJ, Hai FI, Price WE, Ngo HH, Guo W, Nghiem LD. Assessing the integration of forward osmosis and anaerobic digestion for simultaneous wastewater treatment and resource recovery. Bioresour Technol 2018;260:221–6.
[62] Ferrari F, Balcazar JL, Rodriguez-Roda I, Pijuan M. Anaerobic membrane bioreactor for biogas production from concentrated sewage produced during sewer mining. Sci Total Environ 2019;670:993–1000.
[63] Ferrari F, Pijuan M, Rodriguez-Roda I, Blandin G. Exploring submerged forward osmosis for water recovery and pre-concentration of wastewater before anaerobic digestion: a pilot scale study. Membranes 2019;9:97.
[64] Shin C, McCarty PL, Kim J, Bae J. Pilot-scale temperate-climate treatment of domestic wastewater with a staged anaerobic fluidized membrane bioreactor (SAF-MBR). Bioresour Technol 2014;159:95–103.
[65] Huang Z, Ong SL, Ng HY. Submerged anaerobic membrane bioreactor for low-strength wastewater treatment: effect of HRT and SRT on treatment performance and membrane fouling. Water Res 2011;45:705–13.
[66] Wang X, Hu T, Wang Z, Li X, Ren Y. Permeability recovery of fouled forward osmosis membranes by chemical cleaning during a long-term operation of anaerobic osmotic membrane bioreactors treating low-strength wastewater. Water Res 2017;123:505–12.
[67] Meng F, Zhang S, Oh Y, Zhou Z, Shin HS, Chae SR. Fouling in membrane bioreactors: an updated review. Water Res 2017;114:151–80.
[68] Herrera-Robledo M, Cid-León DM, Morgan-Sagastume JM, Noyola A. Biofouling in an anaerobic membrane bioreactor treating municipal sewage. Separ Purif Technol 2011;81:49–55.
[69] Lin H, Zhang M, Wang F, Meng F, Liao BQ, Hong H, et al. A critical review of extracellular polymeric substances (EPSs) in membrane bioreactors: characteristics, roles in membrane fouling and control strategies. J Membr Sci 2014;460:110–25.
[70] Frølund B, Griebe T, Nielsen PH. Enzymatic activity in the activated-sludge floc matrix. Appl Microbiol Biotechnol 1995;43:755–61.
[71] Ruiz-Hernando M, Cabanillas E, Labanda J, Llorens J. Ultrasound, thermal and alkali treatments affect extracellular polymeric substances (EPSs) and improve waste activated sludge dewatering. Process Biochem 2015;50:438–46.
[72] Ding Y, Tian Y, Li Z, Zuo W, Zhang J. A comprehensive study into fouling properties of extracellular polymeric substance (EPS) extracted from bulk sludge and cake sludge in a mesophilic anaerobic membrane bioreactor. Bioresour Technol 2015;192:105–14.
[73] Laspidou CS, Rittmann BE. A unified theory for extracellular polymeric substances, soluble microbial products, and active and inert biomass. Water Res 2002;36:2711–20.
[74] Meng F, Zhang H, Yang F, Li Y, Xiao J, Zhang X. Effect of filamentous bacteria on membrane fouling in submerged membrane bioreactor. J Membr Sci 2006;272:161–8.
[75] Le-Clech P, Chen V, Fane TAG. Fouling in membrane bioreactors used in wastewater treatment. J Membr Sci 2006;284:17–53.
[76] Meng F, Chae SR, Drews A, Kraume M, Shin HS, Yang F. Recent advances in membrane bioreactors (MBRs): membrane fouling and membrane material. Water Res 2009;43:1489–512.
[77] Lin HJ, Xie K, Mahendran B, Bagley DM, Leung KT, Liss SN, et al. Sludge properties and their effects on membrane fouling in submerged anaerobic membrane bioreactors (SAnMBRs). Water Res 2009;43:3827–37.
[78] Arabi S, Nakhla G. Impact of protein/carbohydrate ratio in the feed wastewater on the membrane fouling in membrane bioreactors. J Membr Sci 2008;324:142–50.
[79] Teng J, Shen L, He Y, Liao B-Q, Wu G, Lin H. Novel insights into membrane fouling in a membrane bioreactor: elucidating interfacial interactions with real membrane surface. Chemosphere 2018;210:769–78.
[80] Dong Q, Parker W, Dagnew M. Impact of FeCl3 dosing on AnMBR treatment of municipal wastewater. Water Res 2015;80:281–93.
[81] Yao M, Zhang K, Cui L. Characterization of protein-polysaccharide ratios on membrane fouling. Desalination 2010;259:11–6.
[82] Chen R, Nie Y, Hu Y, Miao R, Utashiro T, Li Q, et al. Fouling behaviour of soluble microbial products and extracellular polymeric substances in a submerged anaerobic membrane bioreactor treating low-strength wastewater at room temperature. J Membr Sci 2017;531:1–9.
[83] Nie Y, Chen R, Tian X, Li YY. Impact of water characteristics on the bioenergy recovery from sewage treatment by anaerobic membrane bioreactor via a comprehensive study on the response of microbial community and methanogenic activity. Energy 2017;139:459–67.
[84] Buntner D, Spanjers H, van Lier JB. The influence of hydrolysis induced biopolymers from recycled aerobic sludge on specific methanogenic activity and sludge filterability in an anaerobic membrane bioreactor. Water Res 2014;51:284–92.
[85] Taimur Khan MM, Takizawa S, Lewandowski Z, Habibur Rahman M, Komatsu K, Nelson SE, et al. Combined effects of EPS and HRT enhanced biofouling on a submerged and hybrid PAC-MF membrane bioreactor. Water Res 2013;47:747–57.
[86] Kimura K, Hane Y, Watanabe Y, Amy G, Ohkuma N. Irreversible membrane fouling during ultrafiltration of surface water. Water Res 2004;38:3431–41.
[87] Gao WJ, Qu X, Leung KT, Liao BQ. Influence of temperature and temperature shock on sludge properties , cake layer structure , and membrane fouling in a submerged anaerobic membrane bioreactor. J Membr Sci 2012;422:131–44.
[88] Aslam A, Khan SJ, Shahzad HMA. Impact of sludge recirculation ratios on the performance of anaerobic membrane bioreactor for wastewater treatment. Bioresour Technol 2019;288:121473.
[89] Luna HJ, Baêta BEL, Aquino SF, Susa MSR. EPS and SMP dynamics at different heights of a submerged anaerobic membrane bioreactor (SAMBR). Process Biochem 2014;49:2241–8.
[90] Wang XM, Waite TD. Role of gelling soluble and colloidal microbial products in membrane fouling. Environ Sci Technol 2009;43:9341–7.
[91] Hong H, Zhang M, He Y, Chen J, Lin H. Fouling mechanisms of gel layer in a submerged membrane bioreactor. Bioresour Technol 2014;166:295–302.
[92] Rosenberger S, Laabs C, Lesjean B, Gnirss R, Amy G, Jekel M, et al. Impact of colloidal and soluble organic material on membrane performance in membrane bioreactors for municipal wastewater treatment. Water Res 2006;40:710–20.
[93] Chen J, Zhang M, Li F, Qian L, Lin H, Yang L, et al. Membrane fouling in a membrane bioreactor: high filtration resistance of gel layer and its underlying mechanism. Water Res 2016;102:82–9.
[94] Teng J, Zhang M, Leung K-T, Chen J, Hong H, Lin H, et al. A unified thermodynamic mechanism underlying fouling behaviors of soluble microbial products (SMPs) in a membrane bioreactor. Water Res 2019;149:477–87.
[95] Chen Y, Yu G, Long Y, Teng J, You X, Liao B, et al. Application of radial basis function arti fi cial neural network to quantify interfacial energies related to membrane fouling in a membrane bioreactor. Bioresour Technol 2019;293:122103.
[96] Li R, Lou Y, Xu Y, Ma G, Liao B, Shen L, et al. Effects of surface morphology on alginate adhesion : molecular insights into membrane fouling based on XDLVO and DFT analysis. Chemosphere 2019;233:373–80.
[97] Miao R, Wang L, Mi N, Gao Z, Liu T, Lv Y, et al. Enhancement and mitigation mechanisms of protein fouling of ultrafiltration membranes under different ionic strengths. Environ Sci Technol 2015;49:6574–80.
[98] Martin-Garcia I, Monsalvo V, Pidou M, Le-Clech P, Judd SJ, McAdam EJ, et al. Impact of membrane configuration on fouling in anaerobic membrane bioreactors. J Membr Sci 2011;382:41–9.
[99] Lin H, Liao BQ, Chen J, Gao W, Wang L, Wang F, et al. New insights into membrane fouling in a submerged anaerobic membrane bioreactor based on characterization of cake sludge and bulk sludge. Bioresour Technol 2011;102:2373–9.
[100] Gao WJ, Han MN, Qu X, Xu C, Liao BQ. Characteristics of wastewater and mixed liquor and their role in membrane fouling. Bioresour Technol 2013;128:207–14.
[101] Christensen ML, Niessen W, Sørensen NB, Hansen SH, Jørgensen MK, Nielsen PH. Sludge fractionation as a method to study and predict fouling in MBR systems. Separ Purif Technol 2018;194:329–37.
[102] Jeison D, van Lier JB. Thermophilic treatment of acidified and partially acidified wastewater using an anaerobic submerged MBR: factors affecting long-term operational flux. Water Res 2007;41:3868–79.
[103] Zhou Z, Tan Y, Xiao Y, Stuckey DC. Characterization and significance of sub-visible particles and colloids in a submerged anaerobic membrane bioreactor (SAnMBR). Environ Sci Technol 2016;50:12750–8.
[104] Zhou Z, Tao Y, Zhang S, Xiao Y, Meng F, Stuckey DC. Size-dependent microbial diversity of sub-visible particles in a submerged anaerobic membrane bioreactor (SAnMBR): implications for membrane fouling. Water Res 2019;20–9.
[105] Wang XM, Waite TD. Impact of gel layer formation on colloid retention in membrane filtration processes. J Membr Sci 2008;325:486–94.
[106] Watanabe R, Nie Y, Wakahara S, Komori D, Li YY. Investigation on the response of anaerobic membrane bioreactor to temperature decrease from 25 °C to 10 °C in sewage treatment. Bioresour Technol 2017;243:747–54.
[107] Gkotsis P, Banti D, Peleka E, Zouboulis A, Samaras P. Fouling issues in membrane bioreactors (MBRs) for wastewater treatment: major mechanisms, prevention and control strategies. Processes 2014;2:795–866.

[108] Chen J, Zhang M, Wang A, Lin H, Hong H, Lu X. Osmotic pressure effect on membrane fouling in a submerged anaerobic membrane bioreactor and its experimental verification. Bioresour Technol 2012;125:97–101.
[109] Zhang M, Peng W, Chen J, He Y, Ding L, Wang A, et al. A new insight into membrane fouling mechanism in submerged membrane bioreactor: osmotic pressure during cake layer filtration. Water Res 2013;47:2777–86.
[110] Teng J, Shen L, Yu G, Wang F, Li F, Zhou X, et al. Mechanism analyses of high specific filtration resistance of gel and roles of gel elasticity related with membrane fouling in a membrane bioreactor. Bioresour Technol 2018;257:39–46.
[111] Ruigómez I, Vera L, González E, Rodríguez-Sevilla J. Pilot plant study of a new rotating hollow fibre membrane module for improved performance of an anaerobic submerged MBR. J Membr Sci 2016;514:105–13.
[112] Chen L, Gu Y, Cao C, Zhang J, Ng JW, Tang C. Performance of a submerged anaerobic membrane bioreactor with forward osmosis membrane for low-strength wastewater treatment. Water Res 2014;50:114–23.
[113] Gu Y, Chen L, Ng JW, Lee C, Chang VWC, Tang CY. Development of anaerobic osmotic membrane bioreactor for low-strength wastewater treatment at mesophilic condition. J Membr Sci 2015;490:197–208.
[114] Wang X, Wang C, Tang CY, Hu T, Li X, Ren Y. Development of a novel anaerobic membrane bioreactor simultaneously integrating micro fi ltration and forward osmosis membranes for low- strength wastewater treatment. J Membr Sci 2017;527:1–7.
[115] Martinez-Sosa D, Helmreich B, Netter T, Paris S, Bischof F, Horn H. Anaerobic submerged membrane bioreactor (AnSMBR) for municipal wastewater treatment under mesophilic and psychrophilic temperature conditions. Bioresour Technol 2011;102:10377–85.
[116] Wei CH, Harb M, Amy G, Hong PY, Leiknes TO. Sustainable organic loading rate and energy recovery potential of mesophilic anaerobic membrane bioreactor for municipal wastewater treatment. Bioresour Technol 2014;166:326–34.
[117] Gouveia J, Plaza F, Garralon G, Fdz-Polanco F, Peña M. Long-term operation of a pilot scale anaerobic membrane bioreactor (AnMBR) for the treatment of municipal wastewater under psychrophilic conditions. Bioresour Technol 2015;185:225–33.
[118] Gouveia J, Plaza F, Garralon G, Fdz-Polanco F, Peña M. A novel configuration for an anaerobic submerged membrane bioreactor (AnSMBR). Long-term treatment of municipal wastewater under psychrophilic conditions. Bioresour Technol 2015;198:510–9.
[119] Prieto AL, Futselaar H, Lens PNL, Bair R, Yeh DH. Development and start up of a gas-lift anaerobic membrane bioreactor (Gl-AnMBR) for conversion of sewage to energy, water and nutrients. J Membr Sci 2013;441:158–67.
[120] Dolejs P, Ozcan O, Bair R, Ariunbaatar J, Bartacek J, Lens PNL, et al. Effect of psychrophilic temperature shocks on a gas-lift anaerobic membrane bioreactor (Gl-AnMBR) treating synthetic domestic wastewater. J Water Process Eng 2017;16:108–14.
[121] Kim J, Kim K, Ye H, Lee E, Shin C, McCarty PL, et al. Anaerobic fluidized bed membrane bioreactor for wastewater treatment. Environ Sci Technol 2011;45:576–81.
[122] Gao DW, Hu Q, Yao C, Ren NQ. Treatment of domestic wastewater by an integrated anaerobic fluidized-bed membrane bioreactor under moderate to low temperature conditions. Bioresour Technol 2014;159:193–8.
[123] Kim J, Shin J, Kim H, Lee JY, hyuk Yoon M, Won S, et al. Membrane fouling control using a rotary disk in a submerged anaerobic membrane sponge bioreactor. Bioresour Technol 2014;172:321–7.
[124] Jørgensen MK, Pedersen MT, Christensen ML, Bentzen TR. Dependence of shear and concentration on fouling in a membrane bioreactor with rotating membrane discs. AIChE J 2014;60:706–15.
[125] Ruigómez I, Vera L, González E, González G, Rodríguez-Sevilla J. A novel rotating HF membrane to control fouling on anaerobic membrane bioreactors treating wastewater. J Membr Sci 2016;501:45–52.
[126] Ruigómez I, González E, Guerra S, Rodríguez-Gómez LE, Vera L. Evaluation of a novel physical cleaning strategy based on HF membrane rotation during the backwashing/relaxation phases for anaerobic submerged MBR. J Membr Sci 2017;526:181–90.
[127] Lindmark J, Thorin E, Bel Fdhila R, Dahlquist E. Effects of mixing on the result of anaerobic digestion: review. Renew Sustain Energy Rev 2014;40:1030–47.
[128] Sauchelli M, Pellegrino G, D'Haese A, Rodríguez-Roda I, Gernjak W. Transport of trace organic compounds through novel forward osmosis membranes: role of membrane properties and the draw solution. Water Res 2018;141:65–73.
[129] Cath TY, Childress AE, Elimelech M. Forward osmosis: principles, applications, and recent developments. J Membr Sci 2006;281:70–87.
[130] Song X, Xie M, Li Y, Li G, Luo W. Salinity build-up in osmotic membrane bioreactors: causes, impacts, and potential cures. Bioresour Technol 2018;257:301–10.
[131] Gao Y, Fang Z, Chen C, Zhu X, Liang P, Qiu Y, et al. Evaluating the performance of inorganic draw solution concentrations in an anaerobic forward osmosis membrane bioreactor for real municipal sewage treatment. Bioresour Technol 2020;307:123254.
[132] Wang F, Zhang M, Peng W, He Y, Lin H, Chen J, et al. Effects of ionic strength on membrane fouling in a membrane bioreactor. Bioresour Technol 2014;156:35–41.
[133] Mo H, Tay KG, Ng HY. Fouling of reverse osmosis membrane by protein (BSA): effects of pH, calcium, magnesium, ionic strength and temperature. J Membr Sci 2008;315:28–35.
[134] Ding Y, Tian Y, Li Z, Wang H, Chen L. Microfiltration (MF) membrane fouling potential evaluation of protein with different ion strengths and divalent cations based on extended DLVO theory. Desalination 2013;331:62–8.
[135] She Q, Tang CY, Wang YN, Zhang Z. The role of hydrodynamic conditions and solution chemistry on protein fouling during ultrafiltration. Desalination 2009;249:1079–87.
[136] Chan R, Chen V. The effects of electrolyte concentration and pH on protein aggregation and deposition: critical flux and constant flux membrane filtration. J Membr Sci 2001;185:177–92.
[137] De Vrieze J, Christiaens MER, Walraedt D, Devooght A, Ijaz UZ, Boon N. Microbial community redundancy in anaerobic digestion drives process recovery after salinity exposure. Water Res 2017;111:109–17.
[138] Gagliano MC, Neu TR, Kuhlicke U, Sudmalis D, Temmink H, Plugge CM. EPS glycoconjugate profiles shift as adaptive response in anaerobic microbial granulation at high salinity. Front Microbiol 2018;9.
[139] Wu Y, Wang X, Tay MQX, Oh S, Yang L, Tang C, et al. Metagenomic insights into the influence of salinity and cytostatic drugs on the composition and functional genes of microbial community in forward osmosis anaerobic membrane bioreactors. Chem Eng J 2017;326:462–9.
[140] Ismail SB, de La Parra CJ, Temmink H, van Lier JB. Extracellular polymeric substances (EPS) in upflow anaerobic sludge blanket (UASB) reactors operated under high salinity conditions. Water Res 2010;44:1909–17.
[141] Muñoz Sierra JD, Oosterkamp MJ, Wang W, Spanjers H, van Lier JB. Impact of long-term salinity exposure in anaerobic membrane bioreactors treating phenolic wastewater: performance robustness and endured microbial community. Water Res 2018;141:172–84.
[142] Muñoz Sierra JD, Oosterkamp MJ, Wang W, Spanjers H, van Lier JB. Comparative performance of upflow anaerobic sludge blanket reactor and anaerobic membrane bioreactor treating phenolic wastewater: overcoming high salinity. Chem Eng J 2019;366:480–90.
[143] Song X, McDonald J, Price WE, Khan SJ, Hai FI, Ngo HH, et al. Effects of salinity build-up on the performance of an anaerobic membrane bioreactor regarding basic water quality parameters and removal of trace organic contaminants. Bioresour Technol 2016;216:399–405.
[144] Wang H, Wang X, Meng F, Li X, Ren Y, She Q. Effect of driving force on the performance of anaerobic osmotic membrane bioreactors: new insight into enhancing water flux of FO membrane via controlling driving force in a two-stage pattern. J Membr Sci 2019;569:41–7.
[145] Wang KM, Soares A, Jefferson B, Wang HY, Zhang LJ, Jiang SF, et al. Establishing the mechanisms underpinning solids breakthrough in UASB configured anaerobic membrane bioreactors to mitigate fouling. Water Res 2020;176:115754.
[146] van Voorthuizen E, Zwijnenburg A, van der Meer W, Temmink H. Biological black water treatment combined with membrane separation. Water Res 2008;42:4334–40.
[147] Chang HM, Sun YC, Chien IC, Chang WS, Ray SS, Cao DTN, et al. Innovative upflow anaerobic sludge osmotic membrane bioreactor for wastewater treatment. Bioresour Technol 2019;287:121466.
[148] Le-Clech P, Jefferson B, Judd SJ. A comparison of submerged and sidestream tubular membrane bioreactor configurations. Desalination 2005;173:113–22.
[149] Aslam M, Charfi A, Lesage G, Heran M, Kim J. Membrane bioreactors for wastewater treatment: a review of mechanical cleaning by scouring agents to control membrane fouling. Chem Eng J 2017;307:897–913.
[150] Yoo R, Kim J, McCarty PL, Bae J. Anaerobic treatment of municipal wastewater with a staged anaerobic fluidized membrane bioreactor (SAF-MBR) system. Bioresour Technol 2012;120:133–9.
[151] Bae J, Shin C, Lee E, Kim J, McCarty PL. Anaerobic treatment of low-strength wastewater: a comparison between single and staged anaerobic fluidized bed membrane bioreactors. Bioresour Technol 2014;165:75–80.
[152] Wu B, Li Y, Lim W, Lee SL, Guo Q, Fane AG, et al. Single-stage versus two-stage anaerobic fluidized bed bioreactors in treating municipal wastewater: performance, foulant characteristics, and microbial community. Chemosphere 2017;171:158–67.
[153] Hu AY, Stuckey DC. Activated carbon addition to a submerged anaerobic membrane bioreactor: effect on performance, transmembrane pressure, and flux. J Environ Eng 2007;133:73–80.
[154] Yang S, Zhang Q, Lei Z, Wen W, Huang X, Chen R. Comparing powdered and granular activated carbon addition on membrane fouling control through evaluating the impacts on mixed liquor and cake layer properties in anaerobic membrane bioreactors. Bioresour Technol 2019;294:122137.
[155] Charfi A, Park E, Aslam M, Kim J. Particle-sparged anaerobic membrane bioreactor with fluidized polyethylene terephthalate beads for domestic wastewater treatment: modelling approach and fouling control. Bioresour Technol 2018;258:263–9.
[156] Aslam M, Charfi A, Kim J. Membrane scouring to control fouling under fluidization of non-adsorbing media for wastewater treatment. Environ Sci Pollut Res 2019;26:1061–71.
[157] Aslam M, McCarty PL, Bae J, Kim J. The effect of fluidized media characteristics on membrane fouling and energy consumption in anaerobic fluidized membrane bioreactors. Separ Purif Technol 2014;132:10–5.
[158] Kim M, Lam TYC, Tan GYA, Lee PH, Kim J. Use of polymeric scouring agent as fluidized media in anaerobic fluidized bed membrane bioreactor for wastewater treatment: system performance and microbial community. J Membr Sci 2020;606:118121.
[159] Shin C, Kim K, McCarty PL, Kim J, Bae J. Integrity of hollow-fiber membranes in a pilot-scale anaerobic fluidized membrane bioreactor (AFMBR) after two-years of operation. Separ Purif Technol 2016;162:101–5.
[160] Shin C, Kim K, McCarty PL, Kim J, Bae J. Development and application of a procedure for evaluating the long-term integrity of membranes for the anaerobic fluidized membrane bioreactor (AFMBR). Water Sci Technol 2016;74:457–65.

[161] Charfi A, Aslam M, Lesage G, Heran M, Kim J. Macroscopic approach to develop fouling model under GAC fluidization in anaerobic fluidized bed membrane bioreactor. J Ind Eng Chem 2017;49:219–29.
[162] Jeong Y, Cho K, Kwon EE, Tsang YF, Rinklebe J, Park C. Evaluating the feasibility of pyrophyllite-based ceramic membranes for treating domestic wastewater in anaerobic ceramic membrane bioreactors. Chem Eng J 2017;328:567–73.
[163] Aslam M, McCarty PL, Shin C, Bae J, Kim J. Low energy single-staged anaerobic fluidized bed ceramic membrane bioreactor (AFCMBR) for wastewater treatment. Bioresour Technol 2017;240:33–41.
[164] Aslam M, Yang P, Lee PH, Kim J. Novel staged anaerobic fluidized bed ceramic membrane bioreactor: energy reduction, fouling control and microbial characterization. J Membr Sci 2018;553:200–8.
[165] Martin Garcia I, Mokosch M, Soares A, Pidou M, Jefferson B. Impact on reactor configuration on the performance of anaerobic MBRs: treatment of settled sewage in temperate climates. Water Res 2013;47:4853–60.
[166] Chu LB, Yang FL, Zhang XW. Anaerobic treatment of domestic wastewater in a membrane-coupled expended granular sludge bed (EGSB) reactor under moderate to low temperature. Process Biochem 2005;40:1063–70.
[167] McKeown RM, Hughes D, Collins G, Mahony T, O'Flaherty V. Low-temperature anaerobic digestion for wastewater treatment. Curr Opin Biotechnol 2012;23:444–51.
[168] Appels L, Baeyens J, Degrève J, Dewil R. Principles and potential of the anaerobic digestion of waste-activated sludge. Prog Energy Combust Sci 2008;34:755–81.
[169] Lettinga G, Rebac S, Zeeman G. Challenge of psychrophilic anaerobic wastewater treatment. Trends Biotechnol 2001;19:363–70.
[170] Dev S, Saha S, Kurade MB, Salama E. Perspective on anaerobic digestion for biomethanation in cold environments. Renew Sustain Energy Rev 2019;103:85–95.
[171] Morris BEL, Henneberger R, Huber H, Moissl-Eichinger C. Microbial syntrophy: interaction for the common good. FEMS Microbiol Rev 2013;37:384–406.
[172] Finke N, Jørgensen BB. Response of fermentation and sulfate reduction to experimental temperature changes in temperate and Arctic marine sediments. ISME J 2008;2:815–29.
[173] Ferry JG. Fundamentals of methanogenic pathways that are key to the biomethanation of complex biomass. Curr Opin Biotechnol 2011;22:351–7.
[174] Smith AL, Skerlos SJ, Raskin L. Anaerobic membrane bioreactor treatment of domestic wastewater at psychrophilic temperatures ranging from 15 °C to 3 °C. Environ Sci Water Res Technol 2015;1:56–64.
[175] Robles A, Ruano MV, Ribes J, Ferrer J. Performance of industrial scale hollow-fibre membranes in a submerged anaerobic MBR (HF-SAnMBR) system at mesophilic and psychrophilic conditions. Separ Purif Technol 2013;104:290–6.
[176] Giménez JB, Martí N, Ferrer J, Seco A. Methane recovery efficiency in a submerged anaerobic membrane bioreactor (SAnMBR) treating sulphate-rich urban wastewater: evaluation of methane losses with the effluent. Bioresour Technol 2012;118:67–72.
[177] Cookney J, Cartmell E, Jefferson B, McAdam EJ. Recovery of methane from anaerobic process effluent using poly-di-methyl-siloxane membrane contactors. Water Sci Technol 2012;65:604–10.
[178] Cashman S, Ma X, Mosley J, Garland J, Crone B, Xue X. Energy and greenhouse gas life cycle assessment and cost analysis of aerobic and anaerobic membrane bioreactor systems: influence of scale, population density, climate, and methane recovery. Bioresour Technol 2018;254:56–66.
[179] Crone BC, Sorial GA, Pressman JG, Ryu H, Keely SP, Brinkman N, et al. Design and evaluation of degassed anaerobic membrane biofilm reactors for improved methane recovery. Bioresour Technol Rep 2020;10:100407.
[180] Mai DT, Kunacheva C, Stuckey DC. A review of posttreatment technologies for anaerobic effluents for discharge and recycling of wastewater. Crit Rev Environ Sci Technol 2018;48:167–209.
[181] Crone BC, Garland JL, Sorial GA, Vane LM. Significance of dissolved methane in effluents of anaerobically treated low strength wastewater and potential for recovery as. Water Res 2016;104:520–31.
[182] Velasco P, Jegatheesan V, Othman M. Recovery of dissolved methane from anaerobic membrane bioreactor using degassing membrane contactors. Front Environ Sci 2018;6:1–6. https://doi.org/10.3389/fenvs.2018.00151.
[183] Rongwong W, Goh K, Bae T-H. Energy analysis and optimization of hollow fiber membrane contactors for recovery of dissolve methane from anaerobic membrane bioreactor effluent. J Membr Sci 2018;554:184–94.
[184] Cookney J, Mcleod A, Mathioudakis V, Ncube P, Soares A, Jefferson B, et al. Dissolved methane recovery from anaerobic effluents using hollow fibre membrane contactors. J Membr Sci 2016;502:141–50.
[185] Bandara WM, Satoh H, Sasakawa M, Nakahara Y, Takahashi M, Okabe S. Removal of residual dissolved methane gas in an upflow anaerobic sludge blanket reactor treating low-strength wastewater at low temperature with degassing membrane. Water Res 2011;45:3533–40.
[186] Sanchis-Perucho P, Robles Á, Durán F, Ferrer J, Seco A. PDMS membranes for feasible recovery of dissolved methane from AnMBR effluents. J Membr Sci 2020;604:118070.
[187] Seco A, Mateo O, Zamorano-López N, Sanchis-Perucho P, Serralta J, Martí N, et al. Exploring the limits of anaerobic biodegradability of urban wastewater by AnMBR technology. Environ Sci Water Res Technol 2018;4:1877–87.
[188] Pretel R, Robles A, Ruano MV, Seco A, Ferrer J. Economic and environmental sustainability of submerged anaerobic MBR-based (AnMBR-based) technology as compared to aerobic-based technologies for moderate-/high-loaded urban wastewater treatment. J Environ Manag 2016;166:45–54.
[189] Pelaz L, Gómez A, Garralón G, Letona A, Fdz-Polanco M. Denitrification of the anaerobic membrane bioreactor (AnMBR) effluent with alternative electron donors in domestic wastewater treatment. Bioresour Technol 2017;243:1173–9.
[190] Alvarino T, Allegue T, Fernandez-Gonzalez N, Suarez S, Lema JM, Garrido JM, et al. Minimization of dissolved methane, nitrogen and organic micropollutants emissions of effluents from a methanogenic reactor by using a preanoxic MBR post-treatment system. Sci Total Environ 2019;671:165–74.
[191] Song X, Luo W, McDonald J, Khan SJ, Hai FI, Guo W, et al. Effects of sulphur on the performance of an anaerobic membrane bioreactor: biological stability, trace organic contaminant removal, and membrane fouling. Bioresour Technol 2018;250:171–7.
[192] Sahinkaya E, Yurtsever A, Isler E, Coban I, Aktaş Ö. Sulfate reduction and filtration performances of an anaerobic membrane bioreactor (AnMBR). Chem Eng J 2018;349:47–55.
[193] Madden P, Al-Raei AM, Enright AM, Chinalia FA, de Beer D, O'Flaherty V, et al. Effect of sulfate on low-temperature anaerobic digestion. Front Microbiol 2014;5.
[194] Chen Y, Cheng JJ, Creamer KS. Inhibition of anaerobic digestion process: a review. Bioresour Technol 2008;99:4044–64.
[195] Abatzoglou N, Boivin S. A review of biogas purification processes. Biofuels, Bioprod Biorefining 2009;3:42–71.
[196] Henze M, van Loosdrecht MCM, Ekama GA, Brdjanovic D. Biological wastewater treatment : principles, modelling and design. London: IWA Pub; 2008.
[197] Silva AFR, Ricci BC, Koch K, Weißbach M, Amaral MCS. Dissolved hydrogen sulfide removal from anaerobic bioreactor permeate by modified direct contact membrane distillation. Separ Purif Technol 2020;233:116036.
[198] Pikaar I, Likosova EM, Freguia S, Keller J, Rabaey K, Yuan Z. Electrochemical abatement of hydrogen sulfide from waste streams. Crit Rev Environ Sci Technol 2015;45:1555–78.
[199] Siles JA, Brekelmans J, Martín MA, Chica AF, Martín A. Impact of ammonia and sulphate concentration on thermophilic anaerobic digestion. Bioresour Technol 2010;101:9040–8.
[200] Ferrer J, Pretel R, Durán F, Giménez JB, Robles A, Ruano MV, et al. Design methodology for submerged anaerobic membrane bioreactors (AnMBR): a case study. Separ Purif Technol 2015;141:378–86.
[201] Pretel R, Robles A, Ruano MV, Seco A, Ferrer J. Environmental impact of submerged anaerobic MBR (SAnMBR) technology used to treat urban wastewater at different temperatures. Bioresour Technol 2013;149:532–40.
[202] Lutchmiah K, Cornelissen ER, Harmsen DJH, Post JW, Lampi K, Ramaekers H, et al. Water recovery from sewage using forward osmosis. Water Sci Technol 2011;64:1443–9.
[203] Valladares Linares R, Li Z, Sarp S, Bucs SS, Amy G, Vrouwenvelder JS. Forward osmosis niches in seawater desalination and wastewater reuse. Water Res 2014;66:122–39.
[204] Cath TY, Hancock NT, Lundin CD, Hoppe-Jones C, Drewes JE. A multi-barrier osmotic dilution process for simultaneous desalination and purification of impaired water. J Membr Sci 2010;362:417–26.
[205] Ansari AJ, Hai FI, Price WE, Drewes JE, Nghiem LD. Forward osmosis as a platform for resource recovery from municipal wastewater - a critical assessment of the literature. J Membr Sci 2017;529:195–206.
[206] Wang Z, Zheng J, Tang J, Wang X, Wu Z. A pilot-scale forward osmosis membrane system for concentrating low-strength municipal wastewater: performance and implications. Sci Rep 2016;6:1–12.
[207] Xue W, Tobino T, Nakajima F, Yamamoto K. Seawater-driven forward osmosis for enriching nitrogen and phosphorous in treated municipal wastewater: effect of membrane properties and feed solution chemistry. Water Res 2015;69:120–30.
[208] Lutchmiah K, Verliefde ARD, Roest K, Rietveld LC, Cornelissen ER. Forward osmosis for application in wastewater treatment: a review. Water Res 2014;58:179–97.
[209] Blandin G, Verliefde ARD, Comas J, Rodriguez-Roda I, Le-Clech P. Efficiently combining water reuse and desalination through forward osmosis-reverse osmosis (FO-RO) hybrids: a critical review. Membranes 2016;6:37.
[210] Shaffer DL, Werber JR, Jaramillo H, Lin S, Elimelech M. Forward osmosis: where are we now? Desalination 2015;356:271–84.
[211] Awad AM, Jalab R, Minier-Matar J, Adham S, Nasser MS, Judd SJ. The status of forward osmosis technology implementation. Desalination 2019;461:10–21.
[212] Achilli A, Cath TY, Childress AE. Power generation with pressure retarded osmosis: an experimental and theoretical investigation. J Membr Sci 2009;343:42–52.
[213] Coday BD, Heil DM, Xu P, Cath TY. Effects of transmembrane hydraulic pressure on performance of forward osmosis membranes. Environ Sci Technol 2013;47:2386–93.
[214] Itliong JN, Villagracia ARC, Moreno JLV, Rojas KIM, Bernardo GPO, David MY, et al. Investigation of reverse ionic diffusion in forward-osmosis-aided dewatering of microalgae: a molecular dynamics study. Bioresour Technol 2019;279:181–8.
[215] Lee DJ, Hsieh MH. Forward osmosis membrane processes for wastewater bioremediation: research needs. Bioresour Technol 2019;290:121795.
[216] Alburquerque JA, de la Fuente C, Ferrer-Costa A, Carrasco L, Cegarra J, Abad M, et al. Assessment of the fertiliser potential of digestates from farm and agroindustrial residues. Biomass Bioenergy 2012;40:181–9.
[217] Alburquerque JA, de la Fuente C, Bernal MP. Chemical properties of anaerobic digestates affecting C and N dynamics in amended soils. Agric Ecosyst Environ 2012;160:15–22.

[218] Ansari AJ, Hai FI, Guo W, Ngo HH, Price WE, Nghiem LD. Selection of forward osmosis draw solutes for subsequent integration with anaerobic treatment to facilitate resource recovery from wastewater. Bioresour Technol 2015;191:30–6.

[219] Feijoo G, Soto M, Méndez R, Lema JM. Sodium inhibition in the anaerobic digestion process: antagonism and adaptation phenomena. Enzym Microb Technol 1995;17:180–8.

[220] Astals S, Batstone DJ, Tait S, Jensen PD. Development and validation of a rapid test for anaerobic inhibition and toxicity. Water Res 2015;81:208–15.

CHAPTER 2:

Forward osmosis pre-concentration before anaerobic membrane bioreactor

2.1 Introduction

Forward osmosis is an emerging technology for the concentration of liquid streams [24]. Municipal sewage pre-concentration is an opportunity to overcome the low sewage organic matter concentration, which is one of the main challenges of mainstream AnMBR application (see Publication I). However, few studies have evaluated the combination of FO and AnMBR technologies for municipal sewage treatment. In this chapter, the key experimental and techno-economic aspects of combining FO and AnMBR are evaluated in Publications II, III and IV.

Publication II evaluates the performance of a continuous lab-scale AnMBR operated at pre-concentration factors of 1, 2, 5 and 10. The lab-scale AnMBR was configured as a continuous stirred tank reactor (CSTR) coupled to a sidestream ultrafiltration membrane module. Figure 2.1 shows the AnMBR set-up used for this study, which was operated at the University of Barcelona. The organic matter and sodium concentrations of the synthetic feed were progressively increased to simulate the different pre-concentration factors and to incorporate the effect of FO reverse solute flux (RSF) on sewage sodium concentration. Finally, an energy-economic study was carried out to evaluate the effect of methane production on the energy and economic balances of an FO+AnMBR system.

Figure 2.1. Lab-scale AnMBR set-up used in Publication II.

Publication III analyses the techno-economic implications of combining FO and AnMBR technologies. RO was considered to regenerate the diluted draw solution while generating fresh water. This modelling study incorporated three FO recovery strategies (50, 80 and 90%) and three different draw solution management strategies. The study also explored the possibility to retrofit a seawater RO plant into a hybrid FO-RO system using wastewater as feed solution for subsequent treatment in the AnMBR.

Publication IV analyses the impact of FO membrane material and draw solute on process economics of an FO+AnMBR system. Specifically, this modelling study evaluated one organic draw solute (CH_3COONa) and seven inorganic draw solutes (NaCl, KCl, $CaCl_2$, $MgCl_2$, $MgSO_4$, Na_2SO_4, $Ca(NO_3)_2$) for cellulose triacetate (CTA) and thin film composite (TFC) FO membranes. The study also modelled the effect of draw solute and FO membrane material on AnMBR effluent quality and anaerobic digestion performance.

Publications II, III and IV included in Chapter 2 covered the following research gaps:

- The impact of forward osmosis pre-concentration on anaerobic digestion performance has been mainly evaluated by means of batch tests [25–27], but limited information is available in the literature concerning the anaerobic digestion of pre-concentrated sewage under continuous conditions [28]. Ferrari et al. [28] evaluated the impact of temperature on the performance of an AnMBR treating four-fold synthetic pre-concentrated sewage. However, the study evaluated one pre-concentration condition and did not include the effect of FO reverse solute flux (RSF) on AnMBR performance. Evaluating the effect of FO pre-concentration factor and RSF on

AnMBR performance is important to understand the technical feasibility of combining FO and AnMBR technologies for municipal sewage treatment (***Publication II***).

- Several studies have evaluated the techno-economic prospect of combining FO and draw solution regeneration technologies for water production [29–31]. However, the use of FO to pre-concentrate municipal sewage before an AnMBR has not been evaluated yet from an economic point of view. Analysing the economic implications of combining both technologies is needed to understand the potential of this configuration for municipal sewage treatment with energy and water production ***(Publication III***).

- Limited information is available in the literature concerning the effect of draw solute on the economic balance of combining FO and anaerobic digestion processes. Bacaksiz et al. [27] evaluated the impact of different draw solutes on the performance of a CTA FO membrane, as well as the potential inhibitory effects of these draw solutes on the anaerobic digestion process. Bacaksiz et al. [27] also conducted an economic analysis to evaluate the chemical purchase cost of each draw solute. However, this study did not include all the costs impacted by the draw solute and FO membrane material. Therefore, a more detailed techno-economic analysis is necessary to evaluate the impact of draw solute and FO membrane material on the economic balance of combining FO and AnMBR technologies (***Publication IV***).

2.2 Publication II: *Anaerobic membrane bioreactor performance at different wastewater pre-concentration factors: An experimental and economic study*

Vinardell, S., Astals, S., Jaramillo, M., Mata-Alvarez, J., Dosta, J. (2021). Anaerobic membrane bioreactor performance at different wastewater pre-concentration factors: An experimental and economic study. Sci. Total Environ. 750, 141625. https://doi.org/10.1016/j.scitotenv.2020.141625

Science of the Total Environment 750 (2021) 141625

Contents lists available at ScienceDirect

Science of the Total Environment

journal homepage: www.elsevier.com/locate/scitotenv

Anaerobic membrane bioreactor performance at different wastewater pre-concentration factors: An experimental and economic study

Sergi Vinardell [a,*], Sergi Astals [a], Marta Jaramillo [a], Joan Mata-Alvarez [a,b], Joan Dosta [a,b]

[a] Department of Chemical Engineering and Analytical Chemistry, University of Barcelona, C/Martí i Franquès 1, 6th floor, 08028 Barcelona, Spain
[b] Water Research Institute, University of Barcelona, 08001 Barcelona, Spain

HIGHLIGHTS

- AnMBR performance was analysed at 1, 2, 5 and 10 sewage pre-concentration factors.
- The AnMBR was satisfactorily operated with an average COD removal of 94 ± 5%.
- CH_4 yields increased from 214 to 322 $mLCH_4\ g^{-1}$ COD with the pre-concentration factor.
- Membrane biofilm contributed to COD removal, especially at the highest salinity.
- A positive net present value could be achieved at a pre-concentration factor of 10.

GRAPHICAL ABSTRACT

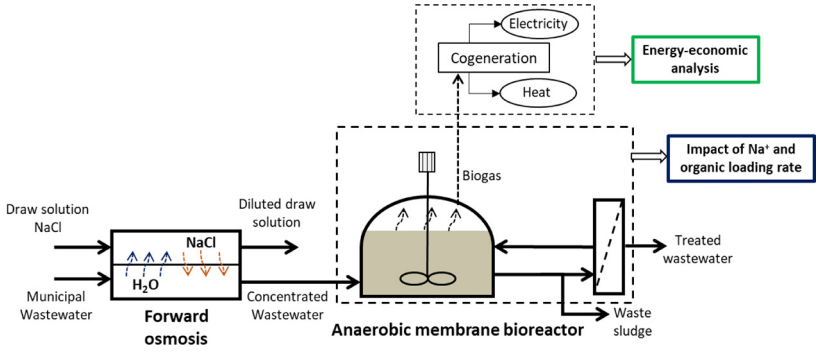

ARTICLE INFO

Article history:
Received 7 July 2020
Received in revised form 4 August 2020
Accepted 9 August 2020
Available online 15 August 2020

Editor: Huu Hao Ngo

Keywords:
Anaerobic digestion
Anaerobic membrane bioreactor (AnMBR)
Forward osmosis (FO)
Water resource recovery facility (WRRF)
Municipal sewage treatment
Sodium inhibition

ABSTRACT

This research evaluated the performance of a lab-scale anaerobic membrane bioreactor (AnMBR) treating municipal sewage pre-concentrated by forward osmosis (FO). The organic loading rate (OLR) and sodium concentrations of the synthetic sewage stepwise increased from 0.3 to 2.0 g COD $L^{-1}\ d^{-1}$ and from 0.28 to 2.30 g $Na^{+}\ L^{-1}$ to simulate pre-concentration factors of 1, 2, 5 and 10. No major operational problems were observed during AnMBR operation, with COD removal efficiencies ranging between 90 and 96%. The methane yield progressively increased from 214 ± 79 to 322 ± 60 mL $CH_4\ g^{-1}$ COD as the pre-concentration factor increased from 1 to 10. This was mainly attributed to the lower fraction of methane dissolved lost in the permeate at higher OLRs. Interestingly, at the highest pre-concentration factor (2.30 g $Na^{+}\ L^{-1}$) the difference between the permeate and the digester soluble COD indicated that membrane biofilm also played a role in COD removal. Finally, a preliminary energy and economic analysis showed that, at a pre-concentration factor of 10, the AnMBR temperature could be increased 10 °C and achieve a positive net present value (NPV) of 4 M€ for a newly constructed AnMBR treating 10,000 $m^3\ d^{-1}$ of pre-concentrated sewage with an AnMBR lifetime of 20 years.

1. Introduction

Economic and environmental requirements are pushing a paradigm shift in municipal wastewater management. Wastewater is progressively being conceived as a source of resources rather than as a source of pollutants (Garrido-Baserba et al., 2018; Guest et al., 2009). Consequently, new technologies are being developed to maximise resource recovery from wastewater with the aim of converting wastewater treatment plants (WWTPs) into resource recovery facilities (RRF) (Puyol et al., 2017).

Anaerobic membrane bioreactor (AnMBR) technology is an emerging mainstream technology for municipal sewage treatment, which allows producing renewable energy in the form of methane and obtaining high-quality effluents free of suspended solids and pathogens

* Corresponding author.
E-mail address: svinardell@ub.edu (S. Vinardell).

https://doi.org/10.1016/j.scitotenv.2020.141625
0048-9697/

(Maaz et al., 2019). Additionally, the membrane separation process provides an excellent decoupling of the solids retention time (SRT) from the hydraulic retention time (HRT), which enables an excellent control on the active biomass in the digester (Robles et al., 2018). The complete biomass retention provided by the membrane is a distinctive feature of AnMBRs over other high-rate anaerobic technologies such as upflow anaerobic sludge blanket (UASB) and expanded granular sludge bed (EGSB) reactors (Ozgun et al., 2015a). Moreover, effluents free of suspended solids and with low residual organic matter facilitate the application of post-treatment technologies to remove dissolved methane and nutrients (Batstone et al., 2015).

AnMBR technology has experienced significant advances towards its implementation as mainstream treatment (Zhen et al., 2019). Many pilot-scale AnMBR plants for municipal sewage treatment have been operated with COD removal efficiencies above 85% and variable methane yields (0.07–0.31 mL CH_4 g^{-1} COD) as reviewed by Shin and Bae (2018). However, some challenges need to be tackled to make AnMBR technology a reality. High volumetric flow rate is a critical challenge for mainstream AnMBR application since (i) it increases AnMBR capital and operating expenditures, (ii) it makes unviable to heat the influent, and (iii) it increases fugitive methane emissions (Ferrari et al., 2019a; Vinardell et al., 2020a; Wei et al., 2014). Sewage pre-concentration could overcome these limitations and improve the applicability of AnMBR as mainstream technology (Ozgun et al., 2013; Vinardell et al., 2020b).

Different membrane technologies have been tested for municipal sewage pre-concentration such as forward osmosis (FO), dynamic membrane filtration and direct membrane filtration (Guven et al., 2019; Nascimento et al., 2020). Among them, FO allows concentrating sewage with a high rejection of organic matter, a low energy input and a low fouling potential (Ansari et al., 2017; Hube et al., 2020). FO is a spontaneous process where water permeation is driven by the osmotic difference between the sewage and the draw solution. Therefore, water permeates from the higher chemical potential solution (sewage) to the lower chemical potential solution (draw solution) (Cath et al., 2006).

FO pre-concentration provides four conceivable advantages for AnMBR: (i) it reduces the AnMBR volume, (ii) it increases the methane energy recovered per m^3 of sewage, (iii) it minimises the losses of methane dissolved in the permeate, and (iv) it reduces the volume of post-treatment units required to remove or recover dissolved methane and nutrients. Additionally, the diluted draw solution can be re-generated by reverse osmosis whilst producing reclaimed water (Blandin et al., 2016; Lee and Hsieh, 2019). However, the integration of FO and AnMBR technologies for municipal sewage treatment also presents some challenges such as (i) the low water fluxes of FO membranes, (ii) the presence of suspended solids in municipal sewage which may lead to FO membrane fouling, (iii) the high energy required to regenerate the draw solution, and (iv) the high salinity in the AnMBR influent after FO pre-concentration (Ferrari et al., 2019b; Ozgun et al., 2013; Vinardell et al., 2020b).

The selection of the draw solute is critical for FO technology since it affects the salinity of the AnMBR influent. Sodium chloride (NaCl) is a widely used draw solute in both natural (seawater) and synthetic draw solutions (Awad et al., 2019; Coday et al., 2013). NaCl has been reported as a suitable solute to achieve high FO fluxes since its high diffusivity allows reducing the impact that dilutive internal concentration polarization (ICP) on the support layer has over FO fluxes (Ansari et al., 2015; Shaffer et al., 2015). However, the high diffusivity of NaCl is also counterproductive for the operability of an FO + AnMBR process. The reverse solute flux (RSF) of NaCl from the draw solution to the sewage through the FO membrane is a drawback of using a NaCl solution as draw solution since it increases the salinity of the AnMBR influent (Corzo et al., 2017; Itliong et al., 2019).

Sodium is a well-known inhibitor of the anaerobic digestion process since high sodium concentrations disintegrate cellular material by generating an osmotic pressure difference between both sides of the membrane cell (Muñoz Sierra et al., 2018, 2019). Inhibitory sodium concentrations have been reported to start at 2–3 g Na^+ L^{-1} (Astals et al., 2015; Feijoo et al., 1995), despite strong inhibition typically occurring at sodium concentrations above 8 g Na^+ L^{-1} (Chen et al., 2008; McCarty, 1964). The potential of sodium to inhibit anaerobic biomass varies depending on several factors such as substrate load, environmental conditions, microbial community or biomass acclimation (Astals et al., 2015). However, the impact of sodium inhibition appears more important during the acclimation of the anaerobic biomass to high and moderate inhibitory concentrations (Chen et al., 2008). Chen et al. (2003) reported that, after biomass acclimation, the sodium concentration that causes total inhibition of methane production increased from 12.7 to 22.8 g Na^+ L^{-1}. Accordingly, biomass acclimation stands as a critical process to develop a microbial community able to work under high sodium concentrations and prevent digester failure during the AnMBR start-up and long-term operation (Appels et al., 2008; Basset et al., 2016).

Several publications have evaluated the effect that progressive salinity increases have on AnMBR performance (Chen et al., 2019; Muñoz Sierra et al., 2018; Song et al., 2016). To the best of our knowledge, only Ferrari et al. (2019a) have evaluated the performance of an AnMBR treating sewage pre-concentrated by FO (four-fold sewage pre-concentration, 1.72 g COD L^{-1}) in a study devoted to assessing the effects of temperature variations on AnMBR performance. However, Ferrari et al. (2019a) did not consider the salinity increase in sewage due to RSF in the FO membrane. The effect of RSF is important since higher influent sodium concentrations can compromise the long-term performance of an AnMBR treating sewage pre-concentrated by FO. Accordingly, evaluating the combined increase in OLR and salinity is needed to better understand the implications of combining FO and AnMBR technologies for municipal sewage treatment.

The present article investigates the performance of an AnMBR treating pre-concentrated municipal sewage by FO. To this end, different pre-concentration factors were applied to evaluate the effects and operational implications that the progressive increase in organic matter and sodium concentrations have on the AnMBR performance. Finally, an energy-economic analysis was conducted to evaluate the opportunities that methane production offers at different FO pre-concentration scenarios.

2. Materials and methods

2.1. Feedstock composition

Synthetic municipal sewage was used as feedstock for the AnMBR. Synthetic sewage was used due to the difficulty to consistently obtain the amount of concentrated sewage needed to feed the AnMBR unit. The composition of synthetic sewage was adapted from Huang et al. (2011): $C_6H_{12}O_6$ = 407 mg L^{-1}, CH_3COONa = 229 mg L^{-1}, NH_4Cl = 95 mg L^{-1}, K_2HPO_4 = 28 mg L^{-1}, $NaHCO_3$ = 600 mg L^{-1}, $MgCl_2 \cdot 4H_2O$ = 4.12 mg L^{-1}, $CaCl_2 \cdot 2H_2O$ = 19.34 mg L^{-1}, $FeCl_3 \cdot 6H_2O$ = 22.5 mg L^{-1}, $MnCl_2 \cdot 4H_2O$ = 0.14 mg L^{-1}, $Na_2MoO_4 \cdot 2H_2O$ = 1.45 mg L^{-1}, $ZnSO_4 \cdot 7H_2O$ = 0.002 mg L^{-1}, H_3BO_3 = 0.002 mg L^{-1}, KI = 0.002 mg L^{-1}. The feedstock was prepared three times a week to minimise organic matter degradation in the feed tank.

Sewage composition was adjusted to simulate four different pre-concentration scenarios based on the pre-concentration factor. The pre-concentration factor is determined by the FO recovery, which can be defined as the percentage of water that permeates the FO membrane. This parameter is particularly relevant for the integration of FO and AnMBR technologies since organic and salinity concentrations increase as FO recovery increases. The increase of salinity in sewage is caused by (i) the reduction in the sewage volumetric flow rate and (ii) the RSF of draw solute through FO membrane. The final sodium concentration in synthetic sewage due to RSF was estimated using Eq. (1) (Ansari et al., 2015):

$$C_f = \frac{1}{J_W/J_s} \cdot \frac{FO_{recovery}}{100-FO_{recovery}} \quad (1)$$

where J_w is the FO water flux (L m^{-2} h^{-1}), J_S is the RSF (g m^{-2} h^{-1}), C_f is the draw solute concentration in the influent sewage (g L^{-1}), and $FO_{recovery}$ is the water recovery in the FO membrane (%).

2.2. AnMBR set-up and operation

The AnMBR set-up consisted of a jacked completely stirred tank reactor (CSTR) of 5.5 L connected to an external membrane module. The membrane module was a flat sheet polyvinylidene difluoride (PVDF) ultrafiltration module (Rayflow Module, Orelis Environment, France) with a membrane area of 0.02 m^2 and a pore size of 0.05 μm. The membrane system was kept at a constant transmembrane pressure (TMP) of approximately 0.1 bar. The membrane was physically and chemically cleaned (see Fig. 2 for further information about cleaning periodicity). The physical cleaning consisted in manually flushing the membrane with distilled water. The chemical cleaning consisted in submerging the membrane into a solution of sodium hypochlorite (0.3% of chlorine) for 2 hours.

The configuration used to feed the AnMBR was similar to the one described in Basset et al. (2016) and consisted of a 500 mL cylinder vessel kept at constant volume and connected to the digester (Fig. S1, supplementary material). This configuration (based on communicating vessels) allows keeping the digester volume constant despite oscillations in membrane flux. The digester was kept at 35 °C by recirculating water from a heated water bath (HUBER 118A-E) through the digester external jacket. The digester was stirred at 80 rpm using an overhead paddle stirrer. The headspace of the AnMBR was connected to a sodium hydroxide solution trap to absorb the CO_2 from biogas. A phenolphthalein indicator was added to ensure that the sodium hydroxide solution was not neutralised. A Ritter MGC-1 gas counter was used to measure the produced volume of methane. All the methane yields reported in this publication refer to the fed COD. The AnMBR was operated at an HRT of 3.1 ± 0.8 d while the SRT was not controlled since biomass was only purged during the sampling events.

The digested sewage sludge used to inoculate the AnMBR was collected from a mesophilic anaerobic digester in a municipal WWTP, which treats a mixed sewage sludge at a solid concentration of 10 g TS L^{-1} and a pH of 7.2. The full-scale WWTP has a treatment capacity of approximately 400,000 population equivalent (Barcelona Metropolitan Area, Spain). The AnMBR was inoculated with a 1:3 dilution of the digested sewage sludge with deionised water to achieve an initial suspended solids concentration of about 3 g L^{-1}. Inoculum dilution aimed to reduce membrane fouling and cleaning events during the AnMBR start-up.

The COD and the sodium concentration of the AnMBR influent varied according to the sewage flow rate reduction and the RSF. Specifically, sewage COD and sodium concentrations were progressively increased to simulate the different pre-concentration factors: (i) without pre-concentration (Period 1), (ii) pre-concentration factor of 2 (Period 2, 50% FO recovery), (iii) pre-concentration factor of 5 (Period 3, 80% FO recovery) and (iv) pre-concentration factor of 10 (Period 4, 90% FO recovery) (see Table 1). The progressive increase in COD and sodium concentrations aimed to favour the acclimation of the anaerobic biomass to harsher conditions (Basset et al., 2016). Each period was operated for a minimum of 5-HRT equivalents.

2.3. Analytical methods

Chemical oxygen demand (COD), total suspended solids (TSS) and volatile suspended solids (VSS) analysis were performed following the Standard Methods 5220C, 2540D and 2540G, respectively (APHA, 2017). Total ammonium nitrogen (TAN) was analysed using a Thermo Fisher Scientific ammonium ion-selective electrode (Orion 9512HPBNWP), following the Standard Methods procedure 4500-NH3D. The pH was analysed with a Crison pH electrode (pH series 52-04). Volatile fatty acids (VFA, i.e. acetic, propionic, i-butyric, n-butyric, i-valeric, n-valeric, i-caproic, n-caproic, heptanoic acid) were analysed using a gas chromatograph (Shimadzu GC-2010 Plus) equipped with a Nukol™ column (15 m × 0.53 mm) and a flame ionisation detector (see Astals et al. (2012) for gas chromatograph configuration and procedure).

2.4. Energy-economic analysis

The energy-economic analysis of the AnMBR process under different FO pre-concentration scenarios was done to evaluate the opportunities that methane production offers to the AnMBR technology. Specifically, the energy-economic analysis evaluated: (i) the sewage temperature increment that could be achieved for each pre-concentration factor and (ii) the impact of sewage pre-concentration on the AnMBR economic balance. Four different scenarios were included in the analysis (i.e. pre-concentration factor of 1, 2, 5 and 10). Energy production was calculated with the average experimental methane yields obtained from each period. It was considered that methane dissolved in the permeate was not recovered.

Two alternatives were considered for on-site energy valorisation: (i) thermal energy valorisation (without methane cogeneration) and (ii) thermal and electrical energy valorisation (with methane cogeneration). A methane calorific value of 38,800 kJ Nm^{-3} was considered for both alternatives. A combined heat and power (CHP) unit was used for energy production with an electricity and heat efficiency of 33 and 55% according to common literature values (Appels et al., 2011; Batstone et al., 2015; Cogert et al., 2019; Pöschl et al., 2010; Ruiz-Hernando et al., 2014). Eq. (2) was used to calculate the potential temperature increase:

$$\Delta T = \frac{q \cdot \eta}{Q \cdot \rho \cdot c_p} \quad (2)$$

where ΔT is the temperature increment of the influent sewage (°C), q is the heat energy (kJ d^{-1}), η is the heat exchange efficiency (90%), ρ is the water density (1000 kg m^{-3}), Q is the sewage flow rate (m^3 d^{-1}) and c_p is the water specific heat (4.18 kJ kg^{-1} °C^{-1}).

The AnMBR capital and operating costs and the revenue from electricity generation were considered for the economic evaluation. The AnMBR capital and operating costs were adapted from Vinardell et al. (2020a) while the electricity was assumed to be sold at a unit price of 0.1149 € kWh^{-1} (Eurostat, 2019). The AnMBR influent flow rate was calculated for each pre-concentration factor considering an influent flow rate before pre-concentration of 100,000 m^3 day^{-1}.

The net present value (NPV) method was used for the AnMBR economic evaluation (Garrido-Baserba et al., 2018; Verrecht et al., 2010) (Eq. (3)).

$$NPV\ (€) = \sum_{t=1}^{T} \frac{I_t - OPEX_t}{(1+i)^t} - CAPEX \quad (3)$$

where I_t is the electricity revenue at year t (€), $OPEX_t$ is the AnMBR operating expenditures at year t (€), CAPEX is the AnMBR capital expenditures (€), i is the discount rate (5%) and T is the plant lifetime (20 years).

3. Results and discussion

3.1. AnMBR performance and operation

The lab-scale AnMBR was successfully operated for 80 days under four different sewage pre-concentration factors. The COD and the

sodium concentrations of the AnMBR influent were increased at each operational period to simulate different pre-concentration factors. Table 1 summarises the main operating conditions and results for the four operational periods.

Fig. 1 shows the OLR, influent sodium concentration, permeate COD concentration, VFA concentration and COD removal efficiency for the four operational periods. Fluctuations in COD removal efficiency with values ranging between 79 and 98% were observed during Period 1, probably caused by the ongoing acclimation of the anaerobic biomass to the AnMBR conditions (Fig. 1). Despite these fluctuations, the average COD removal efficiency was above 90% and the permeate COD met the EU regulations concerning municipal sewage treatment (< 125 mg COD L^{-1}) (CEC, 1991). Period 2 (two-fold sewage pre-concentration) was characterised by a stable AnMBR performance with COD removal efficiencies above 95% and permeate COD concentrations below 60 mg COD L^{-1}.

The performance of the AnMBR decreased during Period 3 (five-fold sewage pre-concentration) since permeate COD concentration progressively increased from 50 to 350 mg COD L^{-1} (day 58). However, the average COD removal efficiency remained high (94 ± 4%) due to the higher influent COD concentration (ca. 3200 mg COD L^{-1}). The increase in the permeate COD concentration could be attributed to the increased OLR rather than the sodium concentration (1.14 g Na^+ L^{-1}) since sodium concentrations below 2 g Na^+ L^{-1} have been reported as not inhibitory for anaerobic microbes (Astals et al., 2015; Wang et al., 2017).

FO pre-concentration reduces influent volumetric flow rate and increases influent COD concentration. However, these experimental results illustrate that while sewage pre-concentration can provide conceivable advantages for municipal sewage treatment, it can also compromise the compliances with COD concentration limits. In this regard, COD removal efficiencies above 96% would be required to meet the EU discharge limits for five-fold pre-concentrated sewage. Furthermore, high effluent COD concentrations could negatively affect nutrient removal post-treatments such as the autotrophic partial nitritation/anammox process (Dai et al., 2015; Giustinianovich et al., 2016).

High COD removal efficiencies (95 ± 5%) were also achieved during Period 4 (ten-fold pre-concentrated sewage), despite the instability occurred between day 66 and 68. On day 65, membrane was chemically cleaned and, therefore, membrane flux significantly increased from 2.1 to 5.6 L m^{-2} h^{-1} (LMH) (see Fig. 2). Consequently, an OLR shock above 3 g COD L^{-1} d^{-1} occurred on day 66, which led to permeate COD concentrations above 900 mg COD L^{-1} (Fig. 1). Moreover, COD removal efficiency was worsened by the removal of the biofilm layer on the membrane, which also played a role in COD removal efficiency (see Section 3.2). During this instability period, VFAs concentration increased from 10 to 706 mg COD L^{-1}, mainly acetate (55%) and propionate (38%) (Fig. S2, supplementary material). To recover the system and prevent further accumulation of VFAs, the membrane system was switched off until the VFA concentration decreased below 100 mg COD L^{-1}. This accumulation of VFA showed that the AnMBR performance is susceptible to OLR shock loads. On day 71, AnMBR performance reached previous operational values and COD removal efficiencies above 95% were sustained until the end of the operational period with COD permeate concentrations below 100 mg COD L^{-1}.

Methane yields progressively increased with the pre-concentration factor (Table 1). Specifically, the methane yield increased from 214 ± 79 to 322 ± 60 mL CH_4 g^{-1} COD as the pre-concentration factor increased from 1 to 10, respectively. The differences in methane yields were primarily attributed to the lower fraction of dissolved methane lost in the permeate with respect to the total fraction of methane produced (i.e. dissolved methane + gas methane) as the OLR increases. Note that the dissolved methane concentration in the permeate is expected to be similar regardless of the influent COD concentration since its equilibrium mainly depends on the temperature (ca. 13.7 mg CH_4 L^{-1} at 35 °C and saturation level). This finding is in agreement with Yeo et al. (2015), who attributed the lower fraction of dissolved methane to the higher methane production and mass transfer rate at higher OLRs.

Fig. 2 shows the membrane flux of the AnMBR for the four operational periods. The membrane system was operated at constant transmembrane pressure (TMP) of 0.1 bar and, consequently, membrane flux progressively decreased between cleaning events. The maximum membrane flux (7.5 LMH) was obtained after the first chemical cleaning (day 5 in Period 1). Physical membrane cleanings were carried out on day 26, 39 and 52 when membrane flux decreased below 3–4 LMH (green vertical lines in Fig. 2). On day 61, membrane flux sharply decreased below 2 LMH. At the early stages of Period 4, MLSS concentration had increased from 4.2 to 5.6 g TSS L^{-1}, which probably exacerbated membrane fouling and decreased membrane flux. The increase in MLSS concentration could be attributed to (i) the non-controlled SRT and (ii) the higher biomass growth due to the higher influent COD concentration (6510 mg COD L^{-1}). On day 65, after a membrane chemical cleaning event, the membrane fluxes increased above 5 LMH. However, a 5 LMH membrane flux was lower than the obtained after the first chemical cleaning in Period 1 (ca. 7.5 LMH). The different response after both chemical cleanings could be explained by (i) the higher MLSS concentration in Period 4 and (ii) the membrane fouling caused by compounds that cannot be removed through chemical cleanings (Basset et al., 2016; Dong et al., 2016).

3.2. The relative importance of suspended biomass and membrane biofilm on AnMBR performance under saline conditions

The AnMBR operation was satisfactory accomplished with sodium concentrations up to 2.3 g Na^+ L^{-1}. The progressive increase of OLR and sodium concentration allowed acclimatising the anaerobic biomass to higher saline concentrations without major disturbances. It has been reported that sodium concentrations below 3.9 g Na^+ L^{-1} do not significantly affect AnMBR performance (Chen et al., 2014, 2019; Song et al., 2016). Song et al. (2016) reported that, after biomass acclimation, high TOC removal (98%) efficiencies can be achieved at sodium

Table 1
Operating conditions and performance of the lab-scale AnMBR.

	Period 1	Period 2	Period 3	Period 4
Pre-concentration factor	1	2	5	10
FO recovery (%)	0	50	80	90
Influent COD (mg COD L^{-1})	576 ± 22	1176 ± 9	3187 ± 98	6510 ± 43
COD removal (%)	90.9 ± 6.0	95.9 ± 0.7	94.2 ± 3.7	95.8 ± 5.6
OLR (g COD L^{-1} d^{-1})	0.25 ± 0.06	0.36 ± 0.04	1.04 ± 0.26	1.96 ± 0.51
HRT (d)	2.4 ± 0.6	3.3 ± 0.4	3.4 ± 0.3	3.6 ± 1.1
Membrane flux (L m^{-2} h^{-1})	4.8 ± 1.5	3.5 ± 0.4	3.5 ± 0.4	3.5 ± 0.9
MLSS (g L^{-1})	3.3	3.4	4.2	5.6
pH	7.6 ± 0.3	8.2 ± 0.1	8.4 ± 0.2	8.4 ± 0.2
Methane yield (mL CH_4 g^{-1} COD)	214 ± 79	259 ± 15	317 ± 61	322 ± 60
Permeate COD (mg COD L^{-1})	53 ± 34	47 ± 7	131 ± 107	254 ± 344
Permeate VFA (mg COD L^{-1})	10 ± 12	12 ± 10	59 ± 88	113 ± 240

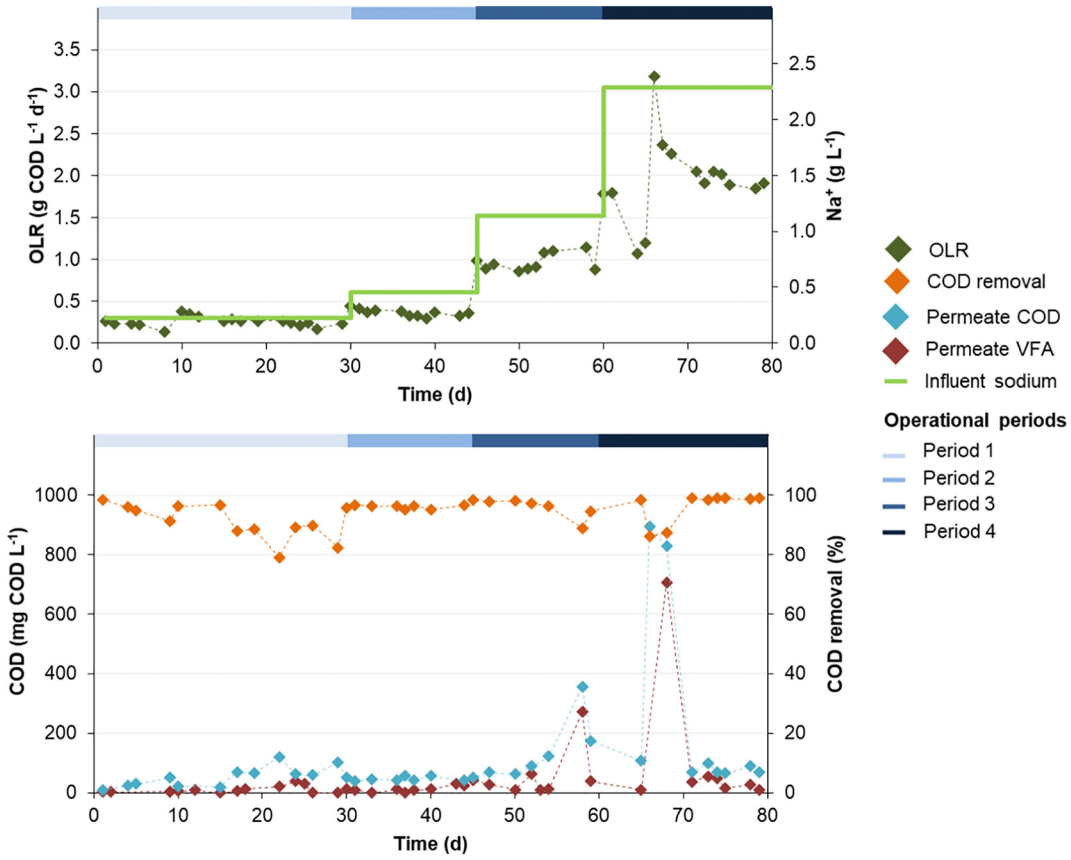

Fig. 1. (top) Influent sodium concentration and OLR; (bottom) permeate VFAs, permeate COD and COD removal efficiency for the four operational periods.

concentrations of 2 g Na^+ L^{-1}. Similarly, Chen et al. (2019) achieved a 94% COD removal efficiency at 2 g Na^+ L^{-1}. These experimental results agree with the results obtained in this study, where AnMBR performance was sustained for sodium concentrations up to 2.3 g Na^+ L^{-1}. However, the increase in sodium concentration and OLR had a direct impact on the role of biofilm in process performance. Fig. 3 shows the differences between digester and permeate soluble COD (sCOD) concentrations for the four operational periods. The sCOD concentration in the digester was consistently higher than in permeate for all the operational periods, clearly indicating that membrane biofilm played a role in COD removal.

Differences between permeate and digester sCOD have been reported in previous AnMBR studies (Martinez-Sosa et al., 2011; Smith et al., 2013). The difference in Period 4 (550 mg COD L^{-1}) was significantly higher than the difference in Period 1, 2 and 3 (80–120 mg COD L^{-1}). These results indicate that the role of biofilm in AnMBR performance is higher under less favourable conditions (2.3 g Na^+ L^{-1}), although the sodium concentration was below the reported strong inhibitory concentrations. It is well-known that many bacteria form biofilm as a survival strategy under stress conditions (e.g. chemical, biological or physical) or non-optimal growth conditions (Jefferson, 2004). Smith et al. (2015) reported that the contribution of membrane biofilm

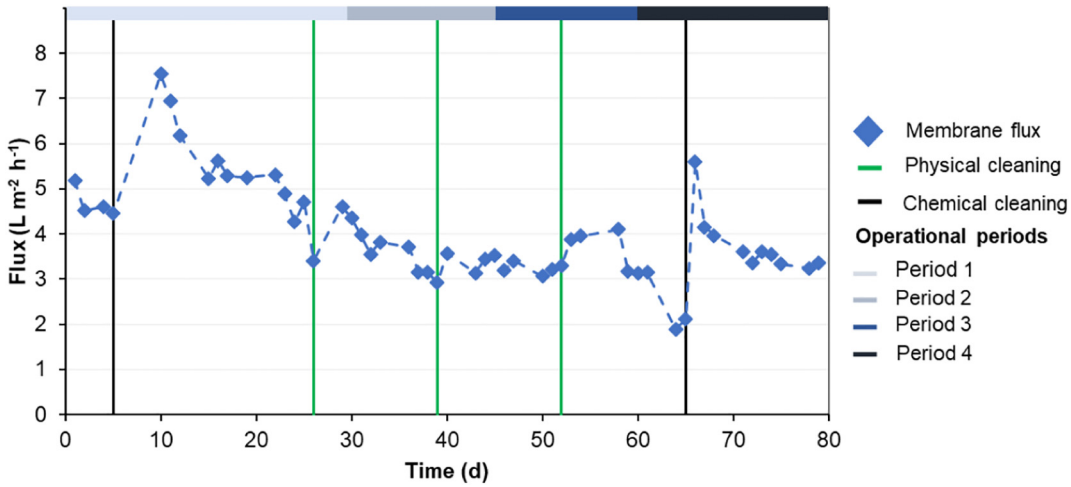

Fig. 2. Membrane flux of the AnMBR for the four operational periods.

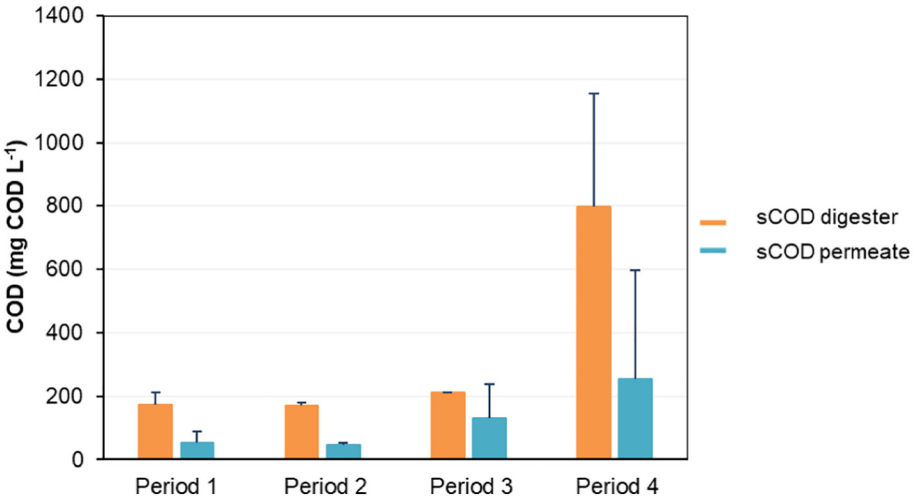

Fig. 3. Soluble COD in permeate and mixed liquor for the four operational periods.

in COD removal efficiency increased from ~40% to ~90% when AnMBR temperature decreased from 15 to 3 °C. In addition, membrane biofilm has been reported to increase dissolved methane supersaturation in the permeate due to the methanisation of acetate and hydrogen in the biofilm (Smith et al., 2013, 2015). However, further research is needed to evaluate the impact of high salinity conditions on membrane biofilm development, activity and microbial community.

3.3. The role of reverse solute flux (RSF) in the operation of an FO + AnMBR system

Experimental results showed that sodium inhibition did not occur at 2.3 g Na^+ L^{-1} (Fig. 1). This is relevant for FO + AnMBR system since it indicates that high process performance can be sustained despite the RSF of sodium through FO membrane. However, sodium RSF may have a direct impact on the performance and profitability of AnMBR process. Besides the changes in membrane biofilm activity and development (Fig. 3), the generation of an AnMBR permeate with 2.3 g Na^+ L^{-1} significantly hinders its application in agriculture. The use of high saline effluents for agricultural irrigation can negatively affect crop growth and soil structure (Beletse et al., 2008; Foglia et al., 2020).

The diffusion of salt has also negative connotations for FO process since it reduces the effective osmotic pressure difference and increases operational costs in areas where natural draw solutions (e.g. seawater) are not available (Blandin et al., 2015; Corzo et al., 2017). The RSF depends on many factors such as FO membrane properties, operational conditions and solute characteristics (Zou et al., 2019). The development of new FO membranes has gained special attention to improve FO membrane performance (Blandin et al., 2015; Lee and Hsieh, 2019; Zhao et al., 2012). The development of new FO membranes has mainly focused on improving water flux. However, little attention has been given to develop FO membranes able to achieve high water fluxes while minimising the RSF (Zou et al., 2019). Most research efforts have focused on (i) reducing ICP effects by modifying the porosity, tortuosity and hydrophilicity of the support layer and (ii) increasing water permeability by modifying membrane characteristics of the active layer (Blandin et al., 2015; Tiraferri et al., 2013). However, these modifications do not necessarily mitigate RSF and the associated increase of sewage salinity. Consequently, the development of FO membranes with limited RSF is important for the success of the FO + AnMBR process.

3.4. Energy-economic analysis

Temperature can limit the application of AnMBR technology in cold and temperate climates since uncontrolled psychrophilic temperatures will be required due to the impossibility to heat the digester (Dev et al., 2019). Psychrophilic temperatures have a direct impact on AnMBR performance and fugitive methane emissions (Martin Garcia et al., 2013; Ozgun et al., 2015b; Smith et al., 2013). Therefore, the increment of sewage temperature has been explored as an option in FO pre-concentration scenarios to improve AnMBR performance and broad the applicability of AnMBR to cooler regions. It is worth highlighting that, although this study focused on pre-concentrated municipal sewage reaching COD concentrations up to 6500 mg L^{-1} (ten-fold sewage pre-concentration), the operational and energy-economic results of the present work could be extendible to high-strength industrial wastewaters.

The energy-economic analysis was conducted (i) to calculate the sewage temperature increments that could be achieved at each FO pre-concentration scenarios and (ii) to determine if FO pre-concentration can make an AnMBR economically self-sufficient. The experimental average methane yields (i.e. 214, 259, 317 and 322 mL CH_4 g^{-1} COD) for each FO pre-concentration scenario (i.e. pre-concentration factor of 1, 2, 5 and 10) were used for the energy-economic analysis.

Table 2 shows the energy and economic results for the four scenarios under study. Scenarios with low pre-concentration factors (≤ 2) do not allow heating the influent sewage more than 2.4 °C and, therefore, increasing the influent temperature is considered unviable. Considering only thermal energy valorisation, a pre-concentration factor of 10 allows increasing sewage temperature up to 16.3 °C, which would approach municipal sewage treatment to mesophilic conditions. Wei et al. (2014) also reported that mesophilic conditions could be achievable at sewage pre-concentration factors above 5. Operating at mesophilic conditions has three relevant positive connotations: (i) it improves anaerobic digestion kinetics, (ii) it reduces methane solubility, and (iii) it improves effluent post-treatments performance, which are sensitive to temperature such as partial nitritation/anammox (Dev et al., 2019; Morales et al., 2015). However, under the circular

Table 2
Energy production and economic results of the AnMBR at different sewage pre-concentration factors.

	Scenario 1	Scenario 2	Scenario 3	Scenario 4
Pre-concentration factor	1	2	5	10
FO recovery (%)	0	50	80	90
AnMBR sewage flow rate (m^3 d^{-1})	100,000	50,000	20,000	10,000
Energy production (kWh m^{-3})	1.2	3.1	10.2	21.1
ΔT without cogeneration (°C)	0.9	2.4	7.8	16.3
ΔT with cogeneration (°C)	0.6	1.4	4.8	10.0
Electricity production (kWh m^{-3})	0.4	1.0	3.4	6.9
NPV (M€)	−163	−68	−9	4

economy framework, this scheme is not conceivable since it fails to recover renewable energy (e.g. electricity, biomethane). The combination of electrical and thermal energy valorisation (i.e. cogeneration) limits sewage temperature increase to 4.8 and 10 °C for pre-concentration factors of 5 and 10, respectively. However, it allows producing renewable electrical energy from biogas (Table 2).

FO pre-concentration decreases AnMBR influent flow rate and increases the energy recovered per m^3 of sewage, which shows the importance of FO pre-concentration on AnMBR economics (Table 2). High pre-concentration factors (i.e. 5 and 10) allow increasing electricity revenue and reducing AnMBR costs. Therefore, the NPV increases from −163 to 4 M€ as the pre-concentration factor increases from 1 to 10, respectively (Table 2). This analysis shows that the economic self-sufficiency of the AnMBR is only achieved with a pre-concentration factor of 10. The potential of AnMBRs to achieve economic and energy self-sufficiency when treating high-strength sewage has also been reported in other studies (Galib et al., 2016; Van Zyl et al., 2008). It should be noted that the methane produced in the scenarios with a pre-concentration factor of 2 and 5 would be enough to offset the AnMBR OPEX. However, economic self-sufficiency is not achieved in these scenarios, mainly due to the high membrane CAPEX.

The reduction in the AnMBR volumetric flow rate also allows reducing the amount of dissolved methane leaving the permeate, which (i) increases energy production, (ii) reduces the size of the methane recovery device (iii) and reduces fugitive methane emission. The latter is especially relevant owing to the high methane global warming potential (Crone et al., 2016; Huete et al., 2018). Smith et al. (2014) showed that dissolved methane accounted for 75% of the global warming impact of an AnMBR. Accordingly, sewage pre-concentration would allow reducing the environmental impacts related to dissolved methane, which makes this approach particularly relevant for mainstream AnMBR application.

Finally, it is worth mentioning that this economic evaluation has not included AnMBR post-treatments nor FO pre-concentration which could significantly increase the overall costs. Indeed, FO pre-concentration has been reported as the main cost contributor of the FO + AnMBR treatment due to the low FO water fluxes (Vinardell et al., 2020a). This is particularly critical at high FO recoveries where the progressive decrease of the driving force leads to lower FO water fluxes and larger FO membrane areas that can compromise the economic feasibility of FO + AnMBR system. Indeed, as discussed above, the economic and technical feasibility of FO + AnMBR requires the development of FO membranes featuring high water fluxes and low sodium RSF from which renewable methane energy production can be maximised in the AnMBR process.

4. Conclusions

The performance of a mesophilic AnMBR at different pre-concentration factors was investigated. OLR and sodium concentration progressively increased from 0.3 to 2.0 g COD L^{-1} d^{-1} and from 0.28 to 2.30 g Na^+ L^{-1}, to simulate pre-concentration factors of 1, 2, 5 and 10. The AnMBR was successfully operated achieving COD removal efficiencies above 90% regardless of the pre-concentration factor. The methane yield progressively increased from 214 ± 79 to 322 ± 60 mL CH_4 g^{-1} COD as the pre-concentration factor increased from 1 to 10. These results were attributed to the lower fraction of dissolved methane lost in the permeate as the OLR increases. Experimental results showed that membrane biofilm plays a role in COD removal efficiency particularly at the highest pre-concentration factor (2.30 g Na^+ L^{-1}). Finally, an energy-economic analysis estimated that, at a pre-concentration factor of 10, the combination of pre-concentration and AnMBR technologies allows increasing sewage temperature 10 °C and achieving a positive net present value (NPV) of 4 M€ for a newly constructed AnMBR with a lifetime of 20 years and treating 10,000 m^3 d^{-1} of pre-concentrated sewage. These results show that sewage pre-concentration stands as an option to make AnMBR economic self-sufficient.

CRediT authorship contribution statement

Sergi Vinardell: Conceptualization, Formal analysis, Investigation, Data curation, Methodology, Writing - original draft, Visualization. **Sergi Astals:** Conceptualization, Methodology, Writing - review & editing, Supervision. **Marta Jaramillo:** Investigation, Data curation, Visualization. **Joan Mata-Alvarez:** Conceptualization, Writing - review & editing, Supervision, Funding acquisition. **Joan Dosta:** Conceptualization, Methodology, Writing - review & editing, Supervision.

Declaration of competing interest

The authors declare that they have no known competing financial interests or personal relationships that could have appeared to influence the work reported in this paper. The authors also declare that this manuscript reflects only the authors' view and that the Executive Agency for SME/EU Commission are not responsible for any use that may be made of the information it contains.

Acknowledgments

The authors acknowledge the European Union LIFE programme for the financial support (LIFE Green Sewer project, LIFE17 ENV/ES/000341). Sergi Vinardell is grateful to the Generalitat de Catalunya for his predoctoral FI grant (2019FI_B 00394). Sergi Astals is grateful to the Spanish Ministry of Science, Innovation and Universities for his Ramon y Cajal fellowship (RYC-2017-22372).

Appendix A. Supplementary data

Supplementary data to this article can be found online at https://doi.org/10.1016/j.scitotenv.2020.141625.

References

Ansari, A.J., Hai, F.I., Guo, W., Ngo, H.H., Price, W.E., Nghiem, L.D., 2015. Selection of forward osmosis draw solutes for subsequent integration with anaerobic treatment to facilitate resource recovery from wastewater. Bioresour. Technol. 191, 30–36. https://doi.org/10.1016/j.biortech.2015.04.119.

Ansari, A.J., Hai, F.I., Price, W.E., Drewes, J.E., Nghiem, L.D., 2017. Forward osmosis as a platform for resource recovery from municipal wastewater - a critical assessment of the literature. J. Memb. Sci. 529, 195–206. https://doi.org/10.1016/j.memsci.2017.01.054.

APHA, 2017. Standard Methods for the Examination of Water and Wastewater. Federation. Water Environmental American Public Health Association (APHA), Washington, DC, USA.

Appels, L., Baeyens, J., Degrève, J., Dewil, R., 2008. Principles and potential of the anaerobic digestion of waste-activated sludge. Prog. Energy Combust. Sci. 34, 755–781. https://doi.org/10.1016/j.pecs.2008.06.002.

Appels, L., Lauwers, J., Degrve, J., Helsen, L., Lievens, B., Willems, K., Van Impe, J., Dewil, R., 2011. Anaerobic digestion in global bio-energy production: potential and research challenges. Renew. Sust. Energ. Rev. 15, 4295–4301. https://doi.org/10.1016/j.rser.2011.07.121.

Astals, S., Nolla-Ardèvol, V., Mata-Alvarez, J., 2012. Anaerobic co-digestion of pig manure and crude glycerol at mesophilic conditions: biogas and digestate. Bioresour. Technol. 110, 63–70. https://doi.org/10.1016/j.biortech.2012.01.080.

Astals, S., Batstone, D.J., Tait, S., Jensen, P.D., 2015. Development and validation of a rapid test for anaerobic inhibition and toxicity. Water Res. 81, 208–215. https://doi.org/10.1016/j.watres.2015.05.063.

Awad, A.M., Jalab, R., Minier-Matar, J., Adham, S., Nasser, M.S., Judd, S.J., 2019. The status of forward osmosis technology implementation. Desalination 461, 10–21. https://doi.org/10.1016/j.desal.2019.03.013.

Basset, N., Santos, E., Dosta, J., Mata-Álvarez, J., 2016. Start-up and operation of an AnMBR for winery wastewater treatment. Ecol. Eng. 86, 279–289. https://doi.org/10.1016/j.ecoleng.2015.11.003.

Batstone, D.J., Hülsen, T., Mehta, C.M., Keller, J., 2015. Platforms for energy and nutrient recovery from domestic wastewater: a review. Chemosphere 140, 2–11. https://doi.org/10.1016/J.CHEMOSPHERE.2014.10.021.

Beletse, Y.G., Annandale, J.G., Steyn, J.M., Hall, I., Aken, M.E., 2008. Can crops be irrigated with sodium bicarbonate rich CBM deep aquifer water? Theoretical and field evaluation. Ecol. Eng. 33, 26–36. https://doi.org/10.1016/j.ecoleng.2007.12.011.

Blandin, G., Verliefde, A.R.D., Tang, C.Y., Le-Clech, P., 2015. Opportunities to reach economic sustainability in forward osmosis–reverse osmosis hybrids for seawater desalination. Desalination 363, 26–36. https://doi.org/10.1016/J.DESAL.2014.12.011.

Blandin, G., Verliefde, A.R.D., Comas, J., Rodriguez-Roda, I., Le-Clech, P., 2016. Efficiently combining water reuse and desalination through forward osmosis-reverse osmosis

(FO-RO) hybrids: a critical review. Membranes (Basel) 6, 37. https://doi.org/10.3390/membranes6030037.
Cath, T.Y., Childress, A.E., Elimelech, M., 2006. Forward osmosis: principles, applications, and recent developments. J. Memb. Sci. 281, 70–87. https://doi.org/10.1016/j.memsci.2006.05.048.
CEC, 1991. Council Directive of 21 May 1991 concerning waste water treatment (91/271/EEC). Off. J. Eur. Communities No. L 135/40–52.
Chen, W.-H., Han, S.-K., Sung, S., 2003. Sodium inhibition of thermophilic methanogens. J. Environ. Eng. 129, 506–512. https://doi.org/10.1061/(ASCE)0733-9372(2003)129:6(506).
Chen, Y., Cheng, J.J., Creamer, K.S., 2008. Inhibition of anaerobic digestion process: a review. Bioresour. Technol. 99, 4044–4064. https://doi.org/10.1016/j.biortech.2007.01.057.
Chen, L., Gu, Y., Cao, C., Zhang, J., Ng, J.W., Tang, C., 2014. Performance of a submerged anaerobic membrane bioreactor with forward osmosis membrane for low-strength wastewater treatment. Water Res. 50, 114–123. https://doi.org/10.1016/j.watres.2013.12.009.
Chen, L., Hu, Q., Zhang, X., Chen, Z., Wang, Y., Liu, S., 2019. Effects of salinity on the biological performance of anaerobic membrane bioreactor. J. Environ. Manag. 238, 263–273. https://doi.org/10.1016/j.jenvman.2019.03.012.
Coday, B.D., Heil, D.M., Xu, P., Cath, T.Y., 2013. Effects of transmembrane hydraulic pressure on performance of forward osmosis membranes. Environ. Sci. Technol. 47, 2386–2393. https://doi.org/10.1021/es304519p.
Cogert, K.I., Ziels, R.M., Winkler, M.K.H., 2019. Reducing cost and environmental impact of wastewater treatment with denitrifying methanotrophs, anammox, and mainstream anaerobic treatment. Environ. Sci. Technol. 53, 12935–12944. https://doi.org/10.1021/acs.est.9b04764.
Corzo, B., de la Torre, T., Sans, C., Ferrero, E., Malfeito, J.J., 2017. Evaluation of draw solutions and commercially available forward osmosis membrane modules for wastewater reclamation at pilot scale. Chem. Eng. J. 326, 1–8. https://doi.org/10.1016/j.cej.2017.05.108.
Crone, B.C., Garland, J.L., Sorial, G.A., Vane, L.M., 2016. Significance of dissolved methane in effluents of anaerobically treated low strength wastewater and potential for recovery as an energy product: a review. Water Res. 104, 520–531. https://doi.org/10.1016/j.watres.2016.08.019.
Dai, W., Xu, X., Liu, B., Yang, F., 2015. Toward energy-neutral wastewater treatment: a membrane combined process of anaerobic digestion and nitritation-anammox for biogas recovery and nitrogen removal. Chem. Eng. J. 279, 725–734. https://doi.org/10.1016/j.cej.2015.05.036.
Dev, S., Saha, S., Kurade, M.B., Salama, E., 2019. Perspective on anaerobic digestion for biomethanation in cold environments. Renew. Sust. Energ. Rev. 103, 85–95.
Dong, Q., Parker, W., Dagnew, M., 2016. Long term performance of membranes in an anaerobic membrane bioreactor treating municipal wastewater. Chemosphere 144, 249–256. https://doi.org/10.1016/j.chemosphere.2015.08.077.
Eurostat, 2019. Electricity price statistics. https://ec.europa.eu/eurostat/statistics-explained/index.php/Electricity_price_statistics. (Accessed 30 September 2019). .
Feijoo, G., Soto, M., Méndez, R., Lema, J.M., 1995. Sodium inhibition in the anaerobic digestion process: antagonism and adaptation phenomena. Enzym. Microb. Technol. 17, 180–188. https://doi.org/10.1016/0141-0229(94)00011-F.
Ferrari, F., Balcazar, J.L., Rodriguez-Roda, I., Pijuan, M., 2019a. Anaerobic membrane bioreactor for biogas production from concentrated sewage produced during sewer mining. Sci. Total Environ. 670, 993–1000. https://doi.org/10.1016/j.scitotenv.2019.03.218.
Ferrari, F., Pijuan, M., Rodriguez-Roda, I., Blandin, G., 2019b. Exploring submerged forward osmosis for water recovery and pre-concentration of wastewater before anaerobic digestion: a pilot scale study. Membranes (Basel) 9, 97. https://doi.org/10.3390/membranes9080097.
Foglia, A., Akyol, Ç., Frison, N., Katsou, E., Eusebi, A.L., Fatone, F., 2020. Long-term operation of a pilot-scale anaerobic membrane bioreactor (AnMBR) treating high salinity low loaded municipal wastewater in real environment. Sep. Purif. Technol. 236, 116279. https://doi.org/10.1016/j.seppur.2019.116279.
Galib, M., Elbeshbishy, E., Reid, R., Hussain, A., Lee, H.S., 2016. Energy-positive food wastewater treatment using an anaerobic membrane bioreactor (AnMBR). J. Environ. Manag. 182, 477–485. https://doi.org/10.1016/j.jenvman.2016.07.098.
Garrido-Baserba, M., Vinardell, S., Molinos-Senante, M., Rosso, D., Poch, M., 2018. The economics of wastewater treatment decentralization: a techno-economic evaluation. Environ. Sci. Technol. 52, 8965–8976. https://doi.org/10.1021/acs.est.8b01623.
Giustinianovich, E.A., Campos, J.L., Roeckel, M.D., 2016. The presence of organic matter during autotrophic nitrogen removal: problem or opportunity? Sep. Purif. Technol. 166, 102–108. https://doi.org/10.1016/j.seppur.2016.04.012.
Guest, J.S., Skerlos, S.J., Barnard, J.L., Beck, M.B., Daigger, G.T., Hilger, H., Jackson, S.J., Karvazy, K., Kelly, L., Macpherson, L., Mihelcic, J.R., Pramanik, A., Raskin, L., Van Loosdrecht, M.C.M., Yeh, D., Love, N.G., 2009. A new planning and design paradigm to achieve sustainable resource recovery from wastewater. Environ. Sci. Technol. 43, 6126–6130. https://doi.org/10.1021/es9010515.
Guven, H., Dereli, R.K., Ozgun, H., Ersahin, M.E., Ozturk, I., 2019. Towards sustainable and energy efficient municipal wastewater treatment by up-concentration of organics. Prog. Energy Combust. Sci. 70, 145–168. https://doi.org/10.1016/j.pecs.2018.10.002.
Huang, Z., Ong, S.L., Ng, H.Y., 2011. Submerged anaerobic membrane bioreactor for low-strength wastewater treatment: effect of HRT and SRT on treatment performance and membrane fouling. Water Res. 45, 705–713. https://doi.org/10.1016/j.watres.2010.08.035.
Hube, S., Eskafi, M., Hrafnkelsdóttir, K.F., Bjarnadóttir, B., Bjarnadóttir, M.Á., Axelsdóttir, S., Wu, B., 2020. Direct membrane filtration for wastewater treatment and resource recovery: a review. Sci. Total Environ. 710, 136375. https://doi.org/10.1016/j.scitotenv.2019.136375.
Huete, A., de los Cobos-Vasconcelos, D., Gómez-Borraz, T., Morgan-Sagastume, J.M., Noyola, A., 2018. Control of dissolved CH4 in a municipal UASB reactor effluent by means of a desorption – biofiltration arrangement. J. Environ. Manag. 216, 383–391. https://doi.org/10.1016/J.JENVMAN.2017.06.061.
Itliong, J.N., Villagracia, A.R.C., Moreno, J.L.V., Rojas, K.I.M., Bernardo, G.P.O., David, M.Y., Manrique, R.B., Ubando, A.T., Culaba, A.B., Padama, A.A.B., Ong, H.L., Chang, J.S., Chen, W.H., Kasai, H., Arboleda, N.B., 2019. Investigation of reverse ionic diffusion in forward-osmosis-aided dewatering of microalgae: a molecular dynamics study. Bioresour. Technol. 279, 181–188. https://doi.org/10.1016/j.biortech.2019.01.109.
Jefferson, K.K., 2004. What drives bacteria to produce a biofilm? FEMS Microbiol. Lett. 236, 163–173. https://doi.org/10.1016/j.femsle.2004.06.005.
Lee, D.J., Hsieh, M.H., 2019. Forward osmosis membrane processes for wastewater bioremediation: research needs. Bioresour. Technol. 290, 121795. https://doi.org/10.1016/j.biortech.2019.121795.
Maaz, M., Yasin, M., Aslam, M., Kumar, G., Atabani, A.E., Idrees, M., Anjum, F., Jamil, F., Ahmad, R., Khan, A.L., Lesage, G., Heran, M., Kim, J., 2019. Anaerobic membrane bioreactors for wastewater treatment: novel configurations, fouling control and energy considerations. Bioresour. Technol. 283, 358–372. https://doi.org/10.1016/j.biortech.2019.03.061.
Martin Garcia, I., Mokosch, M., Soares, A., Pidou, M., Jefferson, B., 2013. Impact on reactor configuration on the performance of anaerobic MBRs: treatment of settled sewage in temperate climates. Water Res. 47, 4853–4860. https://doi.org/10.1016/j.watres.2013.05.008.
Martinez-Sosa, D., Helmreich, B., Netter, T., Paris, S., Bischof, F., Horn, H., 2011. Anaerobic submerged membrane bioreactor (AnSMBR) for municipal wastewater treatment under mesophilic and psychrophilic temperature conditions. Bioresour. Technol. 102, 10377–10385. https://doi.org/10.1016/j.biortech.2011.09.012.
McCarty, P.L., 1964. Anaerobic waste treatment fundamentals. Public Work. 95 (9), 107–112.
Morales, N., Val del Río, Á., Vázquez-Padín, J.R., Méndez, R., Mosquera-Corral, A., Campos, J.L., 2015. Integration of the Anammox process to the rejection water and main stream lines of WWTPs. Chemosphere 140, 99–105. https://doi.org/10.1016/j.chemosphere.2015.03.058.
Muñoz Sierra, J.D., Oosterkamp, M.J., Wang, W., Spanjers, H., van Lier, J.B., 2018. Impact of long-term salinity exposure in anaerobic membrane bioreactors treating phenolic wastewater: performance robustness and endured microbial community. Water Res. 141, 172–184. https://doi.org/10.1016/j.watres.2018.05.006.
Muñoz Sierra, J.D., Oosterkamp, M.J., Wang, W., Spanjers, H., van Lier, J.B., 2019. Comparative performance of upflow anaerobic sludge blanket reactor and anaerobic membrane bioreactor treating phenolic wastewater: overcoming high salinity. Chem. Eng. J. 366, 480–490. https://doi.org/10.1016/j.cej.2019.02.097.
Nascimento, T.A., Fdz-Polanco, F., Peña, M., 2020. Membrane-based technologies for the up-concentration of municipal wastewater: a review of pretreatment intensification. Sep. Purif. Rev. 49, 1–19. https://doi.org/10.1080/15422119.2018.1481089.
Ozgun, H., Dereli, R.K., Ersahin, M.E., Kinaci, C., Spanjers, H., Van Lier, J.B., 2013. A review of anaerobic membrane bioreactors for municipal wastewater treatment: integration options, limitations and expectations. Sep. Purif. Technol. 118, 89–104. https://doi.org/10.1016/j.seppur.2013.06.036.
Ozgun, H., Gimenez, J.B., Evren Ersahin, M., Tao, Y., Spanjers, H., Van Lier, J.B., 2015a. Impact of membrane addition for effluent extraction on the performance and sludge characteristics of upflow anaerobic sludge blanket reactors treating municipal wastewater. J. Memb. Sci. 479, 95–104. https://doi.org/10.1016/j.memsci.2014.12.021.
Ozgun, H., Tao, Y., Ersahin, M.E., Zhou, Z., Gimenez, J.B., Spanjers, H., van Lier, J.B., 2015b. Impact of temperature on feed-flow characteristics and filtration performance of an upflow anaerobic sludge blanket coupled ultrafiltration membrane treating municipal wastewater. Water Res. 83, 71–83. https://doi.org/10.1016/j.watres.2015.06.035.
Pöschl, M., Ward, S., Owende, P., 2010. Evaluation of energy efficiency of various biogas production and utilization pathways. Appl. Energy 87, 3305–3321. https://doi.org/10.1016/j.apenergy.2010.05.011.
Puyol, D., Batstone, D.J., Hülsen, T., Astals, S., Peces, M., Krömer, J.O., 2017. Resource recovery from wastewater by biological technologies: opportunities, challenges, and prospects. Front. Microbiol. 7. https://doi.org/10.3389/fmicb.2016.02106.
Robles, Á., Ruano, M.V., Charfi, A., Lesage, G., Heran, M., Harmand, J., Seco, A., Steyer, J.P., Batstone, D.J., Kim, J., Ferrer, J., 2018. A review on anaerobic membrane bioreactors (AnMBRs) focused on modelling and control aspects. Bioresour. Technol. 270, 612–626. https://doi.org/10.1016/j.biortech.2018.09.049.
Ruiz-Hernando, M., Martín-Díaz, J., Labanda, J., Mata-Alvarez, J., Llorens, J., Lucena, F., Astals, S., 2014. Effect of ultrasound, low-temperature thermal and alkali pretreatments on waste activated sludge rheology, hygienization and methane potential. Water Res. 61, 119–129. https://doi.org/10.1016/j.watres.2014.05.012.
Shaffer, D.L., Werber, J.R., Jaramillo, H., Lin, S., Elimelech, M., 2015. Forward osmosis: where are we now? Desalination 356, 271–284. https://doi.org/10.1016/j.desal.2014.10.031.
Shin, C., Bae, J., 2018. Current status of the pilot-scale anaerobic membrane bioreactor treatments of domestic wastewaters: a critical review. Bioresour. Technol. 247, 1038–1046. https://doi.org/10.1016/j.biortech.2017.09.002.
Smith, A.L., Skerlos, S.J., Raskin, L., 2013. Psychrophilic anaerobic membrane bioreactor treatment of domestic wastewater. Water Res. 47, 1655–1665. https://doi.org/10.1016/J.WATRES.2012.12.028.
Smith, A.L., Stadler, L.B., Cao, L., Love, N.G., Raskin, L., Skerlos, S.J., 2014. Navigating wastewater energy recovery strategies: a life cycle comparison of anaerobic membrane bioreactor and conventional treatment systems with anaerobic digestion. Environ. Sci. Technol. 48, 5972–5981. https://doi.org/10.1021/es5006169.
Smith, A.L., Skerlos, S.J., Raskin, L., 2015. Anaerobic membrane bioreactor treatment of domestic wastewater at psychrophilic temperatures ranging from 15 °C to 3 °C. Environ. Sci. Water Res. Technol. 1, 56–64. https://doi.org/10.1039/c4ew00070f.
Song, X., McDonald, J., Price, W.E., Khan, S.J., Hai, F.I., Ngo, H.H., Guo, W., Nghiem, L.D., 2016. Effects of salinity build-up on the performance of an anaerobic membrane bioreactor regarding basic water quality parameters and removal of trace organic contaminants. Bioresour. Technol. 216, 399–405. https://doi.org/10.1016/j.biortech.2016.05.075.

Tiraferri, A., Yip, N.Y., Straub, A.P., Romero-Vargas Castrillon, S., Elimelech, M., 2013. A method for the simultaneous determination of transport and structural parameters of forward osmosis membranes. J. Memb. Sci. 444, 523–538. https://doi.org/10.1016/j.memsci.2013.05.023.

Van Zyl, P.J., Wentzel, M.C., Ekama, G.A., Riedel, K.J., 2008. Design and start-up of a high rate anaerobic membrane bioreactor for the treatment of a low pH, high strength, dissolved organic waste water. Water Sci. Technol. 57, 291–295. https://doi.org/10.2166/wst.2008.083.

Verrecht, B., Maere, T., Nopens, I., Brepols, C., Judd, S., 2010. The cost of a large-scale hollow fibre MBR. Water Res. 44, 5274–5283. https://doi.org/10.1016/j.watres.2010.06.054.

Vinardell, S., Astals, S., Mata-Alvarez, J., Dosta, J., 2020a. Techno-economic analysis of combining forward osmosis-reverse osmosis and anaerobic membrane bioreactor technologies for municipal wastewater treatment and water production. Bioresour. Technol. 297, 122395. https://doi.org/10.1016/j.biortech.2019.122395.

Vinardell, S., Astals, S., Peces, M., Cardete, M.A., Fernández, I., Mata-Alvarez, J., Dosta, J., 2020b. Advances in anaerobic membrane bioreactor technology for municipal wastewater treatment: a 2020 updated review. Renew. Sust. Energ. Rev. 130, 109936. https://doi.org/10.1016/j.rser.2020.109936.

Wang, S., Hou, X., Su, H., 2017. Exploration of the relationship between biogas production and microbial community under high salinity conditions. Sci. Rep. 7, 1–11. https://doi.org/10.1038/s41598-017-01298-y.

Wei, C.-H., Harb, M., Amy, G., Hong, P.-Y., Leiknes, T., 2014. Sustainable organic loading rate and energy recovery potential of mesophilic anaerobic membrane bioreactor for municipal wastewater treatment. Bioresour. Technol. 166, 326–334. https://doi.org/10.1016/j.biortech.2014.05.053.

Yeo, H., An, J., Reid, R., Rittmann, B.E., Lee, H.S., 2015. Contribution of liquid/gas mass-transfer limitations to dissolved methane oversaturation in anaerobic treatment of dilute wastewater. Environ. Sci. Technol. 49, 10366–10372. https://doi.org/10.1021/acs.est.5b02560.

Zhao, S., Zou, L., Tang, C.Y., Mulcahy, D., 2012. Recent developments in forward osmosis: opportunities and challenges. J. Memb. Sci. 396, 1–21. https://doi.org/10.1016/j.memsci.2011.12.023.

Zhen, G., Pan, Y., Lu, X., Li, Y.-Y., Zhang, Z., Niu, C., Kumar, G., Kobayashi, T., Zhao, Y., Xu, K., 2019. Anaerobic membrane bioreactor towards biowaste biorefinery and chemical energy harvest: recent progress, membrane fouling and future perspectives. Renew. Sust. Energ. Rev. 115, 109392. https://doi.org/10.1016/j.rser.2019.109392.

Zou, S., Qin, M., He, Z., 2019. Tackle reverse solute flux in forward osmosis towards sustainable water recovery: reduction and perspectives. Water Res. 149, 362–374. https://doi.org/10.1016/j.watres.2018.11.015.

SUPPLEMENTARY INFORMATION

Anaerobic membrane bioreactor performance at different wastewater pre-concentration factors: An experimental and economic study

Sergi Vinardell[a,*], Sergi Astals[a], Marta Jaramillo[a], Joan Mata-Alvarez[a,b], Joan Dosta[a,b]

[a] Department of Chemical Engineering and Analytical Chemistry, University of Barcelona, C/Martí i Franquès 1, 6th floor, 08028, Barcelona, Spain

[b] Water Research Institute, University of Barcelona, 08001 Barcelona, Spain

*Corresponding author (e-mail: svinardell@ub.edu)

Figures

Figure S1. Lab-scale anaerobic membrane bioreactor.

Figure S2. Average concentration of acetic acid, propionic acid and butyric acid for the four operational periods.

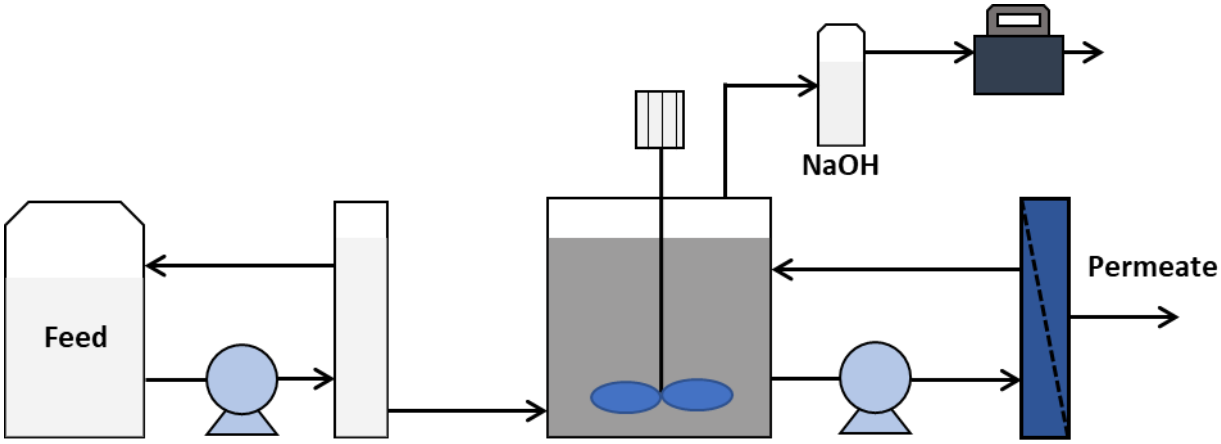

Figure S1. Lab-scale anaerobic membrane bioreactor.

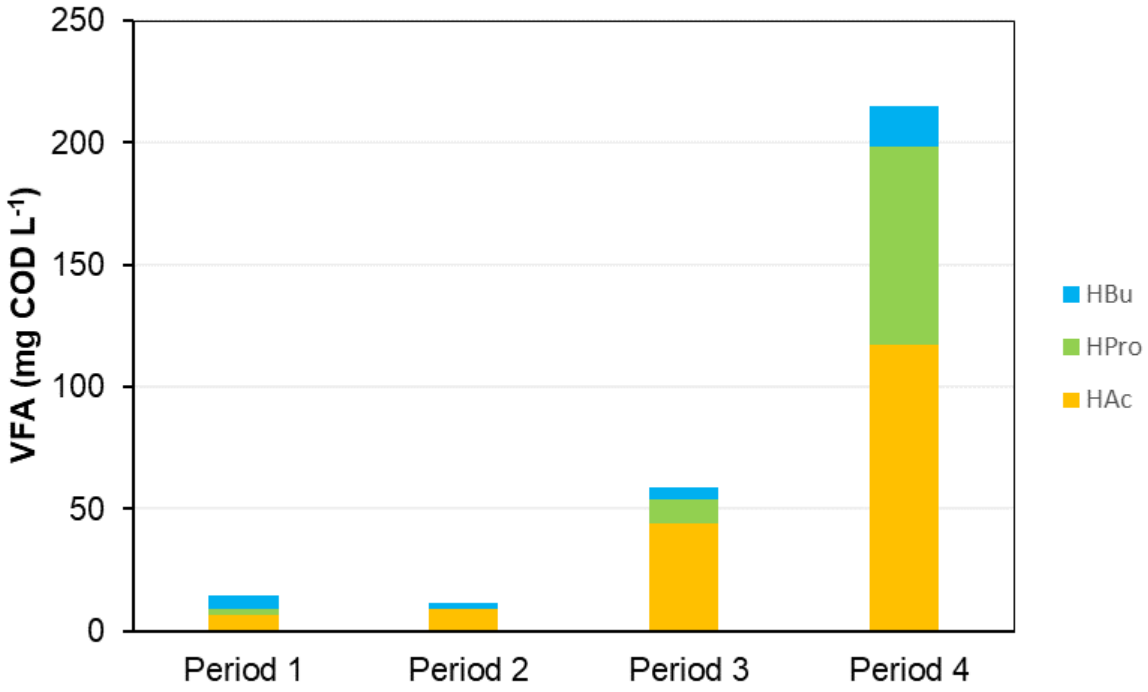

Figure S2. Average concentration of acetic acid, propionic acid and butyric acid in the permeate for the four operational periods.

2.3 Publication III: *Techno-economic analysis of combining forward osmosis-reverse osmosis and anaerobic membrane bioreactor technologies for municipal wastewater treatment and water production*

Vinardell, S., Astals, S., Mata-Alvarez, J., Dosta, J. (2020). Techno-economic analysis of combining forward osmosis-reverse osmosis and anaerobic membrane bioreactor technologies for municipal wastewater treatment and water production. Bioresour. Technol. 297, 122395. https://doi.org/10.1016/j.biortech.2019.122395

Bioresource Technology 297 (2020) 122395

Contents lists available at ScienceDirect

Bioresource Technology

journal homepage: www.elsevier.com/locate/biortech

Techno-economic analysis of combining forward osmosis-reverse osmosis and anaerobic membrane bioreactor technologies for municipal wastewater treatment and water production

Sergi Vinardell*, Sergi Astals, Joan Mata-Alvarez, Joan Dosta

Department of Chemical Engineering and Analytical Chemistry, University of Barcelona, 08028 Barcelona, Spain

ARTICLE INFO

Keywords:
Anaerobic digestion
Anaerobic membrane bioreactor (AnMBR)
Forward osmosis (FO)
Reverse osmosis (RO)
Municipal sewage treatment

ABSTRACT

The economic feasibility of combining forward osmosis (FO), reverse osmosis (RO) and anaerobic membrane bioreactor (AnMBR) technologies for municipal wastewater treatment with energy and water production was analysed. FO was used to pre-concentrate the AnMBR influent, RO for draw solution regeneration and water production, and AnMBR for wastewater treatment and energy production. The minimum wastewater treatment cost was estimated at 0.81 € m^{-3}, achieved when limiting the FO recovery to 50% in a closed-loop scheme. However, the cost increased to 1.01 and 1.27 € m^{-3} for FO recoveries of 80% and 90%, respectively. The fresh water production cost was estimated at 0.80 and 1.16 € m^{-3} for an open-loop scheme maximising water production and a closed-loop scheme, respectively. The low FO membrane fluxes were identified as a limiting factor and a sensitivity analysis revealed that FO membrane fluxes of 10 LMH would significantly improve the competitiveness of FO-RO + AnMBR technology.

1. Introduction

Wastewater treatment plants (WWTPs) based on the conventional activated sludge (CAS) process are not suitable to meet the environmental and economic requirements of the circular biobased economy since they are designed to remove resources rather than recovering them (Guest et al., 2009). Accordingly, new WWTP technologies and configurations have arisen to maximise resources harvesting and support the transition of WWTPs towards the concept of wastewater resource recovery facilities (WRRF) (Puyol et al., 2017).

Anaerobic membrane bioreactor (AnMBR) technology is attracting attention as a mainstream process for municipal wastewater treatment due to its capacity to recover most of the energy potential in wastewater and produce high-quality effluents (McCarty et al., 2011; Puyol et al., 2017). Anaerobic digestion allows to recover the energy content of municipal sewage by transforming its biodegradable organic matter into renewable methane energy. Another noteworthy feature of AnMBR is the high retention of particles provided by the membrane which allows an excellent decoupling of the hydraulic retention time (HRT) from the solids retention time (SRT). This provides a high controllability on the active biomass concentration in the reactor (Maaz et al., 2019).

However, the economic feasibility of AnMBR technology is limited by the low concentration of organics in municipal sewage and the associated high capital (e.g. higher vessel volume, additional membrane modules) and operational (e.g. gas sparging, biomass recirculation) costs. One option to overcome this limitation is the pre-concentration of sewage by means of forward osmosis (FO) (Ansari et al., 2017). The FO process concentrates the total solids contained in sewage by permeating water towards a draw solution using a selective membrane (Cath et al., 2006). The draw solution is a natural (e.g. seawater) or artificial solution (e.g. NaCl, $MgCl_2$) that generates an osmotic gradient (driving force) between both solutions (Itliong et al., 2019; Lee and Hsieh, 2019). Consequently, water flows spontaneously from the sewage to the draw solution through a dense semipermeable membrane: (i) decreasing the sewage flow and increasing the organics concentration and (ii) increasing the draw solution flow and diluting the solute concentration. The concentration of sewage prior to an AnMBR reduces the volumetric flow and, in turn, the volume of the anaerobic reactor (Ansari et al., 2017; Ferrari et al., 2019). Additionally, if a draw solution regeneration step is implemented, it is possible to produce clean water while re-concentrating the diluted draw solution.

Reverse osmosis (RO) stands as the most used technology to produce clean water from diluted draw solutions (Awad et al., 2019; Luo et al., 2014). The combination of FO and RO is particularly interesting for open-loop seawater desalination schemes (once-through systems),

* Corresponding author.
E-mail address: svinardell@ub.edu (S. Vinardell).

https://doi.org/10.1016/j.biortech.2019.122395
Received 30 September 2019; Received in revised form 5 November 2019; Accepted 7 November 2019
Available online 11 November 2019
0960-8524/

where seawater is used as a draw solution and, subsequently, clean water is produced by RO from the diluted seawater (Blandin et al., 2016; Jalab et al., 2019). It is worth to mention that FO-RO system is not thermodynamically favourable when compared to sewage direct RO due to the higher osmotic pressure of the diluted seawater in comparison to municipal sewage (Shaffer et al., 2015). However, the FO-RO system offers important advantages such as a dual barrier to the pollutants and a lower fouling potential in the RO membranes (Blandin et al., 2016). Furthermore, due to its lower osmotic potential, less energy is required to produce clean water from the diluted seawater than from conventional seawater (Hancock et al., 2012; Wan and Chung, 2018).

Several publications have stated that the FO-RO system is a more profitable scenario for seawater desalination than the stand-alone RO system (Cath et al., 2010; Valladares Linares et al., 2016; Wan and Chung, 2018). However, other publications have pointed out that the low FO fluxes and the high FO membrane prices are important limitations for the implementation of such system (Awad et al., 2019; Blandin et al., 2015; Lee and Hsieh, 2019). Regarding FO fluxes, Blandin et al. (2015) reported that an average flux of 30 L m^{-2} h^{-1} (LMH) is needed to guarantee the economic suitability of an FO-RO system for seawater desalination. However, a 30 LMH flux is far from current FO fluxes since reported pilot-scale fluxes range from 2.2 to 10.6 LMH (Awad et al., 2019).

There are evident differences among the published articles regarding the techno-economic feasibility of FO-RO systems. These differences can be related to discrepancies in operational conditions, capital and operational costs, assumptions and omission of some parameters. For instance, the impact of FO recovery and RO strategies for draw solution regeneration and water production have been rarely included in previous studies. To the best of the authors' knowledge, the impact of FO as a pre-concentration step of an AnMBR has not been previously analysed from a techno-economic point of view. Therefore, a detailed and comprehensive techno-economic analysis is needed to determine in which scenarios the combination of FO, RO and AnMBR is economically and technically attractive as well as to identify the process limiting factors.

The goal of this study is to analyse the economic feasibility of a system combining FO for sewage pre-concentration, RO for clean water production and AnMBR for renewable energy production. This theoretical techno-economic analysis includes the impact of different FO recoveries, different draw solution management strategies and the implication of these factors on the AnMBR design. The ultimate goal is to provide a comprehensive tool that allows to evaluate in which scenarios the combination of FO, RO and AnMBR technology is recommendable from both economic and technical points of view.

2. Methodology

2.1. Evaluated wastewater treatment scenarios and design criteria

The economic feasibility of an AnMBR system for mainstream sewage treatment was evaluated for four different scenarios (Table 1). The baseline scenario was the implementation of an AnMBR without FO for sewage pre-concentration nor RO for water production. The other three scenarios resulted from assessing three different FO recoveries, i.e. (i) 50% recovery (Scenario 1), (ii) 80% recovery (Scenario 2), and (iii) 90% recovery (Scenario 3). The FO recovery is an important parameter since it determines (i) the flow rate and concentration of the AnMBR influent and (ii) the flow rate and osmotic pressure of the diluted draw solution feeding the RO stage. Previous economic studies considered FO recoveries around 50% (Blandin et al., 2015; Valladares Linares et al., 2016). However, in this study, the three different recovery scenarios (i.e. 50, 80 and 90%) were selected since (i) high FO recoveries (≥50%) can enhance the operability and applicability of AnMBR technology and (ii) FO recoveries up to 90% have been achieved for municipal wastewater pre-concentration (Ansari et al., 2018).

For each FO recovery scenario, the FO-RO + AnMBR process was assessed for three different draw solution management schemes (Table 1). The three different schemes are as follow (Fig. 1):

- Scheme A: Open-loop system aiming to maximise water production in the RO stage. In this scenario, water production (i.e. RO recovery) from the diluted seawater is determined by permeating the amount of water needed to reach a brine osmotic pressure of 46.7 bar. This is a typical brine osmotic pressure in conventional seawater desalination featuring an RO recovery of 45%.
- Scheme B: Open-loop system where water production in the RO stage is limited by fixing the RO recovery at 45% regardless of the diluted seawater osmotic pressure. RO recovery is fixed at 45% since this is a common value in full-scale desalination plants (Blandin et al., 2016).
- Scheme C: Closed-loop system where the RO stage is used to re-establish the osmotic pressure of the synthetic draw solution. In this system, RO recovery is fixed by FO performance since the amount of water extracted in the RO stage is the same that permeated the FO membrane. NaCl was the solute in the synthetic draw solution.

Open-loop systems are preferred in regions where seawater is available (Blandin et al., 2016). An open-loop is a once-through system where the brine (concentrated seawater) from the RO stage is directly discharged to the sea/ocean. Open-loop schemes provide higher flexibility in RO recoveries since the regenerated seawater does not need to be reused. Another conceivable open-loop scenario would be to directly discharge diluted seawater from the FO stage into the sea/ocean. However, this scenario would only consider FO + AnMBR in coastal areas and would fail to recover the filtered water. Accordingly, this scheme was not included in this publication. On the other hand, closed-loop schemes using synthetic draw solutions are required in non-coastal areas.

This FO-RO + AnMBR process was evaluated for a medium-sized facility (i.e. 30,000 population equivalent (PE)) treating 148 L PE^{-1} day^{-1} of an average strength municipal sewage (COD_T = 420 mg COD L^{-1}; COD_S = 300 mg COD L^{-1}; $COD_{S,inert}$ = 30 mg COD L^{-1}; $COD_{particulate,inert}$ = 40 mg COD L^{-1}) (Garrido-Baserba et al., 2018). An

Table 1
Description and water production for the different FO-RO + AnMBR scenarios.

	Scheme goals	Scenario 1[a] ($FO_{recovery}$ 50%)	Scenario 2[b] ($FO_{recovery}$ 80%)	Scenario 3[c] ($FO_{recovery}$ 90%)
Scheme A (m^3 d^{-1})	Open-loop maximising water production (π_{brine} = 46.7 bar)	4218	5550	5994
Scheme B (m^3 d^{-1})	Open-loop with limited water production (45% RO recovery)	2997	3596	3796
Scheme C (m^3 d^{-1})	Closed-loop using a synthetic draw solution of NaCl ($\pi_{initial}$ = 25.7 bar)	2220	3552	3996

[a] J_WFO = 7.86 LMH and J_SFO = 2.15 g m^{-2} h^{-1}.
[b] J_WFO = 5.90 LMH and J_SFO = 1.96 g m^{-2} h^{-1}.
[c] J_WFO = 3.98 LMH and J_SFO = 1.69 g m^{-2} h^{-1}.

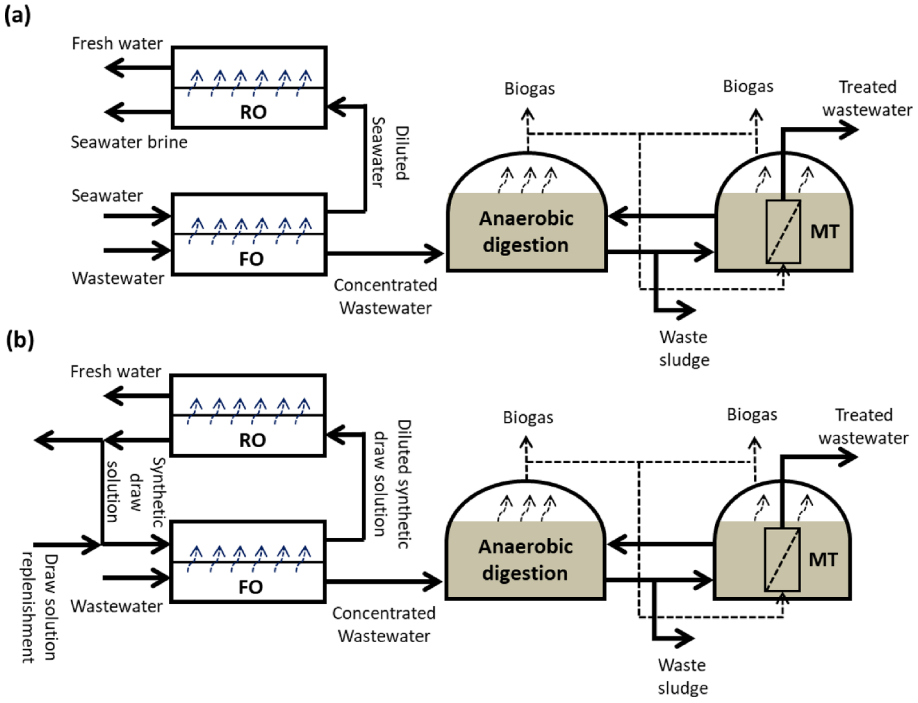

Fig. 1. Schematic representation of FO-RO + AnMBR process. (a) Open-loop scheme; (b) Closed-loop scheme. (MT: Membrane Tank; FO: Forward Osmosis; RO: Reverse Osmosis).

average seawater composition with an osmotic pressure of 25.7 bar was considered (Na^+ = 10,900 mg L^{-1}; Cl^- = 19,700 mg L^{-1}; SO_4^{2-} = 2,740 mg L^{-1}; Mg^{2+} = 1,310 mg L^{-1}; Ca^{2+} = 410 mg L^{-1}; K^+ = 390 mg L^{-1}; HCO_3^- = 152 mg L^{-1}).

2.2. FO-RO process design and costs

2.2.1. Design considerations

FO flux is governed by the osmotic gradient between the sewage and the draw solution. The solution-diffusion model is the most used model to describe water flux across dense FO membranes (Deshmukh et al., 2015; Kim et al., 2017). However, to accurately determine the FO flux, it is important to consider the effective osmotic gradient rather than the simple osmotic gradient. Thus, FO flux calculation needs to include (i) concentrative external concentration polarisation (ECP) on the active layer, (ii) concentrative internal concentration polarisation (ICP) on the support layer, and (iii) reverse salt diffusivity from draw solution to sewage solution (Eq. (1)) (Blandin et al., 2015; Kim et al., 2017). Eq. (1) describes the FO flux when the active layer is facing the feed side. This strategy exacerbates ICP on the support layer. However, it reduces fouling and, therefore, it is the preferred in the long term operation (Blandin et al., 2015).

$$J_W = A\cdot\left[\frac{\pi_{Dbulk}\cdot e^{-J_w\cdot\frac{S}{D}} - \pi_{Fbulk}\cdot e^{\frac{J_w}{k}}}{1-\frac{B}{J_W}\cdot\left(e^{-J_w\cdot\frac{S}{D}} - e^{\frac{J_w}{k}}\right)}\right] \quad (1)$$

where J_w is the water flux (L m^{-2} h^{-1}), $\pi_{D,\ bulk}$ is the osmotic pressure in the draw solution side (bar), $\pi_{F,\ bulk}$ is the osmotic pressure in the sewage side (bar), k is the mass transfer coefficient (38.52 L m^{-2} h^{-1}), D is the solute self-diffusion coefficient (5.33 × 10^{-3} L m^{-1} h^{-1}), S is the structural parameter (6.9 × 10^{-4} m), A is the pure water permeability (1.63 L m^{-2} h^{-1} bar^{-1}), and B is the salt permeability (0.2988 L m^{-2} h^{-1}) (Blandin et al., 2015). Regarding RO flux, an average flux of 15 LMH was considered according to literature (Valladares Linares et al., 2016; Teusner et al., 2017).

2.2.2. FO-RO capital costs

The methodology used to calculate the capital expenditures (CAPEX) of the FO-RO process was adapted from Blandin et al. (2015). Due to the limited data on FO costs some assumptions based on RO values were necessary. Scenario 1A was taken as a benchmark of this study since this scenario presented similar areas for both FO and RO membranes and, consequently, a more reliable estimation of FO CAPEX could be achieved.

CAPEX costs were split in costs directly depending on the surface area of RO unit (e.g. membranes, pressure vessels) and costs independent of the RO unit surface area (e.g. pre-treatment, intake/outfall). The independent costs were considered constant in all the scenarios. This approach made the CAPEX associated with the RO stage just a function of the membrane area. The CAPEX calculations for the FO stage were similar to the ones used for the RO stage. However, some devices such as pressure vessels and pressure exchangers were excluded from the FO CAPEX calculations. Price differences between the FO and RO membrane modules were considered. The lower packing density of FO modules makes FO modules more expensive than RO modules (Blandin et al., 2015). In this study, RO and FO modules were considered to have a cost of 24 and 55 $ m^{-2}, respectively (Teusner et al., 2017; Valladares Linares et al., 2016).

2.2.3. FO-RO operating costs

Energy consumption, membrane replacement, labour, maintenance, chemical reagent consumption and draw solution replenishment were considered as operating expenditures (OPEX).

Energy costs accounted for the energy consumption for: (i) seawater and wastewater pre-treatment, (ii) FO stage, and (iii) RO stage. Although the RO stage is the main energy consumer, to accurately determine the overall energy consumption it is important to include the other two processes (Choi et al., 2017). Pumping energy requirements for seawater pre-treatment were calculated using Eq. (2) (Wan and Chung, 2018).

$$E_{SWP} = \frac{\Delta P_{SWP}\cdot Q_{SW}}{36\cdot\eta_P} \quad (2)$$

where E_{SWP} is the energy consumption (kW), ΔP_{SWP} is the pressure difference (bar), Q_{SW} is the seawater influent flow rate ($m^3\ h^{-1}$), and η_p is the pump efficiency (85%).

The energy consumption of the FO stage was considered 0.3875 kWh m^{-3} which is the average energy consumption value reported for FO pilot-scale plants (Awad et al., 2019). The energy consumption for the RO stage was estimated using the Reverse Osmosis System Analysis (ROSA) software (Filmtec Corporation, US). Energy recovery devices (ERDs) were considered for recovering the energy from the RO brine. The energy recovered was calculated by using Eq. (3) (Wan and Chung, 2018).

$$E_{ERD} = \frac{\Delta P_{ERD} \cdot Q_{ERD} \cdot \eta_{ERD}}{36} \quad (3)$$

where E_{ERD} is the energy recovered by the device (kW), ΔP_{ERD} is the pressure difference (bar), Q_{ERD} is the flowrate feeding the device ($m^3\ h^{-1}$), and η_{ERD} is the efficiency of the ERD (95%).

Draw solution replenishment costs were considered for Scheme C (closed-loop scheme) to account for solute losses due to reverse solute flux (J_S) from draw solution to sewage in the FO stage and the diffusion flux from the diluted draw solution to the permeate in the RO stage. J_S was calculated using Eq. (4) (Kim et al., 2017; Tiraferri et al., 2013), while the solute diffusion in the RO stage was calculated from the final NaCl concentration in the permeate given by the ROSA software.

$$J_s = B \cdot \left[\frac{c_D \cdot e^{-J_W \cdot \frac{S}{D}} - c_F \cdot e^{\frac{J_W}{k}}}{1 + \frac{B}{J_W} \cdot \left(e^{\frac{J_W}{k}} - e^{-J_W \cdot \frac{S}{D}} \right)} \right] \quad (4)$$

where, besides the parameters described for Eq. (1), J_S is the reverse solute flux (g $m^{-2}\ h^{-1}$), c_D is the solute concentration in the draw solution (g L^{-1}), and c_F is the solute concentration in the feed solution (g L^{-1}).

2.3. AnMBR design and costs

2.3.1. Design considerations

The AnMBR was designed for psychrophilic conditions (20 °C). The selected configuration was submerged membranes since this configuration is commonly used for AnMBRs treating municipal sewage (Shin and Bae, 2018). A two-stage scheme consisting of a bioreactor and a separate membrane tank was used owing to the simpler membrane maintenance in comparison to a single-stage scheme. In this configuration, part of the generated biogas is recirculated for membrane scouring and fouling control. A specific gas sparging demand (SGD) of 0.23 $Nm^3\ m^{-2}\ h^{-1}$ was assumed (Giménez et al., 2011; Smith et al., 2014). For the ultrafiltration membrane area calculation, a net flux of 10 LMH was established (Giménez et al., 2011; Robles et al., 2013; Ruigómez et al., 2016; Smith et al., 2014).

The AnMBR was designed at a hydraulic retention time (HRT) of 1 day, and a solids retention time (SRT) of 60 days (Cashman et al., 2018; Hu and Stuckey, 2007; Prieto et al., 2013). Mixed liquor suspended solids (MLSS) concentration in the bioreactor was calculated according to Eq. (5) (Smith et al., 2014).

$$X_M = \frac{SRT}{HRT} \cdot \left[X_I + \frac{(1 + f_D \cdot k_d \cdot SRT) \cdot Y \cdot (S_{S,0} - S_S)}{1 + k_d \cdot SRT} \right] \quad (5)$$

where X_M is the MLSS concentration (mg TSS L^{-1}), SRT is the solids retention time (days), HRT is the hydraulic retention time (days), X_I is the inert solids concentration in the influent (mg L^{-1}), $S_{S,0}$ is the influent soluble organic matter (mg COD L^{-1}), S_S is the effluent soluble organic matter (mg COD L^{-1}), f_D is the decay coefficient (0.20 mg TSS mg TSS^{-1}), k_d is the decay rate (0.02 day $^{-1}$) and Y is the yield (0.076 mg TSS mg COD^{-1}).

Influent pre-concentration increases the concentration of biodegradable COD and inert COD in the AnMBR influent which, if improperly managed, can lead to the accumulation of inert particles in the membrane tank. Therefore, the recirculation flow from the bioreactor to the membrane tank is important to maintain a low solids concentration in the membrane tank and minimise membrane fouling (Ferrer et al., 2015). To determine this flow, a maximum MLSS concentration of 18 g L^{-1} was established for the membrane tank (Martinez-Sosa et al., 2011; Shin and Bae, 2018). However, in Scenario 3 (i.e., 90% pre-concentration) this threshold solids concentration was surpassed owing to the high concentration of inert particles in the influent. To reduce the solids concentration in the membrane tank and associated fouling, an HRT of 2 days was considered in Scenario 3.

2.3.2. AnMBR capital and operating costs

The MBR CAPEX accounts for civil engineering, mechanical and electrical, equipment and land costs (Judd, 2017). However, since the land cost is very site-specific it was excluded in this study. On the other hand, the OPEX analysis of the AnMBR included energy demand, sludge handling, membrane replacement, chemical reagents for membrane cleaning, equipment maintenance and replacement, and labour.

Energy consumption was considered for: (i) pumping and stirring, (iii) gas sparging, and (iii) centrifuge sludge dewatering. The energy consumption for stirring was assumed to be 8 W m^{-3} (Smith et al., 2014). The energy consumption of the centrifugal pumps was calculated using Eq. (6) (Wan and Chung, 2018).

$$E_P = \frac{\Delta P_P \cdot Q_P}{36 \cdot \eta_P} \quad (6)$$

where E_p is the energy consumption (kW), Q_P is the flow rate ($m^3\ h^{-1}$) ΔP_p is the differential head of the pump (bar), and η_p is the pump efficiency (85%).

The blower energy requirements for gas sparging were calculated using Eq. (7) (Pretel et al., 2014).

$$P_B = \frac{M \cdot R \cdot T}{(\alpha - 1) \cdot \eta_B} \cdot \left[\left(\frac{P_2}{P_1} \right)^{\frac{\alpha - 1}{\alpha}} - 1 \right] \quad (7)$$

where P_B is the blower consumption (W), M is the molar flow rate of biogas (mol s^{-1}), R is the gas constant (J $mol^{-1}\ K^{-1}$), T is the biogas temperature (K), α is the adiabatic coefficient, η_B is the blower efficiency (80%), P_2 is the absolute impulsion pressure of the blower (atm), and P_1 is the absolute inlet pressure of the blower (atm).

The energy consumption to dehydrate the AnMBR sludge by centrifugation was 0.045 kWh kg^{-1}TSS (Pretel et al., 2014). Electrolyte dosing was set at 6 kg t^{-1} TSS (Pretel et al., 2014b). No sludge disposal cost nor benefit was included. However, it was considered that the sludge would be highly stable (due to the 60 day SRT), and hence suitable to be reused as fertiliser (Pretel et al., 2015, 2014).

The membrane cleaning protocol included (i) a clean in place (CIP) performed once a week with 500 mg L^{-1} and 2000 mg L^{-1} of sodium hypochlorite and citric acid, respectively, and (ii) two annual cleaning out of place (COP) with 1000 mg L^{-1} and 2000 mg L^{-1} sodium hypochlorite and citric acid, respectively (Brepols et al., 2008; Verrecht et al., 2010).

2.4. FO-RO + AnMBR plant economic evaluation

The CAPEX and OPEX were calculated for the different scenarios. Benefits coming from biogas and water production were not considered in this study, since these benefits are rarely accounted for in the water sector (Maurer, 2009). Therefore, the discounted lifetime costs (DLC) of each option were calculated as the sum of the CAPEX and discounted OPEX during the plant lifetime (Eq. (8)) (Maurer, 2009; Roefs et al., 2016). The levelised cost method was used to obtain the unit cost of water production and wastewater treatment. This method is based on the price at which the outputs would have to be sold to incur a positive net present value. The unit cost was calculated by dividing the DLC by

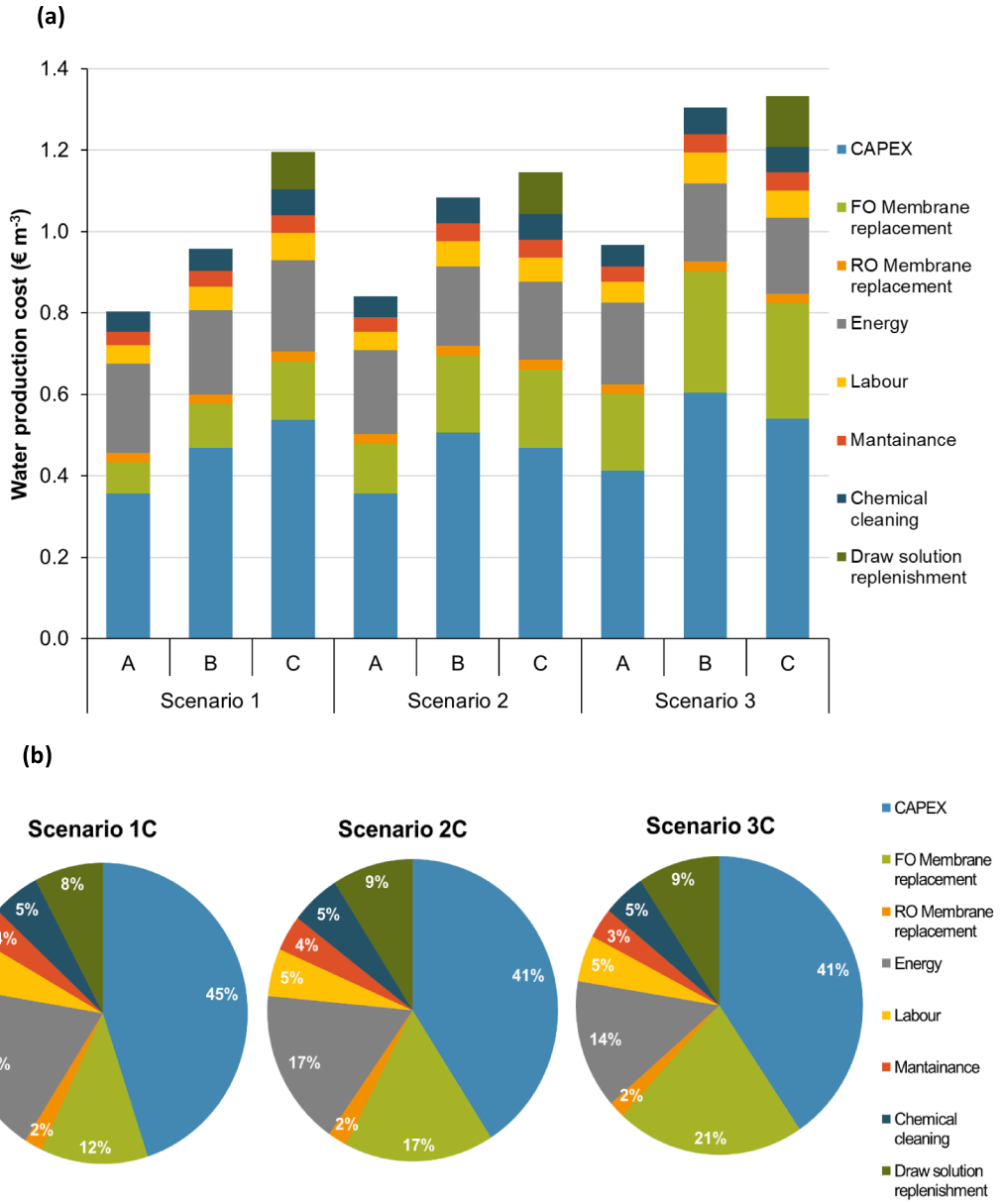

Fig. 2. Water production costs. (a) Costs of the different FO-RO scenarios; (b) Cost distribution of closed-loop scheme (Scheme C) for the different FO recoveries, i.e. 50%, 80% and 90%.

the discounted output produced throughout the lifetime (Eq. (9) and (10)) (Papapetrou et al., 2017).

$$\mathrm{DLC}(€) = \mathrm{CAPEX} + \sum_{t=1}^{T} \frac{\mathrm{OPEX_t}}{(1+i)^t} \tag{8}$$

$$\text{Water production cost}\,(€\cdot m^{-3}) = \frac{\mathrm{DLC}}{\sum_{t=1}^{T} \frac{Mw_t}{(1+i)^t}} \tag{9}$$

$$\text{Wastewater treatment cost}\,(€\cdot m^{-3}) = \frac{\mathrm{DLC}}{\sum_{t=1}^{T} \frac{Mww_t}{(1+i)^t}} \tag{10}$$

where $OPEX_t$ is the OPEX at year t (€), i is the discount rate (5%), T is the plant lifetime (20 years), Mw_t represents the volume of water produced at year t (m^3), and Mww_t represents the volume of wastewater treated at year t (m^3).

3. Results and discussion

3.1. FO-RO costs for reclaimed water production

Fig. 2a shows the unit cost of the water produced by FO-RO system for each scheme and scenario. The economy of FO-RO process is driven by (i) the low water flux performance and the larger number of FO membranes needed to achieve higher FO recoveries (i.e. 50% recovery in Scenario 1, 80% recovery in Scenario 2, and 90% recovery in Scenario 3) and by (ii) the osmotic pressure difference decrease between both sides of the membrane as the FO recovery increases. The latter phenomenon is particularly relevant since it makes the membrane area exponentially increases with FO recovery (Cath et al., 2010). This hinders the economic feasibility of the scenarios with an FO recovery of 80 and 90%.

Regarding the different schemes, Scheme A features the lowest water production cost per m^3 of water produced. The lower unit cost of Scheme A is a result of the much higher water production when compared to Scheme B and Scheme C (Table 1), which minimises the impact

of the FO capital and operating costs. The closed-loop configuration (Scheme C) presents the worst economic prospect for water production, mainly due to the cost related to the replenishment of the synthetic draw solution. In Scheme C, the RO stage is used to re-concentrate the diluted draw solution. Consequently, the diffusion of NaCl through FO and RO membranes requires the addition of NaCl to keep the draw solution osmotic pressure constant that leads to higher OPEX.

Fig. 2b shows the cost distribution of the closed-loop scheme for the three different FO recovery scenarios. CAPEX represents between 41 and 45% of the total cost. Concerning the OPEX, energy consumption and the replacement of the FO membranes are the major OPEX contributors. The contribution of the energy consumption in Scheme C (14–19%) is lower than the values reported for conventional seawater reverse osmosis (SWRO) plants which averages 30–40% (Blandin et al., 2015; Valladares Linares et al., 2016). This difference is attributed to (i) the lower energy consumption of FO-RO system compared to conventional SWRO due to the lower osmotic pressure of the diluted draw solution; and (ii) the significant contribution of the FO stage to the total cost. Fig. 2b shows that higher FO recoveries lower energy costs. However, increasing the FO recovery is accompanied by a significant increase in the costs associated with FO membrane replacement. In the case of 90% FO recovery (Scenario 3C), FO membrane replacement (21%) cost outweighs the cost of energy (14%). These results highlight the importance of improving FO performance and durability on the economic feasibility of the FO-RO system.

The lowest water production cost obtained from the different alternatives is 0.80 € m^{-3} (Scenario 1A), which is an 18% higher than the average cost of 0.76 $ m^{-3} reported for SWRO plants (Blandin et al., 2015). The CAPEX of an FO-RO system will always be higher than that of an SWRO system due to the costs associated with the FO stage. Therefore, the economic reliability of the FO-RO system is linked to potential energy savings which have been reported to reduce OPEX (Cath et al., 2010; Valladares Linares et al., 2016; Wan and Chung, 2018). In this study, energy savings are reached for all FO-RO systems when compared to typical SWRO values. However, these savings do not account for more than 17% of the total energy consumption (see Section 3.4). This value is in agreement with other conservative energy savings reported in the literature (Awad et al., 2019; Choi et al., 2017). The installation of advanced energy recovery devices (e.g. pressure exchangers) in SWRO plants has significantly improved its energy efficiency, thus narrowing the room for improvement of the FO-RO technology. The present study shows that there is a compromise among energy savings, CAPEX and other OPEX such as membrane replacement, labour, maintenance or draw solution replenishment. Therefore, it can be concluded that the economic competitiveness of the FO-RO technology goes beyond energy savings.

3.2. AnMBR costs for sewage treatment and biogas production

Fig. 3a shows the wastewater treatment cost related to the AnMBR stage for the different scenarios under study. The incorporation of the FO stage leads to a noticeable reduction of the AnMBR costs. This cost reduction is related to the lower influent flow and the associated lower digester volume, lower membrane area, and lower energy requirements for gas sparging, among others. Additionally, although it has not been included in this techno-economic analysis, it might also reduce the AnMBR footprint.

CAPEX is the most important contributor to the AnMBR total cost representing between 63 and 77% of it, being the digester construction and membrane acquisition the major capital costs. In this study, an HRT of 1 day was selected, although lower HRTs (less than 10 h) would further decrease CAPEX costs (Stuckey, 2012). However, the technical feasibility of extremely short HRTs is questionable when combined with FO pre-concentration, due to the increased MLSS concentration in the bioreactor and the resulting increase of both the SGD and the recirculation flow from the bioreactor to the membrane tank. Moreover, short HRTs may reduce the COD removal efficiency (Maaz et al., 2019). Therefore, FO + AnMBR systems operated at HRTs below 1 day are not expected to provide economic benefits, particularly when treating highly concentrated influents such as in Scenario 2 (80% FO recovery) and Scenario 3 (90% FO recovery).

OPEX contribution to the AnMBR total cost is relatively low, even more when compared to the conventional activated sludge system, due to the low energy requirements (no aeration requirements) and the low sludge handling cost (less sludge production). The energy consumption of the fouling control method (i.e. gas sparging) and, to a lesser extent, the recirculation pump, are the main OPEX contributors of the AnMBR. Thereby, energy cost optimisation should target these two parameters.

The SRT is an important operational parameter to optimise OPEX of MBR systems (Verrecht et al., 2010). MLSS concentration decreases at lower SRTs and, accordingly, both SGDs and recirculation flow decrease. Furthermore, a lower MLSS concentration is expected to alleviate membrane fouling, which might have a direct influence on the membrane lifespan (i.e. membrane replacement costs) and chemical cleaning requirements (Ozgun et al., 2013). Decreasing SRT and increasing the sludge production would have a minimum impact on the AnMBR OPEX since sludge handling contributes less than 5% to the OPEX. However, in cold climates, decreasing SRT could jeopardise the efficiency of the biological process due to the slower kinetics of the anaerobic microbes at psychrophilic temperatures (Maaz et al., 2019). Regardless of the operational temperature, the influence of SRT on AnMBR performance is expected to progressively increase with the increase of the FO recovery as a result of the higher organic loading rates. Therefore, the SRT should be optimised for each FO recovery with the aim of improving the AnMBR performance while keeping reasonable operating costs. Membrane replacement is the other main contributor to the AnMBR OPEX due to the large membrane area required to achieve the permeate flux and the relatively short lifespan of membrane modules (5–10 years). Low membrane flux is recognised as one of the main economic bottlenecks slowing the progress of the AnMBR technology (Lin et al., 2011; Ozgun et al., 2013).

Increasing membrane fluxes would have a positive effect on the CAPEX costs. However, it can be accompanied by an increase in OPEX owing to the higher SGDs required. Verrecht et al. (2010) noticed that increasing the flux of aerobic MBRs from 15 to 30 LMH reduced the net present value (NPV) by 9% despite the higher OPEX. However, special attention should be given when combining FO pre-concentration with high membrane fluxes (greater than 15 LMH) since the higher MLSS concentrations can exponentially increase the SGDs to keep a stable flux. This could compromise the economic feasibility of AnMBR plants.

3.3. FO-RO + AnMBR cost for integrated sewage treatment and water production

Fig. 3b shows the unit cost of wastewater treatment per m^3 of wastewater treated for the entire FO-RO + AnMBR system. The economy of the system is governed by FO-RO system since it accounts for more than 74% of the total cost in all scenarios. The contribution of the FO-RO system increases as the FO recovery increases. For instance, in Scheme A, the contribution of the FO-RO system to the total cost increases from 75% in Scenario 1 (50% FO recovery) to 90% and 94% for Scenario 2 (80% FO recovery) and Scenario 3 (90% FO recovery), respectively. As discussed in Section 3.2, the higher the FO recovery, the lower the AnMBR cost (Fig. 3a). However, the reduced AnMBR cost does not offset the cost of the FO-RO system. Accordingly, the 50% FO recovery scenarios present the lowest wastewater treatment cost when compared to the 80% and 90% FO recovery scenarios (Fig. 3b).

Scenario 1C (i.e. 50% FO recovery in a closed-loop scheme) is the most economical scenario (0.81 € m^{-3}) owing to the lower water production in the RO step (i.e. 33% recovery), which reduces both CAPEX and OPEX. However, the inclusion of benefits coming from water production could change the economic prospect of this scenario

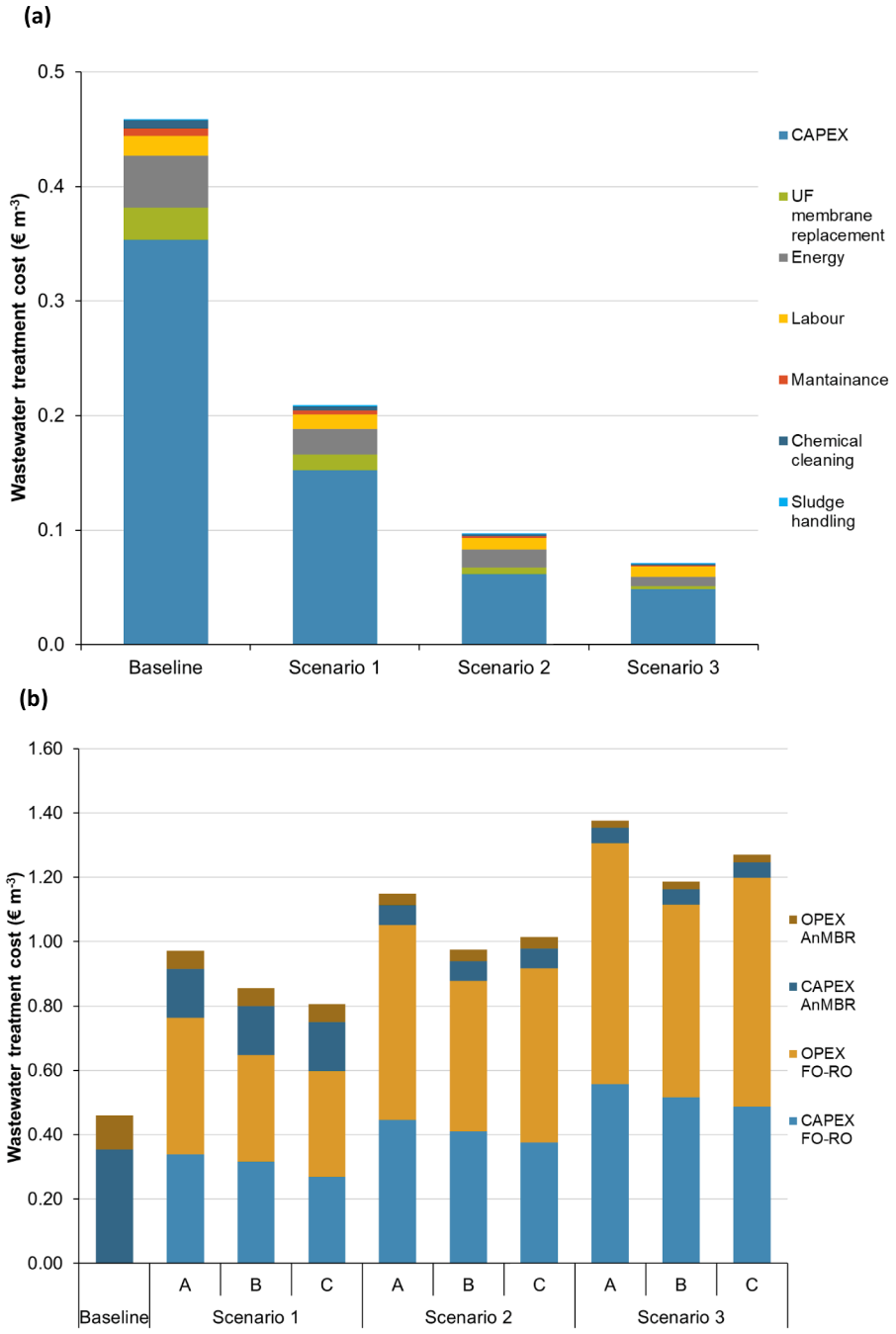

Fig. 3. Wastewater treatment cost for an influent flow rate of 4440 m^3 d^{-1}. (a) AnMBR costs for the different FO scenarios. (b) FO-RO + AnMBR costs for the different scenarios.

since it presents the lowest water production (Table 1). In Scenarios 2 and 3, with higher FO and RO recoveries and higher water productions, Scheme B is cheaper than Scheme C since draw solution replenishment is not needed. NaCl is the most widespread draw solution. However, other solutes (e.g. Mg^{+2}, organic) could be considered to reduce reverse solute flux (Lee and Hsieh, 2019). Alternative solutes would increase the initial chemicals acquisition investment. Nevertheless, these would be negligible compared to the OPEX savings resulting from the reduced draw solution replenishment cost and the higher osmotic pressure of the solution. An ideal solute should have a low reverse solute flux and little impact on microbial activity and digestate quality.

Scheme A, where the production of water is maximised, is the most expensive alternative for wastewater treatment, due to the high cost of the RO installations. Accordingly, this scheme is suitable in coastal regions lacking fresh water, where these higher costs are offset by the benefits obtained from water production. Otherwise, restricting the RO recovery to 45% (Scheme B) is the most favourable condition for areas without water scarcity (Blandin et al., 2015; Teusner et al., 2017).

The estimated cost from plants combining wastewater treatment and fresh water production (e.g. MBR + RO, MBR + RO + AOP and CAS + UF + RO) ranges from 0.6 to 1.0 € per m^3 of wastewater treated (Valladares Linares et al., 2016; Verstraete et al., 2009). Scenario 1 (50% of FO recovery) is the only competitive economic alternative for combining wastewater treatment and water production since the treatment cost ranges between 0.81 and 0.97 € per m^3 of wastewater treated (Fig. 3b). These results corroborate that improving FO

membrane fluxes is paramount to make this technology competitive.

The competitiveness of the FO-RO + AnMBR system is worsened when compared with stand-alone AnMBR (baseline scenario) since the wastewater treatment cost of the stand-alone AnMBR is half than the cheapest FO-RO scenario (Scenario 1C). Nevertheless, including incomes from biogas and water production as well as other factors such as the dual barrier for pollutants provided by FO-RO system (e.g. improving social perception of water produced, increasing pollutants rejection) might improve the overall competitiveness of FO-RO + AnMBR system.

3.4. Economic prospect of retrofitting an SWRO into an FO-RO + AnMBR plant

The FO-RO + AnMBR system is not yet economically feasible when compared to an SWRO plant or stand-alone AnMBR. However, as technology develops, some schemes combining water production and wastewater treatment could make FO-RO + AnMBR a suitable alternative. Indeed, the incorporation of FO stage to an existing SWRO plant has been identified as an attractive scenario for FO technology (Blandin et al., 2016; Teusner et al., 2017). This approach may be an attractive alternative in coastal areas undergoing rapid urbanisation, where the increased population overloads the existing WWTP infrastructure and increases the demand of fresh water (Li et al., 2014). Such coastal areas may require at some point to increase the capacity of the WWTP or construct a new WWTP and, in places where there is a nearby SWRO plant, retrofitting the conventional SWRO to an FO-RO system could be a competitive alternative. Although implementing an FO stage would incur extra capital and operating expenses, these might be compensated by the lower wastewater treatment cost when combining seawater desalination and wastewater treatment plants.

The scheme under study incorporated an FO stage into an SWRO plant since this scenario is considered to be the best approach to reduce an SWRO plant energy consumption (Blandin et al., 2016). The FO recovery (i.e. 50, 80 or 90%) affects both (i) the wastewater concentration and flow rate of the AnMBR influent and (ii) the seawater osmotic pressure and flow rate feeding the RO stage. The concentrated wastewater was fed into a newly constructed AnMBR. The three FO recovery scenarios were compared to the baseline SWRO plant to assess the energy savings related to seawater dilution. All the scenarios were evaluated on the basis of a final water production of 45,000 m^3 day^{-1} (Blandin et al., 2015).

Fig. 4 shows that adding an FO stage in an existing SWRO plant combined with AnMBR treatment is economically competitive for a 50% FO recovery. Fig. 4 also shows that as the FO recovery increases and the FO cost increases, the cost savings from AnMBR also increases (primarily due to the lower digester volume and the lower membrane surface). However, when the FO recovery is 80%, the lower AnMBR cost does not offset the costs associated with the FO stage.

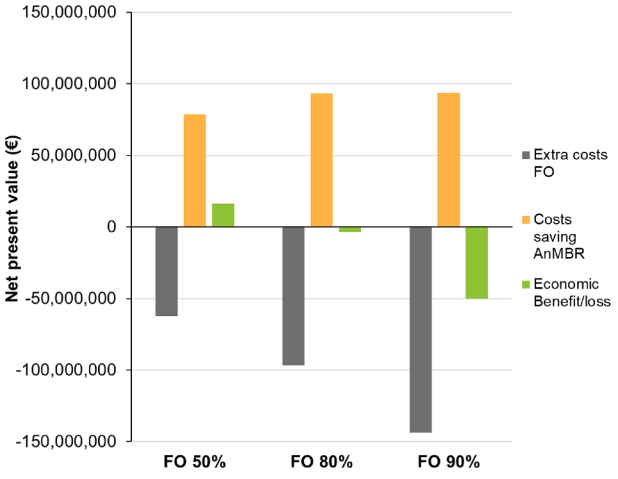

Fig. 4. Economic evaluation of retrofitting SWRO plants to FO-RO + AnMBR plants.

To incorporate the FO process into a SWRO plant leads to improving the energy efficiency of the desalination plant (energy saving = 11.5, 15.0 and 16.2% for FO recoveries of 50, 80 and 90%, respectively). However, this situation does not always relate to a better economic prospect. As a matter of fact, the low fluxes of the FO membranes have a major impact on the process economics than energy consumption. A clear example is Scenario 3 (i.e. 90% FO recovery) which displays the worse economic prospect with a benefit-cost ratio (BCR) of 0.65 despite being the scenario that has the highest energy saving. Accordingly, considering the current development of FO technology, FO recoveries around 50% appear as the most suitable condition to integrate FO-RO + AnMBR technology.

3.5. Sensitivity analysis of the flux impact on FO-RO + AnMBR economics

The low water fluxes reported for FO membranes is the main bottleneck of FO technology. Therefore, improving membrane fluxes is crucial to boost the competitiveness of FO technology. In this regard, the sensitivity analysis shows that the wastewater treatment costs sharply decrease as the FO water fluxes increase from 1 LMH to 10 LMH (Fig. 5). The impact of water fluxes is particularly relevant for Scenario 2 and 3 (i.e. 80 and 90% of recovery) where higher water permeation through the FO membranes is required. Water fluxes above 10 LMH only lead to small improvements in the wastewater treatment costs. This is due to the fact that as the FO fluxes increase the influence of the FO stage (e.g. membrane replacement, labour, maintenance) on the process total cost is minimised.

Scenario 1 is the most competitive, although the differences with Scenario 2 and 3 are substantially narrowed when FO fluxes increase (greater than 10 LMH). In fact, when the water flux is above 20 LMH, Scenario 2B outcompetes Scenario 1B emphasising the windows of opportunities that high FO recoveries would open.

When the FO flux is higher than 10 LMH, closed-loop schemes with FO recoveries below or equal to 80% (Scenario 1 and 2) are more economically competitive than open-loop schemes, due to (i) the reduction in membrane area is accompanied by a reduction in the reverse solute flow rate and (ii) the intake/outfall and pre-treatment of seawater becomes costlier than that required for draw solution replenishment. However, it is important to consider that the accumulation of

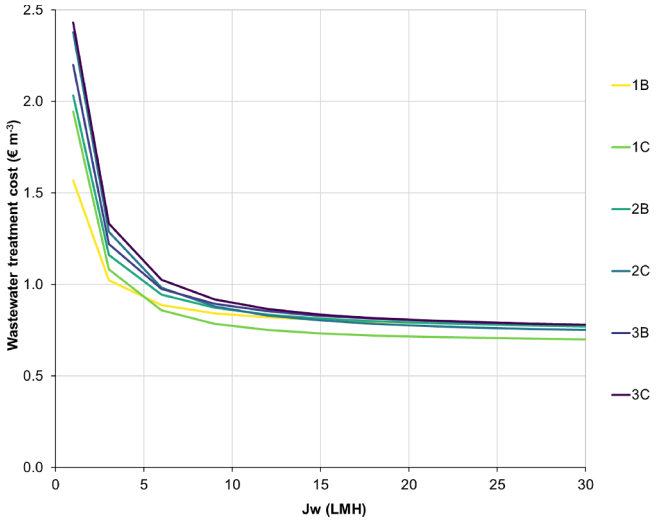

Fig. 5. Sensitivity analysis of FO-RO + AnMBR cost in function to the FO membrane flux for Scheme B and C. Scheme A was not included since it displays the highest treatment cost.

contaminants in the draw solution may occur in closed-loop systems, which may reduce the quality of the recovered water in these schemes (Blandin et al., 2016; D'Haese et al., 2013).

From the sensitivity analysis, it can be concluded that increasing FO flux up to 10 LMH can reduce the wastewater costs to values below 0.80 € m^{-3}, being Scenario 1C the most cost-effective one with a treatment cost of 0.70 € m^{-3} (Fig. 5). This cost would be further reduced if incomes coming from biogas production and, especially, water production were considered. Finally, it is worth to mention that membrane fluxes for FO pilot plants range from 2.2 to 10.6 LMH (Awad et al., 2019). Thus, it is conceivable that fluxes around 10 LMH could be achieved soon for scenarios with water recoveries around 50%. However, in scenarios with higher water recoveries (e.g. 80 and 90%) reaching a flux of 10 LMH still requires further technology advances since it would be required to double or triple current fluxes.

4. Conclusions

The feasibility of combining FO, RO and AnMBR technologies for wastewater treatment with energy and water production was investigated. The minimum wastewater treatment cost was 0.81 € m^{-3} when FO recovery was restricted to 50% in a closed-loop scheme. The treatment cost increased to 1.01 and 1.27 € m^{-3} for FO recoveries of 80% and 90%, respectively. The minimum fresh water production cost was estimated at 0.80 and 1.16 € m^{-3} for an open-loop and a closed-loop scheme. The sensitivity analysis showed that reaching FO fluxes of 10 LMH would significantly improve the competitiveness of FO-RO + AnMBR system for sewage treatment.

Declaration of competing interest

The authors declare that they have no known competing financial interests or personal relationships that could have appeared to influence the work reported in this paper. The authors also declare that this manuscript reflects the author's view and that the European Commission is not responsible for any use that may be made of the information it contains.

Acknowledgments

The authors acknowledge the European Union LIFE programme for the financial support (LIFE Green Sewer project, LIFE17 ENV/ES/000341). Sergi Vinardell is grateful to the Generalitat de Catalunya for his predoctoral FI grant (2019FI_B 00394). Sergi Astals is grateful to the Spanish Ministry of Science, Innovation and Universities for his Ramon y Cajal fellowship (RYC-2017-22372). The authors thank Miriam Peces from Aalborg University (Denmark) for her scientific contribution and proofreading the manuscript.

Appendix A. Supplementary data

Supplementary data to this article can be found online at https://doi.org/10.1016/j.biortech.2019.122395.

References

Ansari, A.J., Hai, F.I., Price, W.E., Drewes, J.E., Nghiem, L.D., 2017. Forward osmosis as a platform for resource recovery from municipal wastewater - A critical assessment of the literature. J. Membr. Sci. 529, 195–206.
Ansari, A.J., Hai, F.I., Price, W.E., Ngo, H.H., Guo, W., Nghiem, L.D., 2018. Assessing the integration of forward osmosis and anaerobic digestion for simultaneous wastewater treatment and resource recovery. Bioresour. Technol. 260, 221–226.
Awad, A.M., Jalab, R., Minier-Matar, J., Adham, S., Nasser, M.S., Judd, S.J., 2019. The status of forward osmosis technology implementation. Desalination 461, 10–21.
Blandin, G., Verliefde, A.R.D., Comas, J., Rodriguez-Roda, I., Le-Clech, P., 2016. Efficiently combining water reuse and desalination through forward osmosis-reverse osmosis (FO-RO) hybrids: a critical review. Membranes (Basel). 6, 37.
Blandin, G., Verliefde, A.R.D., Tang, C.Y., Le-Clech, P., 2015. Opportunities to reach economic sustainability in forward osmosis–reverse osmosis hybrids for seawater desalination. Desalination 363, 26–36.
Brepols, C., Drensla, K., Janot, A., Trimborn, M., Engelhardt, N., 2008. Strategies for chemical cleaning in large scale membrane bioreactors. Water Sci. Technol. 57, 457–463.
Cashman, S., Ma, X., Mosley, J., Garland, J., Crone, B., Xue, X., 2018. Energy and greenhouse gas life cycle assessment and cost analysis of aerobic and anaerobic membrane bioreactor systems: influence of scale, population density, climate, and methane recovery. Bioresour. Technol. 254, 56–66.
Cath, T.Y., Childress, A.E., Elimelech, M., 2006. Forward osmosis: principles, applications, and recent developments. J. Membr. Sci. 281, 70–87.
Cath, T.Y., Hancock, N.T., Lundin, C.D., Hoppe-Jones, C., Drewes, J.E., 2010. A multi-barrier osmotic dilution process for simultaneous desalination and purification of impaired water. J. Membr. Sci. 362, 417–426.
Choi, B.G., Zhan, M., Shin, K., Lee, S., Hong, S., 2017. Pilot-scale evaluation of FO-RO osmotic dilution process for treating wastewater from coal-fired power plant integrated with seawater desalination. J. Membr. Sci. 540, 78–87.
D'Haese, A., Le-Clech, P., Van Nevel, S., Verbeken, K., Cornelissen, E.R., Khan, S.J., Verliefde, A.R.D., 2013. Trace organic solutes in closed-loop forward osmosis applications: influence of membrane fouling and modeling of solute build-up. Water Res. 47, 5232–5244.
Deshmukh, A., Yip, N.Y., Lin, S., Elimelech, M., 2015. Desalination by forward osmosis: identifying performance limiting parameters through module-scale modeling. J. Membr. Sci. 491, 159–167.
Ferrari, F., Balcazar, J.L., Rodriguez-Roda, I., Pijuan, M., 2019. Anaerobic membrane bioreactor for biogas production from concentrated sewage produced during sewer mining. Sci. Total Environ. 670, 993–1000.
Ferrer, J., Pretel, R., Durán, F., Giménez, J.B., Robles, A., Ruano, M.V., Serralta, J., Ribes, J., Seco, A., 2015. Design methodology for submerged anaerobic membrane bioreactors (AnMBR): a case study. Sep. Purif. Technol. 141, 378–386.
Garrido-Baserba, M., Vinardell, S., Molinos-Senante, M., Rosso, D., Poch, M., 2018. The economics of wastewater treatment decentralization: a techno-economic evaluation. Environ. Sci. Technol. 52, 8965–8976.
Giménez, J.B., Robles, A., Carretero, L., Durán, F., Ruano, M.V., Gatti, M.N., Ribes, J., Ferrer, J., Seco, A., 2011. Experimental study of the anaerobic urban wastewater treatment in a submerged hollow-fibre membrane bioreactor at pilot scale. Bioresour. Technol. 102, 8799–8806.
Guest, J.S., Skerlos, S.J., Barnard, J.L., Beck, M.B., Daigger, G.T., Hilger, H., Jackson, S.J., Karvazy, K., Kelly, L., Macpherson, L., Mihelcic, J.R., Pramanik, A., Raskin, L., Van Loosdrecht, M.C.M., Yeh, D., Love, N.G., 2009. A new planning and design paradigm to achieve sustainable resource recovery from wastewater. Environ. Sci. Technol. 43, 6126–6130.
Hancock, N.T., Black, N.D., Cath, T.Y., 2012. A comparative life cycle assessment of hybrid osmotic dilution desalination and established seawater desalination and wastewater reclamation processes. Water Res. 46, 1145–1154.
Hu, A.Y., Stuckey, D.C., 2007. Activated carbon addition to a submerged anaerobic membrane bioreactor: effect on performance, transmembrane pressure, and flux. J. Environ. Eng. 133, 73–80.
Itliong, J.N., Villagracia, A.R.C., Moreno, J.L.V., Rojas, K.I.M., Bernardo, G.P.O., David, M.Y., Manrique, R.B., Ubando, A.T., Culaba, A.B., Padama, A.A.B., Ong, H.L., Chang, J.S., Chen, W.H., Kasai, H., Arboleda, N.B., 2019. Investigation of reverse ionic diffusion in forward-osmosis-aided dewatering of microalgae: a molecular dynamics study. Bioresour. Technol. 279, 181–188.
Jalab, R., Awad, A.M., Nasser, M.S., Minier-Matar, J., Adham, S., Judd, S.J., 2019. An empirical determination of the whole-life cost of FO-based open-loop wastewater reclamation technologies. Water Res. 163, 114879.
Judd, S.J., 2017. Membrane technology costs and me. Water Res. 122, 1–9.
Kim, J.E., Phuntsho, S., Chekli, L., Hong, S., Ghaffour, N., Leiknes, T.O., Choi, J.Y., Shon, H.K., 2017. Environmental and economic impacts of fertilizer drawn forward osmosis and nanofiltration hybrid system. Desalination 416, 76–85.
Lee, D.J., Hsieh, M.H., 2019. Forward osmosis membrane processes for wastewater bioremediation: research needs. Bioresour. Technol. 290, 121795.
Li, Z., Valladares Linares, R., Abu-Ghdaib, M., Zhan, T., Yangali-Quintanilla, V., Amy, G., 2014. Osmotically driven membrane process for the management of urban runoff in coastal regions. Water Res. 48, 200–209.
Lin, H., Chen, J., Wang, F., Ding, L., Hong, H., 2011. Feasibility evaluation of submerged anaerobic membrane bioreactor for municipal secondary wastewater treatment. Desalination 280, 120–126.
Luo, H., Wang, Q., Zhang, T.C., Tao, T., Zhou, A., Chen, L., Bie, X., 2014. A review on the recovery methods of draw solutes in forward osmosis. J. Water Process Eng. 4, 212–223.
Maaz, M., Yasin, M., Aslam, M., Kumar, G., Atabani, A.E., Idrees, M., Anjum, F., Jamil, F., Ahmad, R., Khan, A.L., Lesage, G., Heran, M., Kim, J., 2019. Anaerobic membrane bioreactors for wastewater treatment: novel configurations, fouling control and energy considerations. Bioresour. Technol. 283, 358–372.
Martinez-Sosa, D., Helmreich, B., Netter, T., Paris, S., Bischof, F., Horn, H., 2011. Anaerobic submerged membrane bioreactor (AnSMBR) for municipal wastewater treatment under mesophilic and psychrophilic temperature conditions. Bioresour. Technol. 102, 10377–10385.
Maurer, M., 2009. Specific net present value: an improved method for assessing modularisation costs in water services with growing demand. Water Res. 43, 2121–2130.
McCarty, P.L., Bae, J., Kim, J., 2011. Domestic wastewater treatment as a net energy producer - can this be achieved? Environ. Sci. Technol. 45, 7100–7106.
Ozgun, H., Dereli, R.K., Ersahin, M.E., Kinaci, C., Spanjers, H., Van Lier, J.B., 2013. A review of anaerobic membrane bioreactors for municipal wastewater treatment: integration options, limitations and expectations. Sep. Purif. Technol. 118, 89–104.

Papapetrou, M., Cipollina, A., Commare, U.La., Micale, G., Zaragoza, G., Kosmadakis, G., 2017. Assessment of methodologies and data used to calculate desalination costs. Desalination 419, 8–19.
Pretel, R., Robles, A., Ruano, M.V., Seco, A., Ferrer, J., 2014. The operating cost of an anaerobic membrane bioreactor (AnMBR) treating sulphate-rich urban wastewater. Sep. Purif. Technol. 126, 30–38.
Pretel, R., Shoener, B.D., Ferrer, J., Guest, J.S., 2015. Navigating environmental, economic, and technological trade-offs in the design and operation of submerged anaerobic membrane bioreactors (AnMBRs). Water Res. 87, 531–541.
Prieto, A.L., Futselaar, H., Lens, P.N.L., Bair, R., Yeh, D.H., 2013. Development and start up of a gas-lift anaerobic membrane bioreactor (Gl-AnMBR) for conversion of sewage to energy, water and nutrients. J. Membr. Sci. 441, 158–167.
Puyol, D., Batstone, D.J., Hülsen, T., Astals, S., Peces, M., Krömer, J.O., 2017. Resource recovery from wastewater by biological technologies: opportunities, challenges, and prospects. Front. Microbiol. 7.
Robles, A., Ruano, M.V., Ribes, J., Ferrer, J., 2013. Factors that affect the permeability of commercial hollow-fibre membranes in a submerged anaerobic MBR (HF-SAnMBR) system. Water Res. 47, 1277–1288.
Roefs, I., Meulman, B., Vreeburg, J.H.G., Spiller, M., 2016. Centralised, decentralised or hybrid sanitation systems ? Economic evaluation under urban development uncertainty and phased expansion. Water Res. 109, 274–286.
Ruigómez, I., Vera, L., González, E., Rodríguez-Sevilla, J., 2016. Pilot plant study of a new rotating hollow fibre membrane module for improved performance of an anaerobic submerged MBR. J. Membr. Sci. 514, 105–113.
Shaffer, D.L., Werber, J.R., Jaramillo, H., Lin, S., Elimelech, M., 2015. Forward osmosis: where are we now? Desalination 356, 271–284.
Shin, C., Bae, J., 2018. Current status of the pilot-scale anaerobic membrane bioreactor treatments of domestic wastewaters: a critical review. Bioresour. Technol. 247, 1038–1046.
Smith, A.L., Stadler, L.B., Cao, L., Love, N.G., Raskin, L., Skerlos, S.J., 2014. Navigating wastewater energy recovery strategies: a life cycle comparison of anaerobic membrane bioreactor and conventional treatment systems with anaerobic digestion. Environ. Sci. Technol. 48, 5972–5981.
Stuckey, D.C., 2012. Recent developments in anaerobic membrane reactors. Bioresour. Technol. 122, 137–148.
Teusner, A., Blandin, G., Le-Clech, P., 2017. Augmenting water supply by combined desalination/water recycling methods: an economic assessment. Environ. Technol. (United Kingdom) 38, 257–265.
Tiraferri, A., Yip, N.Y., Straub, A.P., Romero-Vargas Castrillon, S., Elimelech, M., 2013. A method for the simultaneous determination of transport and structural parameters of forward osmosis membranes. J. Membr. Sci. 444, 523–538.
Valladares Linares, R., Li, Z., Yangali-Quintanilla, V., Ghaffour, N., Amy, G., Leiknes, T., Vrouwenvelder, J.S., 2016. Life cycle cost of a hybrid forward osmosis – low pressure reverse osmosis system for seawater desalination and wastewater recovery. Water Res. 88, 225–234.
Verrecht, B., Maere, T., Nopens, I., Brepols, C., Judd, S., 2010. The cost of a large-scale hollow fibre MBR. Water Res. 44, 5274–5283.
Verstraete, W., Van de Caveye, P., Diamantis, V., 2009. Maximum use of resources present in domestic “used water”. Bioresour. Technol. 100, 5537–5545.
Wan, C.F., Chung, T.S., 2018. Techno-economic evaluation of various RO + PRO and RO + FO integrated processes. Appl. Energy 212, 1038–1050.

SUPPLEMENTARY INFORMATION

Techno-economic analysis of combining forward osmosis-reverse osmosis and anaerobic membrane bioreactor technologies for municipal wastewater treatment and water production

Sergi Vinardell[a,*], Sergi Astals[a], Joan Mata-Alvarez[a], Joan Dosta[a]

*Corresponding author (e-mail: svinardell@ub.edu)

Tables

Figure

Table S1. CAPEX Distribution for FO and RO processes. Adapted from Blandin et al. (2015)

	Overall RO plant CAPEX for the benchmark (%)	**% connected to RO**	**% RO CAPEX estimated area dependent**	**% FO Connected to RO benchmark**	**% FO CAPEX estimated area dependent**
Installation/services	7.4	50	0	100	0
Legal	1.0	50	0	100	0
Design	6.9	50	0	100	0
Civil engineering	15.8	50	100	100	100
Pre-treatment[1]	7.9	0	0	0	0
Equipment and materials	25.4	50	75	75	75
Membrane[2]	5.5	100	100	-	100
Pressure vessels	1.5	100	100	0	0
Pumps	7.3	50	75	50	75
Energy recovery	2.0	100	50	0	0
Piping	12.3	50	100	50	100
Intake/Outfall	7.0	0	0	0	0

[1] Pre-treatment costs were considered depending on the scenario (i.e. closed-loop or opened-loop).

[2] Membrane costs of FO and RO were determined depending on the flux and the permeate flow rate for each scenario.

Table S2. Summary of the parameters used for FO-RO OPEX assessment

Parameter (units)	Value	References
FO membranes life time (years)	4	Teusner et al., 2017; Yangali-Quintanilla et al., 2015[a]
RO membranes life time (years)	5	Avlonitis et al., 2003[b]; Yangali-Quintanilla et al., 2015
Labour cost (% to CAPEX)	1	Fritzmann et al., 2015[c]
Maintenance cost (€ m^{-3})	0.022	Fritzmann et al., 2015
Chemical cost (€ m^{-3})	0.0318	Fritzmann et al., 2015
NaCl cost (€ kg^{-1})	0,22	Corzo et al., 2017[d]
FO energy consumption (kWh m^{-3})	0.3875	Awad et al., 2019
Electricity price (€ kWh^{-1})	0.1149	Eurostat, 2018[e]
ΔP pre-treatment (bar)	0.6	Wan and Chung, 2018
Pump efficiency	0.85	Wan and Chung, 2018
ERD efficiency	0.95	Blandin et al., 2015

References that do not appear in the manuscript:

[a] Yangali-Quintanilla, V. et al. 2015. Lowering desalination costs by alternative desalination and water reuse scenarios. Desalin. Water Treat. 55, 2437–2445.

[b] Avlonitis, S.A. et al. 2003. Energy consumption and membrane replacement cost for seawater RO desalination plants. Desalination 157, 151–158.

[c] Fritzmann, C. et al. 2007. State-of-the-art reverse osmosis desalination. Desalination. 216, 1–76.

[d] Corzo, B. et al. 2017. Evaluation of draw solutions and commercially available forward osmosis membrane modules for wastewater reclamation at pilot scale. Chem. Eng. J. 326, 1–8.

[e] Eurostat Electricity price statistics [Online]. Accessed 30 September 2018.

Table S3. Inputs to ROSA software

	Scenario 1			Scenario 2			Scenario 3		
	A	B	C	A	B	C	A	B	C
Permeate production (m^3 h^{-1})	175.74	124.88	92.41	231.25	149.85	147.85	249.74	158.17	166.5
Flux (LMH)	15	15	15	15	15	15	15	15	15
RO Recovery (%)	63.3	45	33.3	69.44	45	44.4	71.05	45	47.37
Seawater classification	Ultrafiltration pre-treatment, SDI<2.5	Ultrafiltration pre-treatment, SDI<2.5	Ultrafiltration pre-treatment, SDI<2.5	Ultrafiltration pre-treatment, SDI<2.5	Ultrafiltration pre-treatment, SDI<2.5	Ultrafiltration pre-treatment, SDI<2.5	Ultrafiltration pre-treatment, SDI<2.5	Ultrafiltration pre-treatment, SDI<2.5	Ultrafiltration pre-treatment, SDI<2.5
Π_{IN} (bar)	16.44	16.44	16.44	13.70	13.70	13.70	12.98	12.98	12.98
T (ºC)	20	20	20	20	20	20	20	20	20
Membrane Type	SW30-4040	SW30-4040	SW30-4040	SW30-4040	SW30-4040	SW30-4040	SW30-4040	SW30-4040	SW30-4040
High pressure pump efficiency	0.9	0.9	0.9	0.9	0.9	0.9	0.9	0.9	0.9
Configuration	1 pass 2 stages	1 pass	1 pass	1 pass 2 stages	1 pass	1 pass	1 pass 2 stages	1 pass	1 pass
Total number of pressure vessels	199	141	105	262	170	168	283	179	189
Elements per pressure vessel	8	8	8	8	8	8	8	8	8

Table S4. Summary of the parameters used for AnMBR CAPEX and OPEX assessment

Parameter (units)	Value	Reference
Anaerobic reactor and membrane tank construction (€ m^{-3})	220	Verrecht et al., 2010
UF Membrane acquisition (€ m^{-2})	50	Brepols et al., 2010[a]; Lin et al., 2011; Verrecht et al., 2010
Blower acquisition (€ Nm^{-3} h^{-1})	4.15	Verrecht et al., 2010
Permeate pump acquisition (€ m^{-3} h^{-1})	58.8	Verrecht et al., 2010
Biomass pump acquisition (€ m^{-3} h^{-1})	12.1	Verrecht et al., 2010
Pipes acquisition[1] (€ m^{-1})	115-520	Ferrer et al., 2015; Pretel et al., 2015
Stirrer acquisition (€ m^{-3})	27.8	Brepols et al., 2010
Mechanical & Engineering (% to CAPEX)	28	DeCarolis et al., 2007[b]; Young et al., 2014[c]
Civil Engineering/legal (% to CAPEX)	36	Brepols et al., 2010
Mixing consumption[2] (W m^{-3})	8	Metcalf & Eddy, 2014[d]; Smith et al., 2014
Electrolyte cost (€ kg^{-1})	2.35	Ferrer et al., 2015; Pretel et al., 2015
Farming cost (€ kg^{-1} TSS)	0.0048	Ferrer et al., 2015; Pretel et al., 2015
Citric acid 50% cost (€ t^{-1})	760	Brepols et al., 2008; Verrecht et al., 2010
NaOCl 14% cost (€ m^{-3})	254	Brepols et al., 2008; Verrecht et al., 2010
UF membrane lifetime (years)	10	Lin et al., 2011; Verrecht et al., 2010
Pumps lifetime (hours)	65,000	Ferrer et al., 2015; Pretel et al., 2015
Blowers lifetime (hours)	50,000	Ferrer et al., 2015; Pretel et al., 2015
Mixer lifetime (hours)	100,000	Ferrer et al., 2015; Pretel et al., 2015
Labour cost[3] (€)	$2E\text{-}09x^3 - 8E\text{-}05x^2 + 3{,}9137x + 15226$	Adham et al., 2004[e]
Blower efficiency	0.8	Pretel et al., 2015
Blower outlet pressure (Pa)	160,300	Judd, 2010; Verrecht et al., 2010
Blower inlet pressure (Pa)	101,325	Judd, 2010; Verrecht et al., 2010

[1] 0.4-1.4 m ø

[2] It was considered that the mixer was working a 10% of the time, since an important degree of mixing is achieved with the sludge recirculation and biogas produced (Smith et al., 2014).

[3] x is the influent flow expressed in m^3 day^{-1}

References that do not appear in the manuscript:

[a] Brepols, C. et al. 2010. Considerations on the design and financial feasibility of full-scale membrane bioreactors for municipal applications. Water Sci. Technol. 61, 2461–8.

[b] DeCarolis. et al. 2007. Evaluation of Newly Developed Membrane Bioreactors for Wastewater Reclamation. Proc. Water Environ. Fed.

[c] Young, T. et al. 2014. Cost-effectiveness of membrane bioreactors treatment system for low-level phosphorus reduction from municipal wastewater. Water Pract. Technol. 9, 316–323.

[d] Metcalf & Eddy, 2014. Wastewater Engineering: Treatment and Resource Recovery, fifth ed. McGraw-Hill, New York.

[e] Adham, S. et al. 2004. Optimization of various MBR systems for water reclamation. Proc. Water Environ. Fed.

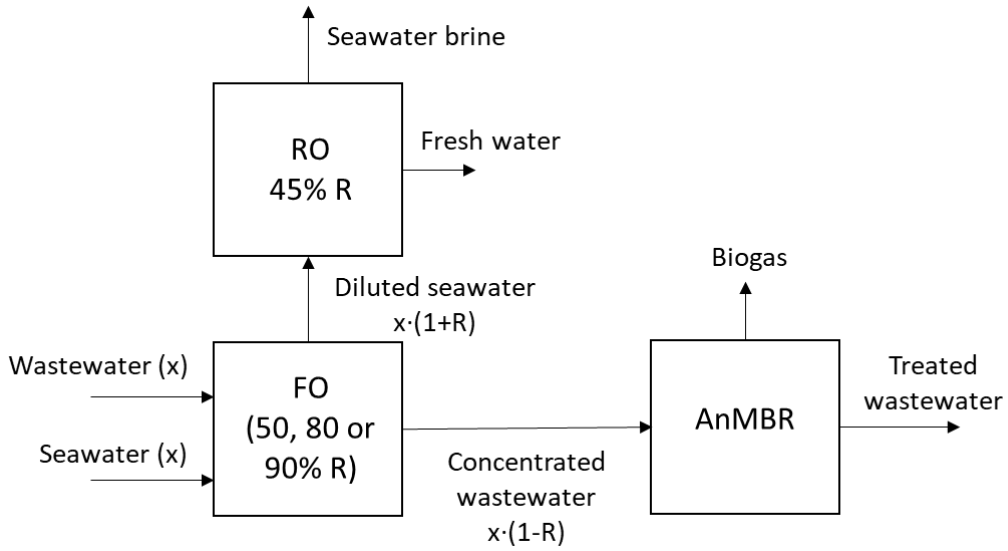

Figure S1: Retrofit scheme from SWRO plants to FO-RO+AnMBR plants.

2.4 Publication IV: *Techno-economic analysis of forward osmosis pre-concentration before an anaerobic membrane bioreactor: Impact of draw solute and membrane material*

Vinardell, S., Blandin, G., Ferrari, F., Lesage, G., Mata-Alvarez, J., Dosta, J., Astals, S. Techno-economic analysis of forward osmosis pre-concentration before an anaerobic membrane bioreactor: Impact of draw solute and membrane material. Submitted to Journal of Cleaner Production with reference number JCLEPRO-D-22-01214.

Techno-economic analysis of forward osmosis pre-concentration before an anaerobic membrane bioreactor: Impact of draw solute and membrane material

Sergi Vinardell[a,*], Gaetan Blandin[b], Federico Ferrari[c], Geoffroy Lesage[d], Joan Mata-Alvarez[a,e], Joan Dosta[a,e], Sergi Astals[a]

[a] Department of Chemical Engineering and Analytical Chemistry, University of Barcelona, 08028, Barcelona, Spain

[b] Laboratory of Chemical and Environmental Engineering (LEQUiA), Institute of the Environment, University of Girona, 17003, Girona, Spain

[c] Eurecat, Centre Tecnològic de Catalunya, Water, Air and Soil Unit, 08242, Manresa, Spain

[d] Institut Européen des Membranes (IEM), Université de Montpellier, CNRS, ENSCM, 34090, Montpellier, France

[e] Water Research Institute, University of Barcelona, 08028, Barcelona, Spain

*Corresponding author (svinardell@ub.edu)

Abstract

This research investigated the impact of draw solute and membrane material on the economic balance of a forward osmosis (FO) system pre-concentrating municipal sewage prior to an anaerobic membrane bioreactor (AnMBR). Eight and three different draw solutes were evaluated for cellulose triacetate (CTA) and polyamide thin film composite (TFC) membranes, respectively. The material of the FO membrane was a key economic driver since the net cost of TFC membrane was substantially lower than the CTA membrane. The draw solute had a moderate impact on the economic balance. The most economically favourable draw solutes were sodium acetate and calcium chloride for the CTA membrane and magnesium chloride for the TFC membrane. The FO+AnMBR performance was modelled for both FO membrane materials and each draw solute considering three FO recoveries (50, 80 and 90%). The estimated COD removal efficiency of the AnMBR was similar regardless of the draw solute and FO membrane material. However, the COD and draw solute concentrations in the permeate and digestate increased as the FO recovery increased. These results highlight that FO membranes with high permselectivity are needed to improve the economic balance of mainstream AnMBR and to ensure the quality of the permeate and digestate.

Keywords

Forward osmosis (FO); Anaerobic membrane bioreactor (AnMBR); Anaerobic digestion; Reverse osmosis (RO); Draw solute; Techno-economic evaluation

1. Introduction

Climate change and resource depletion are pushing a paradigm shift in wastewater treatment plants (WWTPs) to maximise the recovery of resources and reduce the consumption of chemicals and energy (Guest et al., 2009). In this new paradigm, membrane bioreactors play a central role since these technologies provide a physical barrier for solids and pathogens, which allows producing high-quality effluents and improving the performance of the bioreactor (Krzeminski et al., 2017).

Anaerobic membrane bioreactor (AnMBR), which combines membrane technology and anaerobic digestion, is an interesting biotechnology for municipal sewage treatment (Vinardell et al., 2020b). In AnMBRs, the sewage organic matter is transformed into methane-rich biogas and the biomass is completely retained by the membrane (Anjum et al., 2021; Hu et al., 2021). Several full-scale AnMBRs have already been implemented for the treatment of different types of industrial wastewater (Zhen et al., 2019). However, full-scale implementation of AnMBRs for municipal sewage treatment is limited because municipal sewage is typically less concentrated and represents a larger volumetric flow rate than industrial wastewater. The high volumetric flow rate and the low organic matter concentration of municipal sewage: (i) increases the AnMBR capital and operating costs, (ii) decreases the methane productivity per m^3 of sewage, and (iii) increases the total amount of methane dissolved in the effluent (Ansari et al., 2017; Ferrari et al., 2019; Zahedi et al., 2021). Accordingly, it is important to develop technologies for sewage pre-concentration to improve the competitiveness of AnMBR for municipal sewage treatment.

Forward osmosis (FO) is an emerging membrane technology to pre-concentrate municipal sewage with low energy input, low fouling and high rejection of organic matter (Awad et al., 2019; Wang and Liu, 2021). FO is spontaneously driven by the osmotic pressure difference between the feed solution and the saline draw solution (Arcanjo et al., 2020; Blandin et al., 2021). The osmotic pressure gradient between both solutions drives the permeation of water from the feed solution to the draw solution through the dense FO membrane. In this way, the sewage organic matter concentration increases whereas the volumetric flow rate decreases (Ansari et al., 2017). Moreover, a regeneration technology (e.g. reverse osmosis (RO), nanofiltration, membrane distillation) is typically used to re-

concentrate the draw solution and produce high-quality water from the diluted draw solution (Cabrera-Castillo et al., 2021; Kim et al., 2017; Lee and Hsieh, 2019).

Draw solute selection is important since it affects the water and solute fluxes through FO membranes (Achilli et al., 2010; Ansari et al., 2015). Small inorganic solutes (e.g. NaCl, KCl) have been widely used as draw solutes because they feature high diffusivities and mitigate the detrimental effect of internal concentration polarisation (ICP) on water flux (Lutchmiah et al., 2014; Shaffer et al., 2015). However, these solutes generally feature high reverse solute fluxes (RSF) due to their high diffusivity (Shaffer et al., 2015; Zou et al., 2019). The RSF from the draw to the feed solution: (i) increases the salinity of the sewage and (ii) increases the draw solution replenishment costs. The higher salinity in the pre-concentrated sewage could partially inhibit anaerobic bacteria with a direct impact on the AnMBR biogas production and effluent quality (both permeate and digestate) (Vinardell et al., 2021). Therefore, the selection of the draw solute should contemplate both FO and AnMBR performance since solute selection can have a high impact on the technical and economic feasibility of combining both technologies.

Few studies have evaluated the impact of the draw solute on FO and anaerobic digestion performance (Ansari et al., 2015; Bacaksiz et al., 2021). Bacaksiz et al. (2021) evaluated the performance of different inorganic and organic draw solutes in the FO system and the inhibitory impact of these solutes on anaerobic digestion. Bacaksiz et al. (2021) showed that the draw solute has a direct impact on the water flux and RSF of the cellulose triacetate (CTA) FO membrane, where $CaCl_2$, $MgCl_2$, HCOONa and CH_3COONa were the most economically favourable draw solutes. Anaerobic digestion batch experiments showed that the RSF of inorganic draw solutes could inhibit the anaerobic digestion process, while organic draw solutes could increase methane production. However, this study did not consider all the costs influenced by the draw solute since the economic analysis only considered the cost required to purchase the draw solute. Accordingly, a more detailed techno-economic analysis including all the costs impacted by the draw solute is needed to holistically assess its importance on the economic feasibility of an FO+AnMBR system for municipal sewage treatment.

This techno-economic study aims to evaluate the impact of draw solute and FO membrane material on the economic balance of an FO+AnMBR system for municipal sewage

treatment with energy and water production. The costs influenced by the draw solute and FO membrane material were considered in this economic analysis, including FO installation, draw solute replenishment, labour, maintenance, FO membrane replacement, combined heat and power (CHP) unit and electricity production. The ultimate goal is to provide a comprehensive understanding of the techno-economic interdependence between the FO membrane (water flux and reverse solute flux) and the AnMBR for municipal sewage treatment.

2. Methodology

2.1 Design criteria and draw solutes selection

Figure 1 shows the FO+AnMBR configuration evaluated in this study. The chosen configuration was a closed-loop scheme using a synthetic solution as a draw solution. The diluted draw solution was regenerated by means of RO to re-establish the initial osmotic pressure and to produce high-quality water. The draw solute was replenished (by topping up with salts) to keep the osmotic pressure constant in the loop despite losses of the draw solute through FO and RO membranes. The FO recovery was fixed at 80% because this is one of the most used FO recovery values in the literature for FO pre-concentration systems before anaerobic digestion (values range between 50 and 90%) (Ansari et al., 2018, 2015; Ferrari et al., 2019; Vinardell et al., 2020a). The pre-concentrated municipal sewage was considered to be fed to an AnMBR configured as a continuous stirred tank reactor. The membranes were submerged in a separate membrane tank where gas sparging was applied to control the membrane fouling extent since this is the most common strategy for membrane fouling control in AnMBRs (Maaz et al., 2019). The AnMBR was considered to be operated at a solids retention time (SRT) of 60 days and at an hydraulic retention time (HRT) of 1 day (Vinardell et al., 2020a).

The selection of the draw solutes used for the economic evaluation was performed from available data for CTA and polyamide thin film composite (TFC) commercial membranes. Regarding CTA membranes, eight different draw solutes were evaluated: NaCl, $MgCl_2$, KCl, $CaCl_2$, Na_2SO_4, $MgSO_4$, $Ca(NO_3)_2$ and CH_3COONa (Achilli et al., 2010; Ansari et al., 2015). Regarding TFC membranes, three different draw solutes were evaluated: NaCl, $MgCl_2$ and $MgSO_4$ (Sanahuja-Embuena et al., 2019). This research did

not include the same draw solutes for both membranes due to the limited data available in the literature regarding draw solute permeability in TFC membranes. The osmotic pressure of the draw solution before entering to the FO modules was considered to be 28 bar for all the solutes (Achilli et al., 2010).

The economic analysis was conducted for a high-sized WWTP treating 100,000 m^3 d^{-1} of municipal sewage (500,000 population equivalent). The municipal sewage was pre-filtered (~50 µm) before FO to prevent substantial fouling and clogging in the FO membranes and to decrease the amount of suspended solids fed to the AnMBR. The pre-filtered municipal sewage contained a total chemical oxygen demand (COD) concentration of 420 mg COD L^{-1}, which was fractionated in biodegradable soluble COD (64.3%), inert soluble COD (19.1%), biodegradable particulate COD (7.1%) and inert particulate COD (9.5%) (Vinardell et al., 2020a).

2.2 FO process design and modelling

The water flux (J_W) and RSF (J_S) through dense FO membranes were modelled for all draw solutes and both membranes. Eq. (1) and Eq. (2) were used to model J_W and J_S, respectively (Kim et al., 2017; Tiraferri et al., 2013). These equations considered that the active layer faced the feed side and included the effect of (i) dilutive ICP on the support layer, (ii) concentrative external concentration polarisation (ECP) on the active layer and (iii) RSF from the draw solution to the sewage (Blandin et al., 2015).

$$J_W = A \cdot \left[\frac{\pi_D \cdot e^{-J_W \cdot \frac{S}{D}} - \pi_F \cdot e^{\frac{J_W}{k}}}{1 - \frac{B}{J_W} \cdot \left(e^{-J_W \cdot \frac{S}{D}} - e^{\frac{J_W}{k}} \right)} \right] \quad \text{Eq. (1)}$$

$$J_s = B \cdot \left[\frac{c_D \cdot e^{-J_W \cdot \frac{S}{D}} - c_F \cdot e^{\frac{J_W}{k}}}{1 + \frac{B}{J_W} \cdot \left(e^{\frac{J_W}{k}} - e^{-J_W \cdot \frac{S}{D}} \right)} \right] \quad \text{Eq. (2)}$$

where J_w is the water flux (L m^{-2} h^{-1}), J_S is the reverse draw solute flux (g m^{-2} h^{-1}), A is the water permeability (L m^{-2} h^{-1} bar^{-1}), B is the draw solute permeability (L m^{-2} h^{-1}), π_D is the osmotic pressure in the draw solution (bar), π_F is the osmotic pressure in the feed solution (bar), c_D is the draw solute concentration in the draw solution (g L^{-1}), c_F is the draw solute concentration in the feed solution (g L^{-1}), k is the mass transfer coefficient of

the draw solute (L m^{-2} h^{-1}), D is the self-diffusion coefficient of the draw solute (L m^{-1} h^{-1}) and S is the membrane structural parameter (m).

The intrinsic membrane parameters (i.e. A and S) for CTA and TFC membranes were obtained from Coday et al. (2013) and Sanahuja-Embuena et al. (2019), respectively. The parameter B, which depends on both the membrane and the draw solute, was obtained from Achilli et al. (2010) and Ansari et al. (2015) for CTA membrane, and from Sanahuja-Embuena et al. (2019) for TFC membrane. In these publications, the CTA membrane was a commercial flat-sheet FO membrane from Hydration Technology Innovations (Albany, USA) and the TFC membrane was a commercial hollow fibre membrane module from Aquaporin (Kongens Lyngby, Denmark). Detailed information about the A, B and S parameters as well as about the properties of the different draw solutes can be found in Table 1.

2.3 Modelling AnMBR performance

The AnMBR performance was modelled for the different FO alternatives (i.e. draw solutes, membrane materials and FO recoveries) to calculate the COD removal, the amount of methane recovered and the quality of the permeate. The presence of draw solute in the pre-concentrated sewage could partially inhibit anaerobic biomass (i.e. Na^+, K^+, Ca^{2+}, Mg^{2+}), introduce an electron acceptor (i.e. SO_4^{2-} and NO_3^-) and/or introduce an electron donor (i.e. CH_3COO^-). A steady state mass balance was used to model the AnMBR including a non-competitive inhibition function to determine the impact of draw solute concentration on anaerobic digestion performance (Eq. (3)). Subsequently, the total organic matter concentration in the AnMBR permeate was calculated using Eq. (4):

$$Q_0 \cdot S_{S,0} - k_{m,ac} \cdot \frac{S_S}{S_S + K_{S,ac}} \cdot \frac{KI_{50}}{KI_{50} + S_{cat}} X_{ac} \cdot V = Q_e \cdot S_S \qquad \text{Eq. (3)}$$

$$S_e = S_S + S_I \qquad \text{Eq. (4)}$$

where Q_0 is the pre-concentrated sewage flow rate (m^3 d^{-1}), $S_{S,0}$ is the biodegradable organic matter (particulate and soluble) concentration in the pre-concentrated sewage (kg COD m^{-3}), $k_{m,ac}$ is the specific maximum uptake rate for acetogenic methanogens (kg COD kg^{-1} COD_{cell} d^{-1}), Ss is the soluble biodegradable organic matter concentration in the AnMBR and in the permeate (kg COD m^{-3}), $K_{S,ac}$ is the half-saturation constant for

acetogenic methanogens (kg COD m^{-3}), KI_{50} is the 50% inhibitory constant for the draw solute (kg COD m^{-3}), S_{cat} is the cation concentration (i.e. Na^+, K^+, Ca^{2+}, Mg^{2+}) of the draw solute in the AnMBR (kg COD m^{-3}), X_{ac} is the biomass concentration of acetogenic methanogens, which was considered to be a 10% of the biomass (kg COD_{cell} m^{-3}) (Ariesyady et al., 2007), V is the volume of the AnMBR (m^3), Q_e is the permeate flow rate (m^3 d^{-1}), S_e is the total soluble organic matter concentration in the AnMBR permeate (kg COD m^{-3}) and S_I is the soluble inert organic matter concentration in the influent (kg COD m^{-3}). The model parameters used in Eq. (3) can be found in Table S1 of the supplementary material. Eq. (3) and Eq. (4) assumed that: (i) methanogenesis is the rate-limiting step, (ii) all the biodegradable particulate organic matter is solubilised in the AnMBR because of the high SRT (60 days), (iii) particulate organic matter hydrolysis does not generate soluble inert material, (iv) the AnMBR waste sludge flow rate is negligible compared to the permeate flow rate and (v) the KI_{50} values are literature averages and potential acclimation to inhibitors was not considered.

The methane production was calculated considering: (i) the biodegradable COD removed in the AnMBR, (ii) the presence of electron acceptors (i.e. SO_4^{2-} and NO_3^-) from the draw solution that could consume part of the COD and (iii) the presence of external COD coming from the draw solution (i.e. acetate) that could be an additional organic source for methane production. It was considered that the organic matter consumed when sulphate and nitrate were contained in the pre-concentrated sewage corresponded to 2.01 mg COD mg^{-1} SO_4^{2-}-S and 2.86 mg COD mg^{-1} NO_3^--N, respectively (Metcalf & Eddy, 2014).

2.4 Costs and revenue calculation

Draw solution has a direct impact on the FO capital and operating costs since it affects the water and the draw solute RSF through FO membranes. The RSF could also impact the amount of methane recovered in the AnMBR and the quality of the permeate. This section describes the costs and revenue considered for the economic evaluation. The cost calculation was conducted considering a fixed FO recovery of 80% and a draw solution osmotic pressure of 28 bar for all draw solutes and FO membrane materials (see Section 2.1). It is worth mentioning that the costs that were not influenced by the draw solute or the FO membrane material were not considered for the economic evaluation (e.g.

AnMBR capital and operating costs, RO capital costs, energy consumption) since these costs are assumed to be similar regardless of the draw solute and FO membrane material used. Table S2 of the supplementary material shows detailed information about the parameters used for costs and revenue calculations.

2.4.1 FO capital and operating costs

The methodology used to calculate the capital costs of the FO system can be found in Vinardell et al. (2020a), who adapted the methodology proposed by Blandin et al. (2015) to estimate the FO costs. Briefly, the capital costs of the FO system were estimated considering relationships with capital costs of RO systems since (i) RO systems are rather similar to FO systems and (ii) there are more data available concerning the costs of RO systems than FO systems (2015). Firstly, a benchmark RO scenario was established, which corresponded to an RO installation requiring a similar membrane area than the FO installation using NaCl as a draw solute. The capital cost of the benchmark RO scenario was estimated (i) considering an RO membrane cost of 24 £ m^{-2} (21 € m^{-2}) (Valladares Linares et al., 2016) and (ii) using the RO cost distribution shown in Table S3 of the supplementary material. Second, the capital cost of the FO system for the NaCl was estimated (i) considering an FO membrane cost of 55 £ m^{-2} (49 € m^{-2}) (Valladares Linares et al., 2016) and (ii) considering that specific cost contributors of the RO system could be partially (or totally) extendible to FO capital costs (e.g. civil engineering, equipment and materials, pumps) (Table S3). Finally, the FO capital costs for all the other draw solute scenarios were calculated from the FO capital costs of the NaCl scenario and considering that specific cost contributors were dependent on the FO membrane area (Table S3). The capital costs dependent on the FO membrane area were included in the economic evaluation since the costs that did not depend on the FO membrane area were not influenced by the draw solute and, therefore, are out of the scope of the present manuscript.

The operating costs of the FO system accounted for membrane replacement, labour and maintenance. The membrane replacement cost was calculated assuming a membrane lifetime of 4 years (Yangali-Quintanilla et al., 2015). The labour and maintenance costs were considered to be dependent on the size of the FO installation. Specifically, the labour

and maintenance costs accounted for 1% and 2.25% of the capital costs, respectively (Fritzmann et al., 2007; Vinardell et al., 2020a).

2.4.2 Draw solution replenishment costs

The draw solution needs to be replenished due to losses of draw solute through both FO and RO membranes. Draw solute losses through FO membranes were calculated for each solute using Eq. (2) (see Section 2.2), while the draw solute losses through RO membranes were calculated using the Reverse Osmosis System Analysis (ROSA) software (Filmtec Corporation, US). Detailed information of the input parameters to ROSA can be found in Table S4 of the supplementary material. The purchase cost of each draw solute was obtained from Bacaksiz et al. (2021) and is reported in Table 1.

2.4.3 Energy production

The energy production was calculated considering a methane calorific value of 55 MJ kg^{-1} (Metcalf & Eddy, 2014). The produced methane was combusted in a CHP unit with electrical and thermal efficiencies of 33 and 55%, respectively (Riley et al., 2020; Vinardell et al., 2021). The capital and operating costs of the CHP unit were 712 € kW_{el}^{-1} and 0.0119 € kWh_{el}^{-1}, respectively (Riley et al., 2020). The electricity produced in the CHP unit was considered to be sold at a price of 0.1149 € kWh^{-1} (Eurostat, 2019).

2.5 Economic evaluation

The capital expenditures (CAPEX), operating expenditures (OPEX) and electricity revenue were calculated for the different draw solutes and FO membranes. Eq. (5) and Eq. (6) were used to calculate the present value (PV) of the gross cost and electricity revenue, respectively. Subsequently, the PV of the net cost was calculated as the difference between the PV of the gross cost and the PV of the electricity revenue (Eq. (7)).

$$PV_{GC} = CAPEX + \sum_{t=1}^{T} \frac{OPEX_t}{(1+i)^t} \quad \text{Eq. (5)}$$

$$PV_{ER} = \sum_{t=1}^{T} \frac{ER_t}{(1+i)^t} \quad \text{Eq. (6)}$$

$$PV_{NC} = CAPEX + \sum_{t=1}^{T} \frac{OPEX_t - ER_t}{(1+i)^t} \quad \text{Eq. (7)}$$

where PV_{GC} is the PV of the gross cost (€), PV_{ER} is the PV of the electricity revenue (€), PV_{NC} is the PV of the net cost (€), CAPEX is the capital expenditure (€), $OPEX_t$ is the operating expenditure at year t (€), ER_t is the electricity revenue at year t (€), i is the discount rate (5%) and T is the plant lifetime (20 years).

3. Results and discussion

3.1 Impact of draw solute and membrane material on the economic balance of the FO+AnMBR system

Figure 2 illustrates the PV of the gross cost, electricity revenue and net cost for the different draw solutes and both membrane materials. The results show that the net cost of TFC membrane was substantially lower than the net cost of the CTA membrane regardless of the draw solute. The difference between both membranes can be mainly attributed to the higher water permeability and higher solute selectivity of TFC membrane in comparison with CTA membrane (Table 1). From these results, it is possible to conclude that the enhanced permselectivity (A/B ratio) (Shaffer et al., 2015) achieved with TFC membrane is an important factor influencing the economics of the process. The structural parameter (S), which relates to the properties of the membrane support layer, was lower for TFC membrane than for CTA membrane (Table 1). In this study, the membrane properties of the TFC membrane were obtained from Sanahuja-Embuena et al. (2019), who used a commercial Aquaporin membrane module and reported S values lower than commercial CTA membranes. Achieving a low S parameter is important to decrease the effect of ICP on the support layer and to increase the effective osmotic pressure difference between the draw and feed solutions (Blandin et al., 2015). These results illustrate that the improved properties of novel TFC membranes allowed increasing the water flux and reducing the draw solute flow rate through the FO membranes, which had a direct impact on FO installation and draw solution replenishment costs.

The draw solute had a moderate impact on the economic balance of the FO+AnMBR system (Figure 2). Regarding CTA membrane, CH_3COONa and $CaCl_2$ were the most economically competitive draw solutes. CH_3COONa featured a slightly lower net cost than $CaCl_2$ despite the higher gross cost of CH_3COONa. This can be attributed to the

higher electricity revenue achieved in the AnMBR when using CH_3COONa as draw solute since the fraction of CH_3COONa that permeates from the draw solution to the sewage through the FO membrane is converted into methane. The net cost of $MgCl_2$ and Na_2SO_4 were slightly higher than CH_3COONa and $CaCl_2$. Despite its relatively low FO membrane fluxes (~4.6 LMH), Na_2SO_4 was one of the most economically favourable draw solutes (Table 1). The good economic prospect of Na_2SO_4 can be attributed to the relatively low RSF of Na_2SO_4 through FO membranes (~2.5 g m^{-2} h^{-1}) that decreased the replenishment costs of the draw solute. However, the presence of sulphate in the pre-concentrated sewage decreases the amount of energy recovered in the AnMBR because of the competition between methanogens and sulphate reducing bacteria (SRB) for the available organic matter (Figure 2). Additionally, the higher concentration of sulphate in sewage increases the production of H_2S in the AnMBR that could (i) partially inhibit anaerobic microorganisms and (ii) reduce the durability of the infrastructure and hinder the long-term operability of the AnMBR (out of the scope of the present study).

Figure 2 also shows that the economic balance of NaCl, $Ca(NO_3)_2$ and KCl was little attractive since these solutes featured the highest RSF (>4 g m^{-2} h^{-1}) despite achieving relatively high FO membrane fluxes (>5.7 LMH). This is particularly important for $Ca(NO_3)_2$ because high RSF increases the concentration of nitrate in the sewage that, in turn, decreases the amount of organic matter available for methane production (Figure 2). These results illustrate that the selection of a suitable draw solute for FO+AnMBR system requires a compromise solution considering the capability of the draw solute to achieve high water fluxes with limited RSF.

Regarding TFC membrane, $MgCl_2$ was the most economically favourable draw solute followed by NaCl and $MgSO_4$ (Figure 2). This is in agreement with the net cost results obtained with CTA membrane since the same trend was observed for these three solutes. Finally, it is worth mentioning that $MgSO_4$ was not economically favourable for none of the membranes since this draw solute (i) featured a noticeably lower FO membrane flux in comparison to the other draw solutes and (ii) produced a limited amount of methane in the AnMBR due to the presence of sulphate in the pre-concentrated sewage.

3.2 Gross cost distribution

Figure 3 shows the gross cost distribution for the different draw solutes and both membranes. Regarding CTA membrane, the capital cost of the FO system represented the highest cost contributor (33-39%) for $MgCl_2$, $CaCl_2$, Na_2SO_4, $MgSO_4$ and CH_3COONa (Figure 3B). The replacement of the FO membranes during the plant lifetime represented the second highest impact for these five draw solutes (31-37%). This shows that the costs associated with the FO installation had a high impact on the net cost for $MgCl_2$, $CaCl_2$, Na_2SO_4, $MgSO_4$ and CH_3COONa. Similar results were obtained for the TFC membrane since the FO capital cost (33-39%) and FO membrane replacement cost (31-36%) represented the two highest cost contributors for $MgCl_2$ and $MgSO_4$ (Figure 3B). However, in absolute values, the gross cost contribution of the costs related to FO installation (i.e. FO capital cost, FO membrane replacement cost, FO draw solution replenishment cost, maintenance cost and labour cost) were noticeably reduced when using the TFC membrane because of the better flux performance than CTA membrane (Figure 3A). These results highlight the importance of achieving high water permeabilities for the FO+AnMBR system.

The FO draw solution replenishment cost represented the highest cost contributor for CTA membrane using NaCl, KCl and $Ca(NO_3)_2$ (29-39%) as draw solutes (Figure 3B). The high impact of FO draw solution replenishment on the net cost for these three draw solutes can be attributed to: (i) the high RSF (>4 g m^{-2} h^{-1}), which increased the necessity to replenish the solute to keep the draw solute osmotic pressure constant and (ii) the higher water flux (>5.7 LMH) of these solutes, which minimised the contribution of FO installation to the net cost. The draw solution replenishment cost also represented the highest cost contributor for TFC membrane when using NaCl (32%) as draw solute (Figure 3B). However, in absolute values, the gross cost contributor of draw solution replenishment was also reduced with the TFC membrane because TFC membrane featured a lower RSF and a higher permselectivity than CTA membrane (Figure 3A). For all draw solutes, the CHP capital and operating costs did not have a high impact on the net cost since their contribution was below 5% of the gross cost contribution.

3.3 Sensitivity analysis

Figure 4 illustrates the net cost of the different draw solutes and membranes for a ±30% variation of the most relevant economic parameters. The results show that the FO membrane cost variation had the highest impact on the net cost for all the draw solutes except for KCl (CTA membrane) and NaCl (TFC membrane). The variation of FO membrane cost affects both the initial investment and the cost to replace the FO membranes during the plant lifetime. These results highlight that FO membrane flux is a key economic driver in the FO+AnMBR system since this determines the FO membrane area required, which is directly correlated with the FO membrane purchasing and replacement cost. The variation of the FO membranes lifetime also had a high effect on the economic balance, which points out the importance to extend the lifetime of FO membranes to further improve the competitiveness of the system. The chemical cost variation had the highest impact on the net cost for KCl and NaCl in CTA and TFC membranes, respectively (Figure 4). This can be directly attributed to the high RSF of these draw solutes for CTA and TFC membranes.

Figure 4 results also show that the electricity price variation led to small and moderate changes in the net cost for CTA and TFC membranes, respectively. For CTA, the impact of electricity price variation on net cost was nearly negligible for Na_2SO_4, $MgSO_4$ and $Ca(NO_3)_2$ since these solutes substantially decreased the production of methane in the AnMBR and made the electricity revenue irrelevant in comparison to the other cost contributors. Conversely, the impact of the electricity price variation on the net cost was relatively high when using CH_3COONa as a draw solute since this solute increased the methane production in the AnMBR. The electricity price variation had a higher impact on the TFC economic balance since (i) the methane production is similar regardless of the type of FO membrane used and (ii) the FO-related costs are lower for TFC than for CTA membranes. These results imply that the superior performance of the TFC membranes makes the relative importance of electricity revenue higher for TFC membranes than for CTA membranes.

3.4 Impact of draw solute on permeate quality and AnMBR performance

Table 2 shows the COD concentration (both influent and permeate), draw solute concentration and methane production of the AnMBR for the different draw solutes, membrane materials and FO recoveries. Besides the 80% FO recovery used in the previous sections, this section included two additional FO recoveries (i.e. 50 and 90%) to better understand the impact of sewage pre-concentration on the AnMBR performance (i.e. methane production and permeate quality).

Table 2 results show that the AnMBR COD removal efficiency was similar regardless of the draw solute and FO membrane material since the permeate COD concentration remained rather constant at a specific FO recovery condition. These results indicate that, despite the sewage pre-concentration and RSF, inhibition of the anaerobic biomass would have a minor impact on AnMBR performance (Table 2). Besides the great adaptability of anaerobic biomass to operate under harsh conditions, the slight loss of activity due to inhibition could be mitigated by increasing the concentration of active biomass in the AnMBR (Chen et al., 2008). The loss of activity could also be mitigated by the capability of the AnMBR to retain specific microorganisms able to tolerate higher inhibitory concentrations regardless of their doubling time and aggregation properties (Dereli et al., 2012; Puyol et al., 2017).

Methane production was similar for NaCl, $MgCl_2$, KCl and $CaCl_2$ regardless of the FO membrane material and FO recovery (Table 2). However, methane production substantially decreased when using Na_2SO_4, $MgSO_4$ and $Ca(NO_3)_2$ as draw solutes since these solutes decreased the amount of organic matter available for methanisation. For these draw solutes, the amount of methane produced progressively decreased as the FO recovery increased due to the higher concentration of draw solute in the pre-concentrated sewage at higher FO recoveries. This was particularly noticeable for $Ca(NO_3)_2$ since the RSF of $Ca(NO_3)_2$ was substantially higher than $MgSO_4$ and Na_2SO_4. Accordingly, the high presence of nitrate in the pre-concentrated sewage sharply decreased methane production at FO recoveries of 80 and 90%. CH_3COONa achieved the highest methane production among the different draw solutes because this draw solute increased the amount of easily biodegradable organic matter in the pre-concentrated sewage, which allowed maximising methane production in the AnMBR.

Increasing the pre-concentration factor has a direct impact on AnMBR permeate quality. The permeate COD concentration increased as the FO recovery increased, increasing both the concentration of biodegradable organic matter (S_S) and the concentration of soluble inerts (S_I). This phenomenon was particularly important for the high FO recovery scenarios (80 and 90%) since the permeate COD concentration could exceed the European Union COD discharge limits (<125 mg COD L^{-1}) (CEC, 1991). Under these circumstances, it would be necessary to implement post-treatment technologies to ensure that the discharge limits are achieved.

The draw solute concentration also increased with the FO recovery. For the CTA membrane, the NaCl concentration increased from 0.65 to 5.89 mg L^{-1} as the FO recovery increased from 50 to 90% (Table 2). However, the NaCl concentration in the pre-concentrated sewage was substantially decreased using TFC membrane due to its higher permselectivity. Compared to the CTA membrane, TFC membrane decreased the NaCl, $MgCl_2$ and $MgSO_4$ concentrations in the pre-concentrated sewage by 3, 8 and 11 times, respectively (Table 2). These results indicate that high FO recoveries could result in a permeate and digestate with a high salinity concentration, which could limit their application in agriculture as irrigation water and fertilizers (Vinardell et al., 2021). Accordingly, restricting the FO recovery could be used as a strategy to (i) meet the effluent discharge requirements and (ii) improve the quality of the permeate and digestate to make it suitable for agricultural application. These two factors are paramount to make the FO+AnMBR approach environmentally and technically feasibility.

4. Conclusions

The techno-economic analysis of the FO+AnMBR system showed that FO membrane material was a determinant economic factor since the net cost of the TFC membrane was substantially lower than the CTA membrane. The draw solute had a moderate impact on the FO+AnMBR system economic balance. The capital cost of the FO system was the most important cost contributor for $MgCl_2$, $CaCl_2$, Na_2SO_4, $MgSO_4$ and CH_3COONa, while the FO draw solution replenishment was the most important cost contributor for NaCl, KCl and $Ca(NO_3)_2$. The most economically favourable draw solutes were CH_3COONa and $CaCl_2$ for the CTA membrane and $MgCl_2$ for the TFC membrane due to their capacity to achieve relatively high water fluxes with low RSF. The AnMBR COD

removal efficiency was similar regardless of the draw solute and membrane material. However, FO recoveries above 80% could compromise the fulfilment of the permeate discharge requirements. Overall, the results from this techno-economic study highlight that selecting FO membranes and draw solutes capable to achieve high water fluxes with reduced RSF is crucial to boost the economic competitiveness of the system and fulfil the permeate discharge requirements.

Acknowledgments

This work was supported by the European Union LIFE programme (LIFE Green Sewer project, LIFE17 ENV/ES/000341). The authors also acknowledge the grant overseen by the French National Research Agency (ANR) as part of the "JCJC" Program BàMAn (ANR-18-CE04-0001-01). Sergi Vinardell is grateful to the Generalitat de Catalunya for his predoctoral FI grant (2019 FI_B 00394). Sergi Astals is grateful to the Spanish Ministry of Science, Innovation and Universities for his Ramon y Cajal fellowship (RYC-2017-22372). Gaetan Blandin received the support of a fellowship from "la Caixa" Foundation (ID 100010434). The fellowship code is LCF/BQ/PR21/11840009.

Declaration of competing interests

The authors declare that they have no known competing financial interests or personal relationships that could have appeared to influence the work reported in this paper. The authors also declare that this manuscript reflects only the authors' view and that the Executive Agency for SME/EU Commission are not responsible for any use that may be made of the information it contains.

References

Achilli, A., Cath, T.Y., Childress, A.E., 2010. Selection of inorganic-based draw solutions for forward osmosis applications. J. Memb. Sci. 364, 233–241.

Anjum, F., Khan, I.M., Kim, J., Aslam, M., Blandin, G., Heran, M., Lesage, G., 2021. Trends and progress in AnMBR for domestic wastewater treatment and their impacts on process efficiency and membrane fouling. Environ. Technol. Innov. 21, 101204.

Ansari, A.J., Hai, F.I., Guo, W., Ngo, H.H., Price, W.E., Nghiem, L.D., 2015. Selection

of forward osmosis draw solutes for subsequent integration with anaerobic treatment to facilitate resource recovery from wastewater. Bioresour. Technol. 191, 30–36.

Ansari, A.J., Hai, F.I., Price, W.E., Drewes, J.E., Nghiem, L.D., 2017. Forward osmosis as a platform for resource recovery from municipal wastewater - A critical assessment of the literature. J. Memb. Sci. 529, 195–206.

Ansari, A.J., Hai, F.I., Price, W.E., Ngo, H.H., Guo, W., Nghiem, L.D., 2018. Assessing the integration of forward osmosis and anaerobic digestion for simultaneous wastewater treatment and resource recovery. Bioresour. Technol. 260, 221–226.

Arcanjo, G.S., Costa, F.C.R., Ricci, B.C., Mounteer, A.H., de Melo, E.N.M.L., Cavalcante, B.F., Araújo, A. V., Faria, C. V., Amaral, M.C.S., 2020. Draw solution solute selection for a hybrid forward osmosis-membrane distillation module: Effects on trace organic compound rejection, water flux and polarization. Chem. Eng. J. 400, 125857.

Ariesyady, H.D., Ito, T., Okabe, S., 2007. Functional bacterial and archaeal community structures of major trophic groups in a full-scale anaerobic sludge digester. Water Res. 41, 1554–1568.

Awad, A.M., Jalab, R., Minier-Matar, J., Adham, S., Nasser, M.S., Judd, S.J., 2019. The status of forward osmosis technology implementation. Desalination 461, 10–21.

Bacaksiz, A.M., Kaya, Y., Aydiner, C., 2021. Techno-economic preferability of cost-performance effective draw solutions for forward osmosis and osmotic anaerobic bioreactor applications. Chem. Eng. J. 410, 127535.

Blandin, G., Galizia, A., Monclús, H., Lesage, G., Héran, M., Martinez-Lladó, X., 2021. Submerged osmotic processes: Design and operation of hollow fiber forward osmosis modules. Desalination 518, 115281.

Blandin, G., Verliefde, A.R.D., Tang, C.Y., Le-Clech, P., 2015. Opportunities to reach economic sustainability in forward osmosis–reverse osmosis hybrids for seawater desalination. Desalination 363, 26–36.

Cabrera-Castillo, E.H., Castillo, I., Ciudad, G., Jeison, D., Ortega-Bravo, J.C., 2021. FO-

MD setup analysis for acid mine drainage treatment in Chile: An experimental-theoretical economic assessment compared with FO-RO and single RO. Desalination 514, 115164.

CEC, 1991. Council Directive of 21 May 1991 concerning waste water treatment (91/271/EEC). Off. J. Eur. Communities No. L 135/40-52.

Chen, Y., Cheng, J.J., Creamer, K.S., 2008. Inhibition of anaerobic digestion process: A review. Bioresour. Technol. 99, 4044-4064.

Coday, B.D., Heil, D.M., Xu, P., Cath, T.Y., 2013. Effects of transmembrane hydraulic pressure on performance of forward osmosis membranes. Environ. Sci. Technol. 47, 2386–2393.

Dereli, R.K., Ersahin, M.E., Ozgun, H., Ozturk, I., Jeison, D., van der Zee, F., van Lier, J.B., 2012. Potentials of anaerobic membrane bioreactors to overcome treatment limitations induced by industrial wastewaters. Bioresour. Technol. 122, 160–170.

Eurostat, 2019. Electricity price statistics. https://ec.europa.eu/eurostat/statistics-explained/index.php/Electricity_price_statistics (accessed September 30, 2019).

Ferrari, F., Balcazar, J.L., Rodriguez-Roda, I., Pijuan, M., 2019. Anaerobic membrane bioreactor for biogas production from concentrated sewage produced during sewer mining. Sci. Total Environ. 670, 993–1000.

Fritzmann, C., Löwenberg, J., Wintgens, T., Melin, T., 2007. State-of-the-art reverse osmosis desalination. Desalination 216, 1–76.

Guest, J.S., Skerlos, S.J., Barnard, J.L., Beck, M.B., Daigger, G.T., Hilger, H., Jackson, S.J., Karvazy, K., Kelly, L., Macpherson, L., Mihelcic, J.R., Pramanik, A., Raskin, L., Van Loosdrecht, M.C.M., Yeh, D., Love, N.G., 2009. A new planning and design paradigm to achieve sustainable resource recovery from wastewater. Environ. Sci. Technol. 43, 6126–6130.

Hu, Y., Du, R., Nitta, S., Ji, J., Rong, C., Cai, X., Qin, Y., Li, Y.Y., 2021. Identification of sustainable filtration mode of an anaerobic membrane bioreactor for wastewater treatment towards low-fouling operation and efficient bioenergy production. J.

Clean. Prod. 329, 129686.

Irvine, G.J., Rajesh, S., Georgiadis, M., Phillip, W.A., 2013. Ion selective permeation through cellulose acetate membranes in forward osmosis. Environ. Sci. Technol. 47, 13745–13753.

Kim, J.E., Phuntsho, S., Chekli, L., Hong, S., Ghaffour, N., Leiknes, T.O., Choi, J.Y., Shon, H.K., 2017. Environmental and economic impacts of fertilizer drawn forward osmosis and nanofiltration hybrid system. Desalination 416, 76–85.

Krzeminski, P., Leverette, L., Malamis, S., Katsou, E., 2017. Membrane bioreactors – A review on recent developments in energy reduction, fouling control, novel configurations, LCA and market prospects. J. Memb. Sci. 527, 207–227.

Lee, D.J., Hsieh, M.H., 2019. Forward osmosis membrane processes for wastewater bioremediation: Research needs. Bioresour. Technol. 290, 121795.

Lutchmiah, K., Verliefde, A.R.D., Roest, K., Rietveld, L.C., Cornelissen, E.R., 2014. Forward osmosis for application in wastewater treatment: A review. Water Res. 58, 179-197.

Maaz, M., Yasin, M., Aslam, M., Kumar, G., Atabani, A.E., Idrees, M., Anjum, F., Jamil, F., Ahmad, R., Khan, A.L., Lesage, G., Heran, M., Kim, J., 2019. Anaerobic membrane bioreactors for wastewater treatment: Novel configurations, fouling control and energy considerations. Bioresour. Technol. 283, 358–372.

Metcalf & Eddy, 2014. Wastewater Engineering: Treatment and Resource Recovery. Fifth ed. McGraw Hill, New York.

Puyol, D., Batstone, D.J., Hülsen, T., Astals, S., Peces, M., Krömer, J.O., 2017. Resource recovery from wastewater by biological technologies: Opportunities, challenges, and prospects. Front. Microbiol. 7.

Riley, D.M., Tian, J., Güngör-Demirci, G., Phelan, P., Rene Villalobos, J., Milcarek, R.J., 2020. Techno-economic assessment of CHP systems in wastewater treatment plants. Environments 7, 1–32.

Sanahuja-Embuena, V., Khensir, G., Yusuf, M., Andersen, M.F., Nguyen, X.T., Trzaskus, K., Pinelo, M., Helix-Nielsen, C., 2019. Role of operating conditions in a pilot scale investigation of hollow fiber forward osmosis membrane modules. Membranes. 9, 66.

Shaffer, D.L., Werber, J.R., Jaramillo, H., Lin, S., Elimelech, M., 2015. Forward osmosis: Where are we now? Desalination 356, 271–284.

Tiraferri, A., Yip, N.Y., Straub, A.P., Romero-Vargas Castrillon, S., Elimelech, M., 2013. A method for the simultaneous determination of transport and structural parameters of forward osmosis membranes. J. Memb. Sci. 444, 523–538.

Valladares Linares, R., Li, Z., Yangali-Quintanilla, V., Ghaffour, N., Amy, G., Leiknes, T., Vrouwenvelder, J.S., 2016. Life cycle cost of a hybrid forward osmosis – low pressure reverse osmosis system for seawater desalination and wastewater recovery. Water Res. 88, 225–234.

Vinardell, S., Astals, S., Jaramillo, M., Mata-Alvarez, J., Dosta, J., 2021. Anaerobic membrane bioreactor performance at different wastewater pre-concentration factors: An experimental and economic study. Sci. Total Environ. 750, 141625.

Vinardell, S., Astals, S., Mata-Alvarez, J., Dosta, J., 2020a. Techno-economic analysis of combining forward osmosis-reverse osmosis and anaerobic membrane bioreactor technologies for municipal wastewater treatment and water production. Bioresour. Technol. 297, 122395.

Vinardell, S., Astals, S., Peces, M., Cardete, M.A., Fernández, I., Mata-Alvarez, J., Dosta, J., 2020b. Advances in anaerobic membrane bioreactor technology for municipal wastewater treatment: A 2020 updated review. Renew. Sustain. Energy Rev. 130, 109936.

Wang, J., Liu, X., 2021. Forward osmosis technology for water treatment: Recent advances and future perspectives. J. Clean. Prod. 280, 124354.

Yangali-Quintanilla, V., Olesen, L., Lorenzen, J., Rasmussen, C., Laursen, H., Vestergaard, E., Keiding, K., 2015. Lowering desalination costs by alternative

desalination and water reuse scenarios. Desalin. Water Treat. 55, 2437–2445.

Zahedi, S., Ferrari, F., Blandin, G., Balcazar, J.L., Pijuan, M., 2021. Enhancing biogas production from the anaerobic treatment of municipal wastewater by forward osmosis pretreatment. J. Clean. Prod. 315, 128140.

Zhen, G., Pan, Y., Lu, X., Li, Y.-Y., Zhang, Z., Niu, C., Kumar, G., Kobayashi, T., Zhao, Y., Xu, K., 2019. Anaerobic membrane bioreactor towards biowaste biorefinery and chemical energy harvest: Recent progress, membrane fouling and future perspectives. Renew. Sustain. Energy Rev. 115, 109392.

Zou, S., Qin, M., He, Z., 2019. Tackle reverse solute flux in forward osmosis towards sustainable water recovery: reduction and perspectives. Water Res. 149, 362–374.

Table 1. A, B and S parameters as well as main properties and costs for the different draw solutes and membranes under study.

	CTA Membrane								**TFC Membrane**		
	NaCl	**$MgCl_2$**	**KCl**	**$CaCl_2$**	**Na_2SO_4**	**$MgSO_4$**	**$Ca(NO_3)_2$**	**CH_3COONa**	**NaCl**	**$MgCl_2$**	**$MgSO_4$**
A ($L\ m^{-2}\ h^{-1}\ bar^{-1}$)[a]	0.55	0.55	0.55	0.55	0.55	0.55	0.55	0.55	1.71	1.71	1.71
S (mm)[a]	0.463	0.463	0.463	0.463	0.463	0.463	0.463	0.463	0.14	0.14	0.14
B ($L\ m^{-2}\ h^{-1}$)[b]	0.303	0.215	0.363	0.268	0.091	0.04	0.15	0.073	0.240	0.07	0.01
D ($\times 10^{-9}\ m^2\ s^{-1}$)[c]	1.47	1.05	1.86	1.13	0.76	0.37	1.28	1.44	1.47	1.05	0.37
k ($\times 10^{5}\ m\ s^{-1}$)[d]	1.99	1.59	2.32	1.67	1.28	0.79	1.81	1.96	1.99	1.59	0.79
Initial osmotic pressure (bar)	28	28	28	28	28	28	28	28	28	28	28
Initial draw solute concentration ($g\ L^{-1}$)[e]	35.2	34.2	47.0	43.8	84.7	141.3	87.2	55.9	35.2	34.2	141.3
Draw solute purchase cost (€ mol^{-1})[f]	0.016	0.025	0.020	0.015	0.013	0.017	0.038	0.034	0.016	0.025	0.017

[a] Coday et al. (2013) for CTA membrane and Sanahuja-Embuena et al. (2019) for TFC membrane.

[b] Calculated from data provided by Achilli et al. (2010) and Ansari et al. (2015) for CTA membrane and Sanahuja-Embuena et al. (2019) for TFC membrane.

[c] Achilli et al. (2010) for NaCl, $MgCl_2$, KCl, $CaCl_2$, Na_2SO_4 and $MgSO_4$, Irvine et al. (2013) for $Ca(NO_3)_2$ and Ansari et al. (2015) for CH_3COONa.

[d] The k parameter was calculated from Sanahuja-Embuena et al. (2019) equations and parameters.

[e] Achilli et al. (2010) for NaCl, $MgCl_2$, KCl, $CaCl_2$, Na_2SO_4, $MgSO_4$ and $Ca(NO_3)_2$ and calculated from data provided by Arcanjo et al. (2020) for CH_3COONa.

[f] Data obtained from Bacaksiz et al. (2021).

Table 2. AnMBR performance and permeate quality for the different draw solutes and membranes under study. The AnMBR performance was modelled for an FO recovery of 50, 80 and 90%.

		CTA Membrane								**TFC Membrane**		
		NaCl	**$MgCl_2$**	**KCl**	**$CaCl_2$**	**Na_2SO_4**	**$MgSO_4$**	**$Ca(NO_3)_2$**	**CH_3COONa**	**NaCl**	**$MgCl_2$**	**$MgSO_4$**
R=50%	Influent COD concentration (mg L^{-1})	840	840	840	840	840	840	840	929	840	840	840
	Influent solute concentration (g L^{-1})	0.65	0.47	1.02	0.73	0.55	0.45	0.88	0.29	0.19	0.06	0.04
	Permeate COD concentration (mg L^{-1})	83.0	83.7	84.4	83.6	82.7	83.3	83.3	91.1	82.4	82.3	82.2
	Methane production (Nm^3 d^{-1})	11,848	11,836	11,823	11,837	7,481	7,641	4,313	15,653	11,858	11,859	11,485
	Electricity production (kWh d^{-1})	43,080	43,038	42,992	43,041	27,204	27,785	15,682	56,916	43,118	43,123	41,760
R=80%	Influent COD concentration (mg L^{-1})	2,100	2,100	2,100	2,100	2,100	2,100	2,100	2,454	2,100	2,100	2,100
	Influent solute concentration (g L^{-1})	2.61	1.88	4.07	2.93	2.20	1.80	3.53	1.16	0.78	0.23	0.16
	Permeate COD concentration (mg L^{-1})	176.5	179.4	182.7	179.2	175.3	177.7	178.0	189.5	173.9	173.6	173.2
	Methane production (Nm^3 d^{-1})	12,065	12,044	12,021	12,046	5,079	5,334	8	18,288	12,083	12,085	11,486
	Electricity production (kWh d^{-1})	43,870	43,796	43,712	43,8001	18,470	19,395	29	66,498	43,936	43,943	41,764
R=90%	Influent COD concentration (mg L^{-1})	4,200	4,200	4,200	4,200	4,200	4,200	4,200	4,998	4,200	4,200	4,200
	Influent solute concentration (g L^{-1})	5.89	4.22	9.16	6.58	4.96	4.04	7.93	2.60	1.75	0.52	0.36
	Permeate COD concentration (mg L^{-1})	331.6	338.8	347.3	338.3	328.9	334.7	335.3	344.8	325.5	324.8	324.0
	Methane production (Nm^3 d^{-1})	12,139	12,114	12,084	12,116	4,282	4,566	0	19,196	12,161	12,163	11,489
	Electricity production (kWh d^{-1})	44,141	44,050	43,942	44,056	15,569	16,605	0	69,802	44,220	44,228	41,777

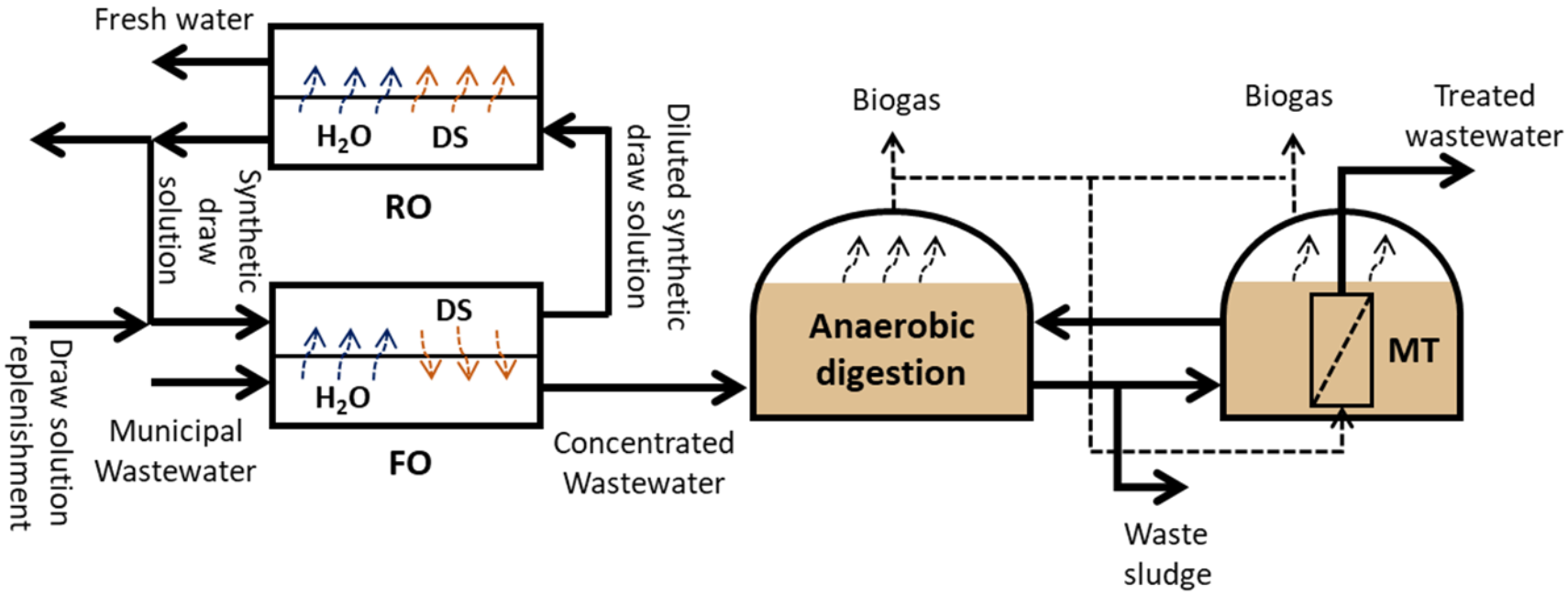

Figure 1. Closed-loop configuration integrating FO, RO and AnMBR technologies for municipal sewage treatment and water production (adapted from Vinardell et al. (2020a)).

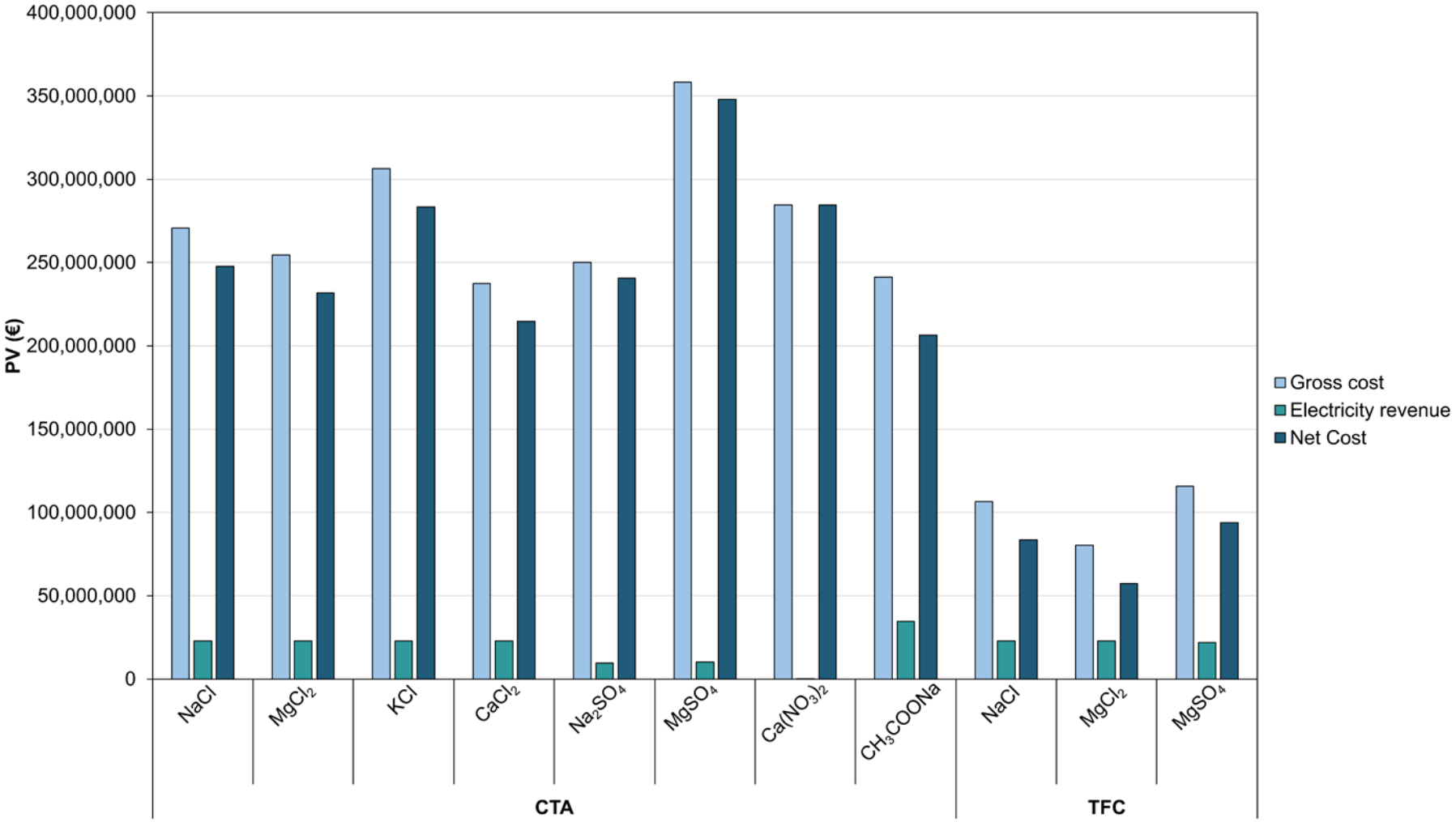

Figure 2. Present value (PV) of the gross cost, electricity revenue and net cost for the different draw solutes and membranes under study.

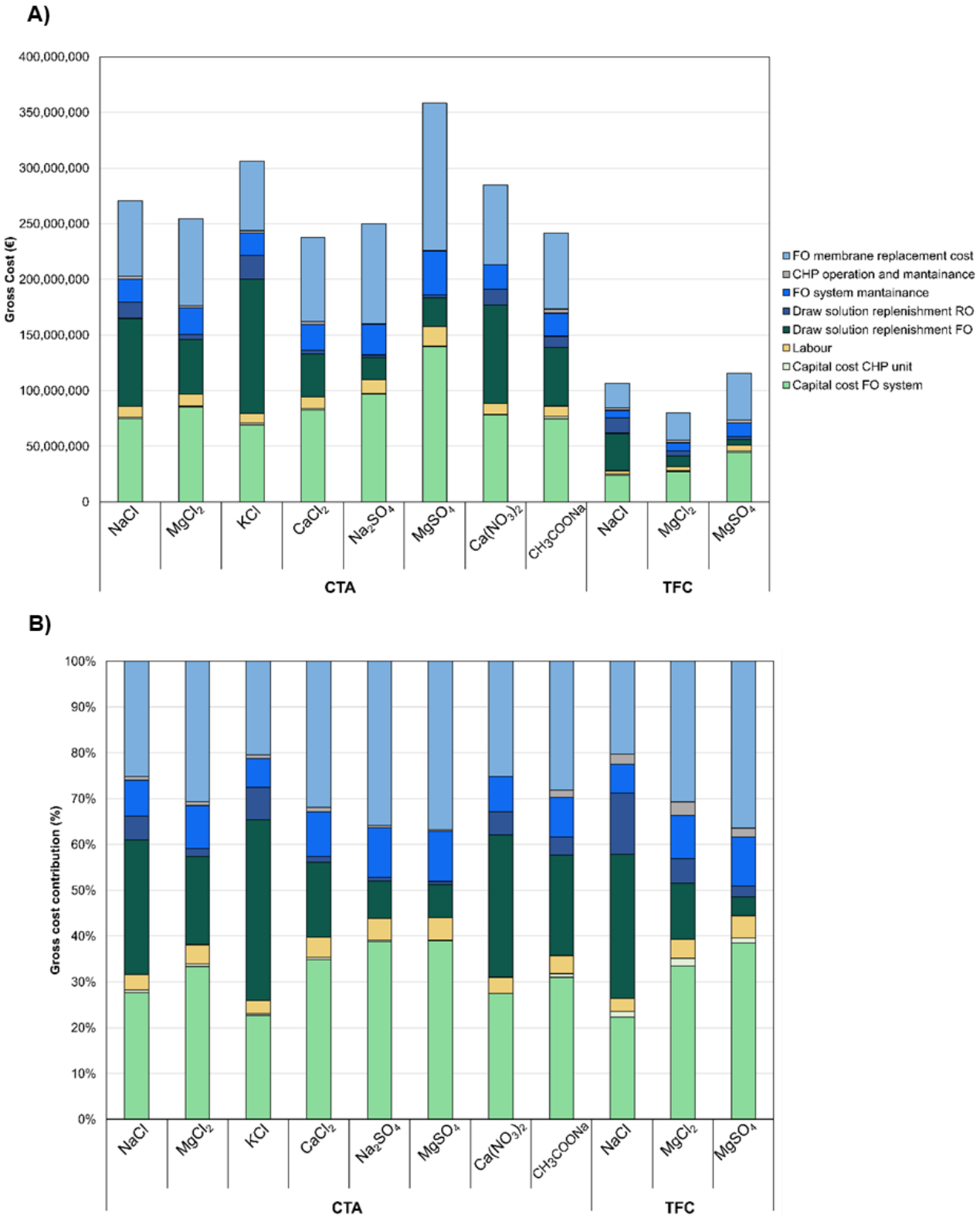

Figure 3. Gross cost contribution for the different draw solutes and membranes under study. (A) Absolute gross costs distribution (€); (B) relative gross cost distribution (%).

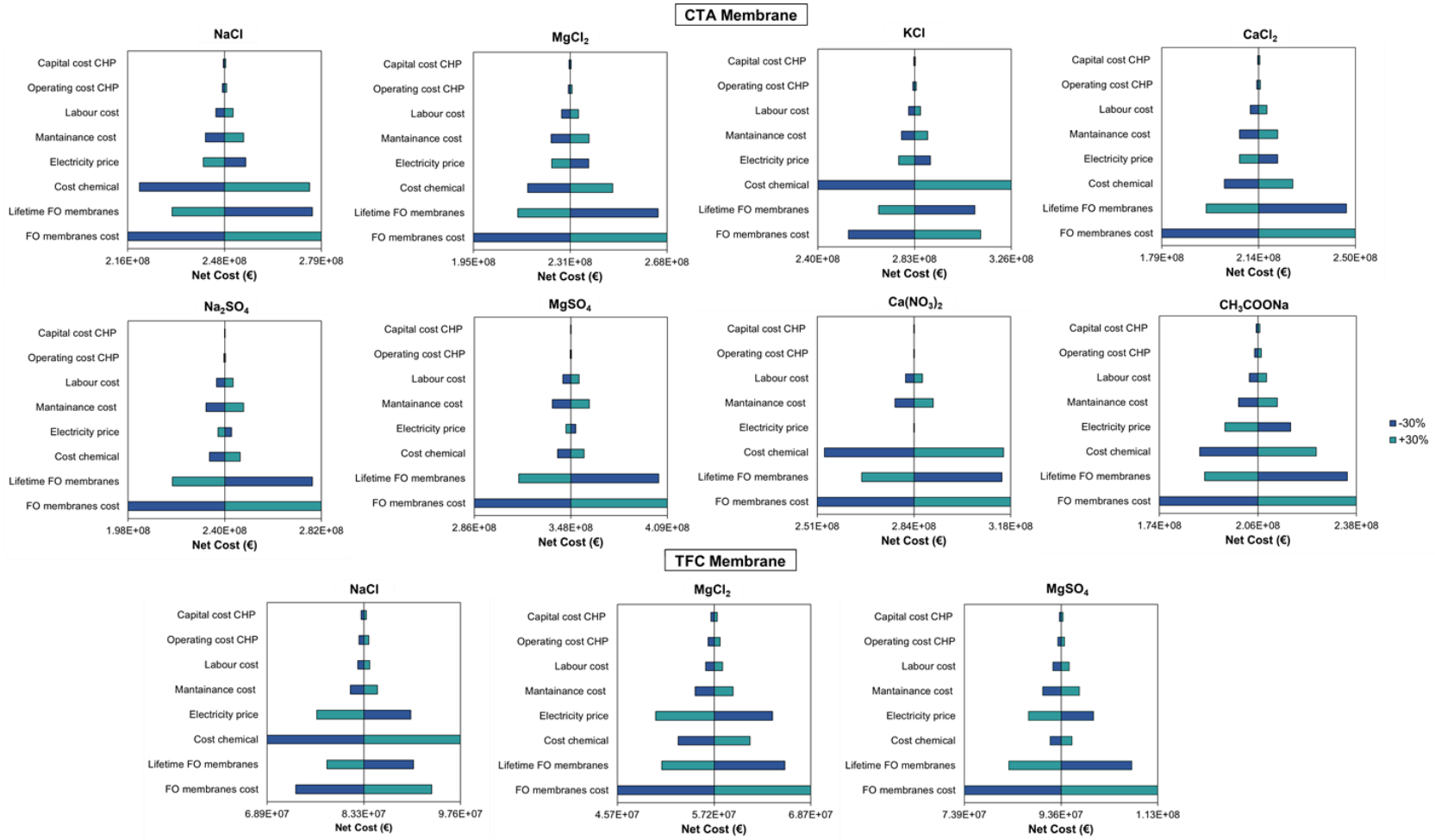

Figure 4. Sensitivity analysis of the net cost for a ±30% variation of the most important economic parameters for the different draw solutes and membranes under study.

SUPPLEMENTARY INFORMATION

Techno-economic analysis of forward osmosis pre-concentration before an anaerobic membrane bioreactor: Impact of draw solute and membrane material

Sergi Vinardell[a,*], Gaetan Blandin[b], Federico Ferrari[c], Geoffroy Lesage[d], Joan Mata-Alvarez[a,e], Joan Dosta[a,e], Sergi Astals[a]

[a] Department of Chemical Engineering and Analytical Chemistry, University of Barcelona, 08028, Barcelona, Spain

[b] Laboratory of Chemical and Environmental Engineering (LEQUiA), Institute of the Environment, University of Girona, 17003, Girona, Spain

[c] Eurecat, Centre Tecnològic de Catalunya, Water, Air and Soil Unit, 08242, Manresa, Spain

[d] Institut Européen des Membranes (IEM), Université de Montpellier, CNRS, ENSCM, 34090, Montpellier, France

[e] Water Research Institute, University of Barcelona, 08028, Barcelona, Spain

*Corresponding author (svinardell@ub.edu)

Table S1. Parameters used to model anaerobic digestion performance (Eq. (3)).

Parameter	Value	Reference
$k_{m,ac}$ (kg COD kg^{-1} COD_{cell} d^{-1})	8	(Batstone et al., 2002)
$K_{S,ac}$ (kg COD m^{-3})	0.15	(Batstone et al., 2002)
kg COD kg^{-1} VSS	1.42	(Henze et al., 2008)
KI_{50} Na^+ (g L^{-1})	7.4	(Kugelman and McCarty, 1964)
KI_{50} K^+ (g L^{-1})	5.9	(Kugelman and McCarty, 1964)
KI_{50} Mg^{2+} (g L^{-1})	1.9	(Kugelman and McCarty, 1964)
KI_{50} Ca^{2+} (g L^{-1})	4.4	(Kugelman and McCarty, 1964)
X_{ac} (g TSS L^{-1})	0.66-1.64[1]	Own Calculation

[1] Calculated from equations reported in Vinardell et al. (2020).

Table S2. Summary of the parameters used for the economic evaluation.

Parameter	Value	References
FO membrane cost (€ m^{-2})	49	(Valladares Linares et al., 2016)
FO membranes life time (years)	4	(Yangali-Quintanilla et al., 2015)
Labour cost (% to CAPEX)	1	(Fritzmann et al., 2007)
Maintenance cost (% to CAPEX)	2.5	(Fritzmann et al., 2007)
Electrical efficiency CHP unit (%)	33	(Riley et al., 2020)
CHP capital cost (€ kW_{el}^{-1})	712	(Riley et al., 2020)
CHP operating cost (€ kWh_{el}^{-1})	0.0119	(Riley et al., 2020)
Electricity price (€ kWh^{-1})	0.1149	(Eurostat, 2019)
NaCl purchase cost (€ mol^{-1})	0.016	(Bacaksiz et al., 2021)
$MgCl_2$ purchase cost (€ mol^{-1})	0.025	(Bacaksiz et al., 2021)
KCl purchase cost (€ mol^{-1})	0.020	(Bacaksiz et al., 2021)
$CaCl_2$ purchase cost (€ mol^{-1})	0.015	(Bacaksiz et al., 2021)
Na_2SO_4 purchase cost (€ mol^{-1})	0.013	(Bacaksiz et al., 2021)
$MgSO_4$ purchase cost (€ mol^{-1})	0.017	(Bacaksiz et al., 2021)
$Ca(NO_3)_2$ purchase cost (€ mol^{-1})	0.038	(Bacaksiz et al., 2021)
CH_3COONa purchase cost (€ mol^{-1})	0.034	(Bacaksiz et al., 2021)

Table S3. Summary of the methodology used for FO CAPEX calculation. This methodology was used by Vinardell et al. (2020), which adapted the methodology previously proposed by Bandin et al. (2015)**.**

	Overall RO plant CAPEX for the benchmark (%)	**% connected to RO stage**	**% FO Connected to RO benchmark**	**% FO CAPEX estimated area dependent[2]**
Installation/services	7.4	50	100	0
Legal	1.0	50	100	0
Design	6.9	50	100	0
Civil engineering	15.8	50	100	100
Pre-treatment	7.9	0	-	0
Equipment and materials	25.4	50	75	75
Membrane[1]	5.5	100	-	100
Pressure vessels	1.5	100	0	0
Pumps	7.3	50	50	75
Energy recovery	2.0	100	0	0
Piping	12.3	50	50	100
Intake/Outfall	7.0	0	0	0

[1] Membrane costs of FO process were determined depending on the flux and the permeate flow rate for each scenario.

[2] The capital costs that were FO flux dependent were included in the economic evaluation since these capital costs changed depending on the draw solution used.

Table S4. Input parameters to the ROSA software.

	NaCl	**$MgCl_2$**	**KCl**	**$CaCl_2$**	**Na_2SO_4**	**$MgSO_4$**	**$Ca(NO_3)_2$**
Permeate production ($m^3\ h^{-1}$)	3,333	3,333	3,333	3,333	3,333	3,333	3,333
Flux (LMH)	15	15	15	15	15	15	15
RO Recovery (%)	44.5	44.5	44.5	44.5	44.5	44.5	44.5
T (ºC)	25	25	25	25	25	25	25
Concentration solute ($g\ L^{-1}$)	19.3	18.6	25.7	24.0	46.8	78.3	48.1
Membrane Type	SW30HR-380	SW30HR-380	SW30HR-380	SW30HR-380	SW30HR-380	SW30HR-380	SW30HR-380
High pressure pump efficiency (%)	90	90	90	90	90	90	90
Configuration	1 pass	1 pass	1 pass	1 pass	1 pass	1 pass	1 pass
Elements per pressure vessel	8	8	8	8	8	8	8

References

Bacaksiz, A.M., Kaya, Y., Aydiner, C., 2021. Techno-economic preferability of cost-performance effective draw solutions for forward osmosis and osmotic anaerobic bioreactor applications. Chem. Eng. J. 410, 127535.

Batstone, D.J., Keller, J., Angelidaki, I., Kalyuzhnyi, S. V., Pavlostathis, S.G., Rozzi, A., Sanders, W.T., Siegrist, H., Vavilin, V.A., 2002. The IWA Anaerobic Digestion Model No 1 (ADM1). Water Sci. Technol. 45, 65–73.

Blandin, G., Verliefde, A.R.D., Tang, C.Y., Le-Clech, P., 2015. Opportunities to reach economic sustainability in forward osmosis–reverse osmosis hybrids for seawater desalination. Desalination 363, 26–36.

Eurostat, 2019. Electricity price statistics. https://ec.europa.eu/eurostat/statistics-explained/index.php/Electricity_price_statistics (accessed 30 September, 2019).

Fritzmann, C., Löwenberg, J., Wintgens, T., Melin, T., 2007. State-of-the-art reverse osmosis desalination. Desalination. 216, 1–76.

Henze, M., van Loosdrecht, M.C.M., Ekama, G.A., Brdjanovic, D., 2008. Biological wastewater treatment : principles, modelling and design. IWA Pub, London.

Kugelman, I.J., McCarty, P.L., 1964. Cation toxicity and stimulation in anaerobic waste treatment. II. Daily feed studies. Proc. Ninet. Ind. Waste Conf. 37, 667–686.

Riley, D.M., Tian, J., Güngör-Demirci, G., Phelan, P., Rene Villalobos, J., Milcarek, R.J., 2020. Techno-economic assessment of CHP systems in wastewater treatment plants. Environments 7, 1–32.

Valladares Linares, R., Li, Z., Yangali-Quintanilla, V., Ghaffour, N., Amy, G., Leiknes, T., Vrouwenvelder, J.S., 2016. Life cycle cost of a hybrid forward osmosis – low pressure reverse osmosis system for seawater desalination and wastewater recovery. Water Res. 88, 225–234.

Vinardell, S., Astals, S., Mata-Alvarez, J., Dosta, J., 2020. Techno-economic analysis of combining forward osmosis-reverse osmosis and anaerobic membrane bioreactor

technologies for municipal wastewater treatment and water production. Bioresour. Technol. 297, 122395.

Yangali-Quintanilla, V., Olesen, L., Lorenzen, J., Rasmussen, C., Laursen, H., Vestergaard, E., Keiding, K., 2015. Lowering desalination costs by alternative desalination and water reuse scenarios. Desalin. Water Treat. 55, 2437–2445.

2.5 Results and discussion

This section summarises the main findings of Publication II, III and IV regarding the experimental and economic implications of combining FO and AnMBR technologies for municipal sewage treatment.

2.5.1 AnMBR performance at different pre-concentration factors

The lab-scale AnMBR achieved COD removal efficiencies above 90% for all the pre-concentration factors (Table 1 in Publication II). COD removal fluctuations were observed during Period 1, 2 and 3, which corresponded to pre-concentration factors of 1, 5 and 10, respectively (Figure 1 in Publication II). In Period 1, COD removal fluctuations were attributed to the ongoing acclimatation of the biomass during the start-up of the AnMBR. In Period 3 and 4, COD removal fluctuations were attributed to organic shocks observed after membrane cleaning events. On day 66, an OLR shock of 3 g COD L^{-1} d^{-1} took place after a chemical cleaning of the membrane (Figure 2 in Publication II). This OLR shock led to unstable AnMBR performance with effluent COD concentrations around 900 mg COD L^{-1}. To avoid system failure, the membrane system was switched off until reaching VFA concentrations below 100 mg COD L^{-1}. The AnMBR performance was recovered and high COD removal efficiencies (>95%) were achieved during the final days of operation.

Effluent COD concentrations progressively increased as the pre-concentration factor increased despite the high COD removal efficiency (Figure 1 in Publication II). The increase in the effluent COD concentration was attributed to the higher organic load at higher pre-concentration factors. This was particularly important at pre-concentration factors of 5 and 10 since the average effluent COD concentration could exceed the discharge limits established in European Union (<125 mg COD L^{-1}) [32].

Sewage sodium concentrations were progressively increased from 0.28 to 2.30 g Na^{+} L^{-1} to simulate the effect of RSF. The results showed that AnMBR biomass was not inhibited since the COD removal efficiency was high regardless of the sodium concentration. This agrees with other studies that did not observe AnMBR biomass inhibition at sodium concentrations below 3.80 g Na^{+} L^{-1} [33,34]. However, the progressive increase of sewage COD and sodium concentrations affected the contribution of membrane biofilm to COD removal efficiency. The results showed that the sCOD concentration in the mixed liquor was higher than in the permeate (Figure 3 in Publication II). The difference between sCOD concentration of the mixed liquor and permeate was substantially higher for Period 4 than for the other three periods. These results suggest that the effect of membrane biofilm on AnMBR performance increased under more restrictive conditions (2.30 g Na^{+} L^{-1}).

Regarding methane production, the methane yield in the AnMBR increased from 214 to 322 mL CH_4 g^{-1} COD at pre-concentration factors of 1 to 10, respectively (Table 1 in Publication II), The higher methane yield at higher pre-concentration factors was attributed to the lower fraction of dissolved methane in the effluent with respect to the total methane produced as the pre-concentration factor increased. This output agrees with other AnMBR studies [35]. Besides the increase in methane yield, sewage pre-concentration allows increasing the AnMBR methane production per unit of wastewater treated as a result of the lower influent flow rate to the AnMBR (Table 2 in Publication II). A preliminary energy and economic evaluation showed that economic self-sufficiency could be achieved in the AnMBR at pre-concentration factors of 10 (Table 2 in Publication II). However, when the cost of the FO-RO stage is included in the economic balance, the total wastewater treatment cost substantially increases as reported in Publication III.

2.5.2 Techno-economic evaluation of FO, RO and AnMBR combination

The cost of the water produced by the hybrid FO-RO system ranged between 0.8 and 1.3 € per m^3 of water produced. The water production cost increased as the FO recovery increased from 50 to 90% (Figure 2a in Publication III). The progressive increase of the water production cost can be primarily attributed to the progressive decrease in water flux as the FO recovery increases. Maximising water production in the RO step was the most favourable strategy to produce water in the FO-RO system (Figure 2a in Publication III). CAPEX was the most important cost contributor in the closed-loop FO-RO system followed by FO membrane replacement and energy consumption (Figure 2b in Publication III). The FO membrane replacement contribution increases with the FO recovery since higher membrane areas are required at higher recoveries. These outputs point out the importance of FO membrane flux and durability on FO-RO economics.

The wastewater treatment cost of the AnMBR stage decreased as the FO recovery increased (Figure 3a in Publication III). FO pre-concentration reduces AnMBR influent flow rate with a direct impact on digester volume, membrane area and gas sparging requirements. CAPEX represented between 63 and 77% of the wastewater treatment cost, with membrane purchasing and digester construction as the most important contributors. OPEX only represented between 23 and 37% of the total costs, being energy consumption for gas sparging the most important contributor (Figure 3a in Publication III). The low contribution of OPEX to the total cost can be attributed to the reduction of energy consumption (no aeration required) and secondary sludge production in the AnMBR in comparison to typical aeration-based WWTPs.

The wastewater treatment cost of the whole FO-RO+AnMBR system ranged between 0.80 and 1.40 € per m^3 of wastewater treated (Figure 3b in Publication III). The AnMBR savings after implementing sewage pre-concentration did not offset the costs of the FO-RO system and, therefore, the stand-alone AnMBR was more economical than any FO-RO+AnMBR scenario. The most favourable FO-RO+AnMBR scenario corresponded to an FO recovery of 50% in a closed-loop scheme. Limiting FO recovery to 50% led to a wastewater treatment cost between 0.81 and 0.97 € per m^3 of wastewater treated (Figure 3b in Publication III), which is between the 0.6-1.0 € m^{-3} range reported in the literature for systems combining water production with wastewater treatment [31,36]. The FO-RO

system accounted for more than 74% of the wastewater treatment cost for all the FO-RO+AnMBR scenarios (Figure 3b in Publication III). The contribution of the FO-RO system to the wastewater treatment cost increased with the FO recovery since higher FO recoveries are associated to larger FO-RO installations. The high impact of FO-RO system on wastewater treatment cost can be primarily attributed to the limited FO water fluxes, particularly at high FO recoveries.

The impact of the FO water flux on the economics of the FO-RO+AnMBR system was evaluated using a sensitivity analysis. The results showed that the wastewater treatment cost sharply decreased when the FO water flux increased from 1 to 10 L m^{-2} h^{-1} (LMH) (Figure 5 in Publication III). However, at fluxes above 10 LMH, the wastewater treatment cost variation was minimal since the contribution of the FO system to the total cost was reduced at higher fluxes (Figure 5 in Publication III). These results demonstrate that achieving FO fluxes above 10 LMH could substantially improve the economic competitiveness of combining FO, RO and AnMBR technologies for municipal sewage treatment with energy and water production.

2.5.3 Impact of draw solute and membrane material on process economics

The type of FO membrane material had a high impact on the economic balance of combining FO and AnMBR technologies since TFC membranes substantially reduced the net cost when compared with CTA membranes (Figure 2 in Publication IV). The lower net cost achieved with TFC membrane can be attributed to (i) the high water flux and low RSF through FO membrane (high permselectivity) and (ii) the low structural parameter of commercial Aquaporin TFC membrane modules [37].

The draw solute featured a moderate impact on the net cost of the system. CH_3COONa and $CaCl_2$ were the most economically favourable draw solutes for CTA membrane, whereas $MgCl_2$ was the most economically favourable draw solute for TFC membrane (Figure 2 in Publication IV). These solutes allowed achieving relatively high water fluxes and low RSF through the FO membranes, which is the main reason behind their promising economic prospect. Conversely, draw solutes achieving high water fluxes such as NaCl or KCl were little attractive since they feature high RSF with a direct impact on draw solute replenishment costs. For both membrane materials, $MgSO_4$ was the most expensive

draw solute since $MgSO_4$ led to low FO membrane fluxes and reduced the amount of methane produced in the AnMBR due to competition between methanogens and sulphate reducing bacteria.

The costs associated with the FO installation (i.e. FO capital cost and FO membrane replacement) were the most important cost contributors for (i) CH_3COONa, $MgCl_2$, $CaCl_2$, Na_2SO_4 and $MgSO_4$ in CTA membrane and (ii) $MgCl_2$ and $MgSO_4$ in TFC membrane (Figure 3A in Publication IV). Conversely, the draw solution replenishment cost was the most important cost contributor for (i) NaCl, KCl and $Ca(NO_3)_2$ in CTA membrane, and (ii) NaCl in TFC membrane (Figure 3A in Publication IV). The high contribution of draw solution replenishment for NaCl, KCl and $Ca(NO_3)_2$ can be primarily attributed to their high RSF, which substantially increased the draw solution replenishment cost. It is worth mentioning that, in absolute values, the costs associated with the FO installation and draw solution replenishment were notably lower for TFC than for CTA membrane due to the improved permselectivity of TFC membranes (Figure 3B in Publication IV).

The FO membrane material and draw solute did not impact the AnMBR COD removal efficiency since the permeate COD concentration was similar at a given FO recovery (Table 2 in Publication IV). The AnMBR methane production, when using Na_2SO_4, $MgSO_4$ and $Ca(NO_3)_2$ as draw solutes, was lower since these solutes would be used as electron acceptors, thus reducing the amount of organic matter converted into methane. Conversely, the AnMBR methane production was increased when using CH_3COONa as draw solute since this solute increased the biodegradable organic matter concentration in the AnMBR influent. Finally, the results showed that the draw solute and COD concentrations in the AnMBR permeate increased with the FO recovery (Table 2 in Publication IV). This finding, which is line with the lab-scale results obtained in Publication II, highlights that restricting the FO recovery could be an strategy to improve the environmental and economic prospects of combining FO and AnMBR technologies.

CHAPTER 3:

Plant-wide impact of anaerobic membrane bioreactor implementation

3.1 Introduction

Changing the wastewater treatment paradigm from AS to AnMBR impacts the WWTP design and operation [38]. First, the combination of anaerobic digestion with membrane separation makes necessary to look for strategies to control long-term membrane fouling because achieving an efficient membrane fouling control is crucial to reduce the operating costs of AnMBR [39]. Second, anaerobic treatment of municipal sewage implies a total re-thinking of the WWTP conception. AnMBR removes organic matter, but it does not remove nitrogen or phosphorus, which means that the AnMBR effluent should undergo posttreatment to remove these nutrients and meet the discharge requirements. Besides nutrients, the AnMBR effluent will contain high amounts of dissolved methane due to the large volumetric flow rate and low temperature of municipal sewage [23,40]. As already reported in Publication I, the recovery or removal of the dissolved methane is paramount, considering the high global warning potential of this gas. In addition, the sludge line of an AnMBR-WWTP needs special attention, particularly considering that the sludge production in the AnMBR would be much lower than in an AS process. In this chapter, all these aspects are covered from a techno-economic point of view. Specifically, the impact of membrane fouling control strategy, AnMBR-WWTP layout and AnMBR waste sludge treatment on process economics are evaluated in Publications V, VI and VII.

Publication V evaluates the effect of specific gas demand (SGD) and membrane flux on membrane performance and process economics of granular AnMBR systems. Unlike the other publications of the thesis, this work is focused on a novel AnMBR configuration using granular sludge for membrane fouling control. The experimental set-up consisted in a vessel configured to mimic hydraulic conditions of granular AnMBRs and equipped with submerged microfiltration flat-sheet membranes. This experimental set-up was operated at the University of Montpellier (France) during the six-months research stay of the author in the research group *Institut Européen des Membranes*. Four SGD conditions and four membrane fluxes were evaluated using short- and long-term filtration tests. This allowed determining the fouling resistance as well as the dissolved and colloidal organic matter (DCOM) rejection for each flux and SGD condition. The most favourable SGD conditions for each membrane flux, obtained from the experimental results, were used to carry out a techno-economic analysis for a modelled full-scale granular AnMBR system.

Publication VI evaluates the economic feasibility of implementing mainstream AnMBR technology in a WWTP. This study modelled five different WWTP layouts, which were a combination of AnMBR with primary settler, degassing membrane for methane recovery, partial-nitritation anammox, chemical phosphorus precipitation and sidestream anaerobic digestion. The study modelled the WWTP layouts under different sewage COD concentrations ranging between 100 and 1100 mg COD L^{-1}. The impact of sewage sulphate on WWTP energy and economic balances were also analysed because sewage sulphate concentration is an important issue to take into account for mainstream AnMBR application (see Section 1.2).

Publication VII focuses on the sludge line of a WWTP based on mainstream AnMBR technology. Specifically, this publication evaluates the techno-economic implications of co-digesting food waste together with primary and AnMBR waste sludge in the sidestream anaerobic digester. To evaluate the most favourable co-digestion strategies, this publication modelled three organic loading rates (1.0, 1.5 and 2.0 kg VS m^{-3} d^{-1}) and two strategies to treat the nitrogen and phosphorus backloads either in the mainstream or in the sidestream of the AnMBR-WWTP.

Publication V, VI and VII included in Chapter 3 covered the following research gaps:

- The impact of SGD on membrane performance of granular AnMBR systems has received little attention in previous publications. Wang et al. [41] reported the importance of filtration mode and gas sparging rate on controlling membrane fouling and reducing the energy consumption of granular AnMBRs. This study evaluated the energy balance of the system but did not include all the capital and operating costs impacted by membrane fouling control strategy. An economic analysis including the costs influenced by the SGD and membrane flux is important to determine the most favourable membrane fouling control strategies in granular AnMBRs from an economic point of view (***Publication V***).

- Different plant layouts have proposed to integrate mainstream AnMBR in a WWTP [13,42,43]. However, the selection of the plant layout has substantially differed among studies and there is not a common criteria for layout selection considering energy and economic aspects. Evaluating different plant layouts including energy and economic aspects is necessary to provide a comprehensive framework for AnMBR-WWTP layout selection (***Publication VI***).

- Co-digestion of food waste and sewage sludge has been evaluated for conventional AS plants [44,45]. However, no studies have analysed the economic feasibility to co-digest food waste and sewage sludge in a future WWTP based on mainstream AnMBR technology. Understanding the implications of implementing co-digestion to maximise energy production in a retrofitted AnMBR-WWTP is important to explore the potential of these plants to further increase energy production in the sidestream anaerobic digester (***Publication VII***).

3.2 Publication V: *Impact of permeate flux and gas sparging rate on membrane performance and process economics of granular anaerobic membrane bioreactors*

Vinardell, S., Sanchez, L., Astals, S., Mata-Alvarez, J., Dosta, J., Heran, M., Lesage, G. Impact of permeate flux and gas sparging rate on membrane performance and process economics of granular anaerobic membrane bioreactors. Accepted for publication in Science of the Total Environment.

Impact of permeate flux and gas sparging rate on membrane performance and process economics of granular anaerobic membrane bioreactors

Sergi Vinardell[a,b,*], Lucie Sanchez[b], Sergi Astals[a], Joan Mata-Alvarez[a,c], Joan Dosta[a,c], Marc Heran[b], Geoffroy Lesage[b]

[a] Department of Chemical Engineering and Analytical Chemistry, University of Barcelona, 08028, Barcelona, Spain

[b] Institut Européen des Membranes (IEM), Université de Montpellier, CNRS, ENSCM, 34090, Montpellier, France

[c] Water Research Institute, University of Barcelona, 08028, Barcelona, Spain

*Corresponding author (svinardell@ub.edu)

Abstract

This research investigated the impact of permeate flux and gas sparging rate on membrane permeability, dissolved and colloidal organic matter (DCOM) rejection and process economics of granular anaerobic membrane bioreactors (AnMBRs). The goal of the study was to understand how membrane fouling control strategies influence granular AnMBR economics. To this end, short- and long-term filtration tests were performed under different permeate flux and specific gas demand (SGD) conditions. The results showed that flux and SGD conditions had a direct impact on membrane fouling. At normalised fluxes (J_{20}) of 4.4 and 8.7 L m^{-2} h^{-1} (LMH) the most favourable SGD condition was 0.5 m^3 m^{-2} h^{-1}, whereas at J_{20} of 13.0 and 16.7 LMH the most favourable SGD condition was 1.0 m^3 m^{-2} h^{-1}. The flux and the SGD did not have a direct impact on DCOM rejection, with values ranging between 31 and 44%. The three-dimensional excitation-emission matrix fluorescence (3DEEM) spectra showed that protein-like fluorophores were predominant in mixed liquor and permeate samples (67-79%) and were retained by the membrane (39-50%). This suggests that protein-like fluorophores could be an important foulant for these systems. The economic analysis showed that operating the membranes at moderate fluxes (J_{20}=7.8 LMH) and SGD (0.5 m^3 m^{-2} h^{-1}) could be the most favourable alternative. Finally, a sensitivity analysis illustrated that electricity and membrane cost were the most sensitive economic parameters, which highlights the importance of reducing SGD requirements and improving membrane permeability to reduce costs of granular AnMBRs.

Keywords

Anaerobic membrane bioreactor (AnMBR); membrane fouling; membrane rejection; upflow anaerobic sludge blanket; dissolved organic matter; techno-economic analysis

1. Introduction

Wastewater treatment plants (WWTP) are undergoing a transformative process where the energy consumption is reduced, the recovery of resources is maximised and the quality of the treated sewage is improved (McCarty et al., 2011). Membrane technologies play an important role in this transition since these technologies allow obtaining high-quality effluents free of suspended solids and pathogens with a high potential for their reuse (Krzeminski et al., 2017). Anaerobic membrane bioreactor (AnMBR) is an emerging technology for municipal sewage treatment that combines anaerobic digestion and membrane separation (Vinardell et al., 2020). This technology has a double positive connotation since it converts the sewage organic matter into methane-rich biogas and provides an excellent retention of the slow-growing anaerobic biomass into the bioreactor with a direct impact on process performance and effluent quality (Ozgun et al., 2013; Stazi and Tomei, 2018).

Several studies have shown the potential of AnMBRs to achieve high organic matter removals with competitive treatment costs (Pretel et al., 2014; Shoener et al., 2016; Vinardell et al., 2021). The technical and economic competitiveness of AnMBR has led to its full-scale implementation for the treatment of different types of industrial wastewater, including alcohol production stillage or food processing wastewater (Dereli et al., 2012; Zhen et al., 2019). However, AnMBR technology still needs to overcome some limitations before widespread implementation in WWTPs, such as membrane fouling, process temperature or low sewage organic matter concentration. Among these limitations, membrane fouling stands as one of the main challenges for full-scale application since it has a large influence on the technical and economic feasibility of the technology (Anjum et al., 2021; De Vela, 2021; Ji et al., 2021). Membrane fouling is a dynamic process that involves the interaction of organic and inorganic foulants with the membrane, which results in a progressive decrease of the membrane permeability (Meng et al., 2017). The decrease of membrane permeability leads to complex chemical and physical cleaning protocols that have a direct impact on the membrane lifetime and operating costs (Aslam et al., 2017; Dong et al., 2016). Furthermore, membrane permeability reduction also increases the AnMBR capital costs since larger membrane areas would be necessary as a result of the reduced flux. Therefore, the development of

configurations and operational strategies able to reach an efficient control of membrane fouling is crucial to achieve relatively high fluxes without an excessive consumption of energy and chemicals.

Different configurations have been proposed in the literature to reduce membrane fouling in AnMBRs (Maaz et al., 2019; Song et al., 2018). The granular AnMBR, which is configured as an upflow anaerobic sludge blanket (UASB), is an interesting alternative to improve fouling control in AnMBRs and improve its full-scale applicability (Chen et al., 2017; Gouveia et al., 2015a; Martin-Garcia et al., 2011). In this configuration, the sewage is fed through the bottom of the bioreactor where a dense granular sludge with good settling characteristics is established. The membrane is typically submerged in an external tank or at the top of the bioreactor to reduce the concentration of solids nearby the membrane. The lower solids concentration close to the membrane aims to reduce cake layer formation and improve membrane fouling control in comparison with AnMBRs configured as continuous stirred tank reactors (Chen et al., 2016; Wang et al., 2018). However, the granular AnMBR system still presents some challenges concerning membrane fouling control. In granular AnMBR, the membrane is in contact with fine particles that are washed out from the granular sludge bed. The removal of these particles from the zones surrounding the membrane is challenging since they feature a poor settleability and back-transport characteristics (Gouveia et al., 2015b). The accumulation of these particles close to the membrane can reduce its permeability since microparticles have been reported to play an important role in AnMBR membrane fouling (Yao et al., 2020; Zhou et al., 2019). Accordingly, it is important to look for strategies able to scour and reduce the concentration of fine solids and dissolved/colloidal organic matter close to the membrane.

Gas sparging is the most used strategy to control membrane fouling in AnMBRs (Fox and Stuckey, 2015; Robles et al., 2013). Gas sparging rates between 0.2 and 2 $m^3\ m^{-2}\ h^{-1}$ have been reported in granular AnMBR systems treating municipal sewage (Gouveia et al., 2015a; Wang et al., 2018). The selection of the sparging rate should consider not only the energy consumption, but also the flux under which the membrane is operated since it also affects the extent of fouling. Wang et al. (2018) evaluated the impact of gas sparging rate on membrane fouling control and energy consumption of a granular AnMBR system.

Continuous and intermittent gas sparging regimes as well as different membrane filtration modes were evaluated. Wang et al. (2018) demonstrated the importance of gas sparging regime, permeate flux and filtration mode on membrane permeability and energy consumption of the granular AnMBR system. However, this study did not evaluate how the different fouling control strategies could influence the costs of the granular AnMBR system. In this regard, an economic analysis including all the costs influenced by the gas sparging rate and permeate flux (e.g. energy consumption, membrane purchase, consumption of chemicals, membrane replacement) is important to holistically evaluate the potential of AnMBR technology for municipal sewage treatment. To the best of the authors' knowledge, the coupling effect of gas sparging rate and permeate flux on capital and operating costs of granular AnMBRs has not yet been evaluated. Accordingly, further research is needed to understand under which sparging rate conditions the granular AnMBR permeate flux can be sustained at an optimum treatment cost.

This study aims to analyse the impact of permeate flux and gas sparging rate on membrane permeability, dissolved and colloidal organic matter (DCOM) rejection and economic feasibility of granular AnMBR systems. Short-term filtration tests were conducted to evaluate the variation of fouling resistance and DCOM rejection for different flux and gas sparging conditions. Subsequently, long-term filtration tests were carried out for the most favourable sparging rate conditions for each flux. The permeability results from the long-term filtration tests were used to conduct an economic analysis to determine the influence of the different membrane fouling control strategies on granular AnMBR economics. The ultimate goal is to understand how the interdependence of different permeate flux and gas sparging rate conditions influence membrane fouling and process economics of granular AnMBRs.

2. Materials and Methods

2.1 Granular anaerobic sludge source

The granular anaerobic sludge used in the short- and long-term filtration tests was collected from a full-scale anaerobic reactor treating wastewater from a recycled paper processing factory (Laveyron, France). The anaerobic granular sludge had a total solids (TS) concentration of 90.6 ± 2.6 g L^{-1} with a volatile solids (VS) fraction of 77.0 ± 0.9

%. The main characteristics of the sludge are shown in Table S1 of the supplementary material. The anaerobic granular sludge was kept refrigerated at 4 ºC before its use.

2.2 Experimental set-up

The experimental set-up for the filtration tests consisted of a cuboid tank (282×100×900 mm) with a working volume of 17 L. The experimental set-up was designed to simulate hydrodynamic conditions of a granular AnMBR system. Three flat-sheet membrane modules with a total membrane area of 0.22 m^2 were submerged in the tank. Each membrane module consisted of two polyvinylidene difluoride (PVDF) microfiltration membranes (Amogreentech, South Korea) with a pore size of 0.3 µm. The permeate was withdrawn using a peristaltic pump (Longer Pump, China). A pressure sensor (Keller, Switzerland) was connected in the permeate line to record the transmembrane pressure (TMP). The permeate was returned back to the tank after the pressure was recorded. A peristaltic pump (Longer Pump, China) was used to recirculate the liquor from the top to the bottom of the tank to provide a liquid upflow velocity of 0.8 m h^{-1}, which is a typical upflow velocity in granular AnMBR systems (Wang et al., 2020, 2018). This recirculation provided additional turbulence in the filtration zone, which is important to reduce the accumulation of fine solids and dissolved/colloidal organic matter close to the membrane (Gouveia et al., 2015a). Pure nitrogen (99.9%) was used for gas sparging. The nitrogen was introduced at the bottom of the tank through three holes (d=1.5 mm) that allowed a homogenous distribution of the gas throughout the tank's height. A rotameter flow meter (Krohne Group, Germany) was connected in the gas line to have a manual record of the nitrogen flow rate. The flow rate was adjusted by means of a regulating valve (Linde Engineering). A schematic representation of the experimental set-up can be found in Figure 1.

Before each filtration test, the anaerobic granular sludge was diluted with distilled water to perform the filtration tests under controlled solids concentration conditions. The TS and VS concentrations in the tank ranged from 8.6 to 9.9 g TS L^{-1} and from 6.5 to 7.4 g VS $L^{.1}$ for the filtration tests (Table S2 of the supplementary material).

2.3 Short-term filtration tests

Short-term filtration tests were conducted to evaluate the impact of flux and gas sparging rate on membrane permeability and DCOM rejection. Short-term filtration tests have been widely used in previous AnMBR studies as screening tool to determine the impact of membrane operational conditions on filtration performance under reproducible conditions (Fox and Stuckey, 2015; Odriozola et al., 2021; Ruigómez et al., 2016). Four specific gas demand (SGD) intensities (0.25, 0.5, 1.0 and 2.0 m^3 m^{-2} h^{-1}) and four flux conditions (5, 10, 15 and 20 L m^{-2} h^{-1} (LMH)) were evaluated in the short-term filtration tests. The SGD and flux conditions were selected based on available literature (Ruigómez et al., 2016; Wang et al., 2018). The SGD conditions are reported at normal conditions of pressure and temperature. Table 1 shows the fluxes and their normalised experimental values at 20 ºC for each SGD condition.

The experimental cycle for the short-term filtration tests comprised four different stages: (1) distilled water filtration to determine the membrane filtration resistance, (2) granular sludge filtration to determine the total filtration resistance, (3) physical cleaning of the membrane with tap water and (4) chemical cleaning of the membrane with a 0.2% sodium hypochlorite solution for 2 h. These four stages were repeated for each flux. The total filtration resistance (Stage 2) for each SGD condition was obtained with a SGD step method adapted from Ruigómez et al. (2016). Specifically, Ruigómez et al. (2016) used the step method proposed by Le Clech et al. (2003) to evaluate the impact of different rotational velocities (fouling control method) on membrane permeability of AnMBRs. In the present study, the SGD step method consisted in progressively increasing/decreasing the SGD intensity for each flux. Firstly, the SGD was progressively increased from 0.25 to 2.0 m^3 m^{-2} h^{-1} following four SGD steps (0.25, 0.5, 1.0 and 2.0 m^3 m^{-2} h^{-1}). Secondly, the SGD was progressively decreased from 2.0 to 0.25 m^3 m^{-2} h^{-1} following the same SGD steps. Each SGD step had a filtration duration of 15 min, whereas a relaxation period of 90 s was applied between steps. The permeate samples were obtained at the end of each SGD step. Permeate flow rate was measured three times per each SGD step to record the experimental flux. The liquor temperature was measured before starting each SGD step and all the fluxes were normalised to 20 ºC by means of Eq. (1) (Wang et al., 2020):

$$J_T = J_{20} \cdot 1.025^{(T-20)} \quad \text{Eq. (1)}$$

where J_T is the measured flux (LMH), J_{20} is the normalised flux at 20 ºC (LMH) and T is the sludge temperature (ºC). The filtration resistance for distilled water and granular sludge filtration was determined by using Eq. (2). Subsequently, the filtration resistance caused by membrane fouling (R_F) was used as indicator to determine the extent of fouling for each condition (Eq. (3)).

$$R = \frac{TMP}{\mu_{20} \cdot J_{20}} \quad \text{Eq. (2)}$$

$$R_F = R_T - R_M \quad \text{Eq. (3)}$$

where R is the filtration resistance (m^{-1}), TMP is the transmembrane pressure (Pa), J_{20} is the normalised flux at 20 ºC ($m^3\ m^{-2}\ s^{-1}$), μ_{20} is the water viscosity at 20ºC (Pa s), R_F is the foulant filtration resistance (m^{-1}), R_T is the total filtration resistance obtained during granular sludge filtration (m^{-1}) and R_M is the membrane resistance obtained during distilled water filtration (m^{-1}).

The short-term filtration tests for each flux and SGD were conducted in triplicate. The anaerobic granular sludge was replaced before each replicate to prevent substantial degradation of the soluble and colloidal compounds that could influence the membrane permeability and DCOM rejection of the system. All the replicates were carried out under similar solids concentration (Table S2 of the supplementary material). Error bars in figures represent the standard deviation.

2.4 Long-term filtration tests

Long-term filtration tests were conducted for four operational conditions: (1) J_{20}=4.1 LMH and SGD=0.5 $m^3\ m^{-2}\ h^{-1}$; (2) J_{20}=7.8 LMH and SGD=0.5 $m^3\ m^{-2}\ h^{-1}$; (3) J_{20}=12.0 LMH and SGD=1.0 $m^3\ m^{-2}\ h^{-1}$; and (4) J_{20}=15.4 LMH and SGD=1.0 $m^3\ m^{-2}\ h^{-1}$. These selected operational conditions represented the most favourable SGD for each membrane flux from the sort-term filtration tests (see Section 3.1).

The experimental cycle for the long-term filtration tests comprised four different stages: (1) distilled water filtration, (2) granular sludge filtration to determine the membrane permeability, (3) physical cleaning of the membrane with tap water and (4) chemical cleaning of the membrane with a 0.2% sodium hypochlorite solution for 4h. These four

stages were repeated for each of the four scenarios evaluated. It is worth mentioning that the duration of the chemical cleaning in the long-term filtration tests was longer than in the short-term tests since the extent of fouling is higher in the long-term trials. This intensive chemical cleaning protocol was applied to ensure the recovery of membrane permeability prior to the next filtration test. The determination of the permeability (Stage 2) comprised five filtration cycles of 45 min with a total duration of 225 min (5×45 min). A relaxation period of 90 s was applied between each filtration cycle. To obtain the experimental flux, the permeate flow rate was measured eight times per each filtration cycle. The liquor temperature was measured three times per each filtration cycle to record possible temperature variations during the experimental period. All the fluxes and membrane permeabilities were normalised to 20 ºC (Eq. (1)). The normalised membrane permeability (k_{20}) at the end of the fifth cycle (225 min) was used for the economic analysis. The k_{20} was calculated by means of Eq. (4).

$$k_{20} = \frac{J_{20}}{TMP} \qquad \text{Eq. (4)}$$

where k_{20} is the normalised permeability at 20 ºC (LMH bar^{-1}), J_{20} is the normalised flux at 20 ºC (LMH) and TMP is the transmembrane pressure (bar).

2.5 Analytical methods

TS and VS were measured following the Standard Method 2540G (APHA, 2017). The soluble total organic carbon (sTOC) analysis was conducted with a TOC analyser (Shimadzu, Japan). The soluble chemical oxygen demand (COD) was measured with COD LCK kits and an UV-VIS spectrophotometer (Hach Lange, Germany). The dissolved and colloidal fractions were obtained after filtering the samples with 1.2 µm filters (Whatman, UK). The pH was analysed with a pH electrode (VWR, USA). The zeta potential of the sludge samples was measured with a zeta potential analyser (Anton Paar, Spain). The particle size distribution of the initial granular sludge was obtained by sieving according to the method reported by Derlon et al (2016).

Three-dimensional excitation-emission matrix fluorescence (3DEEM) was used to evaluate the membrane rejection of DCOM fluorophores. A Perkin-Elmer LS-55 spectrometer was used to obtain the fluorescence spectra for each sample. The samples were diluted with Milli-Q water by a factor of 150 to avoid overlapping signals. The

emission and excitation spectra ranged from 280 to 600 nm and from 200 to 500 nm, respectively. Blank test with Milli-Q water was performed to normalise the spectra. The normalised spectra can be divided into different regions depending on the fluorophore analysed (Chen et al., 2003; Jacquin et al., 2018): (i) Region I+II, which corresponds to protein-like fluorophores; (ii) Region III, which corresponds to fulvic acid-like fluorophores; (iii) Region IV, which corresponds to soluble microbial product-like fluorophores and (iv) Region V, which corresponds to humic acid-like fluorophores. Further information on the methodology used for the 3DEEM analysis can be found in Jacquin et al. (2017).

2.6 Economic evaluation

2.6.1 Scenarios definition

The economic evaluation was conducted modelling a high-sized WWTP with a treatment capacity of 500,000 population equivalent (100,000 m^3 d^{-1}). The WWTP was considered to have a mainstream granular AnMBR system for sewage treatment. Detailed information of the different scenarios and conditions considered for the economic analysis can be found in Table S3 of the supplementary material.

The economic analysis evaluated the four scenarios selected for the long-term filtration tests. Scenario 1: J_{20}=4.1 LMH and SGD=0.5 m^3 m^{-2} h^{-1}; Scenario 2: J_{20}=7.8 LMH and SGD=0.5 m^3 m^{-2} h^{-1}; Scenario 3: J_{20}=12.0 LMH and SGD=1.0 m^3 m^{-2} h^{-1}; and Scenario 4: J_{20}=15.4 LMH and SGD=1.0 m^3 m^{-2} h^{-1}.

Three different chemical cleaning conditions were considered for each scenario. Condition A: clean in place (CIP) and clean out of place (COP) performed 52 and 2 times per year, respectively; Condition B: CIP and COP performed 26 and 1 times per year, respectively; and Condition C: CIP and COP performed 104 and 3 times per year, respectively. Further information on chemical cleaning protocol selection can be found in Section 2.6.2.

2.6.2 Cost calculation

Capital and operating costs for the granular AnMBR system were included in the economic analysis. The capital costs accounted for membrane and blower purchase costs.

The operating costs accounted for energy consumption for gas sparging and permeate pumping, membrane replacement cost and chemical reagents cost. It is worth mentioning that all the costs and revenue that were not influenced by flux and SGD (e.g. capital cost for bioreactor construction, methane production) have not been included in this economic evaluation since they would be similar regardless of the flux and SGD applied. Detailed information of the parameters used for cost calculations can be found in Table S4 of the supplementary material.

The capital costs for membranes and blowers were considered to be 50 € m^{-2} and 4.15 € Nm^{-3} h, respectively (Verrecht et al., 2010; Vinardell et al., 2021). The required power of the blower for gas sparging was calculated by means of Eq. (5) (Pretel et al., 2014):

$$P_B = \frac{M \cdot R \cdot T}{(\alpha - 1) \cdot \eta_B} \cdot \left[\left(\frac{P_2}{P_1} \right)^{\frac{\alpha - 1}{\alpha}} - 1 \right] \quad \text{Eq. (5)}$$

where P_B is the power of the blower (W), M is the biogas molar flow rate (mol s^{-1}), T is the temperature of the biogas (ºK), R is the ideal gas constant (J mol^{-1} K^{-1}), η_B is the blower efficiency (0.80), α is the adiabatic coefficient, P_1 is the absolute pressure in the inlet side of the blower (atm) and P_2 is the absolute pressure in the impulsion side of the blower (atm).

Eq. (6) was used to obtain the required power for the permeate pump (Pretel et al., 2014):

$$P_{PP} = \frac{TMP \cdot Q_P}{\eta_{PP}} \quad \text{Eq. (6)}$$

where P_{PP} is the power of the permeate pump (W), Q_P is the permeate flow rate (m^3 s^{-1}) TMP is transmembrane pressure (Pa), and η_{pp} is the permeate pump efficiency (0.85).

Chemical cleaning requirements depend on the extent of membrane fouling in the AnMBR (Wang et al., 2014). This means that those scenarios with a higher membrane permeability and lower membrane fouling would require a less intensive chemical cleaning. In the present study, the concentration of chemical reagents for the economic analysis was defined considering the membrane permeability of each scenario, obtained from the long-term filtration tests. Scenario 4 was considered the reference scenario from which the concentration of chemical reagents was calculated for the other three scenarios. Scenario 4 was the reference since Scenario 4 features a similar flux (J_T=17.9 LMH) than

typical fluxes for full-scale aerobic MBR plants (Judd, 2010; Verrecht et al., 2010). Therefore, it was considered that typical chemical cleaning protocols reported in the literature for full-scale MBR plants could be extendible to Scenario 4.

The chemical cleaning protocol for Scenario 4 was adapted from Brepols et al. (2008). The chemical cleaning included both CIP and COP protocols. The CIP protocol was assumed to be performed once a week (52 times per year) with a 0.05% sodium hypochlorite solution and a 2,000 mg L^{-1} citric acid solution. The COP protocol was assumed to be performed twice a year with a 0.1% sodium hypochlorite solution and a 2,000 mg L^{-1} citric acid solution (Condition A). The volume of chemicals was considered to be 17.5 L m^{-2} (Ramos et al., 2014). Subsequently, the consumption of chemical reagents for Scenario 1, 2 and 3 was calculated considering that the consumption of chemical reagents was inversely proportional to the membrane permeability. Specifically, the ratio between normalised permeability of the Scenario and normalised permeability of the reference Scenario 4 ($k_{20,x}/k_{20,4}$) was used to calculate the amount of chemical reagents required for each scenario. The duration of the CIP and COP for each chemical reagent was 2 and 16 h, respectively. To evaluate the impact of chemical cleaning protocol frequency on operating costs, two other cleaning frequencies were considered. Condition B: CIP and COP performed 26 and 1 times per year, respectively; and Condition C: CIP and COP performed 104 and 3 times per year, respectively.

The extent of chemical cleaning also has an impact on membrane replacement cost since chemical cleaning reduces the lifetime of the membranes. The membrane replacement cost was calculated considering that the membranes had to be replaced when the maximum cumulative chlorine contact of 500,000 mg L^{-1}-hour was exceeded (Robles et al., 2014). The residual economic value of the membranes at the end of the plant lifetime was included in the economic evaluation.

The capital expenditures (CAPEX) and operating expenditures (OPEX) for the different scenarios and conditions were calculated and Eq. (7) was used to obtain the discounted lifetime cost (DLC) for each scenario:

$$\mathrm{DLC} = \mathrm{CAPEX} + \sum_{t=1}^{T} \frac{\mathrm{OPEX_t}}{(1+i)^t} \qquad \text{Eq. (7)}$$

where CAPEX is the capital expenditure (€), $OPEX_t$ is the OPEX at year t (€), i is the discount rate (5%) and T is the plant lifetime (20 years).

3. Results and discussion

3.1 Effect of flux and SGD on membrane filtration resistance

Figure 2 shows the R_F of the short-term filtration tests for the different fluxes and SGDs. The results show that the extent of membrane fouling was clearly influenced by the SGD intensity since the R_F decreased as the SGD increased. Higher fluxes increased the extent of membrane fouling, which made it necessary to substantially increase SGD intensities to reduce R_F values. Regarding $Flux_1$ and $Flux_2$ (J_T and J_{20} < 10 LMH), a reduction of R_F was observed when the SGD increased from 0.25 to 0.5 m^3 m^{-2} h^{-1}. However, when the SGD was further increased the R_F reduction was minimal. These results show that a SGD of 0.5 m^3 m^{-2} h^{-1} was the most favourable condition for membrane fouling control when the membrane was operated below 10 LMH (Figure 2). Regarding $Flux_3$ and $Flux_4$ (J_T and J_{20} > 10 LMH), a noticeable reduction of R_F was observed as the SGD decreased from 0.25 to 2.0 m^3 m^{-2} h^{-1}. However, the R_F reduction was progressively less pronounced as the SGD increased. This was particularly important when the SGD increased from 1.0 to 2.0 m^3 m^{-2} h^{-1} since this SGD step only provided a relatively moderate R_F reduction at expenses of doubling the gas sparging demand. Accordingly, it is conceivable to state that a SGD of 1.0 m^3 m^{-2} h^{-1} was the most favourable condition for membrane fouling control when the membrane was operated above 10 LMH. These results align with other AnMBR studies that reported that SGDs above 1.0 m^3 m^{-2} h^{-1} did not lead to substantial improvements in membrane fouling control (Ruigómez et al., 2016; Wang et al., 2018).

These results suggest that the extent of membrane fouling was substantially higher when the membrane was operated at fluxes above 10 LMH since the R_F was higher for $Flux_3$ and $Flux_4$ (J_T and J_{20} > 10 LMH) than for $Flux_1$ and $Flux_2$ (J_T and J_{20} < 10 LMH) regardless of the SGD condition applied. These results also highlight that, besides the SGD, it is important to include the impact of flux on fouling extent since the best strategy for fouling control requires a compromise solution considering flux, SGD intensity and fouling extent.

3.2 Effect of flux and SGD on dissolved and colloidal organic matter rejection

Figure 3 shows the sCOD membrane rejection for the different fluxes and SGDs evaluated, where sCOD rejection results have been grouped for each flux and SGD condition. The specific sCOD membrane rejection for each condition is shown in Figure S1 of the supplementary material. The sCOD rejection ranged between 31 and 44% for the different conditions (Figure 3). The capacity of the ultrafiltration/microfiltration membranes to reject DCOM can be attributed to the pore size exclusion phenomenon or chemical/physical interactions of the soluble compounds with the membrane and/or the fouling layer formed on its surface (Jacquin et al., 2018; Liu et al., 2021; Xin et al., 2020). The results show no direct correlation between the SGD/flux and the rejection of sCOD. Regarding the SGD, the sCOD rejection was similar (33-38%) regardless of the SGD applied and no significant differences were observed between the four SGD conditions ($p>0.05$). Regarding the flux, the sCOD rejection was similar for $Flux_1$, $Flux_2$ and $Flux_3$ (31-35%) and no significant differences were observed between them ($p>0.05$). Conversely, $Flux_4$ featured a statistically significantly higher sCOD rejection (44%) when compared to the other flux conditions ($p<0.05$). These differences could be attributed to changes in the concentration and composition of DCOM. The fluorescence intensity of the mixed liquor samples was higher for $Flux_4$ than for $Flux_1$, $Flux_2$ and $Flux_3$, which was particularly noticeable for Region I+II of the 3DEEM spectra (see Figure S2 of the supplementary material). It is hypothesised that the higher sCOD rejection achieved in $Flux_4$ could be attributed to the higher content of DCOM in Region I+II since the DCOM compounds contained in this region are more retained by the membrane (see Table 2).

Table 2 shows the membrane rejection of fluorophores DCOM for the different regions of the 3DEEM spectra. The rejection of fluorophores DCOM ranged between 34 and 44%, which was similar to the sCOD rejection. Table 2 also shows that membrane rejected between 39 and 50% of the fluorophores DCOM of Region I+II. The higher rejection of fluorophores DCOM in Region I+II (protein-like fluorophores) in comparison to the other regions can be mainly attributed to the high molecular weight and hydrophilic nature of proteins (Jacquin et al., 2018; Xin et al., 2020). This is particularly important since Region I+II was predominant in the 3DEEM spectra (67-79%), followed by Region III+V (17-29%) and Region IV (2-4%) (see Figure S3 and Table S5 of the supplementary

material). Considering the predominance of protein-like fluorophores in the 3DEEM spectra and that these fluorophores are more retained by the membrane, it is stated that proteins could play an important role in membrane fouling of anaerobic granular sludge filtration. Finally, it is worth mentioning that the results of Table 2 corroborate that flux and SGD conditions did not feature a direct correlation with the DCOM rejection. However, experiments with a longer filtration duration are necessary to evaluate the impact that the formation and consolidation of a gel or cake layer on the membrane surface have on the DCOM rejection.

3.3 Long-term filtration tests

Table 3 shows the experimental flux, k_{20} and $k_{20,x}/k_{20,4}$ ratio obtained from the long-term filtration tests. The results show that k_{20} increased as the flux decreased, which aligns with the short-term filtration tests since the k_{20} was higher at lower fluxes. This reinforces the idea that studies evaluating the SGD intensity should also consider the impact of flux since this parameter plays a key role in membrane fouling extent. The k_{20} progressively decreased over time and, except for Scenario 1, reached relatively constant values after about 135 min (see Figure S4 of the supplementary material). Table 3 also shows that k_{20} was eight and four times higher in Scenario 1 (J_{20}=4.1 LMH) and Scenario 2 (J_{20}=7.8 LMH) than in Scenario 4 (J_{20}=15.4 LMH), respectively. These results highlight that it is important to evaluate if the higher operating costs required for membrane fouling control could offset the lower costs associated with membrane purchasing when the membrane system is operated at higher fluxes.

3.4 Effect of flux and SGD on process economics

3.4.1 Discounted lifetime cost for the different scenarios and conditions

Figure 4 shows the DLC for the four scenarios and the three chemical cleaning conditions under study. Detailed information of each scenario and chemical cleaning condition can be found in Table S3. The results show that energy consumption for gas sparging was the most important cost contributor for all the scenarios, representing between 35 and 73% of the DLC. Scenario 1 consumed a higher amount of energy for gas sparging than Scenario 3 and 4, although Scenario 1 required a lower SGD (0.5 $m^3\ m^{-2}\ h^{-1}$) than Scenario

3 and 4 (1.0 m^3 m^{-2} h^{-1}). This is due to the higher membrane area (lower flux) of Scenario 1 that increased the total energy required for gas sparging, despite requiring a lower SGD.

The results of Figure 4 also show that membrane purchasing cost represented an important fraction of the DLC, but its contribution decreased from 33-35 to 10-19% as the flux increased from 4.1 to 15.4 LMH, respectively. Chemical and membrane replacement costs also had an impact on DLC, particularly in Scenario 4 (J_{20}=15.4 LMH), where the higher flux required more intensive chemical cleaning to reduce the extent of fouling. In Scenario 4, the membrane replacement cost and chemical cleaning represented 8.5-34.6 and 8.1-18.2% of the DLC, respectively. The increase of chemical cleaning requirements was accompanied by a reduction of the membrane lifetime, which increased the membrane replacement cost. The contribution of blower purchase cost and energy consumption for permeate pumping can be considered negligible since they did not account for more than 2% of the DLC in any of the scenarios and conditions evaluated.

Figure 4 also illustrates that Scenario 2 was the most competitive scenario for chemical cleaning Condition A and C, whereas Scenario 4 was the most competitive scenario for chemical cleaning Condition B. These results highlight that the chemical cleaning strategy had a direct impact on the economic prospect of AnMBR systems. The impact of the chemical cleaning strategy on DLC was higher in Scenario 4 since this scenario featured the highest consumption of chemicals because of its lower membrane permeability. For this reason, Scenario 4 was the most economical scenario for chemical cleaning condition B since the lower frequency of CIP and COP in Condition B led to a noticeable reduction of the DLC in Scenario 4 when compared with Condition A and C (Figure 4). However, Condition B considered that the frequency of CIP and COP would be lower than typical chemical cleaning frequencies reported for aerobic MBR systems. However, this consideration is unlikely to occur in an AnMBR, particularly considering that membrane fouling is generally higher under anaerobic than under aerobic conditions (Yao et al., 2020). Therefore, it is expected that similar (Condition A) or even higher (Condition C) chemical cleaning frequencies in comparison to aerobic MBR systems would be required in future full-scale AnMBR systems. Scenario 2 was the less costly scenario in Condition A and C, followed by Scenario 3 and 4. The DLC difference

between these scenarios was higher for Condition C than for Condition A since Condition C considered a higher frequency of CIP and COP than Condition A.

These results show that Scenario 2 is the most favourable scenario. This indicates that operating the membrane system under moderate fluxes (J_{20}=7.8 LMH) and SGDs (0.5 m^3 m^{-2} h^{-1}) could be the most favourable strategy for membrane fouling control in the granular AnMBR system. Finally, it is worth mentioning that Scenario 1 featured the highest DLC regardless of the chemical cleaning condition applied, which shows that operating the membrane system at fluxes below 5 LMH is not an economical option.

3.4.2 Sensitivity analysis

Figure 5 shows the sensitivity analysis of the DLC for a ±30% variation of the most important economic parameters. The sensitivity analysis was carried out for Condition A since this was considered the most representative condition for the chemical cleaning. The results show that electricity price variation had the highest impact on DLC since an increase or decrease of this parameter substantially affected the energy cost for gas sparging. Membrane cost variation featured the second highest impact on DLC. These results illustrate that lower electricity and membrane costs through improvements in SGD and membrane permeability are crucial to improve the competitiveness of granular AnMBR systems. The DLC variation caused by membrane cost in Scenario 4 was 20 and 34% higher than in Scenario 2 and 3, respectively, although Scenario 4 required a lower membrane area than Scenario 2 and 3 (Figure 5). The higher impact of membrane cost for Scenario 4 can be attributed to the higher membrane replacement cost in this scenario. These results highlight that the variation of the membrane cost does not only affect the initial membrane purchasing cost, but also the cost required to replace the membranes during the plant lifetime. The parameters associated with the chemical cleaning strategy (i.e. chemical reagents price, chemical cleaning concentration and CIP frequency) increased their impact on DLC as the flux increased (higher membrane fouling). As shown in Figure 4, the variation of chemical cleaning strategy affected the amount of chemicals purchased as well as the durability of the membranes. Therefore, these results show the importance of selecting an optimum strategy for chemical cleaning, particularly in those scenarios that require more chemicals to control irreversible membrane fouling.

Figure 6 shows the sensitivity analysis of the DLC for a variation of the $k_{20,x}/k_{20,4}$ ratio in Scenario 1, 2 and 3. This sensitivity analysis was performed to evaluate how possible variations of the $k_{20,x}/k_{20,4}$ ratio could affect the economic prospect of each scenario. The results illustrate that the DLC sharply decreased as the $k_{20,x}/k_{20,4}$ ratio increased from 1 to 4. This is because the increase in membrane permeability decreases the consumption of chemical reagents with a direct impact on membrane durability. However, only marginal reductions of DLC were obtained when the $k_{20,x}/k_{20,4}$ ratio was above 4, which suggests that the contribution of chemical cleaning and membrane replacement to the DLC substantially decreased as the $k_{20,x}/k_{20,4}$ ratio increased. Scenario 2 and Scenario 3 were more competitive than Scenario 4 when the $k_{20,x}/k_{20,4}$ ratio was above 2.5 and 2.0, respectively. Figure 6 also shows that Scenario 2 slightly outcompeted Scenario 3 when the $k_{20,x}/k_{20,4}$ ratio was above 3. This illustrates that Scenario 2 is more economical than Scenario 3 since (i) the membrane permeability of Scenario 2 was higher than Scenario 3 since it was operated at a lower flux and (ii) an experimental $k_{20,x}/k_{20,4}$ ratio of 3.8 (> 3) was obtained for Scenario 2 in the long term-tests (see Table 3). Finally, it is worth mentioning that Scenario 1 was not economically favourable regardless of the $k_{20,x}/k_{20,4}$ ratio, which reinforces the idea that AnMBR operation at low fluxes is not economically feasible.

4. Conclusions

The results of this study showed that the extent of membrane fouling is clearly influenced by membrane flux and SGD conditions. The most favourable SGD condition was 0.5 m^3 m^{-2} h^{-1} at J_{20} of 4.4 and 8.7 LMH, whereas the most favourable SGD condition was 1.0 m^3 m^{-2} h^{-1} at J_{20} of 13.0 and 16.7 LMH. These results show that a suitable SGD needs to consider both gas sparging rate and membrane flux. The membrane rejection of DCOM was between 31 and 44%. No direct correlation between flux/SGD conditions and DCOM rejection was observed. The protein-like fluorophores were predominant (67-79%) in both mixed liquor and permeate samples and were relatively high retained by the membrane (39-50%). This suggests that protein-like fluorophores could play an important role in membrane fouling. The economic analysis indicated that operating the membrane at moderate fluxes (J_{20}=7.8 LMH) and SGDs (0.5 m^3 m^{-2} h^{-1}) is the most favourable strategy for granular AnMBR systems. Finally, a sensitivity analysis illustrated that

electricity and membrane cost had the highest impact on DLC, which highlights the importance of reducing SGD requirements and enhancing membrane permeability to improve the competitiveness of granular AnMBRs.

Supplementary information

E-supplementary data of this work can be found in online version of the paper.

Acknowledgments

This work was supported by a grant overseen by the French National Research Agency (ANR) as part of the "JCJC" program BàMAn (ANR-18-CE04-0001-01). Sergi Vinardell is grateful to the Generalitat de Catalunya for his predoctoral FI grant and the travel stipend (2019 FI_B 00394). Sergi Astals is grateful for his Ramon y Cajal fellowship (RYC-2017-22372).

References

Anjum, F., Khan, I.M., Kim, J., Aslam, M., Blandin, G., Heran, M., Lesage, G., 2021. Trends and progress in AnMBR for domestic wastewater treatment and their impacts on process efficiency and membrane fouling. Environ. Technol. Innov. 21, 101204.

APHA, 2017. Standard Methods for the Examination of Water and Wastewater. Federation. Water Environmental American Public Health Association (APHA), Washington, USA.

Aslam, M., Charfi, A., Lesage, G., Heran, M., Kim, J., 2017. Membrane bioreactors for wastewater treatment: A review of mechanical cleaning by scouring agents to control membrane fouling. Chem. Eng. J. 307, 897–913.

Brepols, C., Drensla, K., Janot, A., Trimborn, M., Engelhardt, N., 2008. Strategies for chemical cleaning in large scale membrane bioreactors. Water Sci. Technol. 57, 457–463.

Chen, C., Guo, W., Ngo, H.H., 2016. Advances in Granular Growth Anaerobic Membrane Bioreactor (G-AnMBR) for Low Strength Wastewater Treatment. J. Energy Environ. Sustain. 1, 77–83.

Chen, C., Guo, W., Ngo, H.H., Chang, S.W., Duc Nguyen, D., Dan Nguyen, P., Bui, X.T., Wu, Y., 2017. Impact of reactor configurations on the performance of a granular anaerobic membrane bioreactor for municipal wastewater treatment. Int. Biodeterior. Biodegrad. 121, 131–138.

Chen, W., Westerhoff, P., Leenheer, J.A., Booksh, K., 2003. Fluorescence Excitation-Emission Matrix Regional Integration to Quantify Spectra for Dissolved Organic Matter. Environ. Sci. Technol. 37, 5701–5710.

De Vela, R.J., 2021. A review of the factors affecting the performance of anaerobic membrane bioreactor and strategies to control membrane fouling, Reviews in Environmental Science and Biotechnology. 20, 607-644.

Dereli, R.K., Ersahin, M.E., Ozgun, H., Ozturk, I., Jeison, D., van der Zee, F., van Lier, J.B., 2012. Potentials of anaerobic membrane bioreactors to overcome treatment limitations induced by industrial wastewaters. Bioresour. Technol. 122, 160–170.

Derlon, N., Wagner, J., da Costa, R.H.R., Morgenroth, E., 2016. Formation of aerobic granules for the treatment of real and low-strength municipal wastewater using a sequencing batch reactor operated at constant volume. Water Res. 105, 341–350.

Dong, Q., Parker, W., Dagnew, M., 2016. Long term performance of membranes in an anaerobic membrane bioreactor treating municipal wastewater. Chemosphere 144, 249–256.

Fox, R.A., Stuckey, D.C., 2015. The effect of sparging rate on transmembrane pressure and critical flux in an AnMBR. J. Environ. Manage. 151, 280–285.

Gouveia, J., Plaza, F., Garralon, G., Fdz-Polanco, F., Peña, M., 2015a. A novel configuration for an anaerobic submerged membrane bioreactor (AnSMBR). Long-term treatment of municipal wastewater under psychrophilic conditions. Bioresour. Technol. 198, 510–519.

Gouveia, J., Plaza, F., Garralon, G., Fdz-Polanco, F., Peña, M., 2015b. Long-term operation of a pilot scale anaerobic membrane bioreactor (AnMBR) for the treatment of municipal wastewater under psychrophilic conditions. Bioresour. Technol. 185, 225–233.

Jacquin, C., Lesage, G., Traber, J., Pronk, W., Heran, M., 2017. Three-dimensional excitation and emission matrix fluorescence (3DEEM) for quick and pseudo-quantitative determination of protein- and humic-like substances in full-scale membrane bioreactor (MBR). Water Res. 118, 82–92.

Jacquin, C., Teychene, B., Lemee, L., Lesage, G., Heran, M., 2018. Characteristics and fouling behaviors of Dissolved Organic Matter fractions in a full-scale submerged membrane bioreactor for municipal wastewater treatment. Biochem. Eng. J. 132, 169–181.

Ji, J., Chen, Y., Hu, Y., Ohtsu, A., Ni, J., Li, Y., Sakuma, S., Hojo, T., Chen, R., Li, Y.Y., 2021. One-year operation of a 20-L submerged anaerobic membrane bioreactor for real domestic wastewater treatment at room temperature: Pursuing the optimal HRT and sustainable flux. Sci. Total Environ. 775, 145799.

Judd, S., 2010. The MBR book : principles and applications of membrane bioreactors for water and wastewater treatment. Butterworth-Heinemann, Oxford.

Krzeminski, P., Leverette, L., Malamis, S., Katsou, E., 2017. Membrane bioreactors – A review on recent developments in energy reduction, fouling control, novel configurations, LCA and market prospects. J. Memb. Sci. 527, 207–227.

Le Clech, P., Jefferson, B., Chang, I.S., Judd, S.J., 2003. Critical flux determination by the flux-step method in a submerged membrane bioreactor. J. Memb. Sci. 227, 81–93.

Liu, J., Zhao, M., Duan, C., Yue, P., Li, T., 2021. Removal characteristics of dissolved organic matter and membrane fouling in ultrafiltration and reverse osmosis membrane combined processes treating the secondary effluent of wastewater treatment plant. Water Sci. Technol. 83, 689–700.

Maaz, M., Yasin, M., Aslam, M., Kumar, G., Atabani, A.E., Idrees, M., Anjum, F., Jamil, F., Ahmad, R., Khan, A.L., Lesage, G., Heran, M., Kim, J., 2019. Anaerobic membrane bioreactors for wastewater treatment: Novel configurations, fouling control and energy considerations. Bioresour. Technol. 283, 358–372.

Martin-Garcia, I., Monsalvo, V., Pidou, M., Le-Clech, P., Judd, S.J., McAdam, E.J., Jefferson, B., 2011. Impact of membrane configuration on fouling in anaerobic membrane bioreactors. J. Memb. Sci. 382, 41–49.

McCarty, P.L., Bae, J., Kim, J., 2011. Domestic wastewater treatment as a net energy producer - can this be achieved? Environ. Sci. Technol. 45, 7100–6.

Meng, F., Zhang, S., Oh, Y., Zhou, Z., Shin, H.S., Chae, S.R., 2017. Fouling in membrane bioreactors: An updated review. Water Res. 114, 151–180.

Odriozola, M., Lousada-Ferreira, M., Spanjers, H., van Lier, J.B., 2021. Effect of sludge characteristics on optimal required dosage of flux enhancer in anaerobic membrane bioreactors. J. Memb. Sci. 619, 118776.

Ozgun, H., Dereli, R.K., Ersahin, M.E., Kinaci, C., Spanjers, H., Van Lier, J.B., 2013. A review of anaerobic membrane bioreactors for municipal wastewater treatment: Integration options, limitations and expectations. Sep. Purif. Technol. 118, 89–104.

Pretel, R., Robles, A., Ruano, M. V., Seco, A., Ferrer, J., 2014. The operating cost of an anaerobic membrane bioreactor (AnMBR) treating sulphate-rich urban wastewater. Sep. Purif. Technol. 126, 30–38.

Ramos, C., Zecchino, F., Ezquerra, D., Diez, V., 2014. Chemical cleaning of membranes from an anaerobic membrane bioreactor treating food industry wastewater. J. Memb. Sci. 458, 179–188.

Robles, A., Ruano, M. V., Ribes, J., Seco, A., Ferrer, J., 2014. Model-based automatic tuning of a filtration control system for submerged anaerobic membrane bioreactors (AnMBR). J. Memb. Sci. 465, 14–26.

Robles, A., Ruano, M. V, Ribes, J., Ferrer, J., 2013. Factors that affect the permeability of commercial hollow-fibre membranes in a submerged anaerobic MBR (HF-SAnMBR) system. Water Res. 47, 1277–1288.

Ruigómez, I., Vera, L., González, E., González, G., Rodríguez-Sevilla, J., 2016. A novel rotating HF membrane to control fouling on anaerobic membrane bioreactors treating wastewater. J. Memb. Sci. 501, 45–52.

Shoener, B.D., Zhong, C., Greiner, A.D., Khunjar, W.O., Hong, P.Y., Guest, J.S., 2016. Design of anaerobic membrane bioreactors for the valorization of dilute organic carbon waste streams. Energy Environ. Sci. 9, 1102–1112.

Song, X., Luo, W., Hai, F.I., Price, W.E., Guo, W., Ngo, H.H., Nghiem, L.D., 2018. Resource recovery from wastewater by anaerobic membrane bioreactors: Opportunities and challenges. Bioresour. Technol. 270, 669–677.

Stazi, V., Tomei, M.C., 2018. Enhancing anaerobic treatment of domestic wastewater: State of the art, innovative technologies and future perspectives. Sci. Total Environ. 635, 78–91.

Verrecht, B., Maere, T., Nopens, I., Brepols, C., Judd, S., 2010. The cost of a large-scale hollow fibre MBR. Water Res. 44, 5274–5283.

Vinardell, S., Astals, S., Peces, M., Cardete, M.A., Fernández, I., Mata-Alvarez, J., Dosta, J., 2020. Advances in anaerobic membrane bioreactor technology for municipal wastewater treatment: A 2020 updated review. Renew. Sustain. Energy Rev. 130, 109936.

Vinardell, S., Dosta, J., Mata-Alvarez, J., Astals, S., 2021. Unravelling the economics behind mainstream anaerobic membrane bioreactor application under different plant layouts. Bioresour. Technol. 319, 124170.

Wang, K.M., Cingolani, D., Eusebi, A.L., Soares, A., Jefferson, B., McAdam, E.J., 2018. Identification of gas sparging regimes for granular anaerobic membrane bioreactor to enable energy neutral municipal wastewater treatment. J. Memb. Sci. 555, 125–133.

Wang, K.M., Soares, A., Jefferson, B., Wang, H.Y., Zhang, L.J., Jiang, S.F., McAdam, E.J., 2020. Establishing the mechanisms underpinning solids breakthrough in UASB configured anaerobic membrane bioreactors to mitigate fouling. Water Res. 176, 115754.

Wang, Z., Ma, J., Tang, C.Y., Kimura, K., Wang, Q., Han, X., 2014. Membrane cleaning in membrane bioreactors: A review. J. Memb. Sci. 468, 276–307.

Xin, C., Cheng, Z., You, Z., Bai, H., Wang, J., 2020. Using EEM fluorescence to characterize the membrane integrity of membrane bioreactor (MBR). J. Memb. Sci. 610, 118356.

Yao, Y., Zhou, Z., Stuckey, D.C., Meng, F., 2020. Micro-particles-A Neglected but Critical Cause of Different Membrane Fouling between Aerobic and Anaerobic Membrane Bioreactors. ACS Sustain. Chem. Eng. 8, 16680–16690.

Zhen, G., Pan, Y., Lu, X., Li, Y.-Y., Zhang, Z., Niu, C., Kumar, G., Kobayashi, T., Zhao, Y., Xu, K., 2019. Anaerobic membrane bioreactor towards biowaste biorefinery and chemical energy harvest: Recent progress, membrane fouling and future perspectives. Renew. Sustain. Energy Rev. 115, 109392.

Zhou, Z., Tao, Y., Zhang, S., Xiao, Y., Meng, F., Stuckey, D.C., 2019. Size-dependent microbial diversity of sub-visible particles in a submerged anaerobic membrane bioreactor (SAnMBR): Implications for membrane fouling. Water Res. 159, 20–29.

Table 1. Permeate fluxes and their normalised values at 20ºC for each SGD and flux condition evaluated in the short-term filtration tests. Errors represent standard deviations (n=18). No statistical difference was observed between the fluxes for the different SGDs at a specific flux condition ($p>0.05$).

		SGD_1 ($0.25\ m^3\ m^{-2}\ h^{-1}$)	**SGD_2 ($0.5\ m^3\ m^{-2}\ h^{-1}$)**	**SGD_3 ($1.0\ m^3\ m^{-2}\ h^{-1}$)**	**SGD_4 ($2.0\ m^3\ m^{-2}\ h^{-1}$)**
$Flux_1$	**$J_{T,1}$ (LMH)**	4.8 ± 0.2	4.8 ± 0.3	4.7 ± 0.1	4.7 ± 0.1
	$J_{20,1}$ (LMH)	4.4 ± 0.3	4.4 ± 0.3	4.3 ± 0.2	4.4 ± 0.2
$Flux_2$	**$J_{T,2}$ (LMH)**	9.6 ± 0.2	9.6 ± 0.1	9.6 ± 0.2	9.5 ± 0.3
	$J_{20,2}$ (LMH)	8.7 ± 0.2	8.8 ± 0.2	8.7 ± 0.2	8.6 ± 0.3
$Flux_3$	**$J_{T,3}$ (LMH)**	14.1 ± 0.6	14.4 ± 0.5	14.6 ± 0.4	14.5 ± 0.3
	$J_{20,3}$ (LMH)	12.8 ± 0.8	13.0 ± 0.8	13.2 ± 0.7	13.1 ± 0.6
$Flux_4$	**$J_{T,4}$ (LMH)**	18.6 ± 1.4	18.5 ± 1.5	18.5 ± 1.4	18.6 ± 1.5
	$J_{20,4}$ (LMH)	16.8 ± 1.0	16.7 ± 1.1	16.7 ± 1.1	16.7 ± 1.1

Table 2. Membrane rejection of the fluorophores DCOM compounds for the different regions of the 3DEEM spectra. Errors represent standard deviations (n=4). $Flux_1$=4.4 LMH; $Flux_2$=8.7 LMH; $Flux_3$=13.0 LMH; $Flux_4$=16.7 LMH; SGD_1=0.25 m^3 m^{-2} h^{-1}; SGD_2=0.50 m^3 m^{-2} h^{-1}; SGD_3=1.0 m^3 m^{-2} h^{-1}; SGD_4=2.0 m^3 m^{-2} h^{-1}.

	$Flux_1$	**$Flux_2$**	**$Flux_3$**	**$Flux_4$**	**SGD_1**	**SGD_2**	**SGD_3**	**SGD_4**
Rejection region I+II (%)	45.2 ± 6.8	44.3 ± 3.1	39.1 ± 10.9	50.2 ± 6.3	40.2 ± 10.0	48.5 ± 4.7	43.9 ± 4.9	46.7 ± 10.7
Rejection region IV (%)	47.2 ± 8.5	26.4 ± 3.4	26.3 ± 8.3	39.8 ± 4.6	34.6 ± 10.6	38.2 ± 12.9	28.1 ± 8.8	43.0 ± 4.4
Rejection region III+V (%)	16.1 ± 12.6	18.1 ± 3.8	23.1 ± 9.1	18.8 ± 6.8	13.7 ± 5.6	26.2 ± 4.6	15.8 ± 6.4	21.3 ± 13.5
Total Rejection (%)	40.2 ± 7.6	38.6 ± 2.2	34.8 ± 9.9	43.7 ± 5.9	34.8 ± 8.9	43.6 ± 4.6	37.9 ± 4.4	41.7 ± 9.7

Table 3. Summary of the results obtained in the long-term filtration tests. Figure S4 shows the evolution of membrane permeability over time. Errors represent standard deviations (n=40).

	SGD ($m^3\ m^{-2}\ h^{-1}$)	**J_T** (LMH)	**J_{20}** (LMH)	**$k_{20,t=225}$** (LMH bar^{-1})	**$k_{20,x}/k_{20,4}$**
Scenario 1	0.5	4.7 ± 0.1	4.1 ± 0.1	1175	8.8
Scenario 2	0.5	9.2 ± 0.1	7.8 ± 0.1	506	3.8
Scenario 3	1.0	13.7 ± 0.1	12.0 ± 0.1	315	2.4
Scenario 4	1.0	17.9 ± 0.3	15.4 ± 0.1	133	1.0

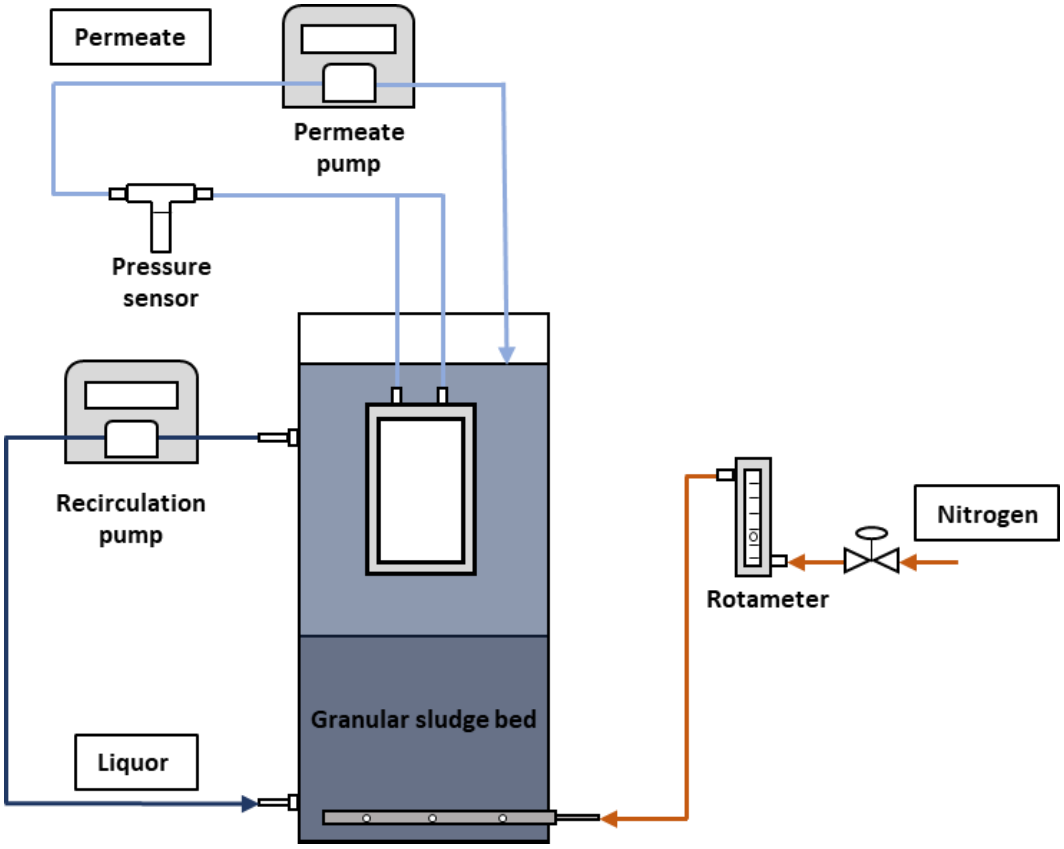

Figure 1. Schematic representation of the experimental set-up.

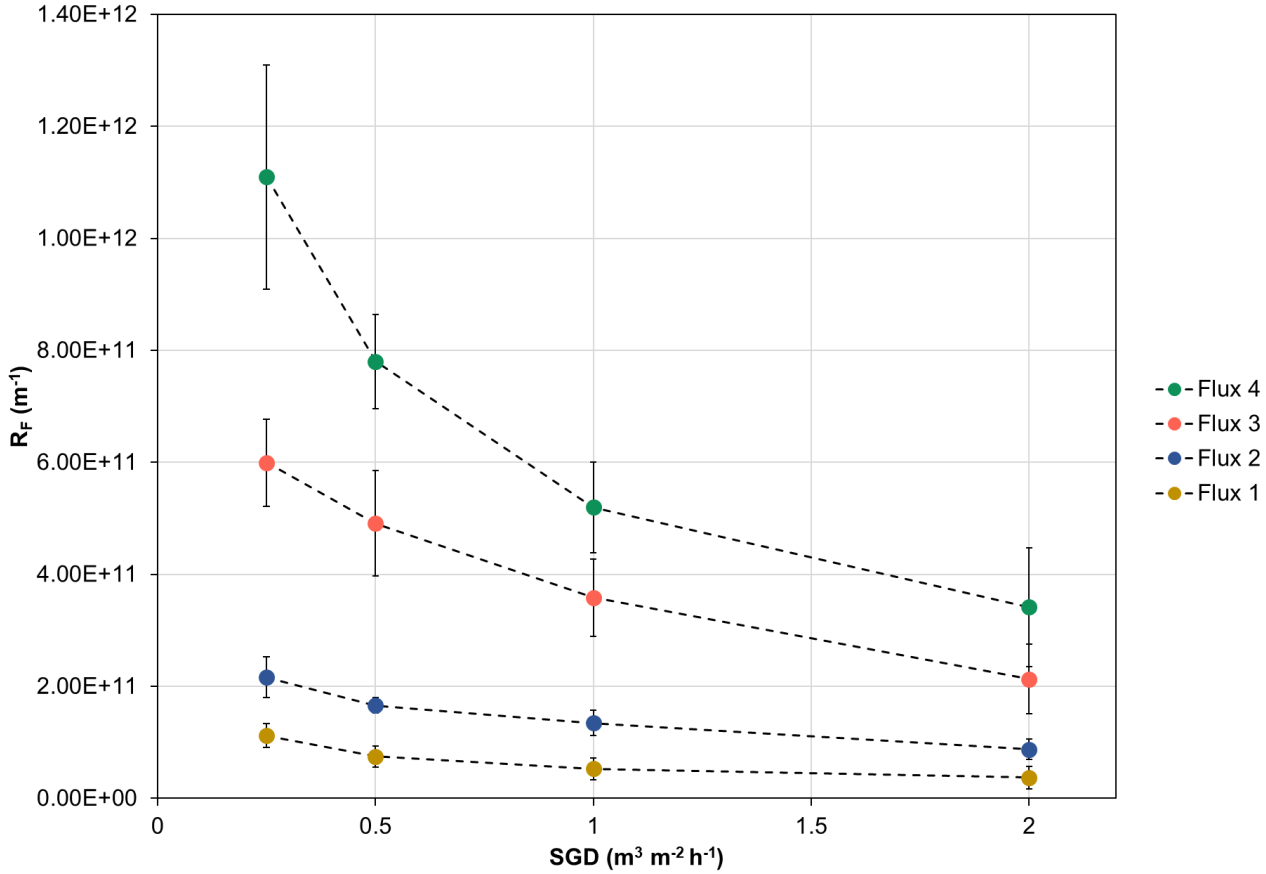

Figure 2. R_f for the four SGD and fluxes evaluated. Error bars represent standard deviations (n=6). $Flux_1$=4.4 LMH; $Flux_2$=8.7 LMH; $Flux_3$=13.0 LMH; $Flux_4$=16.7 LMH.

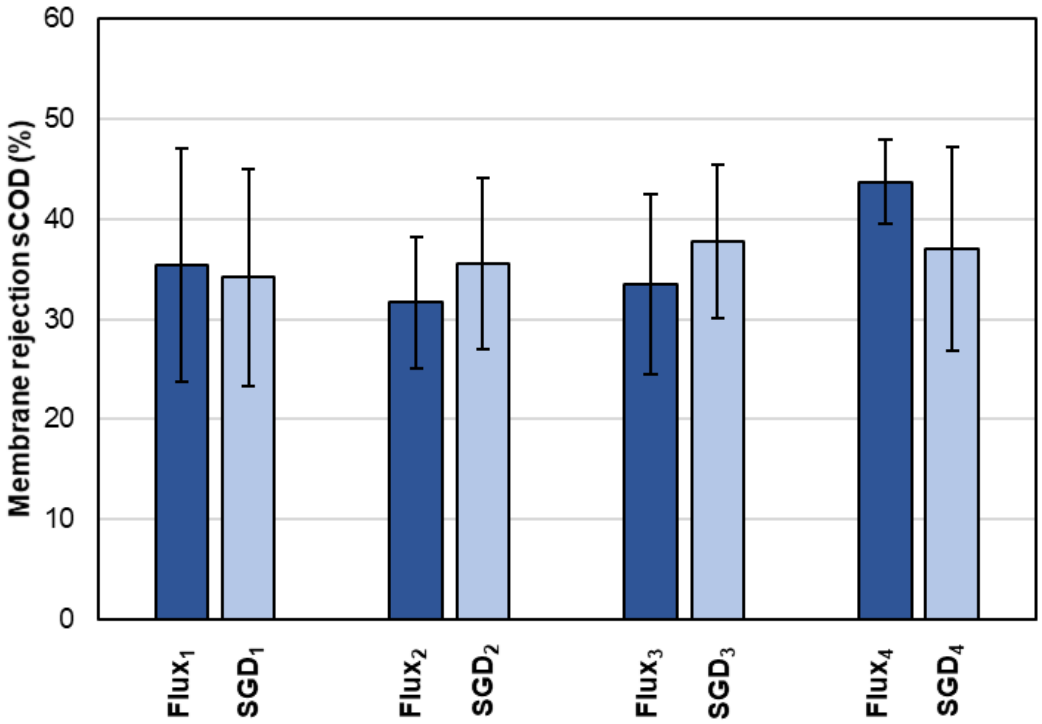

Figure 3. Membrane rejection of sCOD for the four SGD and fluxes evaluated. Error bars represent standard deviations (n=12). $Flux_1$=4.4 LMH; $Flux_2$=8.7 LMH; $Flux_3$=13.0 LMH; $Flux_4$=16.7 LMH; SGD_1=0.25 m^3 m^{-2} h^{-1}; SGD_2=0.50 m^3 m^{-2} h^{-1}; SGD_3=1.0 m^3 m^{-2} h^{-1}; SGD_4=2.0 m^3 m^{-2} h^{-1}.

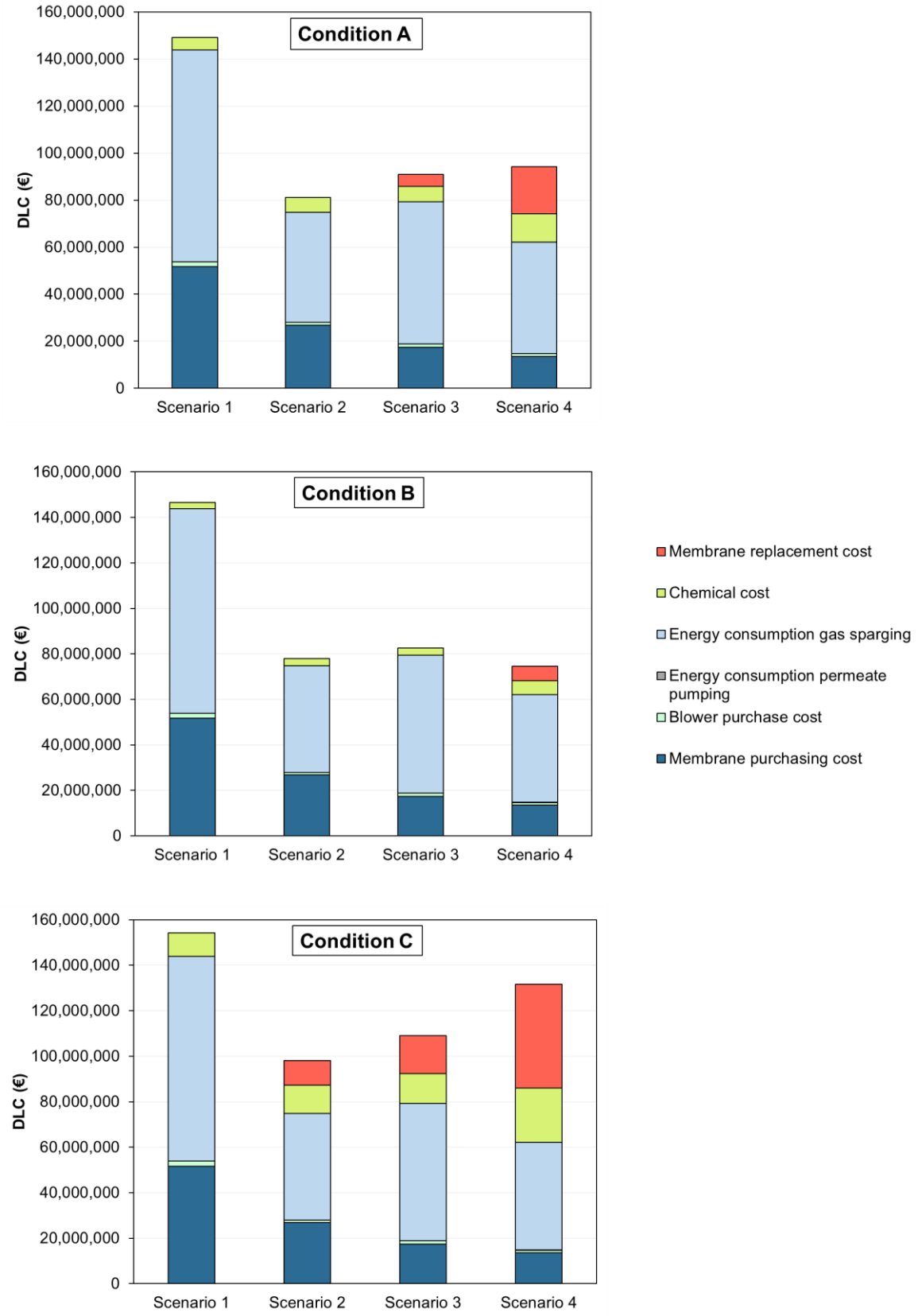

Figure 4. Discounted lifetime cost (DLC) for the four scenarios and three chemical cleaning conditions evaluated. Table S3 shows detailed information of each scenario and chemical cleaning condition.

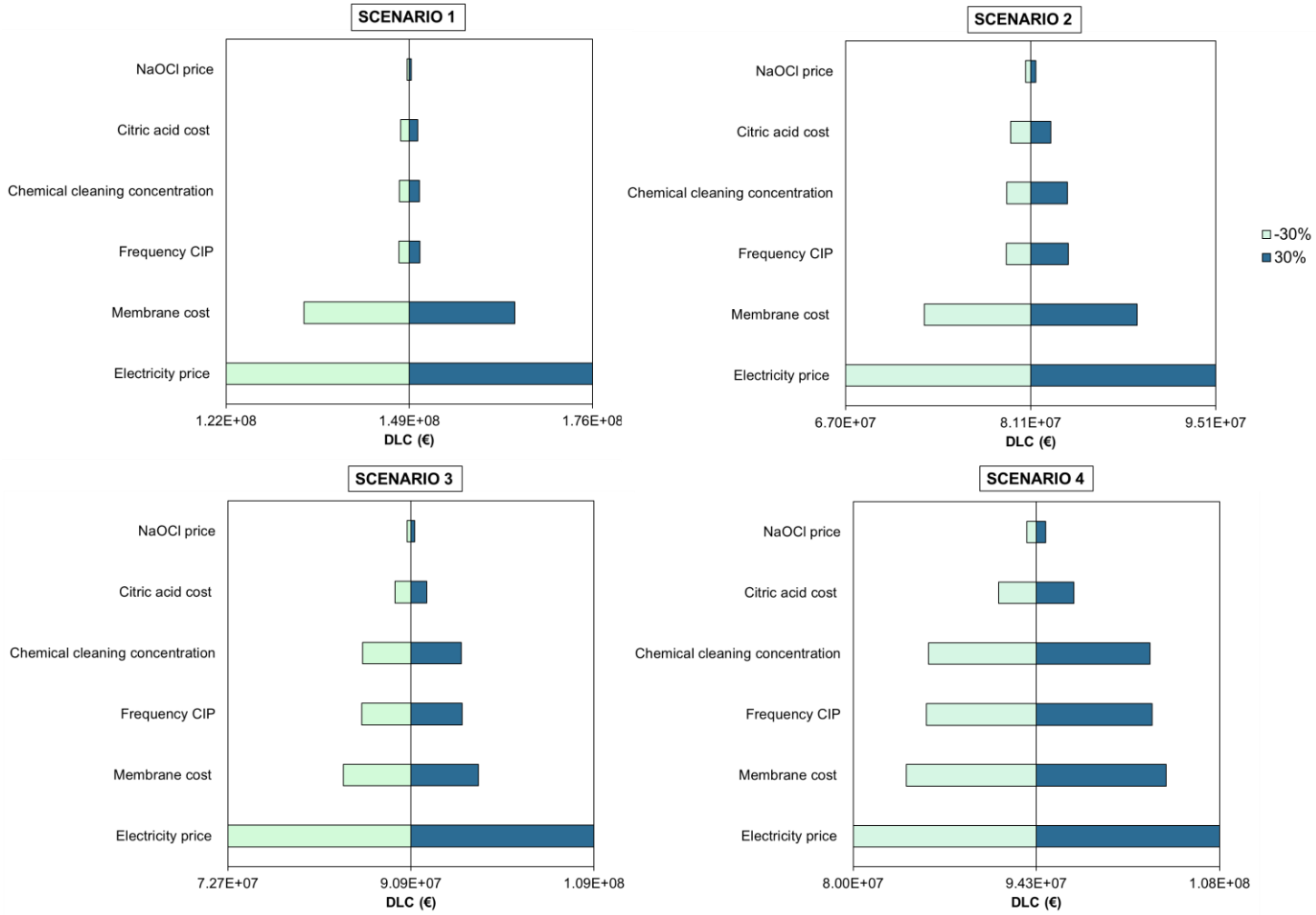

Figure 5. Sensitivity analysis of the discounted lifetime cost (DLC) for a ±30% variation of the most important economic parameters for the four scenarios. The sensitivity analysis was carried out for chemical cleaning Condition A.

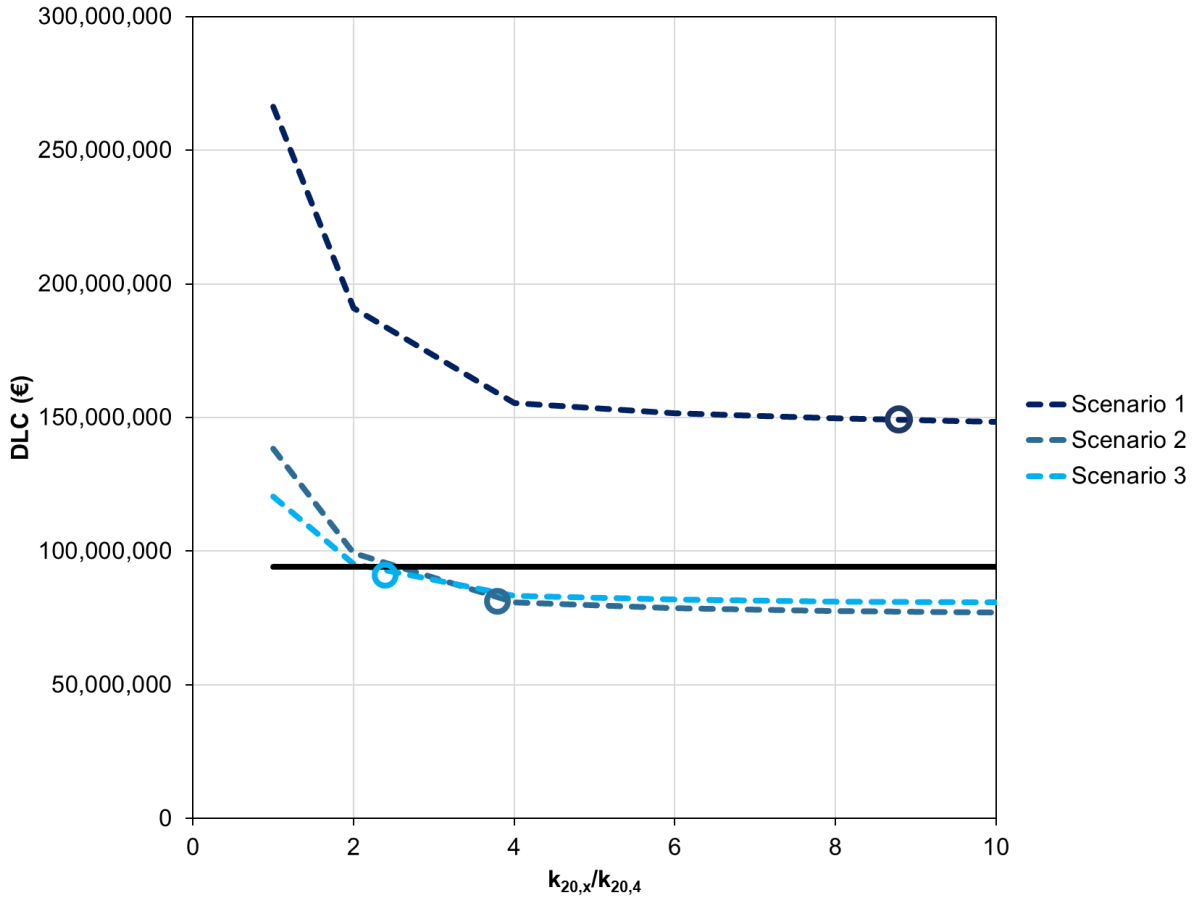

Figure 6. Sensitivity analysis of the discounted lifetime cost (DLC) variation for Scenario 1, 2 and 3 in function to the $k_{20,x}/k_{20,4}$ ratio. The horizontal black bar represents the DLC of Scenario 4 that remains constant because this is the reference scenario. The circles indicate the experimental $k_{20,x}/k_{20,4}$ ratio. The sensitivity analysis was carried out for chemical cleaning Condition A.

SUPPLEMENTARY INFORMATION

Impact of permeate flux and gas sparging rate on membrane performance and process economics of granular anaerobic membrane bioreactors

Sergi Vinardell[a,b,*], Lucie Sanchez[b], Sergi Astals[a], Joan Mata-Alvarez[a,c], Joan Dosta[a,c], Marc Heran[b], Geoffroy Lesage[b]

[a] Department of Chemical Engineering and Analytical Chemistry, University of Barcelona, 08028, Barcelona, Spain

[b] Institut Européen des Membranes (IEM), Université de Montpellier, CNRS, ENSCM, 34090, Montpellier, France

[c] Water Research Institute, University of Barcelona, 08028 Barcelona, Spain

*Corresponding author (e-mail: svinardell@ub.edu)

Table S1. Main characteristics of the granular sludge. Errors represent standard deviation (n=3).

TS (g L^{-1})	90.6 ± 2.6
VS (g L^{-1})	69.7 ± 1.2
VS/TS (%)	77.0 ± 0.7
sCOD (mg L^{-1})	536.3 ± 11.7
DOC (mg L^{-1})	167.3 ± 3.5
pH (-)	7.2 ± 0.1
Zeta potential (mV)	-8.9
Particle size distribution (% fraction TS)	
diameter<0.125 mm	0.8
0.125<diameter<0.25 mm	2.1
0.25<diameter<0.63 mm	4.7
0.63<diameter<1 mm	14.8
diameter>1 mm	77.6

Table S2. Solids concentration in the tank for the short- and long-term filtration tests. Errors represent standard deviations (n=3).

	TS (g L^{-1})	**VS (g L^{-1})**	**VS/TS (%)**
Short-term Test 1	9.9 ± 0.2	7.4 ± 0.1	75.0 ± 0.3
Short-term Test 2	8.6 ± 0.3	6.5 ± 0.2	75.6 ± 0.2
Short-term Test 3	9.4 ± 0.3	7.0 ± 0.2	75.1 ± 0.1
Long-term Test	9.0 ± 0.4	7.1 ± 0.2	78.9 ± 1.4

Table S3. Description of the different scenarios and conditions evaluated for the economic analysis.

	Condition description	**Scenario 1**	**Scenario 2**	**Scenario 3**	**Scenario 4**
Condition A	CIP frequency=52 times year^{-1} COP frequency=2 times year^{-1}	J_{20}=4.1 LMH J_T=4.7 LMH; SGD=0.5 m^3 m^{-2} h^{-1}	J_{20}=7.8 LMH J_T=9.2 LMH SGD=0.5 m^3 m^{-2} h^{-1}	J_{20}=12.0 LMH J_T=13.7 LMH SGD=1.0 m^3 m^{-2} h^{-1}	J_{20}=15.4 LMH J_T=17.9 LMH SGD=1.0 m^3 m^{-2} h^{-1}
Condition B	CIP frequency=26 times year^{-1} COP frequency=1 times year^{-1}	J_{20}=4.1 LMH J_T=4.7 LMH SGD=0.5 m^3 m^{-2} h^{-1}	J_{20}=7.8 LMH J_T=9.2 LMH SGD=0.5 m^3 m^{-2} h^{-1}	J_{20}=12.0 LMH J_T=13.7 LMH SGD=1.0 m^3 m^{-2} h^{-1}	J_{20}=15.4 LMH J_T=17.9 LMH SGD=1.0 m^3 m^{-2} h^{-1}
Condition C	CIP frequency=104 times year^{-1} COP frequency=3 times year^{-1}	J_{20}=4.1 LMH J_T=4.7 LMH SGD=0.5 m^3 m^{-2} h^{-1}	J_{20}=7.8 LMH; J_T=9.2 LMH SGD=0.5 m^3 m^{-2} h^{-1}	J_{20}=12.0 LMH J_T=13.7 LMH SGD=1.0 m^3 m^{-2} h^{-1}	J_{20}=15.4 LMH J_T=17.9 LMH SGD=1.0 m^3 m^{-2} h^{-1}

Table S4. Summary of the parameters used for granular AnMBR cost calculation.

	Parameter (units)	Value	Reference
Economic parameters	Membrane purchase (€ m^{-2})	50	Verrecht et al., 2010; Vinardell et al., 2021
	Blower purchase (€ m^{-3} h)	4.15	Verrecht et al., 2010
	Citric acid 50% cost (€ t^{-1})	760	Brepols et al., 2008; Verrecht et al., 2010
	NaOCl 14% cost (€ m^{-3})	254	Brepols et al., 2008; Verrecht et al., 2010
	Electricity price (€ kWh^{-1})	0.1149	Eurostat, 2019
	Discount rate (-)	0.05	Vinardell et al., 2021
	Plant lifetime (years)	20	Vinardell et al., 2021
Equation parameters	Blower efficiency (-)	0.80	Pretel et al., 2014
	Pump efficiency (-)	0.85	Wan and Chung, 2018
	Temperature (ºK)	293	-
	Ideal gas constant (J mol^{-1} $ºK^{-1}$)	8.31	-
	Adiabatic coefficient at 20ºC (-)	1.32	-
	Blower outlet pressure (Pa)	160,300	Judd, 2010; Verrecht et al., 2010
	Blower inlet pressure (Pa)	101,325	Judd, 2010; Verrecht et al., 2010

Table S5. Average volume contribution of each region of the 3DEEM spectra in permeate and mixed liquor samples for each membrane flux and SGD conditions. ML refers to mixed liquor samples.

	$Flux_1$	$Flux_2$	$Flux_3$	$Flux_4$	SGD_1	SGD_2	SGD_3	SGD_4	ML_1	ML_2	ML_3	ML_4
Volume region I+II (%)	72.3	70.2	67.7	68.5	70.0	70.0	69.1	69.3	78.9	77.4	72.7	77.6
Volume region IV (%)	3.0	3.4	3.5	2.9	3.0	3.2	3.5	3.0	3.4	2.8	3.0	2.7
Volume region III+V (%)	24.6	26.4	28.8	28.6	26.9	26.7	27.4	27.6	17.6	19.8	24.2	19.7

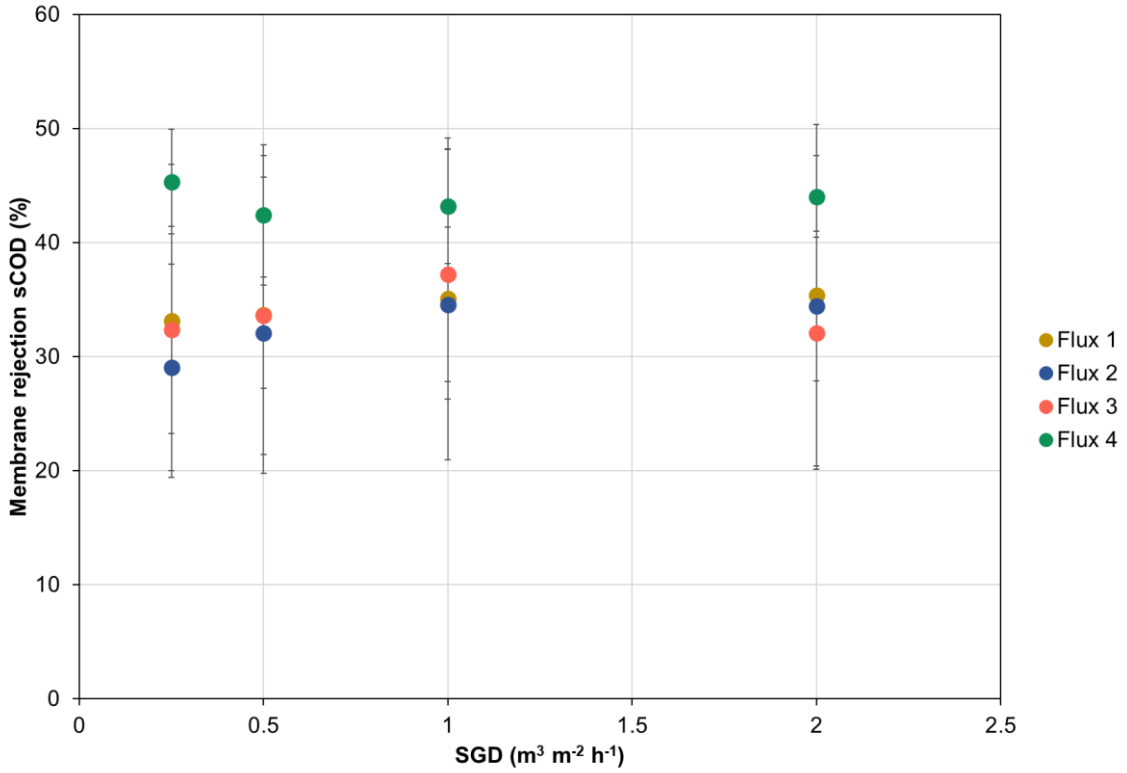

Figure S1. Membrane rejection of sCOD for each specific SGD and flux condition evaluated. Error bars represent standard deviations (n=3). $Flux_1$=4.4 LMH; $Flux_2$=8.7 LMH; $Flux_3$=13.0 LMH; $Flux_4$=16.7 LMH.

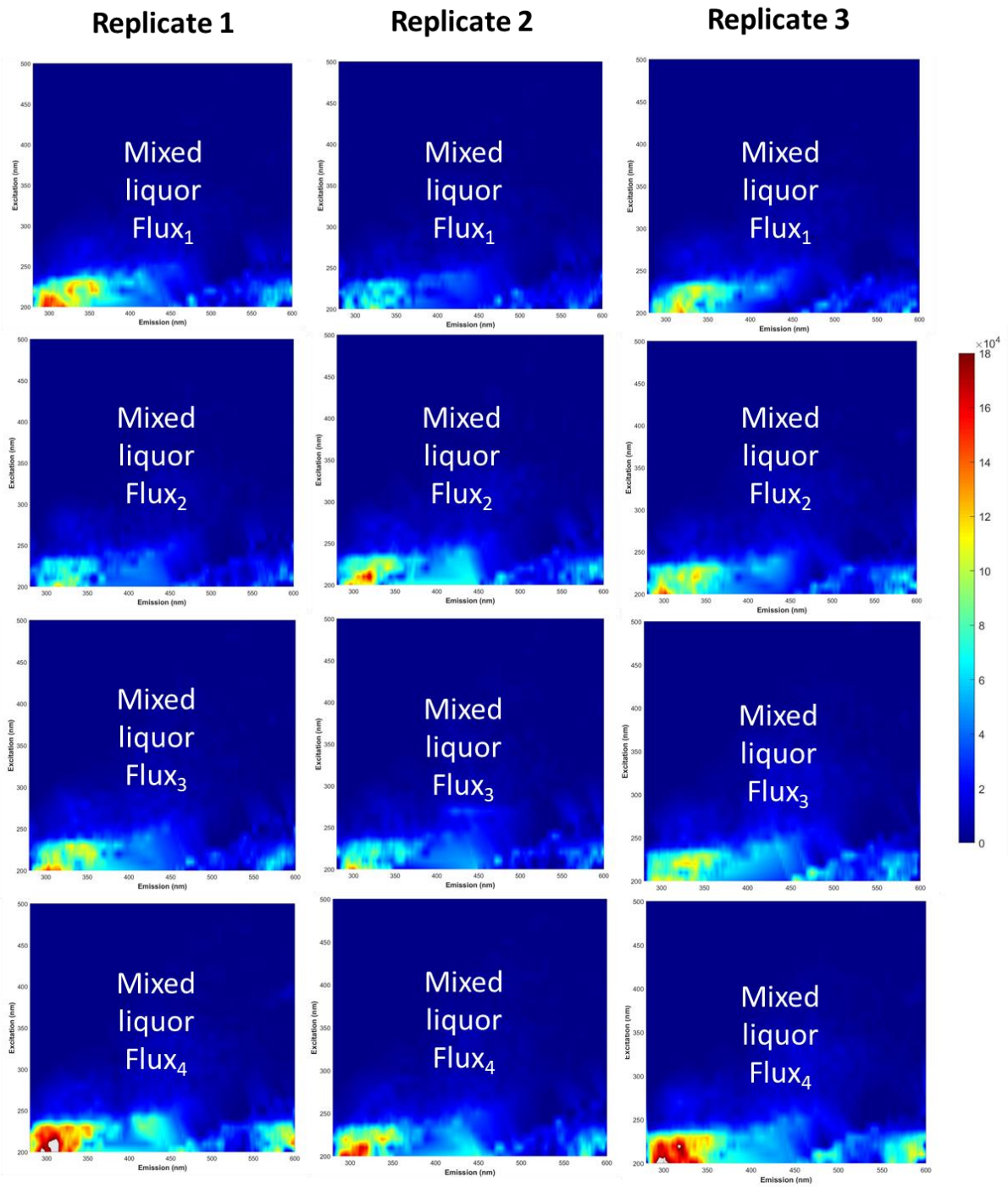

Figure S2. 3DEEM spectra of the mixed liquor samples of the three replicates for each permeate flux condition.

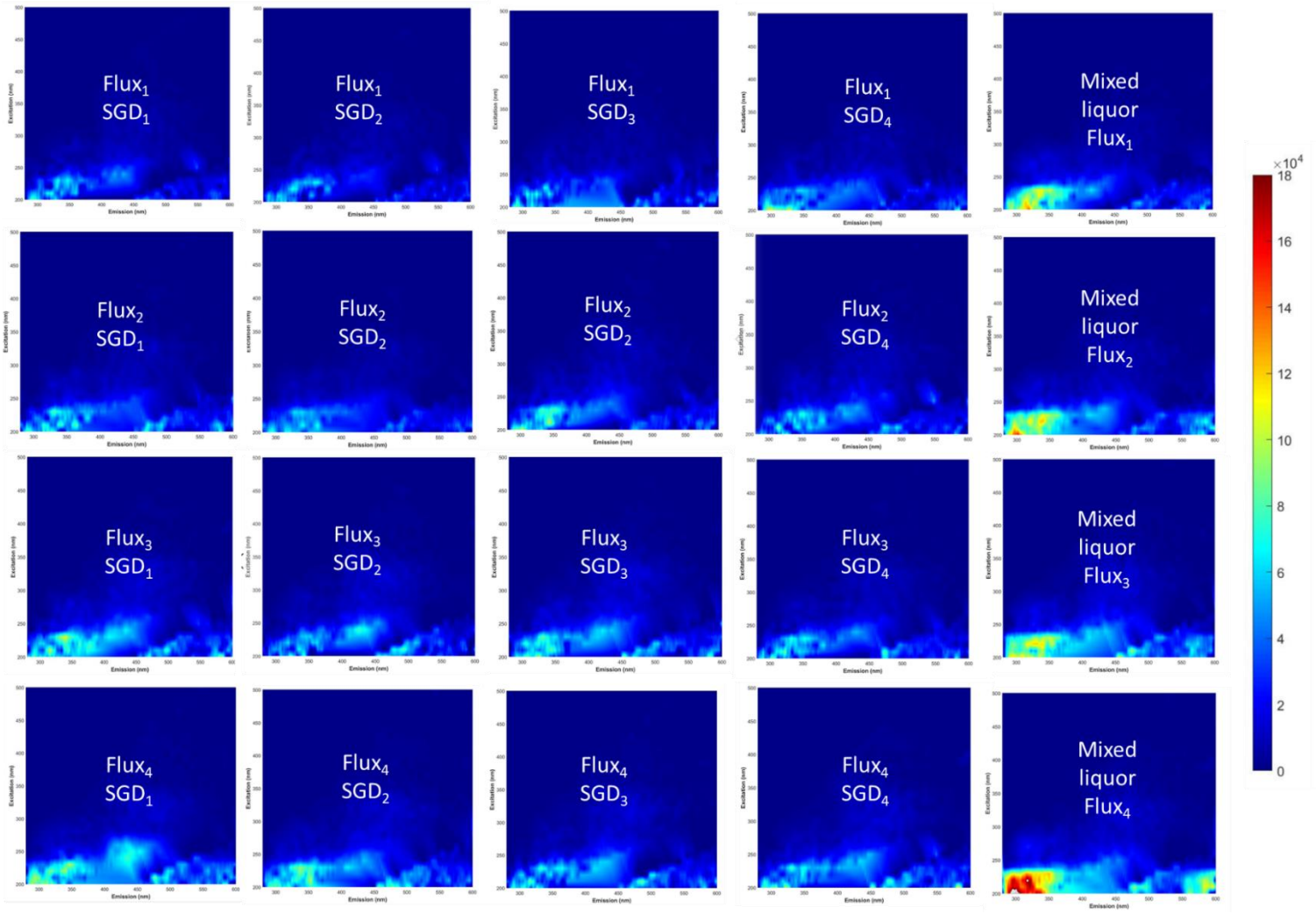

Figure S3. 3DEEM spectra for the permeate and mixed liquor samples for the different membrane flux and SGD conditions.

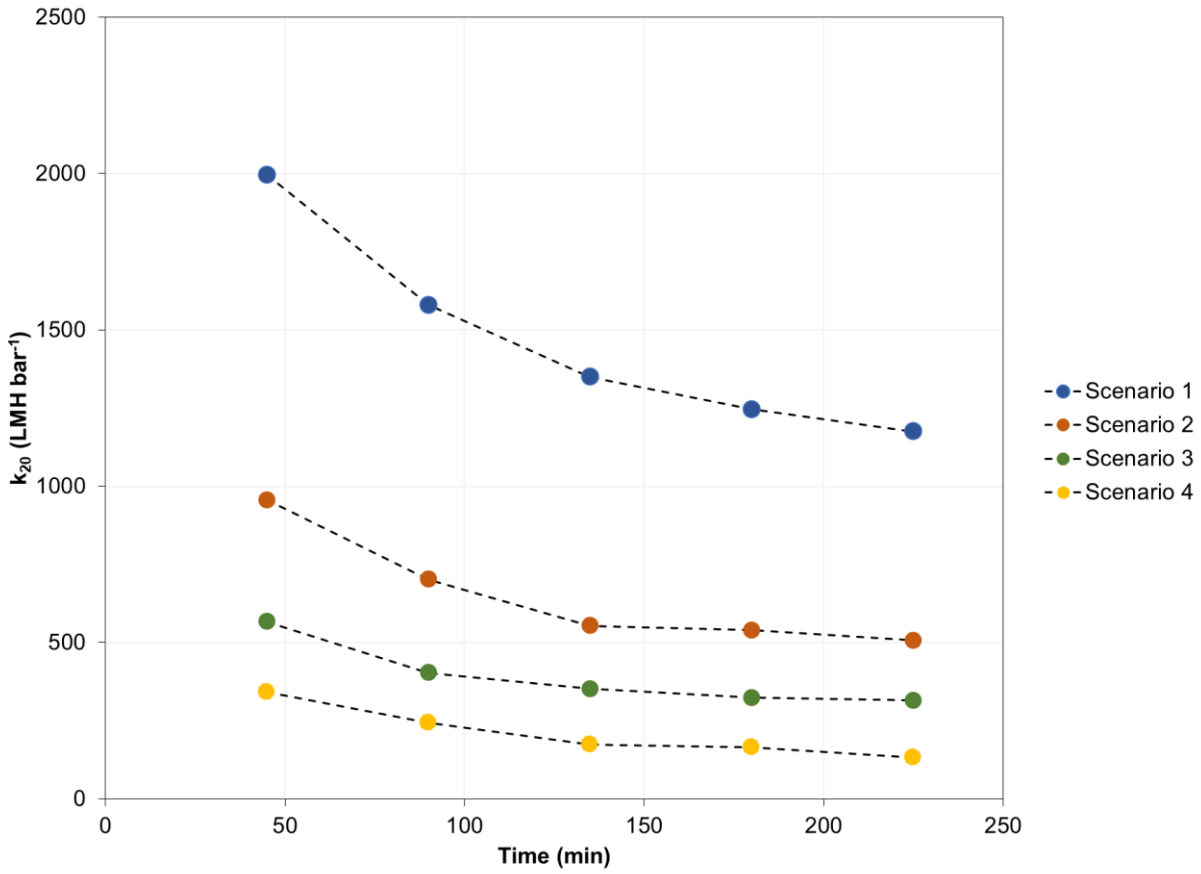

Figure S4. Normalised membrane permeability at 20ºC (k_{20}) evolution over time for the four scenarios of the long-term experiments..

References

Brepols, C., Drensla, K., Janot, A., Trimborn, M., Engelhardt, N., 2008. Strategies for chemical cleaning in large scale membrane bioreactors. Water Sci. Technol. 57, 457–463.

Eurostat, Electricity price statistics. https://ec.europa.eu/eurostat/statistics-explained/index.php/Electricity_price_statistics, 2019 (accessed 30 September 2019).

Judd, S., 2010. The MBR book : principles and applications of membrane bioreactors for water and wastewater treatment. Butterworth-Heinemann, Oxford.

Pretel, R., Robles, A., Ruano, M. V., Seco, A., Ferrer, J., 2014. The operating cost of an anaerobic membrane bioreactor (AnMBR) treating sulphate-rich urban wastewater. Sep. Purif. Technol. 126, 30–38.

Verrecht, B., Maere, T., Nopens, I., Brepols, C., Judd, S., 2010. The cost of a large-scale hollow fibre MBR. Water Res. 44, 5274–5283.

Vinardell, S., Dosta, J., Mata-Alvarez, J., Astals, S., 2021. Unravelling the economics behind mainstream anaerobic membrane bioreactor application under different plant layouts. Bioresour. Technol. 319.

Wan, C.F., Chung, T.S., 2018. Techno-economic evaluation of various RO+PRO and RO+FO integrated processes. Appl. Energy 212, 1038–1050.

3.3 Publication VI: *Unravelling the economics behind mainstream anaerobic membrane bioreactor application under different plant layouts*

Vinardell, S., Dosta, J., Mata-Alvarez, J., Astals, S. (2021). Unravelling the economics behind mainstream anaerobic membrane bioreactor application under different plant layouts. Bioresour. Technol. 319, 124170. https://doi.org/10.1016/j.biortech.2020.124170

Bioresource Technology 319 (2021) 124170

Contents lists available at ScienceDirect

Bioresource Technology

journal homepage: www.elsevier.com/locate/biortech

Unravelling the economics behind mainstream anaerobic membrane bioreactor application under different plant layouts

Sergi Vinardell *, Joan Dosta, Joan Mata-Alvarez, Sergi Astals

Department of Chemical Engineering and Analytical Chemistry, University of Barcelona, 08028 Barcelona, Spain

HIGHLIGHTS

- The economic feasibility of mainstream AnMBR application was analysed.
- Net treatment cost decreased from 0.42 to 0.35 € m^{-3} as the influent COD increased.
- Net treatment cost was above 0.51 € m^{-3} when N and P nutrient removal was included.
- AnMBR and partial nitritation-Anammox represented 58 and 30% of the treatment cost.
- Energy autarky was achieved at 1000 mg COD L^{-1} and COD:SO_4^{2-}-S ratios above 40.

ARTICLE INFO

Keywords:
Anaerobic digestion
Anaerobic membrane bioreactor (AnMBR)
Water resource recovery facility (WRRF)
Plant-wide assessment
Techno-economic analysis

ABSTRACT

This research evaluated the economic feasibility of anaerobic membrane bioreactor (AnMBR) as a mainstream technology for municipal sewage treatment. To this end, different wastewater treatment plant (WWTP) layouts were considered, including primary settler, AnMBR, degassing membrane, partial nitritation-Anammox, phosphorus precipitation and sidestream anaerobic digestion. The net treatment cost of an AnMBR-WWTP decreased from 0.42 to 0.35 € m^{-3} as the sewage COD concentration increased from 100 to 1100 mg COD L^{-1} due to revenue from electricity production. However, the net treatment cost increased above 0.51 € m^{-3} when nutrient removal technologies were included. The AnMBR and partial nitritation-Anammox were the costliest processes representing a 57.6 and 30.3% of the treatment cost, respectively. Energy self-sufficiency was achieved for high-strength municipal sewage treatment (1000 mg COD L^{-1}) and a COD:SO_4^{2-}-S ratio above 40. Overall, the results showed that mainstream AnMBR has potential to be an economically competitive option for full-scale implementation.

1. Introduction

Most wastewater treatment plants (WWTPs) were designed and constructed decades ago when sewage was considered a source of pollution rather than a source of resources (Sheik et al., 2014). These WWTPs, based on the conventional activated sludge (CAS) process, do not make an efficient use of the energy, water and nutrients contained in municipal sewage. The development and implementation of novel technologies able to maximise resource recovery while obtaining high-quality effluents is crucial to transform WWTPs into water resource recovery facilities (WRRF) (Guest et al., 2009).

Anaerobic membrane bioreactor (AnMBR) is a promising technology for mainstream municipal sewage treatment (Vinardell et al., 2020a). In contrast to the CAS process, AnMBR converts sewage organic matter into renewable biogas energy with no oxygen requirements and low sludge production. Additionally, the membrane system allows producing high-quality effluents and providing an excellent decoupling of the hydraulic retention time (HRT) from the solids retention time (SRT) (Stuckey, 2012).

The application of mainstream AnMBR technology represents an opportunity for WWTPs to become energy neutral, reduce treatment costs and produce high-quality effluents. Several publications have demonstrated that AnMBRs can achieve energy self-sufficiency at net treatment costs between 0.1 and 0.4 € m^{-3} (Batstone et al., 2015; Cogert et al., 2019; Evans et al., 2019; Lim et al., 2019; Pretel et al., 2015b; Shoener et al., 2016; Smith et al., 2014). However, some of these studies

* Corresponding author.
E-mail address: svinardell@ub.edu (S. Vinardell).

https://doi.org/10.1016/j.biortech.2020.124170
Received 11 August 2020; Received in revised form 18 September 2020; Accepted 21 September 2020
Available online 24 September 2020

limited their analysis to the AnMBR unit, omitting the implications and impact that AnMBR implementation has on sewage primary treatment, AnMBR post-treatment and sludge management. The incorporation of all these factors in the AnMBR-WWTP economic evaluation is paramount to obtain a realistic picture since the feasibility of AnMBR for mainstream WWTP application goes beyond its capacity to achieve high COD removal efficiencies and produce biogas.

The sensitivity of the AnMBR process to the sewage chemical oxygen demand (COD) and sulphate concentrations is critical for the AnMBR profitability (Batstone et al., 2015; Song et al., 2018). On the one hand, the higher the sewage COD concentration, the higher the amount of COD available for methane production (Shin and Bae, 2018). On the other hand, the presence of sulphate makes sulphate reducing bacteria (SRB) compete with acetogenic and methanogenic microorganisms for easily biodegradable substrate while reducing sulphate to sulphide (Serrano et al., 2019). Additionally, the presence of sulphide partially inhibits methanogenic archaea activity and makes necessary the use of equipment and instrumentation resistant to corrosion (Madden et al., 2014). Some previous publications have considered the impact of sewage COD concentration (Batstone et al., 2015; Cogert et al., 2019; Smith et al., 2014) and sewage sulphate concentration (Pretel et al., 2015a) on AnMBR-WWTP feasibility. However, little attention has been given to the relative and combined impact of sewage COD and sulphate concentrations on AnMBR-WWTP costs.

The presence of dissolved methane and nutrients (i.e. N, P) in the permeate (AnMBR effluent) is a major bottleneck for AnMBR application (Vinardell et al., 2020a). Dissolved methane can account for 50% of the total methane produced at psychrophilic conditions (ca. 15 °C) and its recovery is important to maximise energy production and minimise greenhouse gas emissions (Sanchis-Perucho et al., 2020; Smith et al., 2013). Furthermore, the mobilisation of nutrients in the AnMBR as a result of organic matter degradation makes necessary the implementation of post-treatments able to recover or remove nitrogen and phosphorus to fulfil the discharge requirements and reduce the environmental impact on aquatic systems (Robles et al., 2020). Accordingly, the inclusion of all treatment units (i.e. dissolved methane recovery, nutrients recovery/removal, and sludge management) in the economic evaluation is necessary to obtain a reliable estimation of the AnMBR-WWTP costs.

The selection of suitable plant layouts able to solve the aforementioned challenges is critical to support AnMBR full-scale implementation. Several plant layouts have been proposed for AnMBR-WWTPs, including (i) downstream processes for the recovery/removal of nutrients (Ab Hamid et al., 2020; Batstone et al., 2015; Cogert et al., 2019; Harclerode et al., 2020; Lim et al., 2019), (ii) downstream processes for the recovery/removal of dissolved methane (Cogert et al., 2019; Harclerode et al., 2020; Lim et al., 2019; Pretel et al., 2015a), and (iii) sludge treatment processes for sludge hygienisation and conditioning (Ab Hamid et al., 2020; Batstone et al., 2015; Harclerode et al., 2020; Pretel et al., 2015a). Although some of these studies considered similar operational conditions and sewage characteristics, they differed in the AnMBR-WWTP layout. These different selection criteria show that AnMBR-WWTP layout does not have yet a common baseline framework. Consequently, the plant layout selection is sometimes made intuitively and subjectively omitting important factors such as the plant cost or the plant energy consumption. However, energy and economic aspects should be particularly considered for the selection of the AnMBR-WWTP layout.

The goal of this study is to evaluate the economic feasibility of WWTPs based on mainstream AnMBR technology under different plant layouts. To this end, this research evaluated the impact of sewage COD and sulphate concentrations on the AnMBR-WWTP energy and economic balances, as well as their impact on the plant layout selection. The AnMBR-WWTP layout comprises a combination of primary settler, AnMBR, dissolved methane recovery, nutrients removal and sidestream anaerobic digestion. The ultimate goal is to provide a comprehensive understanding of the implications that different factors and their combination have on the AnMBR-WWTP economic feasibility.

2. Methodology

2.1. AnMBR-WWTP scenarios definition

Fig. 1 illustrates the three scenarios considered for the energy-economic evaluation, while Table 1 shows the treatments included in each scenario. The different scenarios were evaluated for an AnMBR-WWTP treating 100,000 m^3 d^{-1} of municipal sewage with different COD and sulphate concentrations. The lifetime of the AnMBR-WWTP was 20 years. The three scenarios conceived in this publication are summarised below.

Scenario 1 represents the implementation of an AnMBR and a downstream dissolved methane recovery unit (see Fig. 1A). Degassing membrane was selected for dissolved methane recovery since this technology achieves relatively high recovery efficiencies (ca. 70%) at a relatively low energy input (0.01 kWh m^{-3}) (Cookney et al., 2016; Lim et al., 2019). In Scenario 1, primary settler, sidestream anaerobic digestion (AD) and nutrients treatment were not included.

Scenario 2 was an extension of Scenario 1 and included three different plant layouts integrating primary settler and/or sidestream AD (see Fig. 1B and Table 1). The primary settler controls the amount of COD fed to the AnMBR, which affects (i) the amount of methane produced in the AnMBR unit and (ii) the energy consumption for membrane fouling control. The sidestream AD maximises biogas energy production and further stabilises the WWTP sludge. The three plant layouts were: (i) Scenario 2A with a primary settler and sidestream AD, (ii) Scenario 2B with a primary settler and without sidestream AD, and (iii) Scenario 2C with sidestream AD and without primary settler.

Scenario 3 was an extension of the most favourable alternative in Scenario 2 (i.e. Scenario 2C) and included downstream treatments for nitrogen and phosphorus removal (see Fig. 1C). Phosphorus precipitation with ferric chloride was used for mainstream phosphorus removal (Fig. 1C) (Harclerode et al., 2020; Lim et al., 2019), while partial nitritation-Anammox (PN-Anammox) was selected for nitrogen removal since this is a suitable treatment for sewage with a low COD:N ratio (Batstone et al., 2015; Cogert et al., 2019). Specifically, a MBR PN-Anammox system was considered for nitrogen removal due to its capacity to achieve an effective retention of the slow-growing Anammox bacteria in the system at ambient temperature (Dai et al., 2015; Kwak et al., 2020). The PN-Anammox was placed before phosphorus precipitation unit: (i) to prevent phosphorus limitation in PN-Anammox and (ii) to allow a better control of phosphorus removal, which is important to meet the increasingly stringent regulations concerning phosphorus discharge.

2.2. Sewage composition and variability

Municipal sewage COD concentrations ranging from 100 to 1200 mg COD L^{-1} were considered. This interval is representative for municipal sewage and comprises typical concentrations for low-, medium-, and high-strength sewage. Sewage COD consisted of biodegradable soluble COD ($COD_{S,B}$), inert soluble COD ($COD_{S,I}$), biodegradable particulate COD ($COD_{X,B}$) and inert particulate COD ($COD_{X,I}$) representing individual fractions of 0.36, 0.04, 0.40 and 0.20, respectively (Henze et al., 2008). Total nitrogen and phosphorus concentrations were obtained through a lineal COD-dependent function adapted from data provided by Henze et al. (2008). Specifically, the ratios for nitrogen and phosphorus were 12.5 mg COD mg^{-1} N and 51 mg COD mg^{-1} P, respectively. Therefore, the sewage N and P concentrations increased as the sewage COD concentration increased. In Section 3.3.2, where the influence of PN-Anammox energy consumption was evaluated, the sewage nitrogen concentration ranged from 10 to 100 mg N L^{-1} for a fixed sewage COD concentration of 700 mg COD L^{-1}.

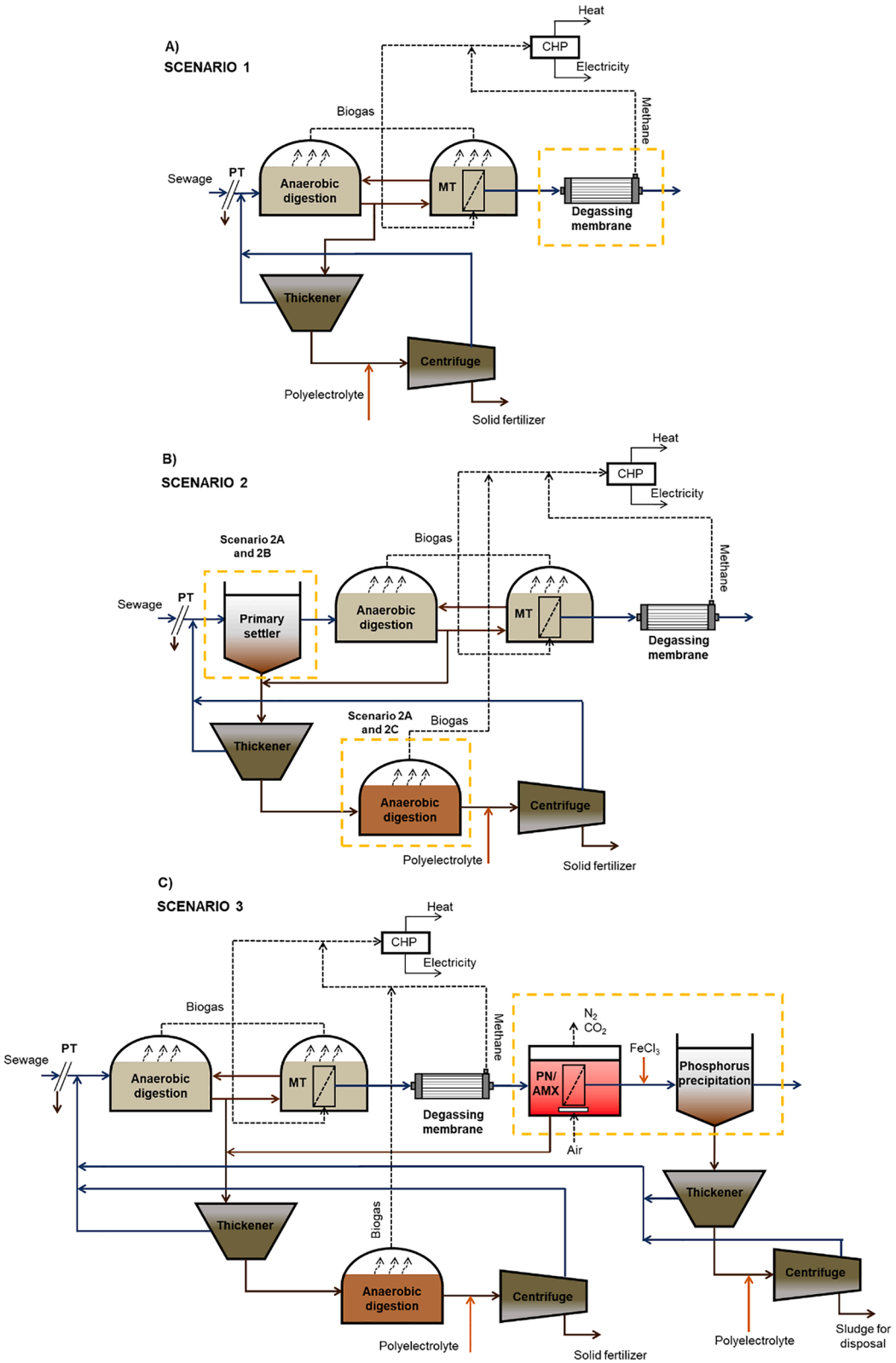

Fig. 1. Schematic representation of the different scenarios. (Scenario 1) AnMBR and degassing membrane; (Scenario 2) AnMBR, degassing membrane, primary settler and sidestream anaerobic digestion; (Scenario 3) AnMBR, degassing membrane, sidestream anaerobic digestion, and nutrients treatment. (PT: Preliminary treatment; MT: Membrane tank; CHP: Combined heat and power unit; PN/AMX: Partial nitritation-Anammox).

Table 1
Treatment units included in each scenario.

	PT	PS	AnMBR	DM	PN/AMX	PP	TK	AD	CG	CHP
Scenario 1	x	–	x	x	–	–	x	–	x	x
Scenario 2A	x	x	x	x	–	–	x	x	x	x
Scenario 2B	x	x	x	x	–	–	x	–	x	x
Scenario 2C	x	–	x	x	–	–	x	x	x	x
Scenario 3	x	–	x	x	x	x	x	x	x	x

PT: Preliminary treatment; PS: Primary settler; AnMBR: Anaerobic membrane bioreactor; DM: Degassing membrane; PN/AMX: Partial nitritation-Anammox; PP: Phosphorus precipitation; TK: Thickener; AD: Sidestream anaerobic digestion; CG: Centrifuge; CHP: Combined heat and power unit.

A COD:SO_4^{2-}-S ratio of 57 was considered in the scenarios where the influence of sulphate was not evaluated since this is a typical ratio for sewage with a low sulphate content (Ferrer et al., 2015). However, in Section 3.2 and 3.3.1, where the influence of sulphate concentration was evaluated, the COD:SO_4^{2-}-S ratio ranged from 2 to 100.

2.3. System design and costs

The AnMBR-WWTP was designed (i) using data reported from lab-, pilot- and full-scale applications and (ii) well-stablished model equations (ASCE et al., 1996; Cogert et al., 2019; Metcalf & Eddy, 2014; Pretel et al., 2015a; Qasim, 1999; Smith et al., 2014). This section summarises the main design and cost considerations for the different technologies considered in this study, including AnMBR, PN-Anammox, phosphorus precipitation, primary settler, sludge treatment processes (i.e. sidestream AD, sludge thickener, and centrifuge), dissolved methane recovery and methane valorisation. Detailed information about the equations and parameters used for cost and energy calculations can be found in the electronic supplementary material.

2.3.1. AnMBR

The AnMBR was designed as a two-stage process operated at ambient temperature (20 °C). The AnMBR system consisted of two tanks: (i) the anaerobic digester and (ii) the membrane tank equipped with submerged ultrafiltration membrane modules. A two-stage system was chosen since the maintenance procedures are simpler than for one stage-systems (Shin and Bae, 2018). The membrane area was calculated considering a net flux of 10 L m^{-2} h^{-1} (LMH) (Giménez et al., 2011; Smith et al., 2014). The membrane replacement cost was calculated considering a membrane lifetime of 10 years (Harclerode et al., 2020; Smith et al., 2014). Gas sparging was used to control long-term membrane fouling assuming a specific gas demand (SGD) of 0.23 Nm^3 m^{-2} h^{-1} (Giménez et al., 2011; Smith et al., 2014). An SRT of 60 days and an HRT of 1 day were considered (Lim et al., 2019; Vinardell et al., 2020b). The recirculation flow rate from the bioreactor to the membrane tank is an important parameter for two-stage AnMBRs since it allows controlling the mixed liquor suspended solids (MLSS) concentration in the membrane tank and reducing membrane fouling (Aslam et al., 2019; Ferrer et al., 2015). In this study, the recirculation flow rate was calculated considering a MLSS concentration in the membrane tank of 18 g L^{-1} (Shin and Bae, 2018). This approach allowed evaluating the influence of sewage strength on energy consumption for fouling control. The MLSS concentration and sludge production were calculated through steady-state equations (see electronic supplementary material).

AnMBR energy consumption accounted for pumping requirements (i.e. influent pump, recirculation pump and permeate/backwash pump), stirring requirements and gas sparging. The energy required to operate centrifugal pumps and gas blowers were calculated through theoretical equations (see electronic supplementary material). The other operating costs (i.e. membrane replacement, chemical reagents for membrane cleaning, labour and equipment maintenance) and capital costs (i.e. civil engineering, mechanical/electrical and equipment) were adapted from Vinardell et al (2020b).

2.3.2. PN-Anammox

The PN-Anammox process was designed for a nitrogen loading rate (NLR) of 0.3 kg N m^{-3} d^{-1}. This is a typical NLR for mainstream PN-Anammox applications (Batstone et al., 2015; Dai et al., 2015). It was assumed that 90% of sewage nitrogen remained in the AnMBR effluent mainly as ammonium ion (Bair et al., 2015), and that nitrogen removal efficiencies of 81% were achieved in the PN-Anammox process (Dai et al., 2015; Schaubroeck et al., 2015). PN-Anammox sludge production was calculated through a steady-state equation considering the growth rates of ammonia oxidising bacteria (AOB) and anammox bacteria (see electronic supplementary material). Theoretically, the PN-Anammox process can significantly reduce the energy requirements for nitrogen removal when compared with the conventional nitrification–denitrification process (Morales et al., 2015). However, the selective inhibition of nitrite oxidising bacteria (NOB), the retention of anammox bacteria at low temperatures, and the presence of residual organic matter in the anaerobic effluent increase PN-Anammox energy requirements (Cruz et al., 2019; Schaubroeck et al., 2015). An energy consumption of 5 kWh per kg of N removed was used for the economic evaluation of the PN-Anammox process (Schaubroeck et al., 2015). However, future technological advances could improve the PN-Anammox process and, subsequently, reduce its energy requirements. In Section 3.3.2, the impact of reducing PN-Anammox energy consumption on AnMBR-WWTP energy balance was evaluated through a sensitivity analysis.

2.3.3. Phosphorus precipitation

The chemical precipitation of phosphorus included a settler, a sludge thickener and a centrifuge. It was considered that 89% of sewage phosphorus remained in the AnMBR effluent mainly as phosphate (Bair et al., 2015) and that phosphorus removal efficiencies in the precipitation unit were 90% (Taboada-Santos et al., 2020). Ferric chloride ($FeCl_3$) was used for phosphorus precipitation considering a cost of 220 € t^{-1} (Taboada-Santos et al., 2020). Sludge thickening and sludge dewatering were designed considering that the sludge production differed for the different sewage P concentrations (see Section 2.3.5 for further details on thickener and centrifuge design).

2.3.4. Primary settler

The primary settler efficiency determines the amount of COD fed to the AnMBR, which has a direct impact on the AnMBR biogas production as well as on the MLSS concentration in the bioreactor. A 40% of the sewage COD was separated in the primary sludge in those scenarios with primary settler (Metcalf & Eddy, 2014). The primary sludge was composed of 6% of TSS and a COD biodegradable fraction of 0.66 (Andreoli et al., 2007). The COD biodegradable fraction was calculated considering that the amount of soluble COD contained in primary sludge is negligible.

2.3.5. Sludge treatment processes

Sludge thickening, sidestream AD and sludge dewatering processes were designed considering that the sludge production differed for the different sewage COD concentrations and for the different scenarios and layouts. It was assumed that the combined thickened sludge contained a

5% of TSS and that no solids were washed out in the thickener. The AD was designed to treat a VS loading rate of 1.6 kg VS m^{-3} d^{-1} at mesophilic conditions (Andreoli et al., 2007) with a VS removal ranging between 17 and 59% depending on the sludge biodegradability of each scenario. The biodegradability of the combined sludge (including primary and secondary) was calculated considering (i) the biodegradable particulate fraction of the sewage that is separated in the primary settler, and (ii) the amount of sludge that is biologically produced in the AnMBR and PN-Anammox processes. The energy consumption for sludge treatment accounted for sludge thickening, digester mixing and sludge dewatering. Polyelectrolyte was dosed at 6 kg t^{-1} TSS with a cost of 2.35 € kg^{-1} (Pretel et al., 2015b). It was considered that the biosolids (dewatered sludge) after AD were stable and thus suitable to be used as fertiliser with a cost of 4.8 € t^{-1} TSS (Ferrer et al., 2015). However, a higher disposal cost was considered in Scenario 2B and Scenario 3. Scenario 2B does not have sidestream AD for mixed sludge and, therefore, the mixed sludge needs to be incinerated or disposed in a landfill. In Scenario 3, the sludge produced from phosphorus removal is disposed in a landfill since it is not suitable for land application.

2.3.6. Methane recovery and valorisation

The methane produced in the AnMBR and the sidestream AD was calculated considering that: (i) all biodegradable COD was biologically degraded in the anaerobic digesters, (ii) a fraction of COD was used for biomass growth (0.076 mg TSS mg^{-1} COD), (iii) SRB consumed 2.01 mg of biodegradable COD per mg of SO_4^{2-}-S (Giménez et al., 2011), and (iv) a fraction of methane remained dissolved in the AnMBR effluent (17.8 mg L^{-1}). The dissolved methane concentration was calculated with Henry's law at ambient temperature (20 °C). The methane produced was combusted in a combined heat and power (CHP) unit with an electricity yield of 33% (Appels et al., 2011). The methane calorific power was 38,800 kJ m^{-3} (0 °C and 1 atm) (Metcalf & Eddy, 2014).

Dissolved methane was partially recovered through degassing membrane, which was designed for a membrane flux of $3{\cdot}10^{-8}$ kmol CH_4 m^{-2} s^{-1} (Rongwong et al., 2017; Sethunga et al., 2019), and a lifetime of 7 years (Cookney et al., 2016). A methane recovery efficiency of 70% was considered based on pilot-scale reported efficiencies (Lim et al., 2019; Seco et al., 2018). It was considered that degassing membrane was operated at an energy input of 0.01 kWh m^{-3} (Evans et al., 2019; Lim et al., 2019). The methane recovered by the degassing membrane was accounted for energy production.

2.4. Economic evaluation

Capital expenditure (CAPEX) and operating expenditure (OPEX) for the different scenarios were calculated. Electricity revenue from the energy produced through biogas cogeneration was also included in the economic evaluation. CAPEX was annualised over the project lifetime with Eq. (1). The net treatment cost, including CAPEX, OPEX and electricity revenue (ER), was calculated using Eq. (2). Finally, the net treatment cost was referred to the volume of sewage treated to facilitate the comparison with other studies and treatment configurations.

$$\text{Annualised CAPEX}\left(€\ y^{-1}\right) = \frac{i\cdot(1+i)^t}{(1+i)^t-1}\cdot\text{CAPEX} \quad (1)$$

$$\text{Net treatment cost}\left(€\ y^{-1}\right) = \frac{i\cdot(1+i)^t}{(1+i)^t-1}\cdot\text{CAPEX} + \text{OPEX} - \text{ER} \quad (2)$$

where CAPEX is the investment cost (€), OPEX is the operating cost (€ y^{-1}), ER is the electricity revenue (€ y^{-1}), i is the discount rate, and t is the plant lifetime (20 years). The discount rate was established at 5% in the scenarios where the influence of the discount rate was not analysed. In Section 3.4, four discount rates (i.e. 5, 10, 15 and 20%) were used to evaluate the influence of the discount rate on treatment costs.

3. Results and discussion

3.1. Energy and economic evaluation of an AnMBR-WWTP with dissolved methane recovery

Fig. 2 shows the energy balance and the net treatment cost of Scenario 1 for COD concentrations between 100 and 1200 mg COD L^{-1}. The energy balance (green line in Fig. 2) shows that (i) the AnMBR process with dissolved methane recovery achieves energy self-sufficiency for COD concentrations above 550 mg COD L^{-1} and (ii) the maximum net energy production (0.32 kWh m^{-3}) is reached when sewage has a COD concentration of 1100 mg COD L^{-1}. The energy recovery increases from 0.05 to 1.01 kWh m^{-3} as the COD concentration increases from 100 to 1200 mg COD L^{-1} (yellow line in Fig. 2). The energy consumption suddenly increases at 1100 mg COD L^{-1} (blue line in Fig. 2), due to the higher recirculation flow rate from the bioreactor to the membrane tank. A higher recirculation flow rate is needed to keep the MLSS concentration in the membrane tank constant at 18 g L^{-1} since the MLSS concentration in the bioreactor increases as a result of the higher sewage COD concentration. Controlling the MLSS concentration in the membrane tank (i) reduces the gas sparging energy requirements, (ii) minimises the use of intensive and complex membrane cleaning protocols and (iii) lowers the membrane replacement frequency.

Scenario 1 features a net treatment cost (brown line in Fig. 2) between 0.42 and 0.35 € m^{-3} for COD concentrations between 100 and 1200 mg COD L^{-1}. These results agree with Smith et al. (2014), who reported similar net treatment costs (ca. 0.37–0.41 $ m^{-3}, i = 5%, 40 years plant lifetime) for an AnMBR-WWTP without degassing membrane and treating 18,950 m^3 d^{-1} of sewage. The production of energy is a distinctive feature of AnMBRs compared with other aerobic technologies such as CAS and MBRs with energy costs between 0.04 and 0.08 and 0.06–0.11 € m^{-3}, respectively (Iglesias et al., 2017).

For the WWTP under study, methane production allows achieving net energy production for COD concentrations above 550 mg COD L^{-1}. However, the methane dissolved in the permeate represents 8–100% of the methane produced under these operational conditionals. Therefore, its recovery is required to increase energy production and reduce uncontrolled methane emissions (Cookney et al., 2016; Lim et al., 2019). In the present study, the benefit-cost ratio for the degassing membrane is estimated at 1.1. The economic prospect of degassing membrane improves if environmental incomes are considered because degassing membrane reduces mainstream greenhouse gas emissions from 0.308 to 0.113 kg CO_2–eq m^{-3} (Sanchis-Perucho et al., 2020). The benefit-cost ratio of degassing membrane increases to 2.0 when the current European Union carbon price (27 € t^{-1} CO_2–eq) is considered (EMBER, 2020). Although degassing membrane technology still needs to be tested at full-scale, the recovery of methane from AnMBR effluents appears crucial to reduce environmental impacts of mainstream anaerobic digestion (Smith et al., 2014).

3.2. Economic evaluation of an AnMBR-WWTP integrating primary settler and sidestream AD

Fig. 3A shows the net treatment cost of Scenario 2 for COD concentrations between 100 and 1200 mg COD L^{-1}. The scenario without primary settler (i.e. Scenario 2C) is the most competitive for COD concentrations below 1100 mg COD L^{-1}. Specifically, the net treatment cost of this scenario decreases from 0.42 to 0.35 € m^{-3} as the sewage COD concentration increases from 100 to 1100 mg COD L^{-1}. The net treatment cost of Scenario 2C is nearly the same than Scenario 1, which does not include neither primary settler nor sidestream AD (see Fig. 2). These results show that the biogas produced from the sludge wasted from the AnMBR in Scenario 2C could offset the costs related to the construction and operation of the sidestream AD. Besides environmental incomes (out of the scope of this publication), further electricity revenue for the sidestream AD could be achieved by implementing co-digestion

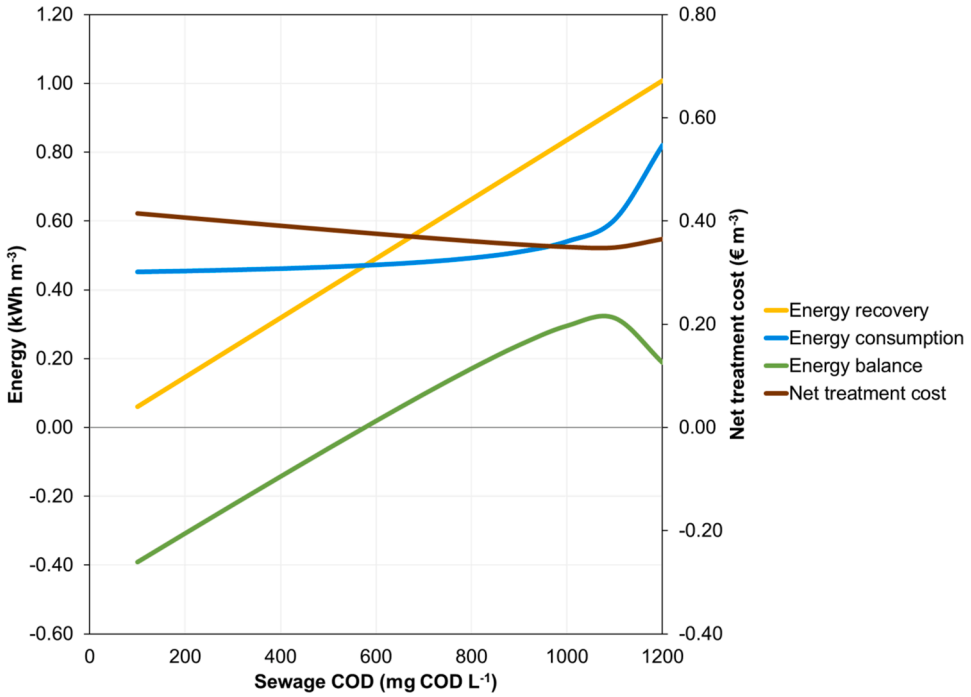

Fig. 2. Energy balance and net treatment cost of Scenario 1 for different sewage COD concentrations (COD:SO_4^{2-}-S = 57).

strategies (Macintosh et al., 2019).

Scenario 2A, which includes both primary settler and sidestream AD, features a net treatment cost 0.01 € m^{-3} higher than Scenario 2C (scenario without primary settler) for COD concentrations below 1100 mg COD L^{-1}. However, Scenario 2A displays the cheapest cost at sewage COD concentrations above 1100 mg COD L^{-1} (Fig. 3A). These results highlight that an AnMBR-WWTP treating high-strength sewage (>1100 mg COD L^{-1}) should integrate primary settler to reduce chemicals and energy consumption associated with fouling control. In Scenario 2A, the high methane yield of primary sludge (ca. 400 mL CH_4 g^{-1} VS) is recovered in the sidestream AD instead of the AnMBR. The importance of the sidestream AD when the AnMBR-WWTP includes a primary settler is shown in Scenario 2B (scenario without sidestream AD), which presents the worse cost among the three configurations considered in Scenario 2 (Fig. 3A). Scenario 2B fails to recover energy and to stabilise primary sludge and, therefore, it is considered unsuitable from both economic and environmental points of view.

The sewage COD:SO_4^{2-}-S ratio has been highlighted as a critical factor for AnMBR profitability and plant layout selection (Pretel et al., 2015a; Vinardell et al., 2020a). COD:SO_4^{2-}-S ratios between 43 and 60 have been reported in previous AnMBR publications (Harclerode et al., 2020; Pretel et al., 2015b; Smith et al., 2014). However, a lower COD:SO_4^{2-}-S ratio is possible when treating sulphate-rich sewage. Accordingly, evaluating the impact of COD:SO_4^{2-}-S ratio on net treatment cost is important to understand the influence of this variable on AnMBR-WWTP profitability.

Fig. 3B shows the net treatment cost of Scenario 2 for COD:SO_4^{2-}-S ratios between 2 and 100 at a constant COD concentration of 700 mg COD L^{-1}. The impact of low COD:SO_4^{2-}-S ratios on methane yield is particularly relevant in Scenario 2C (scenario without primary settler) where the net treatment cost suddenly increases from 0.38 to 0.44 € m^{-3} as the COD:SO_4^{2-}-S ratio decreases from 15 to 2, respectively. The integration of a primary settler (Scenario 2A) should be considered when the COD:SO_4^{2-}-S ratio is below 8 since primary settler allows valorising a fraction of the sewage COD to methane in the sidestream AD (Fig. 3B). However, Scenario 2A decreases the COD:SO_4^{2-}-S ratio in the AnMBR influent and, subsequently, most of the COD is used to convert sulphate into sulphide rather than for methane production. Accordingly, mainstream AnMBR application does not appear suitable to treat sewage with a COD:SO_4^{2-} ratio below 15 (700 mg COD L^{-1}) regardless of the presence of a primary settler in the WWTP layout.

Overall, Scenario 2C (including sidestream AD and without primary settler) presents the most favourable energy and economic prospects for AnMBR-WWTP treating sewage with COD concentrations between 100 and 1100 mg COD L^{-1} and COD:SO_4^{2-}-S ratios above 8. Scenario 2C appears also the most appropriate configuration when the nutrient-rich effluent can be directly used for agricultural irrigation. However, in most applications, the AnMBR effluent has to be discharged into the environment and, therefore, a certain level of post-treatment would be required to comply with N and P discharge limits. In Section 3.3 and 3.4, an energy-economic evaluation of an AnMBR-WWTP is conducted, including nitrogen and phosphorus nutrient removal technologies.

3.3. Energy evaluation of an AnMBR-WWTP with dissolved methane recovery, sidestream AD and nutrients removal

3.3.1. Impact of COD concentration and COD:SO_4^{2-}-S ratio

Fig. 4A shows the energy balance of Scenario 3 for a low-, medium-, and high-strength sewage (400, 700 and 1000 mg COD L^{-1}, respectively) and for COD:SO_4^{2-}-S ratios between 2 and 100. For COD:SO_4^{2-}-S ratios higher than 5, the treatment of medium- and high-strength sewage features a more favourable energy balance than the treatment of low-strength sewage. The energy balance for COD:SO_4^{2-}-S ratios below 5 is unfavourable regardless of the sewage strength with values ranging between –0.47 and –0.87 kWh m^{-3} (Fig. 4). These results reinforce the idea that mainstream AnMBR is not suitable to treat sulphate-rich sewage. Furthermore, sulphide production has a direct negative impact on biological performance, membrane permeability and infrastructure durability (not included in this analysis), further worsening the economic and energetic prospects of AnMBR-WWTPs treating sulphate-rich sewage (Harclerode et al., 2020; Song et al., 2018).

Fig. 4A also shows that the effect of COD:SO_4^{2-}-S ratio on the energy balance has a tipping point at 10, 15 and 20 for sewage concentrations of 400, 700 and 1000 mg COD L^{-1}, respectively. This tipping point represents the COD:SO_4^{2-}-S ratio where the impact of sulphate reduction on the energy balance and process profitability lowers its influence.

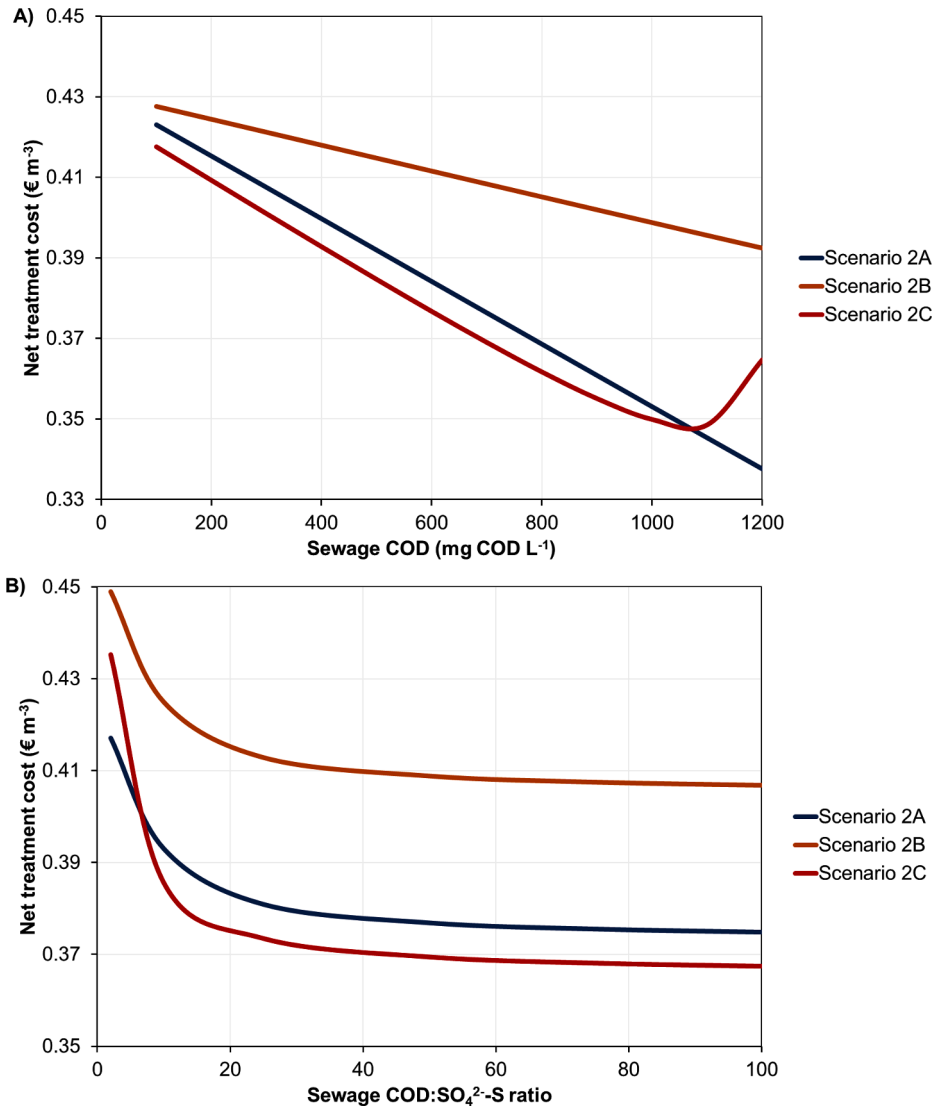

Fig. 3. Net treatment cost of Scenario 2A, Scenario 2B and Scenario 2C. (A) Influence of sewage COD concentration (COD:SO_4^{2-}-S = 57); (B) Influence of COD:SO_4^{2-}-S ratio (700 mg COD L^{-1}).

Accordingly, the application of mainstream AnMBR for the treatment of low-, medium- and high-strength sewage should be considered for COD:SO_4^{2-}-S ratios above 10, 15 and 20, respectively. Operating below this threshold implies not only a poor energy balance, but also a high sensitivity of the energy balance towards sewage COD:SO_4^{2-}-S ratio fluctuations.

The energy balance plotted for the low-, medium-, and high-strength sewage is asymptotic to −0.28, −0.10 and +0.04 kWh m^{-3}, respectively. These results show that an AnMBR-WWTP, including dissolved methane recovery, AnMBR, PN-Anammox, phosphorus precipitation and side-stream AD, has potential to reduce the net energy requirements in comparison with aerobic-based WWTP configurations such as CAS process (0.3–0.6 kWh m^{-3}) (Fernández-Arévalo et al., 2017), aerobic MBR (0.4–0.6 kWh m^{-3}) (Xiao et al., 2019), or high-rate activated sludge (0.39 kWh m^{-3}) (Taboada-Santos et al., 2020). However, although the AnMBR allows reducing the WWTP energy consumption, energy neutrality is only achieved when treating the high-strength sewage with COD:SO_4^{2-}-S ratios above 40. For low- and medium-strength sewage, the energy consumption should be further reduced to achieve an energy self-sufficient AnMBR-WWTP. For low- and medium-strength sewage, the PN-Anammox process consumes 0.11 and 0.19 kWh m^{-3} accounting for 17 and 25% of the total energy consumption, respectively. Future PN-Anammox improvements could reduce its treatment cost and, consequently, overcome the constraints associated with nitrogen removal towards achieving an energy self-sufficient AnMBR-WWTP.

3.3.2. *Impact of PN-Anammox energy consumption*

Fig. 4B illustrates the energy balance of Scenario 3 for nitrogen concentrations between 10 and 100 mg N L^{-1} and considering three PN-Anammox energy consumptions (i.e. 1, 3, and 5 kWh kg^{-1}N removed). This interval was selected because energy consumptions between 1 and 5 kWh kg^{-1}N have been previously reported for mainstream PN-Anammox (Batstone et al., 2015; Schaubroeck et al., 2015). Fig. 4B shows that the AnMBR-WWTP energy consumption could be reduced up to 0.27 kWh m^{-3} if the PN-Anammox energy consumption is reduced from 5 to 1 kWh kg^{-1}N (100 mg N L^{-1}). A PN-Anammox energy consumption of 1 kWh kg^{-1}N would make the AnMBR-WWTP energy self-sufficient regardless of the sewage nitrogen concentration. However, further technological advances are still required to operate mainstream PN-Anammox process at 1 kWh kg^{-1}N (Schaubroeck et al., 2015). On the other hand, energy self-sufficiency is only achieved for nitrogen concentrations below 35 and 25 mg N L^{-1} when PN-Anammox has an energy consumption of 3 and 5 kWh kg^{-1}N, respectively. These results

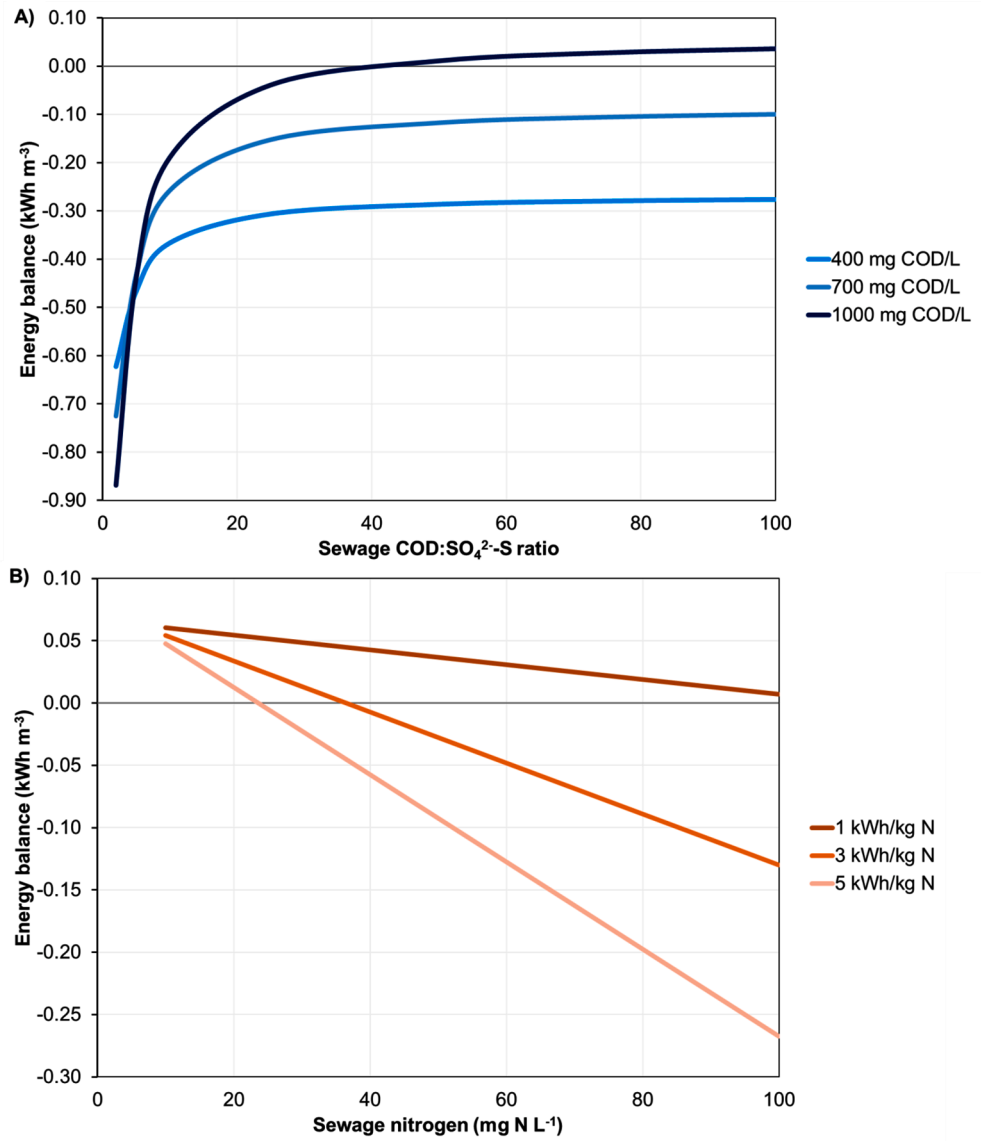

Fig. 4. Energy balance of Scenario 3. (A) Influence of COD:SO_4^{2-} ratio for three sewage COD concentrations (400, 700 and 1000 mg COD L^{-1}). (B) Influence of PN-Anammox energy consumptions (1, 3 and 5 kWh kg^{-1}N) for different sewage nitrogen concentrations (700 mg COD L^{-1}; COD:SO_4^{2-}-S = 57; COD:P = 51).

indicate that reducing the energy consumption of mainstream PN-Anammox is important to achieve a self-sufficient AnMBR-WWTP for medium- or low-strength sewage treatment. However, the economic prospects of the MBR PN-Anammox process also requires considering the energy consumption for membrane fouling control. To overcome the limitations associated with mainstream PN-Anammox, alternative physical methods are being researched. Specifically, ion exchange processes appear to be a promising alternative to valorise nitrogen from AnMBR effluents with relatively low costs (Cruz et al., 2019; Huang et al., 2020; Lim et al., 2019). Overall, the development of efficient technologies for nitrogen removal or recovery is crucial to make AnMBR technology competitive for municipal sewage treatment.

3.4. Economic evaluation of AnMBR-WWTP with dissolved methane recovery, sidestream AD and nutrients removal

The AnMBR-WWTP under assessment includes innovative technologies primarily tested at lab- and pilot-scale but still lacking demonstration at full-scale. The risk associated with the implementation of these novel technologies can be reflected in the discount rate. The discount rate is a financial parameter that allows including the value of money over time and the uncertainty related to future cash flows (Papapetrou et al., 2017). Since the use of mainstream AnMBR application is riskier than aerobic technologies, it is important to evaluate the influence that the discount rate has on AnMBR-WWTP treatment costs.

Fig. 5 shows the net treatment cost of Scenario 3 for sewage COD concentrations between 100 and 1200 mg COD L^{-1} and considering discount rates of 5, 10, 15 and 20%. The net treatment cost does not experience important variations as the sewage COD concentration increases despite the tipping point observed at 1100 mg COD L^{-1} (see Section 3.1). Importantly, these results show that higher COD concentrations do not lead to lower net treatment costs in Scenario 3 because the increased methane production does not offset the higher CAPEX and OPEX associated with nutrients removal and membrane fouling control. For the lowest discount rate (5%), the net treatment cost ranges between 0.51 and 0.56 € m^{-3}, which is competitive compared with the 0.30–0.60 € m^{-3} treatment cost reported for CAS and MBR technologies (including CAPEX and OPEX) (Verstraete et al., 2009). However, a discount rate of 5% is applied for well-stablished technologies and, therefore, it is little realistic for an AnMBR-WWTP. A discount rate of 10% increases the net

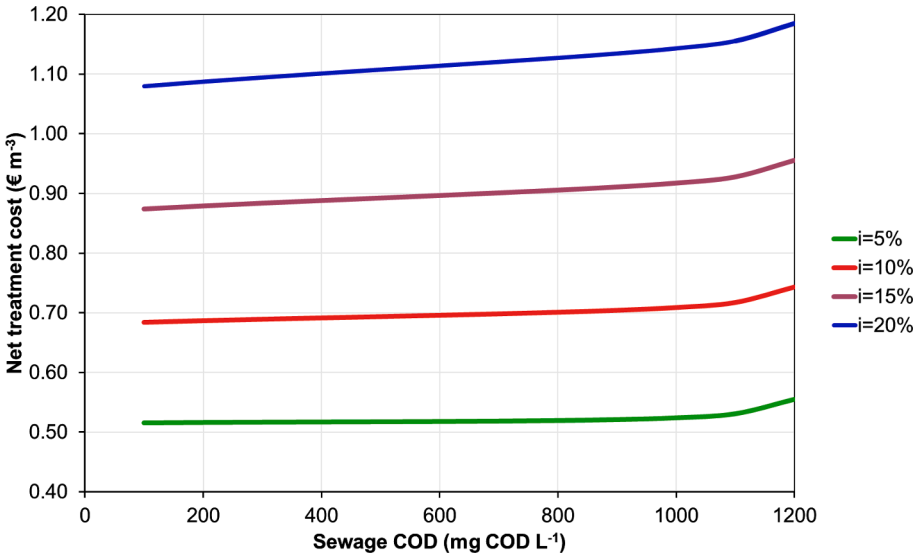

Fig. 5. Net treatment cost of Scenario 3 for different sewage COD concentrations and considering discount rates of 5, 10, 15, and 20% (COD:SO_4^{2-}-S = 57; COD:N = 12.5; COD:P = 51).

treatment cost to 0.68–0.74 € m^{-3}, whereas a discount rate above 15% leads to net treatment cost above 0.90 € m^{-3}. These results show that the net treatment cost of mainstream AnMBR application can be competitive compared with aerobic treatments. However, the risk associated with implementing a range of innovative technologies can significantly compromise the AnMBR-WWTP economic feasibility. Therefore, research at demonstration-scale is crucial to reduce the risk and uncertainty associated with these novel technologies and support the transition from WWTPs to WRRFs.

Fig. 6 shows the costs distribution of AnMBR-WWTPs with AnMBR, dissolved methane recovery, PN-Anammox, phosphorus precipitation and sidestream AD for sewage COD concentration of 700 mg COD L^{-1}. The AnMBR is the most expensive unit, representing 57.6% of the treatment cost. The PN-Anammox process also represents an important fraction of the treatment cost (30.3%). Since AnMBR and PN-Anammox account for 87.9% of the treatment cost, future research efforts should aim to reduce costs associated with these technologies. Sludge treatment cost only represents 3.4% of the treatment cost since mainstream AnMBR application notably reduces sludge production compared with aerobic technologies. The revenue coming from methane production allows reducing 10.8% the treatment cost. Besides electricity, further revenue from the reutilisation of the high-quality effluent free of suspended solids and nutrients could be obtained in future AnMBR-WWTPs.

The OPEX of the AnMBR-WWTP only represents between 30.5 and 36.5% of the treatment cost since net energy consumption and sludge production are reduced in anaerobic systems (see electronic supplementary material). Accordingly, reducing CAPEX is crucial to reduce treatment costs. In this regard, retrofitting existing aerobic-based WWTPs to AnMBR-WWTPs stands as a promising alternative to implement mainstream AnMBR technology with reduced CAPEX. Indeed, the net treatment cost of AnMBR-WWTP could be reduced to 0.12 € m^{-3} if only OPEX and the revenue from energy production were considered

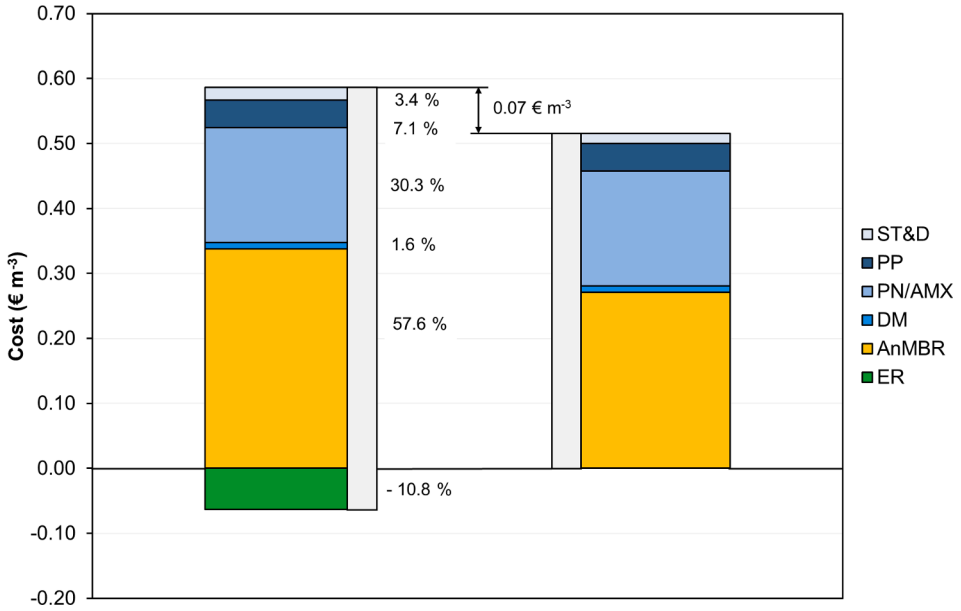

Fig. 6. Cost distribution of Scenario 3 for a sewage COD concentration of 700 mg COD L^{-1} (COD:SO_4^{2-}-S = 57; COD:N = 12.5; COD:P = 51). (left) Without including electricity revenue (treatment cost); (right) including electricity revenue (net treatment cost). (ST&D: Sludge treatment and disposal; PP: Phosphorus precipitation; PN/AMX: Partial nitritation-Anammox; DM: Degassing membrane; AnMBR: Anaerobic membrane bioreactor; ER electricity revenue).

(see electronic supplementary material). Finally, it is worth mentioning that in a retrofitted AnMBR-WWTP the existing sidestream anaerobic digester would be oversized due to the lower amount of sludge produced in the AnMBR process. However, this represents an opportunity to implement co-digestion in the AnMBR-WWTP as a strategy to further increase biogas energy production and reduce the net treatment cost.

4. Conclusions

The economic feasibility of mainstream AnMBR-WWTP was investigated. The net treatment cost of a WWTP, including AnMBR, degassing membrane and sidestream AD, was between 0.42 and 0.35 € m^{-3} for a sewage COD concentration between 100 and 1200 mg COD L^{-1}. The incorporation of nutrient removal technologies increased the net treatment cost above 0.51 € m^{-3} despite a net energy production of 0.04 kWh m^{-3} was achieved for high-strength municipal sewage treatment (1000 mg COD L^{-1}). The results showed that reducing the treatment cost of AnMBR and PN-Anammox is important to make AnMBR-WWTP competitive for municipal sewage treatment.

CRediT authorship contribution statement

Sergi Vinardell: Conceptualization, Formal analysis, Investigation, Data curation, Methodology, Writing - original draft, Visualization. **Joan Dosta:** Conceptualization, Writing - review & editing, Supervision. **Joan Mata-Alvarez:** Conceptualization, Supervision, Funding acquisition. **Sergi Astals:** Conceptualization, Writing - review & editing, Supervision.

Declaration of Competing Interest

The authors declare that they have no known competing financial interests or personal relationships that could have appeared to influence the work reported in this paper. The authors also declare that this manuscript reflects only the authors' view and that the Executive Agency for SME/EU Commission are not responsible for any use that may be made of the information it contains.

Acknowledgments

This work was supported by the European Union LIFE programme (LIFE Green Sewer project, LIFE17 ENV/ES/000341). Sergi Vinardell is grateful to the Generalitat de Catalunya for his predoctoral FI grant (2019FI_B 00394). Sergi Astals is grateful to the Spanish Ministry of Science, Innovation and Universities for his Ramon y Cajal fellowship (RYC-2017-22372).

Appendix A. Supplementary data

Supplementary data to this article can be found online at https://doi.org/10.1016/j.biortech.2020.124170.

References

Ab Hamid, N.H., Smart, S., Wang, D.K., Koh, K.W.J., Ng, K.J.C., Ye, L., 2020. Economic, energy and carbon footprint assessment of integrated forward osmosis membrane bioreactor (FOMBR) process in urban wastewater treatment. Environ. Sci. Water Res. Technol. 6, 153–165.

Andreoli, C.V., von Sperling, M., Fernandes, F., 2007. Biological Wastewater Treatment, Sludge treatment and disposal. IWA Publishing, London.

Appels, L., Lauwers, J., Degrve, J., Helsen, L., Lievens, B., Willems, K., Van Impe, J., Dewil, R., 2011. Anaerobic digestion in global bio-energy production: Potential and research challenges. Renew. Sustain. Energy Rev. 15, 4295–4301.

ASCE, AWWA, EPA, 1996. Management of water treatment plant residuals : technology transfer handbook. ASCE and AWWA. New York.

Aslam, A., Khan, S.J., Shahzad, H.M.A., 2019. Impact of sludge recirculation ratios on the performance of anaerobic membrane bioreactor for wastewater treatment. Bioresour. Technol. 288, 121473.

Bair, R.A., Ozcan, O.O., Calabria, J.L., Dick, G.H., Yeh, D.H., 2015. Feasibility of anaerobic membrane bioreactors (AnMBR) for onsite sanitation and resource recovery (nutrients, energy and water) in urban slums. Water Sci. Technol. 72, 1543–1551.

Batstone, D.J., Hülsen, T., Mehta, C.M., Keller, J., 2015. Platforms for energy and nutrient recovery from domestic wastewater: A review. Chemosphere 140, 2–11.

Cogert, K.I., Ziels, R.M., Winkler, M.K.H., 2019. Reducing Cost and Environmental Impact of Wastewater Treatment with Denitrifying Methanotrophs, Anammox, and Mainstream Anaerobic Treatment. Environ. Sci. Technol. 53, 12935–12944.

Cookney, J., Mcleod, A., Mathioudakis, V., Ncube, P., Soares, A., Jefferson, B., McAdam, E.J., 2016. Dissolved methane recovery from anaerobic effluents using hollow fibre membrane contactors. J. Memb. Sci. 502, 141–150.

Cruz, H., Law, Y.Y., Guest, J.S., Rabaey, K., Batstone, D., Laycock, B., Verstraete, W., Pikaar, I., 2019. Mainstream ammonium recovery to advance sustainable urban wastewater management. Environ. Sci. Technol. 53, 11066–11079.

Dai, W., Xu, X., Liu, B., Yang, F., 2015. Toward energy-neutral wastewater treatment: A membrane combined process of anaerobic digestion and nitritation-anammox for biogas recovery and nitrogen removal. Chem. Eng. J. 279, 725–734.

EMBER, 2020. https://ember-climate.org/carbon-price-viewer/. (Accessed 8/9/2020).

Evans, P.J., Parameswaran, P., Lim, K., Bae, J., Shin, C., Ho, J., McCarty, P.L., 2019. A comparative pilot-scale evaluation of gas-sparged and granular activated carbon-fluidized anaerobic membrane bioreactors for domestic wastewater treatment. Bioresour. Technol. 288, 120949.

Fernández-Arévalo, T., Lizarralde, I., Fdz-Polanco, F., Pérez-Elvira, S.I., Garrido, J.M., Puig, S., Poch, M., Grau, P., Ayesa, E., 2017. Quantitative assessment of energy and resource recovery in wastewater treatment plants based on plant-wide simulations. Water Res. 118, 272–288.

Ferrer, J., Pretel, R., Durán, F., Giménez, J.B., Robles, A., Ruano, M.V., Serralta, J., Ribes, J., Seco, A., 2015. Design methodology for submerged anaerobic membrane bioreactors (AnMBR): A case study. Sep. Purif. Technol. 141, 378–386.

Giménez, J.B., Robles, A., Carretero, L., Durán, F., Ruano, M.V., Gatti, M.N., Ribes, J., Ferrer, J., Seco, A., 2011. Experimental study of the anaerobic urban wastewater treatment in a submerged hollow-fibre membrane bioreactor at pilot scale. Bioresour. Technol. 102, 8799–8806.

Guest, J.S., Skerlos, S.J., Barnard, J.L., Beck, M.B., Daigger, G.T., Hilger, H., Jackson, S. J., Karvazy, K., Kelly, L., Macpherson, L., Mihelcic, J.R., Pramanik, A., Raskin, L., Van Loosdrecht, M.C.M., Yeh, D., Love, N.G., 2009. A new planning and design paradigm to achieve sustainable resource recovery from wastewater. Environ. Sci. Technol. 43, 6126–6130.

Harclerode, M., Doody, A., Brower, A., Vila, P., Ho, J., Evans, P.J., 2020. Life cycle assessment and economic analysis of anaerobic membrane bioreactor whole-plant configurations for resource recovery from domestic wastewater. J. Environ. Manage. 269, 110720.

Henze, M., van Loosdrecht, M.C.M., Ekama, G.A., Brdjanovic, D., 2008. Biological wastewater treatment : principles, modelling and design. IWA Publishing, London.

Huang, X., Guida, S., Jefferson, B., Soares, A., 2020. Economic evaluation of ion-exchange processes for nutrient removal and recovery from municipal wastewater. npj Clean Water 3, 7.

Iglesias, R., Simón, P., Moragas, L., Arce, A., Rodriguez-Roda, I., 2017. Cost comparison of full-scale water reclamation technologies with an emphasis on membrane bioreactors. Water Sci. Technol. 75, 2562–2570.

Kwak, W., Rout, P.R., Lee, E., Bae, J., 2020. Influence of hydraulic retention time and temperature on the performance of an anaerobic ammonium oxidation fluidized bed membrane bioreactor for low-strength ammonia wastewater treatment. Chem. Eng. J. 386, 123992.

Lim, K., Evans, P.J., Parameswaran, P., 2019. Long-Term Performance of a Pilot-Scale Gas-Sparged Anaerobic Membrane Bioreactor under Ambient Temperatures for Holistic Wastewater Treatment. Environ. Sci. Technol. 53, 7347–7354.

Macintosh, C., Astals, S., Sembera, C., Ertl, A., Drewes, J.E., Jensen, P.D., Koch, K., 2019. Successful strategies for increasing energy self-sufficiency at Grüneck wastewater treatment plant in Germany by food waste co-digestion and improved aeration. Appl. Energy 242, 797–808.

Madden, P., Al-Raei, A.M., Enright, A.M., Chinalia, F.A., de Beer, D., O'Flaherty, V., Collins, G., 2014. Effect of sulfate on low-temperature anaerobic digestion. Front. Microbiol. 5.

Metcalf & Eddy, 2014. Wastewater Engineering: Treatment and Resource Recovery, fifth ed. McGraw Hill, New York.

Morales, N., Val del Río, Á., Vázquez-Padín, J.R., Méndez, R., Mosquera-Corral, A., Campos, J.L., 2015. Integration of the Anammox process to the rejection water and main stream lines of WWTPs. Chemosphere 140, 99–105.

Papapetrou, M., Cipollina, A., Commare, U.La., Micale, G., Zaragoza, G., Kosmadakis, G., 2017. Assessment of methodologies and data used to calculate desalination costs. Desalination 419, 8–19.

Pretel, R., Durán, F., Robles, A., Ruano, M.V., Ribes, J., Serralta, J., Ferrer, J., 2015a. Designing an AnMBR-based WWTP for energy recovery from urban wastewater: The role of primary settling and anaerobic digestion. Sep. Purif. Technol. 156, 132–139.

Pretel, R., Shoener, B.D., Ferrer, J., Guest, J.S., 2015b. Navigating environmental, economic, and technological trade-offs in the design and operation of submerged anaerobic membrane bioreactors (AnMBRs). Water Res. 87, 531–541.

Qasim, S.R., 1999. Wastewater treatment plants : planning, design, and operation, second ed. Technomic Publishing Co, Lancaster.

Robles, Á., Aguado, D., Barat, R., Borrás, L., Bouzas, A., Giménez, J.B., Martí, N., Ribes, J., Ruano, M.V., Serralta, J., Ferrer, J., Seco, A., 2020. New frontiers from removal to recycling of nitrogen and phosphorus from wastewater in the Circular Economy. Bioresour. Technol. 300, 122673.

Rongwong, W., Wongchitphimon, S., Goh, K., Wang, R., Bae, T.H., 2017. Transport properties of CO2 and CH4 in hollow fiber membrane contactor for the recovery of biogas from anaerobic membrane bioreactor effluent. J. Memb. Sci. 541, 62–72.
Sanchis-Perucho, P., Robles, Á., Durán, F., Ferrer, J., Seco, A., 2020. PDMS membranes for feasible recovery of dissolved methane from AnMBR effluents. J. Memb. Sci. 604, 118070.
Schaubroeck, T., De Clippeleir, H., Weissenbacher, N., Dewulf, J., Boeckx, P., Vlaeminck, S.E., Wett, B., 2015. Environmental sustainability of an energy self-sufficient sewage treatment plant: Improvements through DEMON and co-digestion. Water Res. 74, 166–179.
Seco, A., Mateo, O., Zamorano-López, N., Sanchis-Perucho, P., Serralta, J., Martí, N., Borrás, L., Ferrer, J., 2018. Exploring the limits of anaerobic biodegradability of urban wastewater by AnMBR technology. Environ. Sci. Water Res. Technol. 4, 1877–1887.
Serrano, A., Peces, M., Astals, S., Villa-Gómez, D.K., 2019. Batch assays for biological sulfate-reduction: a review towards a standardized protocol. Crit. Rev. Environ. Sci. Technol. 50, 1195–1223.
Sethunga, G.S.M.D.P., Karahan, H.E., Wang, R., Bae, T.H., 2019. PDMS-coated porous PVDF hollow fiber membranes for efficient recovery of dissolved biomethane from anaerobic effluents. J. Memb. Sci. 584, 333–342.
Sheik, A.R., Muller, E.E.L., Wilmes, P., Clark, K.B., Zhang, X., 2014. A hundred years of activated sludge: time for a rethink. Frointiers Microbiol. 5, 1–7.
Shin, C., Bae, J., 2018. Current status of the pilot-scale anaerobic membrane bioreactor treatments of domestic wastewaters: A critical review. Bioresour. Technol. 247, 1038–1046.
Shoener, B.D., Zhong, C., Greiner, A.D., Khunjar, W.O., Hong, P.Y., Guest, J.S., 2016. Design of anaerobic membrane bioreactors for the valorization of dilute organic carbon waste streams. Energy Environ. Sci. 9, 1102–1112.
Smith, A.L., Skerlos, S.J., Raskin, L., 2013. Psychrophilic anaerobic membrane bioreactor treatment of domestic wastewater. Water Res. 47, 1655–1665.
Smith, A.L., Stadler, L.B., Cao, L., Love, N.G., Raskin, L., Skerlos, S.J., 2014. Navigating Wastewater Energy Recovery Strategies: A Life Cycle Comparison of Anaerobic Membrane Bioreactor and Conventional Treatment Systems with Anaerobic Digestion. Environ. Sci. Technol. 48, 5972–5981.
Song, X., Luo, W., McDonald, J., Khan, S.J., Hai, F.I., Guo, W., Ngo, H.H., Nghiem, L.D., 2018. Effects of sulphur on the performance of an anaerobic membrane bioreactor: Biological stability, trace organic contaminant removal, and membrane fouling. Bioresour. Technol. 250, 171–177.
Stuckey, D.C., 2012. Recent developments in anaerobic membrane reactors. Bioresour. Technol. 122, 137–148.
Taboada-Santos, A., Rivadulla, E., Paredes, L., Carballa, M., Romalde, J., Lema, J.M., 2020. Comprehensive comparison of chemically enhanced primary treatment and high-rate activated sludge in novel wastewater treatment plant configurations. Water Res. 169.
Verstraete, W., Van de Caveye, P., Diamantis, V., 2009. Maximum use of resources present in domestic “used water”. Bioresour. Technol. 100, 5537–5545.
Vinardell, S., Astals, S., Peces, M., Cardete, M.A., Fernández, I., Mata-Alvarez, J., Dosta, J., 2020a. Advances in anaerobic membrane bioreactor technology for municipal wastewater treatment: A 2020 updated review. Renew. Sustain. Energy Rev. 130, 109936.
Vinardell, S., Astals, S., Mata-Alvarez, J., Dosta, J., 2020b. Techno-economic analysis of combining forward osmosis-reverse osmosis and anaerobic membrane bioreactor technologies for municipal wastewater treatment and water production. Bioresour. Technol. 297, 122395.
Xiao, K., Liang, S., Wang, X., Chen, C., Huang, X., 2019. Current state and challenges of full-scale membrane bioreactor applications: A critical review. Bioresour. Technol. 271, 473–481.

SUPPLEMENTARY INFORMATION

Unravelling the economics behind mainstream anaerobic membrane bioreactor application under different plant layouts

Sergi Vinardell[a,*], Joan Dosta[a], Joan Mata-Alvarez[a], Sergi Astals[a]

*Corresponding author (e-mail: svinardell@ub.edu)

Tables

Table S1. Equations used to calculate (i) capital costs, operating costs and electricity revenue, (ii) energy requirements, (iii) sludge production, and (iv) dissolved methane concentration in the AnMBR permeate.

Table S2. Parameters used for the equations illustrated in Table S1.

Figures

Figure S1. Energy balance of Scenario 3 for different influent COD concentrations.

Figure S2. Energy distribution of Scenario 3 for an influent COD concentration of 700 mg COD L^{-1}.

Figure S3. Net operating costs and OPEX to CAPEX relationship of Scenario 3 for different influent COD concentrations.

Table S1. Equations used to calculate (i) capital costs, operating costs and benefits, (ii) energy requirements, (iii) sludge production, and (iv) dissolved methane concentration in the AnMBR permeate.

Capital costs	
Preliminary treatment	$\mathrm{Cost_{PT}}(€) = \mathrm{CC_{PT}} \cdot \mathrm{Q}$
Settler	$\mathrm{Cost_{PS}}(€) = -0.00002 \cdot \mathrm{Q} + 19.29 \cdot \mathrm{Q} + 220{,}389$
AnMBR	$\mathrm{Cost_{AnMBR}}(€) = \mathrm{Q} \cdot \mathrm{CC_{AnMBR}}$
Degassing membrane	$\mathrm{Cost_{DM}}(€) = \frac{\mathrm{CH_{4,dissolved}} \cdot \mathrm{Q_{IN,DM}} \cdot \eta_{\mathrm{DM}}}{\mathrm{J_{DM}} \cdot 86.4 \cdot 10^6 \cdot \mathrm{M_{CH_4}}} \cdot \mathrm{CC_{DM}}$
Phosphorus precipitation	$\mathrm{Cost_{PP}}(€) = -0.00002 \cdot \mathrm{Q_{IN,PP}} + 19.29 \cdot \mathrm{Q_{IN,PP}} + 220{,}389 + \left(34{,}600 + 206 \cdot \left(\frac{\mathrm{W_{T1,PP}}}{0.0038}\right)^{0.50} + 110 \cdot \left(\frac{\mathrm{W_{T1,PP}}}{0.0038}\right)^{0.55}\right) \cdot \mathrm{R_{\$,€}} + \left(138{,}400 + 666 \cdot \left(\frac{\mathrm{W_{T2,PP}}}{0.0038}\right)^{0.50} + 15{,}400 + 59 \cdot \left(\frac{\mathrm{W_{T2,PP}}}{0.0038}\right)^{0.50}\right) \cdot \mathrm{R_{\$,€}}$
PN-Anammox reactor	$\mathrm{Cost_{PN-AMX}}(€) = \mathrm{C_1} \cdot \left(\frac{\mathrm{L_N}}{\frac{\mathrm{NLR}}{\mathrm{k_1}}}\right)^{0.85} + \frac{\mathrm{Q_{P,PN-AMX}} \cdot 41.7}{\mathrm{J_{w,}}} \cdot \mathrm{CC_{UF}}$
Thickener	$\mathrm{Cost_{TK}}(€) = \left(34{,}600 + 206 \cdot \left(\frac{\mathrm{W_{T1}}}{0.0038}\right)^{0.50} + 110 \cdot \left(\frac{\mathrm{W_{T1}}}{0.0038}\right)^{0.55}\right) \cdot \mathrm{R_{\$,€}}$
Centrifuge	$\mathrm{Cost_{CG}}(€) = \left(138{,}400 + 666 \cdot \left(\frac{\mathrm{W_{T2}}}{0.0038}\right)^{0.50} + 15{,}400 + 59 \cdot \left(\frac{\mathrm{W_{T2}}}{0.0038}\right)^{0.50}\right) \cdot \mathrm{R_{\$,€}}$
Sidestream anaerobic digestion	$\mathrm{Cost_{AD}}(€) = \frac{\mathrm{VS_I}}{\mathrm{VSLR}} \cdot \mathrm{CC_{AD}}$
CHP	$\mathrm{Cost_{CHP}}(€) = \mathrm{P_{CHP}} \cdot \mathrm{CC_{CPH}} \cdot \mathrm{R_{\$,€}}$
Others	$\mathrm{Cost_{M\&E,CE}} = \mathrm{Q} \cdot \mathrm{C_{M\&E,CE}} + \mathrm{Q} \cdot \mathrm{C_{CE}}$
Energy	
Centrifugal pumps	$\mathrm{E_P(kW)} = \sum_{i=1}^{N} \frac{\Delta \mathrm{P_P} \cdot \mathrm{Q_P}}{36 \cdot \eta_{\mathrm{P}}}$
Blower	$\mathrm{P_B(W)} = \frac{\mathrm{M_{Biogas}} \cdot \mathrm{R} \cdot \mathrm{T}}{(\alpha - 1) \cdot \eta_{\mathrm{B}}} \cdot \left[\left(\frac{\mathrm{P_2}}{\mathrm{P_1}}\right)^{\frac{\alpha-1}{\alpha}} - 1\right]$
Operating costs	

AnMBR	$\text{Cost}_{\text{AnMBR}}(€\,y^{-1}) = Q \cdot OC_{\text{AnMBR}} \cdot 365 + \left(\frac{\Delta P_{P1} \cdot Q}{36 \cdot \eta_P} + \frac{\Delta P_{P2} \cdot Q_R}{36 \cdot \eta_P} + \frac{\Delta P_{P3} \cdot Q_P}{36 \cdot \eta_P} + \frac{P_B}{1000}\right) \cdot 8{,}760 \cdot UC_{El}$
Degassing membrane	$\text{Cost}_{DM}(€\,y^{-1}) = E_{DM} \cdot Q \cdot 365 \cdot UC_{El} + DM_{\text{Replacement}}$
Phosphorus precipitation	$\text{Cost}_{PP}(€\,y^{-1}) = (E_{TK} \cdot Q + E_{CG} \cdot Q) \cdot 365 \cdot UC_{El} + TSS_{PP} \cdot k_{\text{Poly,sludge}} \cdot UC_{\text{Poly}} \cdot 365 + TSS_{PP} \cdot UC_{\text{Disposal}} \cdot 365 + \frac{L_P}{M_P} \cdot M_{FeCl_3} UC_{FeCl_3} \cdot 365$
PN-Anammox	$\text{Cost}_{PN-AMX}(€\,y^{-1}) = E_{PN-AMX} \cdot L_N \cdot x_N \cdot 365 \cdot UC_{El} + UF_{\text{Replacement}}$
Sludge line	$\text{Cost}_{\text{SludgeLine}}(€\,y^{-1}) = \left(E_{TK} \cdot Q + E_{CG} \cdot Q + E_{Mix} \cdot 24 \cdot \frac{VS_I}{VSLR}\right) \cdot 365 \cdot UC_{El} + TSS_{SL} \cdot k_{\text{Poly,sludge}} \cdot UC_{\text{Poly}} \cdot 365 + TSS_{SL} \cdot UC_{\text{Disposal}} \cdot 365$
Benefits	
Electricity production	$\text{Revenue}_{\text{Electricity}}(€\,y^{-1}) = Q_{CH_4} \cdot LHV \cdot \eta_{El} \cdot \frac{365}{3600} \cdot UC_{El}$
Sludge production	
MLSS concentration in the AnMBR (mg TSS L^{-1})	$X_M(\text{mg TSS } L^{-1}) = \frac{SRT}{HRT} \cdot \left[X_I + \frac{(1 + f_D \cdot b_H \cdot SRT) \cdot Y_T \cdot (S_{S,0} - S_S)}{1 + b_H}\right]$
Sludge production in the AnMBR (kg TSS day^{-1})	$W_{\text{AnMBR}}(\text{kg TSS } d^{-1}) = \frac{Q}{10^3} \cdot \left[X_I + \frac{(1 + f_D \cdot b_H \cdot SRT) \cdot Y_T \cdot (S_{S,0} - S_S)}{1 + b_H}\right]$
Sludge production in the PN-Anammox process	$W_{PN/AMX}(\text{kg VSS } d^{-1}) = L_N \cdot f_{N,AOB} Y_{AOB} + L_N \cdot f_{N,AMX} Y_{AMX}$
Dissolved methane	
Permeate dissolved methane (mg L^{-1})	$CH_{4,\text{dissolved}}(\text{mg } L^{-1}) = P_{CH_4} \cdot K_{H,CH_4} \cdot M_{CH_4} \cdot OS \cdot 1000$

Table S2. Parameters used for the equations illustrated in Table S1.

Capital Costs	**Parameter**	**Description**	**Units**	**Value**	**Reference[f]**
Preliminary treatment	Q	Sewage flow rate	$m^3\ d^{-1}$	100000	Assumption
	CC_{PT}	Capital cost preliminary treatment	€ $m^{-3}\ d$	23	Smith et al., 2014
Primary Settler	Q	Sewage flow rate	$m^3\ d^{-1}$	100000	Assumption
AnMBR	CC_{AnMBR}	AnMBR capital costs (equipment cost)[a]	€ $m^{-3}\ d$	498	Vinardell et al., 2020
	Q	Sewage flow rate	$m^3\ d^{-1}$	100000	Assumption
Degassing membrane (DM)	$Q_{IN,DM}$	Degassing membrane influent flow rate	$m^3\ d^{-1}$	98833	Calculation
	$CH_{4,dissolved}$	Dissolved methane	mg $CH_4\ L^{-1}$	17.8	Calculation
	η_{DM}	Recovery efficiency	-	0.70	Lim et al., 2019
	J_{DM}	Methane flux	kmol $CH_4\ m^{-2}\ s^{-1}$	$3 \cdot 10^{-8}$	Rongwong et al., 2017; Sethunga et al., 2019
	M_{CH4}	Molar mass methane	kg $kmol^{-1}$	16	Metcalf & Eddy, 2014
	CC_{DM}	Capital cost degassing membrane	€ m^{-2}	40	Cookney et al., 2016
Phosphorus precipitation	$Q_{IN,PP}$	Influent flow rate to the phosphorus precipitation unit	$m^3\ d^{-1}$	98833	Calculation
	$W_{T1,PP}$	Sludge flow rate	$m^3\ d^{-1}$	41-502	Calculation
	$W_{T2,PP}$	Sludge flow rate after thickener	$m^3\ d^{-1}$	25-301	Calculation
	$R_{\$,€}$	Conversion $ to €	€ $\$^{-1}$	0.89	ECB, 2020
PN-Anammox	$Q_{P,PN\text{-}AMX}$	PN-Anammox permeate flow rate	$m^3\ d^{-1}$	97659-98277	Calculation
	J_W	Net membrane flux	L $m^{-2}\ h^{-1}$	10	Giménez et al., 2011; Smith et al., 2014
	CC_{UF}	Capital cost ultrafiltration membranes	€ m^{-2}	50	Brepols et al., 2010; Verrecht et al., 2010
	L_N	Nitrogen load	kg N d^{-1}	645-7742	Calculation
	NLR	Nitrogen loading rate	kg N $m^{-3}\ d^{-1}$	0.30	Dai et al., 2015; Batstone et al., 2015
	k_1	PN-Anammox reference volume k_1	m^3	310	Astals et al., 2019
	C_1	Cost of PN-Anammox reactor with volume k_1	€	350000	Astals et al., 2019
Thickener	W_{T1}	Sludge flow rate before thickener	$m^3\ d^{-1}$	1680-2471	Calculation

	$R_{\$,€}$	Conversion $ to €	€ $^{-1}$	0.89	ECB, 2020
Centrifuge	W_{T2}	Sludge flow rate before centrifuge	$m^3 d^{-1}$	50-1177	Calculation
	$R_{\$,€}$	Conversion $ to €	€ $^{-1}$	0.89	ECB, 2020
Sidestream anaerobic digestion	VS_I	Volatile solids load	kg VS d^{-1}	1691-41122	Calculation
	VSLR	Volatile solids loading rate	kg VS m^3 d^{-1}	1.6	Andreoli et al., 2007
	CC_{AD}	Capital cost anaerobic digester	€ m^{-3}	220	Verrecht et al., 2010
CHP	P_{CHP}	Power	kW	184-4569	Calculated
	CC_{CHP}	Capital cost CHP	$ Kw^{-1}	800	Smith et al., 2014
	$R_{\$,€}$	Conversion $ to €	€ $^{-1}$	0.89	ECB, 2020
Others	Q	Sewage flow rate	$m^3 d^{-1}$	100000	Assumption
	$C_{M\&E}$	Mechanical and Electrical	€ $m^3 d^{-1}$	387	Vinardell et al., 2020; DeCarolis et al., 2007
	C_{CE}	Civil Engineering	€ $m^3 d^{-1}$	498	Vinardell et al., 2020; Brepols et al., 2010
Operating Costs	**Parameter**	**Description**	**Units**	**Value**	**Reference[f]**
AnMBR	ΔP_1	Influent pump head	bar	0.6	Assumption
	ΔP_2	Recirculation pump head	bar	0.8	Assumption
	ΔP_3	Permeate pump head	bar	0.8	Assumption
	Q	Sewage flow rate	$m^3 d^{-1}$	100000	Assumption
	Q_R	Recirculation flow rate	$m^3 d^{-1}$	103000-1515700	Calculation
	Q_P	Permeate flow rate	$m^3 d^{-1}$	98833	Calculation
	η_P	Pump efficiency	-	0.85	Wan and Chung, 2018
	M_{Biogas}	Molar flow rate biogas	mol s^{-1}	1170	Calculation
	R	Gas constant	J mol^{-1} K^{-1}	8.31	Metcalf & Eddy, 2014
	T	Biogas temperature	K	293	Assumption
	η_B	Blower efficiency	-	0.80	Ferrer et al., 2015
	P_1	Blower absolute inlet pressure	atm	1	Judd and Judd, 2006; Verrecht et al., 2010

	P_2	Blower absolute impulsion pressure	atm	1.58	Judd and Judd, 2006; Verrecht et al., 2010
	α	Adiabatic coefficient (20ºC)	-	1.32	Metcalf & Eddy, 2014
	UC_{El}	Unit cost of electricity	€ kWh^{-1}	0.1149	Eurostat, 2019
	OC_{AnMBR}	Operating costs AnMBR (including labour, maintenance and chemical reagents)	€ m^{-3}_{WW}	0.06	Vinardell et al., 2020
Degassing membrane (DM)	E_{DM}	Degassing membrane energy consumption	kWh m^{-3}	0.01	Cookney et al., 2016; Crone et al., 2016
	$DM_{Replacement}$	Degassing membrane replacement cost	€ y^{-1}	[b]	Calculation
	UC_{El}	Unit cost of electricity	€ kWh^{-1}	0.1149	Eurostat, 2019
Phosphorus precipitation	Q	Sewage flow rate	m^3 d^{-1}	100,000	Assumption
	E_{TK}	Thickener energy consumption	kWh m^{-3}	0.02	Taboada-Santos et al., 2020
	E_{CG}	Centrifuge energy consumption	kWh m^{-3}	0.03	Taboada-Santos et al., 2020
	UC_{El}	Unit cost of electricity	€ kWh^{-1}	0.1149	Eurostat, 2019
	TSS_{PP}	Suspended solids load (Phosphorus precipitation sludge)	kg TSS d^{-1}	1254-15056	Calculation
	$k_{Poly,sludge}$	Polyelectrolyte dose	kg Poly kg^{-1} TSS	0.006	Pretel et al., 2014
	UC_{Poly}	Unit cost polyelectrolyte	€ kg^{-1} Poly	2.35	Pretel et al., 2015
	$UC_{Disposal}$	Unit cost land application/disposal	€ kg^{-1} TSS	0.0048/0.043[d]	Pretel et al., 2015; Verrecht et al., 2010
	L_P	Phosphorus load	kg P d^{-1}	174-2093	Calculation
	M_P	Molar mass phosphorus	kg $kmol^{-1}$	30.98	Metcalf & Eddy, 2014
	M_{FeCl3}	Molar mass ferric chloride	kg $kmol^{-1}$	162.20	Metcalf & Eddy, 2014
	UC_{FeCl3}	Unit cost ferric chloride	€ kg^{-1} $FeCl_3$	0.22	Taboada-Santos et al., 2020
PN-Anammox	E_{PN-AMX}	PN-Anammox energy consumption	kWh kg^{-1}N	5	Schaubroeck et al., 2015
	L_N	Nitrogen load	kg N d^{-1}	645-7742	Calculation
	x_N	Removal efficiency	-	0.81	Dai et al., 2015; Schaubroeck et al., 2015
	UC_{El}	Unit cost electricity	€ kWh^{-1}	0.1149	Eurostat, 2019
	$UF_{Replacement}$	Ultrafiltration membrane replacement cost	€ y^{-1}	[c]	Calculation
Sludge line	Q	Sewage flow rate	m^3 d^{-1}	100,000	Assumption

	E_{TK}	Thickener energy consumption	kWh m^{-3}	0.02	Taboada-Santos et al., 2020
	E_{CG}	Centrifuge energy consumption	kWh m^{-3}	0.03	Taboada-Santos et al., 2020
	E_{MIX}	Anaerobic digester mixing energy consuption	kWh $m^{-3}_{Digester}$	0.007	Appels et al., 2008
	VS_I	Volatile solids load	kg VS d^{-1}	1691-41122	Calculation
	VSLR	Volatile solids loading rate	kg VS m^3 d^{-1}	1.6	Andreoli et al., 2007
	UC_{EL}	Unit cost electricity	€ kWh^{-1}	0.1149	Eurostat, 2019
	TSS_{SL}	Suspended solids load (mixed primary and secondary sludge)	kg TSS d^{-1}	2337-24144	Calculation
	$k_{Poly,sludge}$	Polyelectrolyte dose	kg Poly kg^{-1} TSS	0.006	Pretel et al., 2014
	$UC_{Poly,sludge}$	Unit cost polyelectrolyte	€ kg^{-1} Poly	2.35	Pretel et al., 2015
	$UC_{Disposal}$	Unit cost land application/disposal	€ kg^{-1} TSS	0.0048/0.043[d]	Pretel et al., 2015; Verrecht et al., 2010
Benefits	**Parameter**	**Description**	**Units**	**Value**	**Reference[f]**
Electricity production	Q_{CH4}	Methane flow rate (0 ºC, 1 atm)	m^3 d^{-1}	1237-30799	Calculation
	LHV	Methane low heating value (0 ºC, 1 atm)	kJ m^{-3}	38846	Metcalf & Eddy, 2014
	η_{El}	Electrical efficiency CHP unit	-	0.33	Pöschl et al., 2010; Metcalf & Eddy, 2014
	UC_{El}	Unit cost of electricity	€ kWh^{-1}	0.1149	Eurostat, 2019
Biological model equations	**Parameter**	**Description**	**Units**	**Value**	**Reference[f]**
MLSS concentration (AnMBR)	SRT	Solids retention time	d	60	Cashman et al., 2018
	HRT	Hydraulic retention time	d	1	Hu and Stuckey, 2007
	X_I	Influent inert solids	mg TSS L^{-1}	7-241	Calculation
	f_D	Decay coefficient	mg TSS mg^{-1} TSS	0.2	Smith et al., 2014
	b_H	Decay rate	d^{-1}	0.02	Smith et al., 2014
	Y_T	Yield	mg TSS mg^{-1} COD	0.076	Smith et al., 2014
	$S_{S,0}$	Influent biodegradable organic matter	mg COD L^{-1}	50-912	Calculation
	S_S	Effluent biodegradable organic matter	mg COD L^{-1}	[e]	Assumption
Sludge production (AnMBR)	Q	Sewage flow rate	m^3 d^{-1}	100000	Assumption
	X_I	Influent inert solids	mg TSS L^{-1}	7-241	Calculation

	f_0	Decay coefficient	mg TSS mg^{-1} TSS	0.2	Smith et al., 2014
	b_H	Decay rate	d^{-1}	0.02	Smith et al., 2014
	Y_T	Biomass Yield	mg TSS mg^{-1} COD	0.076	Smith et al., 2014
	$S_{S,0}$	Influent biodegradable organic matter	mg COD L^{-1}	50-912	Calculation
	S_S	Effluent biodegradable organic matter	mg COD L^{-1}	[e]	Assumption
Sludge production (PN-AMX)	L_N	Nitrogen load	kg N d^{-1}	645-7742	Calculation
	$f_{N,AOB}$	Fraction of influent nitrogen undergoing partial nitritation	-	0.565	Cogert et al., 2019
	Y_{AOB}	Biomass yield of AOB	g VSS g^{-1} N	0.12	Cogert et al., 2019
	$f_{N,AMX}$	Fraction of influent nitrogen undergoing anammox	-	0.435	Cogert et al., 2019
	Y_{AMX}	Biomass yield anammox bacteria	kg VSS kg^{-1} N	0.13	Cogert et al., 2019
Dissolved methane	**Parameter**	**Description**	**Units**	**Value**	**Reference[f]**
Permeate dissolved methane	P_{CH4}	Partial pressure of methane	atm	0.75	Calculation
	$K_{H,CH4}$	Henry constant of methane	mol atm^{-1} kg^{-1}	0.00148	Calculation
	M_{CH4}	Molar mass methane	g mol^{-1}	16	Metcalf & Eddy, 2014
	OS	Oversaturation	-	1	Assumption

[a] The AnMBR equipment included: anaerobic reactor and membrane tank construction, membranes, gas blowers, influent pump, permeate pump, biomass recirculation pump, pipes and stirrer.

[b] The degassing membrane replacement cost was calculated considering that membrane was replaced twice along the plant lifetime.

[c] The ultrafiltration membrane replacement cost was calculated considering that membrane was replaced once along the plant lifetime.

[d] Land application/disposal.

[e] It is considered that all biodegradable COD feeding the AnMBR is removed.

[f] References that do not appear in the manuscript.

Appels, L. et al. 2008. Principles and potential of the anaerobic digestion of waste-activated sludge. Prog. Energy Combust. Sci. 34, 755–781.
Astals, S. et al. 2019. Post treatment of effluents from anaerobic digestion of organic fraction of municipal solid waste. In: Post Treatments of Anaerobically Treated Effluents. IWA Publishing. London.
Brepols, C. et al. 2010. Considerations on the design and financial feasibility of full-scale membrane bioreactors for municipal applications. Water Sci. Technol. 61, 2461–8.
Cashman, S. et al. 2018. Energy and greenhouse gas life cycle assessment and cost analysis of aerobic and anaerobic membrane bioreactor systems: Influence of scale, population density, climate, and methane recovery. Bioresour. Technol. 254, 56–66.
Crone, B.C. et al. 2016. Significance of dissolved methane in effluents of anaerobically treated low strength wastewater and potential for recovery as an energy product: A review. Water Res. 104, 520–531.
DeCarolis. et al. 2007. Evaluation of Newly Developed Membrane Bioreactors for Wastewater Reclamation. Proc. Water Environ. Fed.
ECB, 2020. https://www.ecb.europa.eu/stats/policy_and_exchange_rates/euro_reference_exchange_rates/html/eurofxref-graph-usd.en.html (accessed 28 February of 2020)
Eurostat, 2019. Electricity price statistics. https://ec.europa.eu/eurostat/statistics-explained/index.php/Electricity_price_statistics (accessed 30 September of 2019).
Hu, A.Y., Stuckey, D.C., 2007. Activated Carbon Addition to a Submerged Anaerobic Membrane Bioreactor: Effect on Performance, Transmembrane Pressure, and Flux. J. Environ. Eng. 133, 73–80.
Judd, S., Judd, C., 2006. The MBR book: principles and applications of membrane bioreactors for water and wastewater treatment. Elsevier, Oxford.
Pöschl, M. et al. 2010. Evaluation of energy efficiency of various biogas production and utilization pathways. Appl. Energy 87, 3305–3321.
Pretel, R. et al. 2014. The operating cost of an anaerobic membrane bioreactor (AnMBR) treating sulphate-rich urban wastewater. Sep. Purif. Technol. 126, 30-38.
Verrecht, B. et al. 2010. The cost of a large-scale hollow fibre MBR. Water Res. 44, 5274–5283.
Wan, C.F., Chung, T.S., 2018. Techno-economic evaluation of various RO+PRO and RO+FO integrated processes. Appl. Energy 212, 1038–1050.

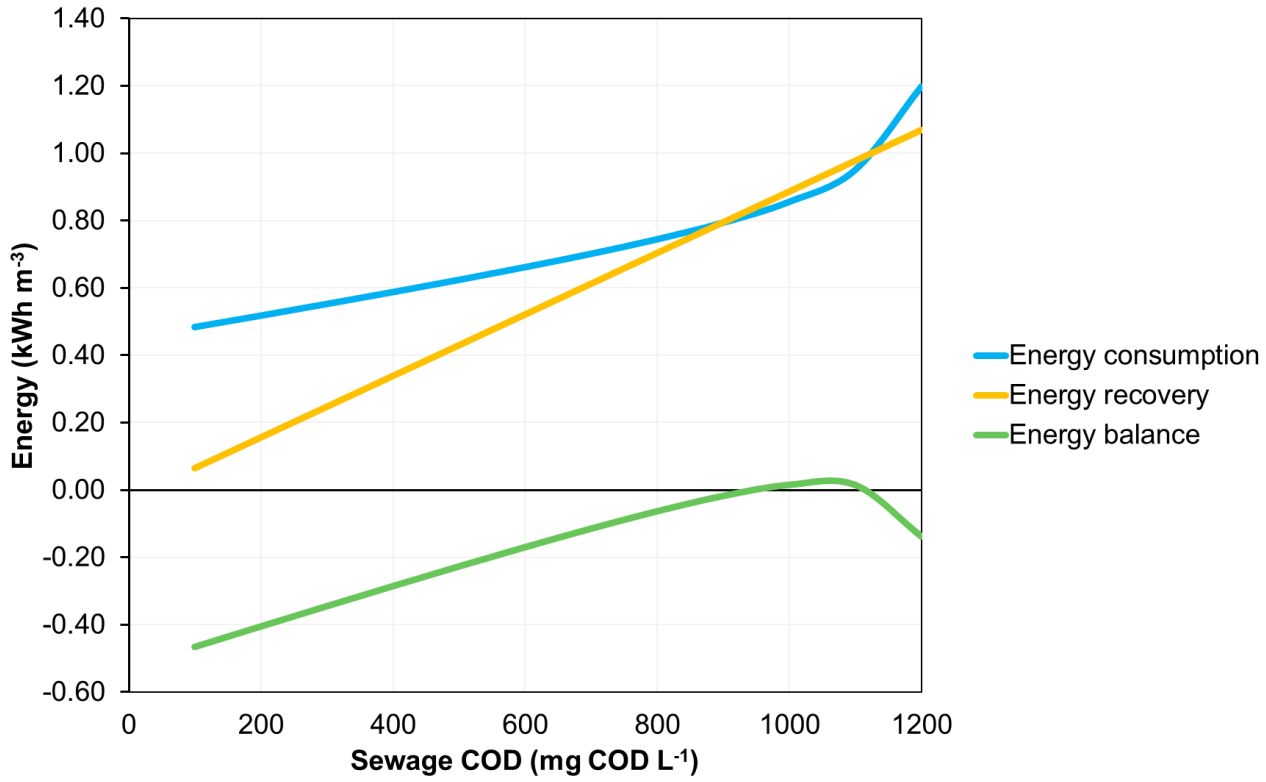

Figure S1. Energy balance of Scenario 3 for different sewage COD concentrations (COD:SO_4^{2-}-S=57; COD:N= 12.5; COD:P=51).

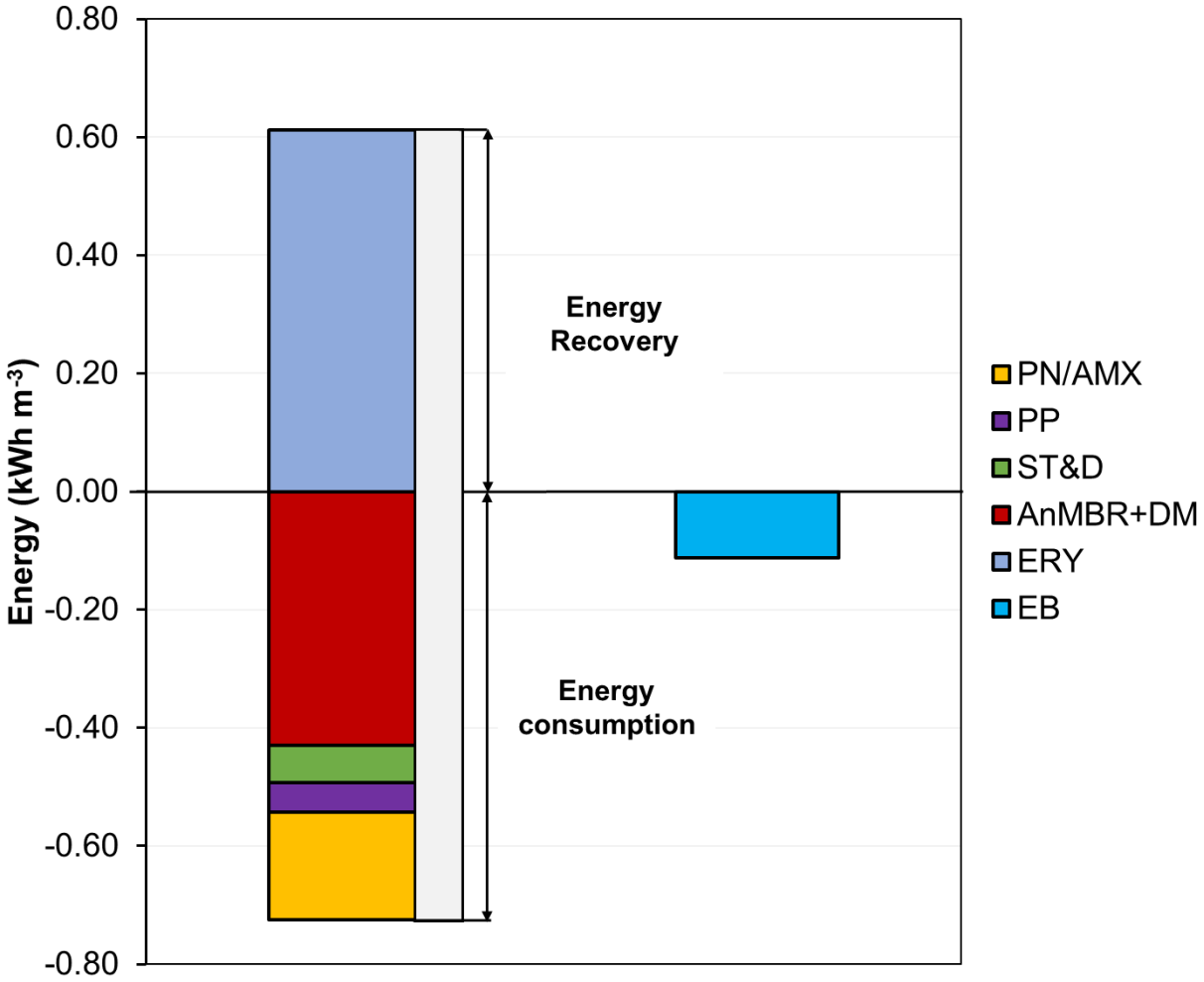

Figure S2. Energy distribution of Scenario 3 for an influent COD concentration of 700 mg COD L^{-1} (COD:SO_4^{2-}-S=57; COD:N= 12.5; COD:P=51). (left) Energy recovery and energy consumption. (right) (Energy balance. EB: Energy balance; ERY: Energy recovery; PN/AMX: Partial nitritation-anammox; SR: Struvite reactor; ST&D: Sludge treatment and disposal; AnMBR+DM: Anaerobic membrane bioreactor and degassing membrane).

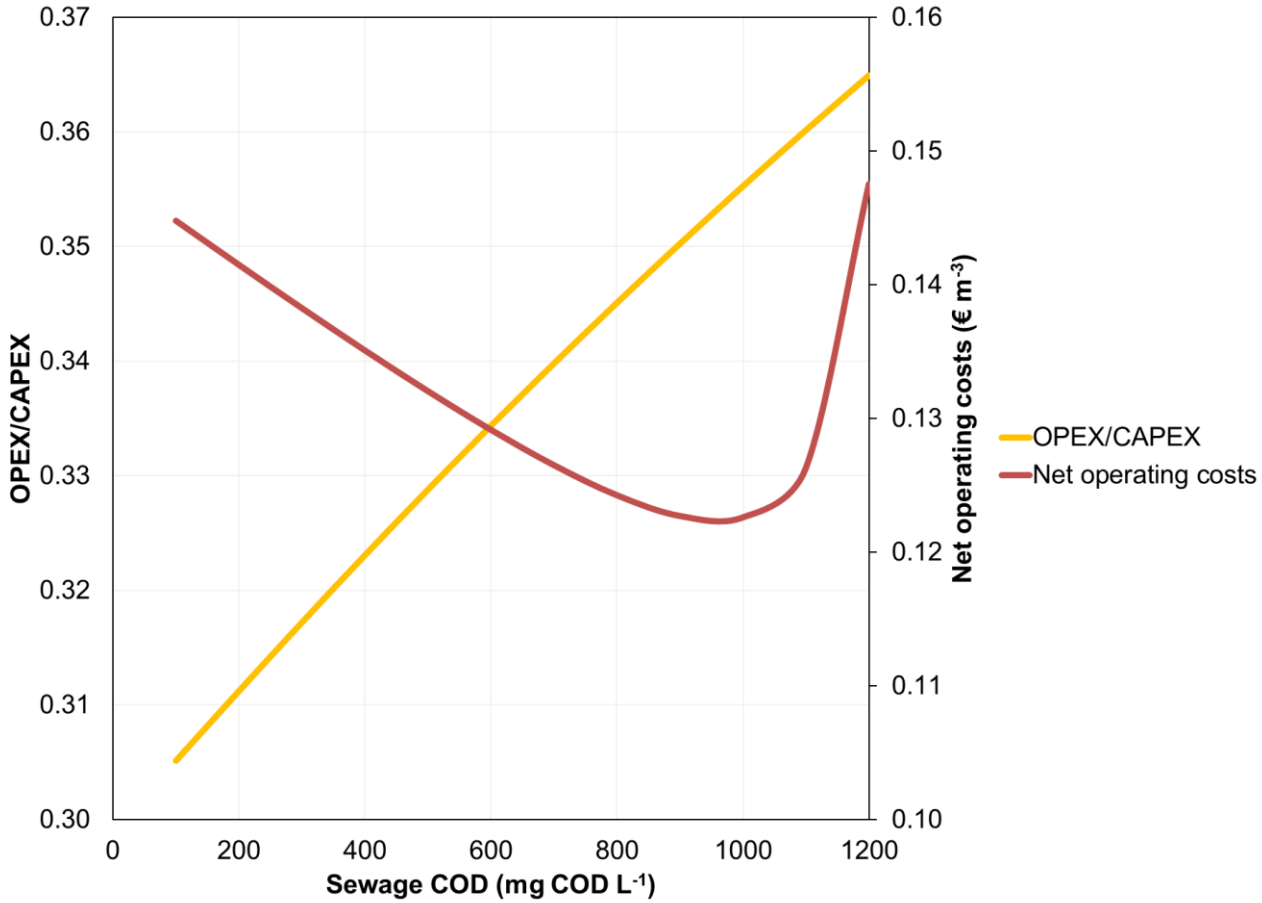

Figure S3. Net operating costs and OPEX to CAPEX relationship of Scenario 3 for different sewage COD concentrations (COD:SO_4^{2-}-S=57; COD:N= 12.5; COD:P=51).

3.4 Publication VII: Co-digestion of sewage sludge and food waste in a wastewater treatment plant based on mainstream anaerobic membrane bioreactor technology: A techno-economic evaluation

Vinardell, S., Astals, S., Koch, K., Mata-Alvarez, J., Dosta, J. (2021). Co-digestion of sewage sludge and food waste in a wastewater treatment plant based on mainstream anaerobic membrane bioreactor technology: A techno-economic evaluation. Bioresour. Technol. 330, 124978. https://doi.org/10.1016/j.biortech.2021.124978

Bioresource Technology 330 (2021) 124978

Contents lists available at ScienceDirect

Bioresource Technology

journal homepage: www.elsevier.com/locate/biortech

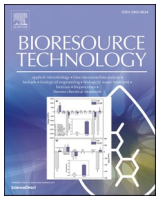

Co-digestion of sewage sludge and food waste in a wastewater treatment plant based on mainstream anaerobic membrane bioreactor technology: A techno-economic evaluation

Sergi Vinardell [a,*], Sergi Astals [a], Konrad Koch [b], Joan Mata-Alvarez [a], Joan Dosta [a]

[a] Department of Chemical Engineering and Analytical Chemistry, University of Barcelona, 08028 Barcelona, Spain
[b] Chair of Urban Water Systems Engineering, Technical University of Munich, 85748 Garching, Germany

HIGHLIGHTS

- The economic feasibility to co-digest sewage sludge and food waste was evaluated.
- The higher electricity revenue offsets the higher cost in co-digestion scenarios.
- Treating nutrient backloads in the sidestream was costlier than in the mainstream.
- Biosolids disposal cost was the most important gross cost contributor.
- Food waste gate fee had a noticeable impact on co-digestion economic feasibility.

ARTICLE INFO

Keywords:
Anaerobic digestion
Anaerobic co-digestion
Anaerobic membrane bioreactor (AnMBR)
Food waste
Techno-economic analysis

ABSTRACT

The implementation of anaerobic membrane bioreactor as mainstream technology would reduce the load of sidestream anaerobic digesters. This research evaluated the techno-economic implications of co-digesting sewage sludge and food waste in such wastewater treatment plants to optimise the usage of the sludge line infrastructure. Three organic loading rates (1.0, 1.5 and 2.0 kg VS m^{-3} d^{-1}) and different strategies to manage the additional nutrients backload were considered. Results showed that the higher electricity revenue from co-digesting food waste offsets the additional costs of food waste acceptance infrastructure and biosolids disposal. However, the higher electricity revenue did not offset the additional costs when the nutrients backload was treated in the sidestream (partial-nitritation/anammox and struvite precipitation). Biosolids disposal was identified as the most important gross cost contributor in all the scenarios. Finally, a sensitivity analysis showed that food waste gate fee had a noticeable influence on co-digestion economic feasibility.

1. Introduction

Wastewater treatment plants (WWTPs) are essential facilities in our society. Aerobic-based technologies, which are widely used in WWTPs, have successfully improved worldwide sanitation for more than a century (Van Loosdrecht and Brdjanovic, 2014). However, these technologies are not suitable in the current context of climate change and resource depletion as they fail to recover the resources contained in municipal sewage (Akyol et al., 2020). Pursuing sustainable technologies able to valorise these resources is required to promote the circular economy in WWTPs (Guest et al., 2009).

At present, anaerobic digestion is widely used to transform the organic matter contained in sewage sludge into biogas (Foladori et al., 2015). However, the development of technologies able to provide an effective retention of the slow growing anaerobic microorganisms at ambient temperature has broadened the applicability of anaerobic digestion to the mainstream of the WWTP (Akyol et al., 2020; Stazi and Tomei, 2018). Anaerobic membrane bioreactor (AnMBR) is an emerging technology for municipal sewage treatment where the membrane provides an excellent retention of the anaerobic microorganisms in the bioreactor while providing a high-quality effluent suitable for reuse (Vinardell et al., 2020).

The transition from aerobic-WWTPs to AnMBR-WWTPs is challenging since most aerobic-WWTPs are already constructed and under

* Corresponding author.
E-mail address: svinardell@ub.edu (S. Vinardell).

https://doi.org/10.1016/j.biortech.2021.124978
Received 25 January 2021; Received in revised form 7 March 2021; Accepted 8 March 2021
Available online 14 March 2021

operation. However, existing facilities are ageing, which makes it necessary to retrofit WWTPs to meet the stricter discharge requirements and achieve a cost-effective long-term operation (Garrido-Baserba et al., 2018; Tian et al., 2020). Infrastructure retrofit could allow reducing the initial investment and land use in comparison with a newly constructed AnMBR-WWTP. Understanding the main implications of retrofitting an existing WWTP to implement mainstream AnMBR is important to make an efficient use of the different process units in the retrofitted plant.

A lower sludge production is one of the main implications of implementing mainstream AnMBR technology in a WWTP. This is because the biomass yield of anaerobic microorganisms (ca. 0.10 $gCOD_x/gCOD_s$) is significantly lower than the biomass yield of aerobic microorganisms (ca. 0.60 $gCOD_x/gCOD_s$) (Henze et al., 2008; Stazi and Tomei, 2018). Accordingly, the organic loading rates (OLR) of the sidestream anaerobic digester (AD) would be reduced after retrofitting the aerobic-WWTP to an AnMBR-WWTP. This would result in a lower biogas production and a poor operation of the existing sludge line infrastructure. Therefore, it is important to look for strategies to increase biogas production and take full advantage of the existing infrastructure in the retrofitted AnMBR-WWTP.

Anaerobic co-digestion (AcoD) is a strategy to increase biogas production of the sidestream AD in the retrofitted AnMBR-WWTP (Nghiem et al., 2017; Vinardell et al., 2021). AcoD consists of the combined digestion of sewage sludge with one or more co-substrates to increase biogas production (Macintosh et al., 2019; Mata-Alvarez et al., 2014). Food waste is the most used co-substrate in WWTP full-scale applications due to its easy accessibility and relatively high methane yield (Nghiem et al., 2017). The high biodegradability of food waste allows increasing the biogas production with a minor increase in the amount of biosolids to be managed (Capson-Tojo et al., 2016; Nghiem et al., 2017). Accordingly, AcoD of sewage sludge and food waste has the potential to increase the profitability of the AnMBR-WWTP.

The economic and technical feasibility of food waste AcoD cannot be limited to its capacity to increase biogas and power production since AcoD has a plant-wide impact on the WWTP (Aichinger et al., 2015; Macintosh et al., 2019). In the sludge line, the higher amount of biosolids would increase the consumption of polyelectrolyte and the biosolids management cost (Aichinger et al., 2015). In the mainstream, the higher nutrients concentration in the backload due to AcoD increases the consumption of energy and chemicals for their removal (Sembera et al., 2019). Moreover, food waste AcoD involves the implementation of a new installation for food waste acceptance and processing, as well as the negotiation of a gate or delivery fee for food waste (Nghiem et al., 2017; Sembera et al., 2019). The economic evaluation of sewage sludge and food waste AcoD needs to consider all these factors to have a reliable estimation of the costs associated with the implementation of AcoD.

Some studies have analysed the economic feasibility of co-digesting sewage sludge and food waste in a WWTP (Morelli et al., 2020; Sembera et al., 2019). However, an economic analysis evaluating the co-digestion of sewage sludge and food waste in the sidestream AD of a future AnMBR-WWTP has not yet been analysed. Evaluating the economic drivers and constraints of implementing AcoD strategies in a retrofitted AnMBR-WWTP is important to better understand the impact that the implementation of mainstream AnMBR has on sludge line and on the sidestream AD biogas production.

This theoretical study aims to analyse the techno-economic feasibility of implementing sewage sludge and food waste AcoD in the sludge line of a retrofitted AnMBR-WWTP. To this end, different factors influencing the economics of AcoD were considered such as biogas production, nutrients backload, combined heat and power (CHP) unit upgrading, polyelectrolyte consumption, dewatering energy consumption, biosolids management, food waste acceptance installation and food waste gate/delivery fee.

2. Methodology

2.1. Scenarios definition

Fig. 1 shows the different scenarios evaluated in this study. A high-sized WWTP with a population equivalent (PE) capacity of 500,000 PE (100,000 $m^3\ d^{-1}$) was considered in this economic evaluation. The four scenarios evaluated in the present study are described below:

- Baseline Scenario represented the WWTP before retrofitting (Fig. 1A). The sewage sludge consisted of a mixture of primary and secondary sludge. The secondary sludge was produced in an activated sludge (AS) process using a modified Ludzack-Ettinger configuration (see supplementary material). The thickened sewage sludge (50% primary sludge and 50% secondary sludge on VS basis) was treated in a sidestream AD working at an OLR of 1.0 kg VS $m^{-3}\ d^{-1}$. The biogas produced in the sidestream AD was combusted in a CHP unit. The digestate was dewatered with a centrifuge before its final disposal.
- Scenario 1 was the retrofitted AnMBR-WWTP without implementing AcoD in the sidestream AD (Fig. 1A). In this scenario, the AS from the Baseline Scenario was retrofitted to an AnMBR and partial nitritation-anammox (PN/Anammox) processes for the removal of organic matter and nitrogen, respectively (see supplementary material). The AnMBR was a two-stage system where the membrane was submerged in a separated membrane tank. The AnMBR was considered to be operated at an HRT and SRT of 1 and 60 days, respectively (Vinardell et al., 2021). The sewage sludge was a mixture of primary and secondary sludge. The secondary sludge consisted of the wasted sludge from the mainstream AnMBR and excess sludge from PN/Anammox. In Scenario 1, no additional equipment nor equipment upgrading was needed for the sludge line since the existing infrastructure was oversized due to the lower amount of sludge produced in the AnMBR and PN/Anammox processes in comparison with the AS process. Therefore, Scenario 1 had the same sludge line infrastructure than the Baseline Scenario (Fig. 1A). In this scenario, the OLR of the sidestream AD was 0.63 kg VS $m^{-3}\ d^{-1}$ considering (i) the amount of primary and secondary sludge produced and (ii) the volume of the exiting sidestream AD.
- Scenario 2 was the retrofitted AnMBR-WWTP with AcoD of sewage sludge and food waste in the sidestream AD (Fig. 1B). In Scenario 2, new infrastructure for food waste acceptance was necessary and the CHP unit was upgraded to adapt the existing infrastructure to the higher biogas production. In this scenario, three AcoD alternatives were evaluated based on the total OLR ($OLR_{sludge} + OLR_{food\ waste}$) of the sidestream AD: (A) 1.0 kg VS $m^{-3}\ d^{-1}$, (B) 1.5 kg VS $m^{-3}\ d^{-1}$ and (C) 2.0 kg VS $m^{-3}\ d^{-1}$. Considering that the sludge OLR was 0.63 kg VS $m^{-3}\ d^{-1}$, the OLR provided by the food waste was 0.37, 0.87 and 1.37 kg VS $m^{-3}\ d^{-1}$, respectively. The OLR range was chosen based on the OLR of full-scale digesters at WWTPs co-digesting sewage sludge and food waste (Aichinger et al., 2015; Koch et al., 2016; Macintosh et al., 2019). The first alternative (1.0 kg VS $m^{-3}\ d^{-1}$) only added the amount of food waste needed to compensate the VS load reduced by the AnMBR.
- Scenario 3 was an extension of Scenario 2 and included nutrients treatment of the centrate in the sidestream (Fig. 1C). Specifically, PN-Anammox and struvite crystallisation were used to reduce the impact of nutrients backload on the mainstream of the WWTP (Caffaz et al., 2008; Rodriguez-Garcia et al., 2014). Struvite crystallisation was placed after PN/Anammox process since this configuration reduces the sodium hydroxide requirements for struvite crystallisation as a result of the alkalinity consumption in the previous PN/Anammox process (Campos et al., 2017). In Scenario 3, the same three OLRs of Scenario 2 were evaluated: (A) 1.0 kg VS $m^{-3}\ d^{-1}$, (B) 1.5 kg VS $m^{-3}\ d^{-1}$ and (C) 2.0 kg VS $m^{-3}\ d^{-1}$.

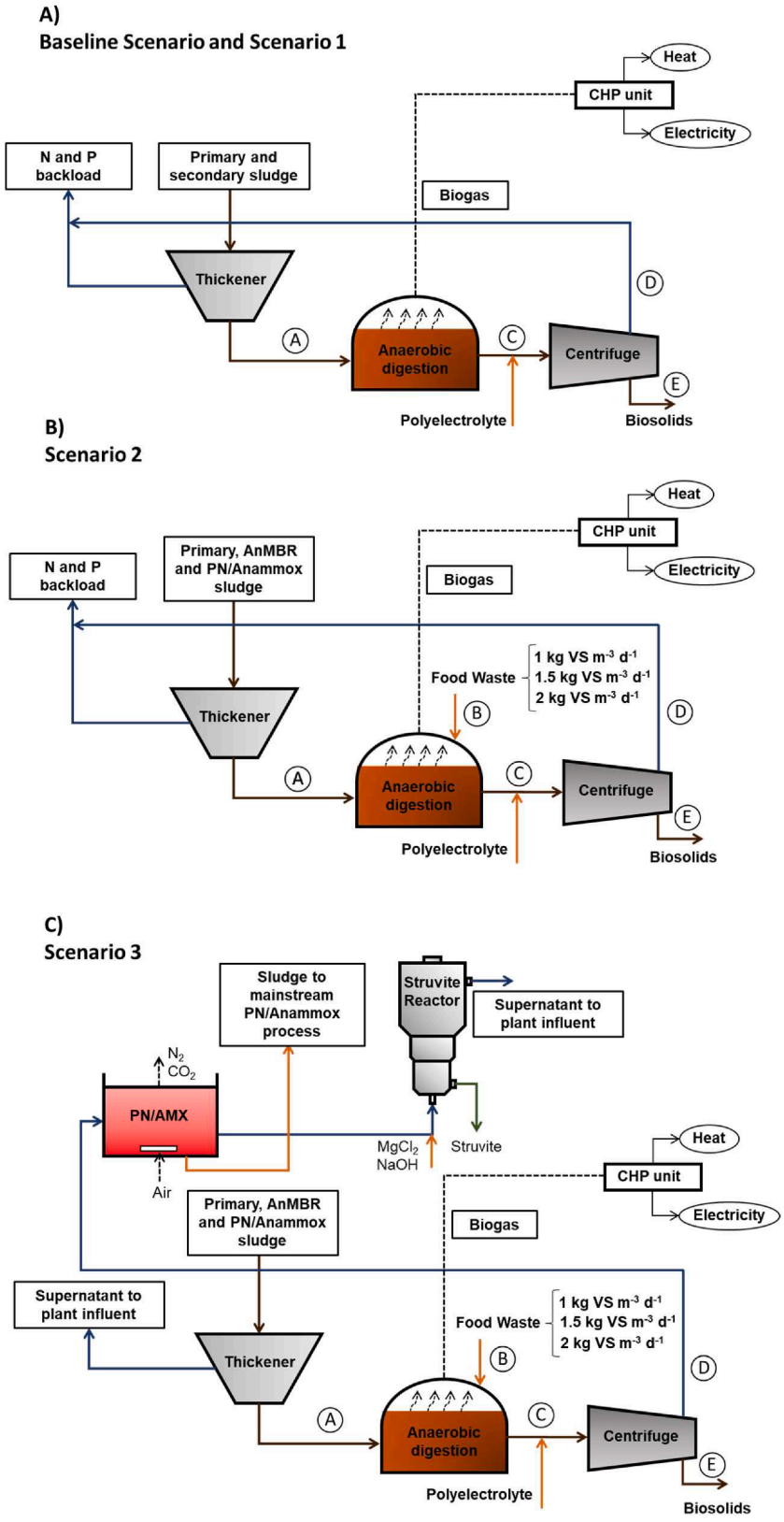

Fig. 1. Schematic representation of the different scenarios under study. (top) Baseline Scenario (aerobic-WWTP) and Scenario 1 (AnMBR-WWTP without AcoD); (middle) Scenario 2 (AnMBR-WWTP including food waste AcoD); (bottom) Scenario 3 (AnMBR-WWTP with food waste AcoD and sidestream nutrients backload treatment).

2.2. Sludge and food waste production and characterisation

The sludge production for the different scenarios was calculated considering a municipal sewage with a chemical oxygen demand (COD) concentration of 700 mg COD L^{-1} and 56 mg N L^{-1}, respectively (Henze et al., 2008). The COD content of sewage, before primary settling, was fractioned in biodegradable soluble COD (36%), biodegradable particulate COD (40%), inert soluble COD (4%) and inert particulate COD (20%) (Henze et al., 2008).

The sludge production of the aerobic-WWTP (before retrofitting) was calculated to obtain the capacity of the existing sludge line infrastructure. The primary sludge production was calculated assuming that 67% of the particulate COD was separated in the primary settler. This means that 40% of the total sewage COD was separated in the primary settler (Henze et al., 2008). The secondary sludge production of the aerobic-WWTP was calculated through steady-state equations considering the growth rate of autotrophic nitrifiers, heterotrophic denitrifiers and heterotrophic oxidisers (see supplementary material). The thickened sewage sludge consisted of a total solids (TS) concentration of 3.5% (Astals et al., 2013). Sewage sludge composition was obtained as the average of the seven different sewage sludges reported by Astals et al. (2013).

In the retrofitted AnMBR-WWTP, the sewage sludge production was lower than in the aerobic-WWTP. The sludge produced in the AnMBR and PN/Anammox processes was calculated through steady-state equations (see supplementary material). The sewage sludge was mixed with food waste in Scenario 2 and Scenario 3. The amount of food waste added was calculated from the OLR of each alternative. The food waste had a TS concentration of 23.4% and a VS/TS ratio of 91.0%, which was obtained as the average of seven different food wastes reported in literature (see supplementary material).

2.3. Modelling AD performance

Model equations for a continuous stirred tank reactor (CSTR) at steady-state conditions were used to calculate the VS removal, methane yield and nutrients solubilisation in the sidestream AD. The model was applied for each substrate, namely, primary sludge, secondary sludge and food waste. The sewage sludge composition was used as representative for both primary and secondary sludge due to the limited data available in literature. No synergism was considered in the AcoD process. The model parameters (i.e. first-order kinetic constant and biodegradability) used for each substrate were obtained as the average of five different studies (see supplementary material).

The biodegradable VS concentration in the AD effluent was calculated by using a mass balance in VS (Eq. (1)), which considers that the degradation of VS over time follows a first-order kinetic (Garcia-Heras, 2003).

$$S_{eff,bio} = S_{0,bio} \cdot \frac{1}{1 + k \cdot HRT} \quad (1)$$

where $S_{eff,bio}$ is the biodegradable VS concentration in the AD effluent (g VS L^{-1}), $S_{0,bio}$ is the biodegradable VS concentration in the AD influent (g VS L^{-1}), k is the first-order kinetic constant (d^{-1}), and HRT is the hydraulic retention time (d).

The methane yield of a CSTR digester can be calculated at steady-state conditions by means of Eq. (2) as shown elsewhere (Garcia-Heras, 2003).

$$B = B_0 \cdot \frac{k \cdot HRT}{1 + k \cdot HRT} \quad (2)$$

where, besides the described above, B is the methane yield (mL CH_4 g^{-1} VS) and B_0 is the substrate ultimate methane yield (mL CH_4 g^{-1} VS).

Finally, the amount of NH_4^+-N and PO_4^{3-}-P in the AD effluent were calculated using Eq. (3) and Eq. (4), respectively. These equations consider that the release of nutrients is proportional to organic matter degradation.

$$N_{eff,NH_4^+} = N_{0,NH_4^+} N_{0,org} \cdot \frac{S_{0,bio} - S_{eff,bio}}{S} \quad (3)$$

$$P_{eff,PO_4^{3-}} = P_{0,PO_4^{3-}} + P_{0,org} \cdot \frac{S_{0,bio} - S_{eff,bio}}{S} \quad (4)$$

where $N^+_{eff,NH4}$ is the NH_4^+-N concentration in the AD effluent (g N L^{-1}), $N_{0,org}$ is the organic nitrogen concentration in the AD influent (g N L^{-1}), $N^+_{0,NH4}$ is the NH_4^+-N concentration in the AD influent (g N L^{-1}), $P_{eff,PO4}^{3-}$ is the PO_4^{3-}-P concentration in the AD effluent (g P L^{-1}), $P_{0,org}$ is the organic phosphorus concentration in the AD influent (g P L^{-1}), $P_{0,PO4}^{3-}$ is the PO_4^{3-}-P concentration in the AD influent (g P L^{-1}), $S_{eff,bio}$ is the biodegradable VS concentration in the AD effluent (g VS L^{-1}), $S_{0,bio}$ is the biodegradable VS concentration in the AD influent (g VS L^{-1}), and S is the total VS concentration in the AD influent (g VS L^{-1}). Organic matter and nutrient initial concentrations were calculated considering the flow of each substrate to the digester.

2.4. Costs and revenue calculation

The implementation of AcoD is expected to increase the revenue of the sidestream AD due to the higher biogas production. However, AcoD increases the capital and operating costs of the sludge line and the consumption of energy and chemical reagents in the mainstream to remove the nutrients backload. The most sensitive factors to AcoD were included in this economic evaluation. These factors were classified into four groups: (i) food waste acceptance, (ii) digestate dewatering and biosolids management, (iii) nutrients backload treatment and (iv) energy production. In this study, the costs and revenue that are not influenced by AcoD were not included since they are expected to be similar regardless of AcoD implementation (e.g. operation of the AS and AnMBR in the mainstream of the WWTP). The following subsections discuss the parameters and considerations used to calculate the costs and revenue for the different scenarios. The parameters used for cost and electricity revenue calculations can be found in the supplementary material.

2.4.1. Food waste acceptance

The use of food waste as co-substrate for AcoD requires the installation of a new infrastructure for food waste acceptance and processing as well as the negotiation of a gate/delivery fee for the co-substrate. These costs were obtained from the Grüneck WWTP (Germany), where co-digestion of sewage sludge and food waste is used since 2014. In this WWTP, the construction of the facility for food waste acceptance cost 150,000 € (Macintosh et al., 2019). The plant receives 2,100 t y^{-1} of food waste from a processing plant. The transportation cost from the processing plant to the Grüneck WWTP is paid by the WWTP at 3 € t^{-1} (Macintosh et al., 2019). However, the criteria to establish a gate/delivery fee is still unclear and differs depending on the WWTP and the food waste source (Sembera et al., 2019). In Section 3.3.4, the impact of gate/delivery fee on AcoD profitability was analysed through a sensitivity analysis.

2.4.2. Digestate dewatering and biosolids disposal

The digestate from the anaerobic digester was considered to be dewatered to 30% TS before its final disposal. Polyelectrolyte was dosed to improve sludge dewaterability and to achieve the final biosolids concentration. A polyelectrolyte dosage of 9 kg t^{-1} TS was considered (Aichinger et al., 2015). After polyelectrolyte dosage, the digestate was centrifuged at an energy consumption of 0.045 kWh kg^{-1} TSS (Pretel et al., 2014).

The biosolids were transported for its final disposal at 54 € t^{-1} TS, which represents the average cost in Europe for the transportation of dewatered digestate with a TS content of 30% (Foladori et al., 2015). The biosolids were used for agriculture at a cost of 93 € t^{-1} TS since land

Table 1
Main operation and flow data for the different scenarios under study.

			Baseline Scenario	Scenario 1	Scenario 2A	Scenario 2B	Scenario 2C	Scenario 3A	Scenario 3B	Scenario 3C
Description	WWTP configuration		Aerobic-WWTP	AnMBR-WWTP	AnMBR-WWTP	AnMBR-WWTP	AnMBR-WWTP	AnMBR-WWTP	AnMBR-WWTP	AnMBR-WWTP
	AcoD application		No	No	Yes	Yes	Yes	Yes	Yes	Yes
	OLR_{sludge} (kg VS m^{-3} d^{-1})		1.0	0.63	0.63	0.63	0.63	0.63	0.63	0.63
	$OLR_{food\ waste}$ (kg VS m^{-3} d^{-1})		–	–	0.37	0.87	1.37	0.37	0.87	1.37
	OLR_{total} (kg VS m^{-3} d^{-1})		1.0	0.63	1.0	1.5	2.0	1.0	1.5	2.0
	Nutrients backload treatment		Mainstream	Mainstream	Mainstream	Mainstream	Mainstream	Sidestream	Sidestream	Sidestream
Mass and volumetric flows[1]	(A) Sewage sludge	TS (%)	3.5	3.5	3.5	3.5	3.5	3.5	3.5	3.5
		VS/TS (%)	75	75	75	75	75	75	75	75
		Q (m^3 d^{-1})	1,192	746	746	746	746	746	746	746
	(B) Food waste	TS (%)	–	–	23.4	23.4	23.4	23.4	23.4	23.4
		VS/TS (%)	–	–	91	91	91	91	91	91
		Q (m^3 d^{-1})	–	–	57	133	208	57	133	208
	(C) Digestate	TS (%)	2.5	2.3	2.6	3.0	3.3	2.6	3.0	3.3
		VS/TS (%)	64	60	61	63	64	61	63	64
		Q (m^3 d^{-1})	1,175	733	781	845	908	781	845	908
	(D) Centrate	$F_{NH4\text{-}N}$ (kg NH_4^+-N d^{-1})	1,051	776	1,037	1,375	1,702	1,037	1,375	1,702
		$F_{PO4\text{-}P}$ (kg PO_4^{3-}-P d^{-1})	242	162	222	301	378	222	301	378
		Q (m^3 d^{-1})	1,077	678	714	761	807	714	761	807
	(E) Biosolids	TS (%)	30	30	30	30	30	30	30	30
		VS/TS (%)	64	60	61	63	64	61	63	64
		Q (m^3 d^{-1})	98	55	67	84	101	67	84	101
Chemicals	Polyelectrolyte consumption (kg d^{-1})		274	155	189	236	284	189	236	284
	$MgCl_2{\cdot}6H_2O$ consumption (kg d^{-1})		–	–	–	–	–	1,313	1,824	2,319
	NaOH consumption (kg d^{-1})		–	–	–	–	–	331	439	541
Energy	Methane yield (L CH_4 kg^{-1} VS)		268	324	343	353	358	343	353	358
	Methane production (m^3 d^{-1})		8,389	6,345	10,887	16,903	22,858	10,887	16,903	22,858
	Biogas production (t d^{-1})		17	13	22	34	46	22	34	46
	Electricity production (kWh d^{-1})		30,505	23,072	39,587	61,462	83,117	39,587	61,462	83,117
	Energy requirements sludge line (kWh d^{-1})		3,634	2,487	3,254	4,260	5,247	3,484	4,603	5,702

[1]The different flows (A, B, C, D and E) are illustrated in Fig. 1.

application is still the main management route in Europe (Foladori et al., 2015). Therefore, the total disposal cost (transport + disposal) was 147 € t^{-1} TS. Nevertheless, the cost of biosolids disposal largely depends on its final use (i.e. agriculture, landfill, composting or incineration) and country, which may have a big impact on total costs. In Section 3.3.1, the impact of biosolids disposal cost was analysed through a sensitivity analysis.

2.4.3. Nutrients backload treatment

Food waste contains a high content of organic nitrogen and phosphorus, which are partially solubilised into ammonium and phosphate during anaerobic digestion (Nghiem et al., 2017). Accordingly, food waste AcoD increases the concentration of these compounds in the centrate. In this study, two approaches were considered to remove the nutrients backload of the centrate: (i) mainstream nutrients treatment (Baseline Scenario, Scenario 1 and 2) and (ii) sidestream nutrients treatment by PN/Anammox and struvite crystallisation (Scenario 3).

2.4.3.1. Mainstream nutrients treatment. Energy consumption for nitrogen removal and ferric chloride ($FeCl_3$) consumption for phosphorus precipitation were considered to calculate the cost to remove the nutrients backload in the mainstream of the WWTP. A specific energy consumption for mainstream nitrogen removal of 2.38 kWh kg^{-1}N was used according to Horstmeyer et al. (2018). It was considered that nitrification/denitrification (Baseline Scenario) and mainstream PN/Anammox (Scenario 1, 2 and 3) processes had the same specific energy consumption since PN/Anammox is still not fully optimised for mainstream nitrogen removal (Schaubroeck et al., 2015). The amount of ferric chloride necessary to precipitate phosphate was estimated considering that 30 mg $FeCl_3$ L^{-1} are needed to decrease phosphate concentration from ~ 2.3 mg PO_4^{3-}-P L^{-1} to ~ 0.2 mg PO_4^{3-}-P L^{-1} (Taboada-Santos et al., 2020).

2.4.3.2. Sidestream nutrients treatment. The PN/Anammox process was also selected for sidestream nitrogen removal of the centrate since it is an autotrophic nitrogen removal process suitable to treat streams with a low COD/N ratio (Guo et al., 2020; Vázquez-Padín et al., 2009). The PN/Anammox process was designed to treat a nitrogen loading rate (NLR) of 0.42 kg N m^{-3} d^{-1} and achieved a nitrogen removal efficiency of 89%, which are average values from full-scale PN/Anammox processes (Lackner et al., 2014; Schaubroeck et al., 2015). The sludge produced in the sidestream PN/Anammox system was transferred to the mainstream system to enrich its anammox and ammonia oxidising bacteria biomass of the full-scale PN/Anammox (Schaubroeck et al., 2015; Wett et al., 2013). The capital cost for PN/Anammox was assumed to be 1,600 €/(kg N/day), between the 1,300 and 1,900 €/(kg N/day) reported in literature (Van Eekert et al., 2012; Vandekerckhove et al., 2020). This capital cost range was obtained by dividing the initial investment (€) by the nitrogen load (kg N/day) reported by Van Eekert et al. (2012) and Vandekerckhove et al. (2020). The PN/Anammox specific energy consumption was 1.5 kWh kg^{-1}N, which is a typical energy consumption for nitrogen removal of the centrate (Lackner et al., 2014; Schaubroeck et al., 2015). Finally, the total operating cost of the PN/Anammox process was calculated considering a unit cost of 0.8 € kg^{-1}N (Van Eekert et al., 2012; Vandekerckhove et al., 2020).

Struvite crystallisation was used to recover the phosphorus from the centrate since this is the most mature technology for phosphorus recovery (Bolzonella et al., 2006; Münch and Barr, 2001) and struvite ($MgNH_4PO_4{\cdot}6H_2O$) can be valorised as a slow release fertiliser (Peng et al., 2018). An average capital cost of 10,000 €/(kg P/day) was considered (Vaneeckhaute et al., 2017). Phosphate removal efficiencies of 90% were considered for the struvite reactor (Peng et al., 2018). The energy consumption for struvite crystallisation was 5.9 kWh kg^{-1}P, between the 2.2 and 10 kWh kg^{-1}P reported in literature (Ghosh et al., 2019). Magnesium chloride hexahydrate ($MgCl_2{\cdot}6H_2O$) was used for struvite crystallization at a unit cost of 370 € t^{-1} (Bouzas et al., 2019). The $MgCl_2{\cdot}6H_2O$ dosage was calculated with the stoichiometric relationship with phosphate and considering that the centrate contained 27.2 mg Mg^{2+} L^{-1} (Campos et al., 2017). Sodium hydroxide (NaOH) was dosed to increase the pH from 7.3 to 9.0, which is the optimum pH for struvite crystallisation (Peng et al., 2018). The previous PN/Anammox process allowed reducing the NaOH consumption in the struvite crystalliser since it already consumes alkalinity (i.e. HCO_3^- and NH_4^+). In this research, a molar HCO_3^-:NH_4^+ ratio of 1:1 in the centrate was considered (Campos et al., 2017). Subsequently, the NaOH consumption was calculated through acid-base equilibrium after subtracting the alkalinity consumed in the PN/Anammox process. The NaOH cost was 620 € t^{-1} (Bouzas et al., 2019). No revenue was considered from the struvite produced since this is still managed as a waste in many countries (Peng et al., 2018). In Section 3.3.3, the impact of struvite commercialisation was evaluated through a sensitivity analysis.

2.4.4. Energy production

An electrical efficiency of 33% for the CHP unit was considered, which represents the average electrical efficiency reported in literature (Riley et al., 2020; Vinardell et al., 2021). The methane yield of the sidestream AD for each scenario was used for the energy calculations (see Section 2.3 for further details on methane yield calculations). The higher methane production in AcoD scenarios makes it necessary to upgrade the existing CHP unit to utilise all the produced biogas (minimise biogas flaring) and increase the WWTP energy production. The capital cost to upgrade existing CHP unit was calculated considering a unit cost of 712 € kW_{el}^{-1} (Riley et al., 2020; Smith et al., 2014). The operating cost of the CHP unit was 0.0119 € kWh_{el}^{-1} (Riley et al., 2020; Smith et al., 2014). A lifetime of 20 years was considered for the CHP unit (Whiting and Azapagic, 2014). All methane volumetric flows are reported in standard temperature and pressure conditions (0 °C and 1 atm).

The electricity produced through cogeneration was considered to be sold at a price of 0.1149 € kWh^{-1} (Eurostat, 2019). However, the electricity price is very variable and can range between 0.06 and 0.18 € kWh^{-1} depending on the country or region (Eurostat, 2019). In Section 3.3.2, the impact of electricity price on process profitability was analysed through a sensitivity analysis.

2.5. Economic evaluation

Capital expenditures (CAPEX), operating expenditures (OPEX) and revenue were calculated to evaluate the economic feasibility of each scenario. The CAPEX was annualised by using Eq. (5), while the net cost was calculated as the difference between gross cost and revenue (Eq. (6)) (Bolzonella et al., 2018; Vinardell et al., 2021).

$$\text{Annualised CAPEX}\left(€\ y^{-1}\right) = \frac{i\cdot(1+i)^t}{(1+i)^t-1}\cdot\text{CAPEX} \quad (5)$$

$$\text{Net cost}\left(€\ y^{-1}\right) = \frac{i\cdot(1+i)^t}{(1+i)^t-1}\cdot\text{CAPEX} + \text{OPEX} - \text{R} \quad (6)$$

where CAPEX is the capital expenditures (€), R is the revenue (€ y^{-1}), OPEX is the operating expenditures (€ y^{-1}), i is the discount rate (5%) and t is the project lifetime (20 years). The electricity revenue from the sidestream AD was included in all sections since this is the main revenue obtained in all scenarios. The revenue from selling struvite was only considered in Section 3.3.3.

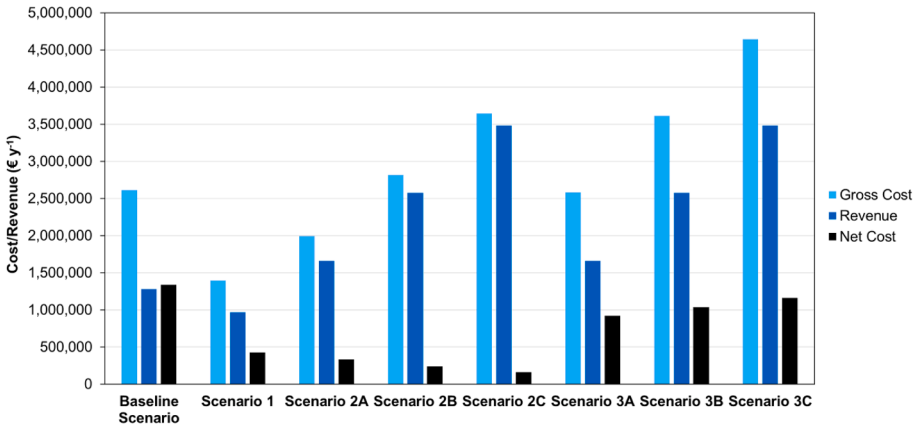

Fig. 2. Cost, revenue and net cost for the different scenarios under study.

3. Results and discussion

3.1. Economic feasibility of co-digesting sewage sludge and food waste in an AnMBR-WWTP

Table 1 shows a summary of the main operation data for each scenario, while Fig. 2 illustrates the gross cost, revenue and net cost for each scenario. The gross cost (light blue bar in Fig. 2) includes the capital and operating costs. The gross cost is mainly driven by the operating cost since the capital cost has a relatively low influence on gross cost (7–23%) because retrofitting the existing sludge line infrastructure allows reducing the initial investment in comparison with the construction of a new infrastructure. The Baseline Scenario is the worst scenario since it presents the highest net cost (1,336,000 € y^{-1}). This is mainly caused by the large amount of secondary sludge produced, which is characterised by its poor biodegradability (~37%) and methane yield (~200 mL CH_4 g^{-1} VS). Scenario 1 results show that retrofitting an aerobic-WWTP to an AnMBR-WWTP would reduce the net cost of the sludge line, primarily due to the lower secondary sludge production. The implementation of AcoD in the AnMBR-WWTP (Scenario 2 and 3) significantly increases the revenue from electricity production (dark blue bar in Fig. 2), which has a direct impact on the net cost (black bar in

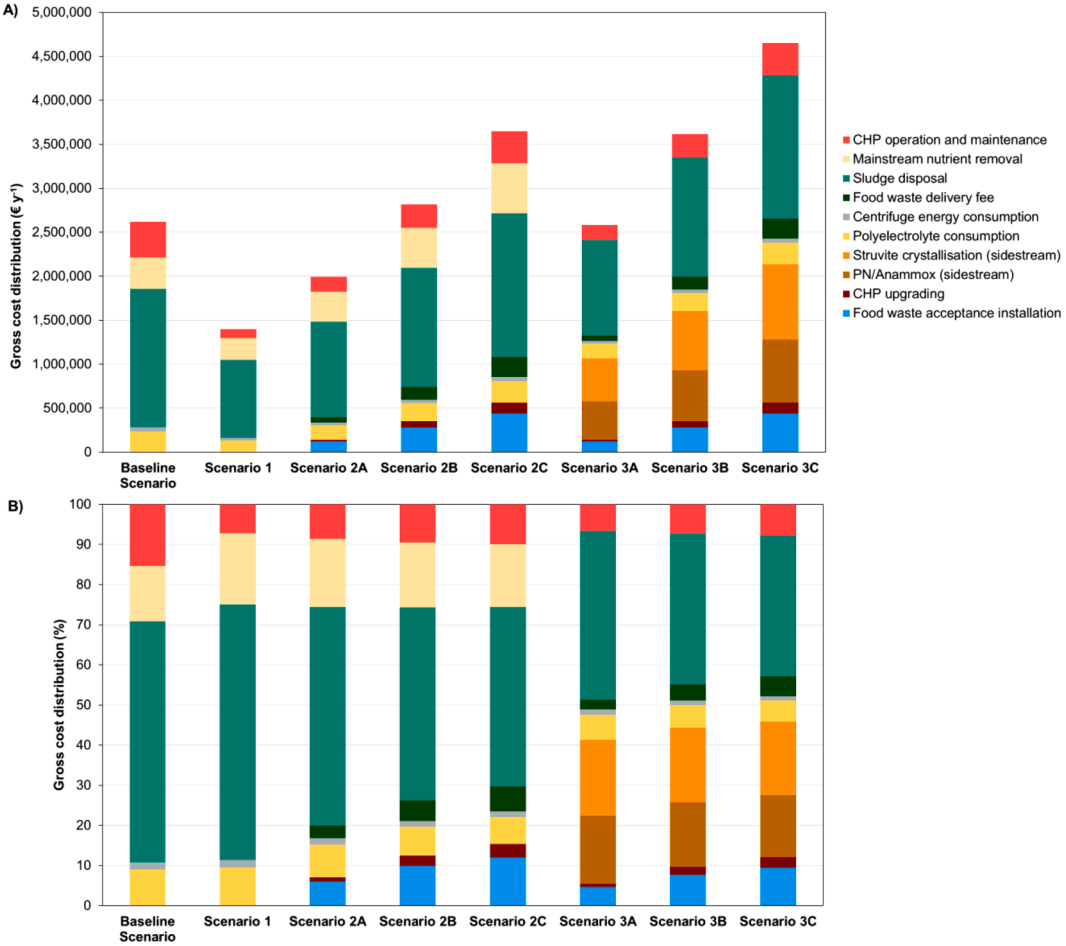

Fig. 3. Gross cost contribution for the different scenarios under study. (A) Absolute gross cost distribution (€ y^{-1}); (B) relative gross cost distribution (%).

Fig. 2). The electricity revenue from food waste co-digestion exceeds the underlying costs associated with food waste acceptance infrastructure and biosolids management/disposal. However, the higher electricity revenue did not offset the additional costs when the nutrients backload was treated in the sidestream (Scenario 3) rather than in the mainstream (Scenario 2).

Scenario 2, where food waste is co-digested with sewage sludge and the nutrients backload is treated in the mainstream, features the lowest net cost among the different scenarios. Scenario 2C is the most competitive alternative in Scenario 2 as a result of the higher biogas production (due to the higher OLR) in the sidestream AD. Specifically, the net cost decreased from 333,000 to 160,000 € y^{-1} as the OLR increased from 1.0 to 2.0 kgVS m^{-3} d^{-1}, respectively (Fig. 2). These results clearly show that the increased electricity production at higher OLRs improves the economic balance of Scenario 2. However, increasing the OLR of the sidestream AD would not always imply a better economic prospect since high OLRs could compromise: (i) the performance and stability of the AD due to overloading, (ii) the quality and stability of the biosolids and (iii) the capacity of the mainstream units to handle the nutrients backload (Mata-Alvarez et al., 2014; Usack et al., 2018; Xie et al., 2018). Therefore, a compromise solution considering the electricity revenue and the technical and environmental prospects of the WWTP is needed to maximise the profit from AcoD.

Scenario 3, where food waste is co-digested with sewage sludge and the nutrients backload is treated in the sidestream, features a net cost higher than Scenario 2. Unlike Scenario 2, the economic balance of Scenario 3 worsens as the OLR increases. Specifically, the net cost increased from 922,000 to 1,162,000 € y^{-1} as the OLR increased from 1 to 2 kg VS m^{-3} d^{-1}, respectively. In Scenario 3, the higher revenue from electricity production from food waste co-digestion does not offset the higher gross cost as the OLR increases. The higher gross cost of Scenario 3 is attributed to the implementation of PN/Anammox and struvite crystallisation for the removal of N and P from the centrate. The addition of food waste increases the content of N and P in the centrate, which has a direct impact on the capital and operating costs of both processes. It was estimated that the NH_4^+-N and PO_4^{3-}-P backload increased from 1,037 to 1,702 kg N d^{-1} and from 222 to 378 kg P d^{-1} as the OLR increased from 1 to 2 kg VS m^{-3} d^{-1}, respectively. These results suggest that treating the N and P in the sidestream is costlier than treating these compounds in the mainstream of the WWTP. However, the treatment of the extra N and P backload in the mainstream of the WWTP could make necessary to expand existing facilities with a direct impact on capital costs (out of the scope of the present study). Additionally, revenue from struvite crystallisation would have a noticeable influence on the economic balance of Scenario 3 as discussed in Section 3.3.3. Besides economic considerations, implementing N and P removal technologies in the sidestream of the WWTP (i) reduces disturbances in the mainstream biological nitrogen removal step (Sembera et al., 2019), (ii) prevents piping blockage because of uncontrolled and spontaneous struvite precipitation (Bouzas et al., 2019) and (iii) reduces the environmental impacts related to eutrophication if the mainstream does not have the spare capacity to handle the extra nutrients load (Rodriguez-Garcia et al., 2014).

3.2. Cost distribution for the different scenarios

Fig. 3 shows the gross cost distribution for the different scenarios under study. Biosolids disposal (including transport) is the most important cost contributor in all the scenarios. In absolute values, the biosolids disposal cost increases as the OLR increases due to the higher biosolids production at higher OLRs (Fig. 3A). However, in relative values, the disposal contribution to the gross cost decreases as the OLR increases in AcoD scenarios due to the presence of other cost contributors in the AcoD scenarios (Fig. 3B). It is worth mentioning that biosolids disposal cost does not increase linearly with the OLR since food waste digestion produces a relatively low amount of biosolids as a result of its high biodegradability (~85%).

Food waste AcoD implies the construction of a new facility for food waste acceptance. The capital cost to construct a food waste acceptance facility ranges between 4 and 12% in AcoD scenarios (Fig. 3B). The

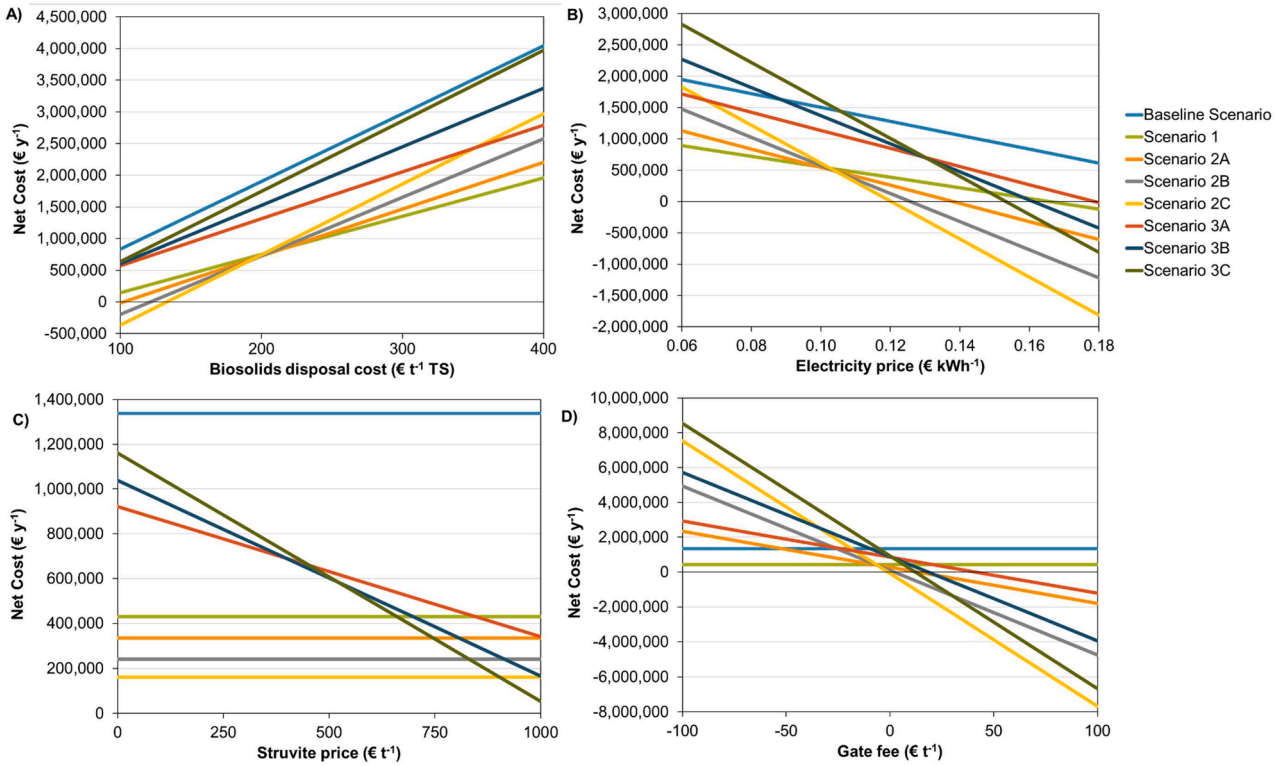

Fig. 4. Sensitivity analysis for: (A) biosolids disposal cost, (B) electricity price, (C) struvite price, and (D) gate fee.

contribution of the food waste acceptance facility increases as the OLR increases since larger amounts of food waste are needed at higher OLRs. Food waste AcoD also implies the negotiation of a gate/delivery fee for food waste acceptance. For a delivery fee of 3 € t^{-1}, the cost contribution of the food waste delivery fee ranges between 2 and 7% of the gross cost. This delivery fee represents the amount of money that the WWTP has to pay to obtain the food waste. However, some WWTPs obtain a revenue for the acceptance of the food waste (gate fee). For instance, Nghiem et al. (2017) reported a gate fee of 86 € t^{-1} for Rovereto WWTP (Italy). The difference between Grüneck and Rovereto could be attributed to the non-processed origin of food waste in the Rovereto WWTP (Sembera et al., 2019). The quality of the food waste received at the WWTP determines the need to implement a food waste processing infrastructure to remove impurities (e.g. glass, debris, metals and plastics) before feeding the food waste into the digester. However, the criteria to establish a gate/delivery fee by the WWTP is still unclear regardless of the food waste origin. Therefore, it is important to evaluate how the gate/delivery fee influences the net cost to better understand the role of this parameter in AcoD economics (see Section 3.3.4).

Treating the nutrients backload in the mainstream represents between 13 and 18% of the gross cost (Fig. 3B). This contribution is much lower than when the nutrients backload is treated in the sidestream of the WWTP, where the contribution represents 33–36% of the gross cost. These results support the idea that PN/Anammox and struvite crystallisation sidestream implementation is potentially costlier than treating the nutrients backload in the existing mainstream facility. However, in those WWTPs operating close to their design capacity, the implementation of nutrients backload treatment in the sidestream could be more economical than expanding the existing mainstream processes. In Scenario 3, the gross cost contribution of the sidestream nutrients backload treatment is close to the biosolids disposal contribution, which highlights the impact of sidestream PN/Anammox and struvite crystallisation on AcoD economics. Struvite crystallisation is slightly costlier (18–19%) than PN/Anammox (15–17%) as a result of the high consumption of NaOH needed to adjust the pH to 9 and $MgCl_2$ needed to provide the amount of Mg^{2+} to precipitate struvite (Table 1).

3.3. Sensitivity analysis of the most critical factors for sewage sludge and food waste co-digestion

Fig. 4 shows the sensitivity analysis for the four parameters evaluated: (i) biosolids disposal cost, (ii) electricity price, (iii) struvite price and (iv) food waste gate fee.

3.3.1. Biosolids disposal cost

Fig. 4A shows the net cost variation when the biosolids disposal cost (including transport) ranges between 100 and 400 € t^{-1} TS (Foladori et al., 2015). This interval was chosen since it comprises biosolids disposal costs for other disposal alternatives such as incineration, landfilling or composting (Foladori et al., 2015). Scenario 2C is the most competitive scenario for disposal costs below 200 € t^{-1} TS. However, when disposal cost is above 200 € t^{-1} TS, Scenario 1, 2A and 2B outcompete Scenario 2C due to the lower amount of biosolids to be managed in these scenarios. Interestingly, Scenario 1 is the most competitive scenario when the disposal cost is above 200 € t^{-1} TS. These results suggest that implementing AcoD of sewage sludge and food waste in an AnMBR-WWTP is recommendable for economical management options (<200 € t^{-1} TS) such as agriculture and composting; however, it is less economically attractive for costly management options (>200 € t^{-1} TS) such as landfilling or incineration. Scenario 3 is costlier than Scenario 1 and 2 regardless of the biosolids disposal cost as a result of the extra cost needed to implement PN/Anammox and struvite crystallisation in the sidestream of the WWTP. The Baseline Scenario presents the worst economic prospect since it produces a large amount of poorly biodegradable secondary sludge.

3.3.2. Electricity price

Fig. 4B shows the net cost variation when the electricity purchase price ranges between 0.06 and 0.18 € kWh^{-1}. This interval was chosen since it represents the current electricity prices in the European Union (Eurostat, 2019). Scenario 2C is the most favourable scenario when the electricity price is above 0.10 € kWh^{-1} due to the high amount of energy produced when the sidestream AD co-digests sewage sludge and food waste at an OLR of 2 kg VS m^{-3} d^{-1}. All AcoD scenarios feature a net benefit (net cost < 0 € y^{-1}) at an electricity price of 0.18 € kWh^{-1}. Conversely, Scenario 1 is the most favourable scenario when the electricity price is below 0.10 € kWh^{-1}. At low electricity prices, the higher electricity revenue of AcoD scenarios is not enough to offset their higher gross costs. These results show that implementing AcoD is particularly attractive when the price of electricity is high since a negative impact on AcoD profitability is observed as the price of the electricity decreases. Another example of this factor is that Scenario 3C and 3B are the less favourable scenarios at an electricity price of 0.10 and 0.09 € kWh^{-1}, respectively. Overall, these results show that the application of AcoD in the AnMBR-WWTP is particularly attractive when the electricity price is above 0.10 € kWh^{-1}, where the higher amount of energy recovered and sold compensates the higher gross costs needed to implement AcoD. This is relevant considering that energy prices are expected to increase in the future as a result of the increased fuel and CO_2 prices (Panos and Densing, 2019). Future higher energy prices would make AcoD more attractive to WWTP operators to maximise the revenue from electricity generation.

3.3.3. Struvite price

Fig. 4C shows the net cost variation of the different scenarios when the struvite price ranges between 0 and 1,000 € t^{-1}, which comprises struvite prices reported in literature (Akyol et al., 2020; Molinos-Senante et al., 2011). It should be noted that the impact of struvite price is only applicable in Scenario 3 because this is the only scenario that included struvite precipitation in the sidestream of the WWTP (Fig. 1). The net cost of Scenario 3 decreases from 921,000–1,161,000 to 54,000–340,000 € y^{-1} as the struvite price increases from 0 to 1,000 € t^{-1}, respectively. Scenario 3C is more competitive than Scenario 3A and 3B when the struvite price is above 450 € t^{-1} since Scenario 3C achieves the highest revenue from struvite commercialisation. This is mainly attributed to the higher amount of phosphorus released in Scenario 3C in comparison with Scenario 3A and Scenario 3B. Scenario 3C becomes the most favourable scenario when the struvite price is above 850 € t^{-1} (Fig. 4C). However, a struvite price of 850 € t^{-1} is little realistic since struvite prices between 188 and 763 € t^{-1} have been reported in literature (Akyol et al., 2020; Molinos-Senante et al., 2011). Besides economic considerations, novel legislations forcing the recovery of phosphorus can be a major driver for the implementation of struvite recovery in WWTPs.

3.3.4. Food waste gate fee

Fig. 4D shows the net cost variation when the food waste gate fee ranges between –100 and 100 € t^{-1}, which is a representative interval for full-scale plants using food waste as co-substrate (Nghiem et al., 2017). The gate fee has a big impact on net cost since Scenario 2 and 3 achieve net benefit (net cost < 0 € y^{-1}) when the gate fee is above 43 € t^{-1}. Scenario 2C and 3C are the most favourable scenarios at gate fees above 30 € t^{-1} since these scenarios accept large amounts of food waste (OLR of 2.0 kg VS m^{-3} d^{-1}), which leads to the highest revenue from the gate fee. For a gate fee of 86 € t^{-1}, the gate fee represents 51, 61 and 65% of the total revenue in Scenario 3A, 3B and 3C, respectively. This agrees with Sembera et al. (2019), who reported that the gate fee could represent an important revenue for WWTPs. However, the increasing interest in AcoD would also increase the number of WWTPs performing AcoD, which would increase the competition for co-substrates, implying a drop in gate fee prices that could even become negative (delivery fee). As shown in Fig. 4D, paying a delivery fee for the food waste would have

a negative impact on net cost. Indeed, Scenario 1 is the most favourable scenario when the delivery fee is above 10 € t^{-1} (gate fee < -10 € t^{-1}) since this scenario does not implement AcoD and does not have to pay for the food waste. Thus, the implementation of AcoD in an AnMBR-WWTP would only be economically attractive when the food waste delivery fee is below 10 € t^{-1} (gate fee > -10 € t^{-1}). These results reinforce the idea that the gate/delivery fee is a key factor in AcoD economics.

4. Conclusions

The economic feasibility of implementing sewage sludge and food waste co-digestion in the sidestream AD of an AnMBR-WWTP was evaluated. Results showed that the higher electricity revenue derived from co-digestion offsets the higher costs associated with the food waste acceptance infrastructure and biosolids management/disposal. However, the electricity revenue did not offset the additional costs when the nutrients backload was treated using sidestream equipment (partial-nitritation/anammox, struvite crystallisation). Biosolids disposal was the most important gross cost contributor in all scenarios. Finally, a sensitivity analysis revealed that the food waste gate fee had a noticeable impact on the net cost.

CRediT authorship contribution statement

Sergi Vinardell: Conceptualization, Formal analysis, Investigation, Data curation, Methodology, Visualization, Writing - original draft, Writing - review & editing. **Sergi Astals:** Conceptualization, Methodology, Supervision, Writing - review & editing. **Konrad Koch:** Supervision, Writing - review & editing. **Joan Mata-Alvarez:** Supervision, Writing - review & editing, Funding acquisition. **Joan Dosta:** Supervision, Writing - review & editing.

Declaration of Competing Interest

The authors declare that they have no known competing financial interests or personal relationships that could have appeared to influence the work reported in this paper. The authors also declare that this manuscript reflects only the authors' view and that the Executive Agency for SME/EU Commission are not responsible for any use that may be made of the information it contains.

Acknowledgments

This work was supported by the European Union LIFE programme (LIFE Green Sewer project, LIFE17 ENV/ES/000341). Sergi Vinardell is grateful to the Generalitat de Catalunya for his predoctoral FI grant (2019FI_B 00394). Sergi Astals is grateful to the Spanish Ministry of Science, Innovation and Universities for his Ramon y Cajal fellowship (RYC-2017-22372).

Appendix A. Supplementary data

Supplementary data to this article can be found online at https://doi.org/10.1016/j.biortech.2021.124978.

References

Aichinger, P., Wadhawan, T., Kuprian, M., Higgins, M., Ebner, C., Fimml, C., Murthy, S., Wett, B., 2015. Synergistic co-digestion of solid-organic-waste and municipal-sewage-sludge: 1 plus 1 equals more than 2 in terms of biogas production and solids reduction. Water Res. 87, 416–423.

Akyol, Ç., Foglia, A., Ozbayram, E.G., Frison, N., Katsou, E., Eusebi, A.L., Fatone, F., 2020. Validated innovative approaches for energy-efficient resource recovery and re-use from municipal wastewater: From anaerobic treatment systems to a biorefinery concept. Crit. Rev. Environ. Sci. Technol. 50, 869–902.

Astals, S., Esteban-Gutiérrez, M., Fernández-Arévalo, T., Aymerich, E., García-Heras, J.L., Mata-Alvarez, J., 2013. Anaerobic digestion of seven different sewage sludges: A biodegradability and modelling study. Water Res. 47, 6033–6043.

Bolzonella, D., Fatone, F., Gottardo, M., Frison, N., 2018. Nutrients recovery from anaerobic digestate of agro-waste: Techno-economic assessment of full scale applications. J. Environ. Manage. 216, 111–119.

Bolzonella, D., Pavan, P., Battistoni, P., Cecchi, F., 2006. Anaerobic co-digestion of sludge with other organic wastes and phosphorus reclamation in wastewater treatment plants for biological nutrients removal. Water Sci. Technol. 53, 177–186.

Bouzas, A., Martí, N., Grau, S., Barat, R., Mangin, D., Pastor, L., 2019. Implementation of a global P-recovery system in urban wastewater treatment plants. J. Clean. Prod. 227, 130–140.

Caffaz, S., Bettazzi, E., Scaglione, D., Lubello, C., 2008. An integrated approach in a municipal WWTP: Anaerobic codigestion of sludge with organic waste and nutrient removal from supernatant. Water Sci. Technol. 58, 669–676.

Campos, J.L., Mosquera-Corral, A., Val del Río, A., Pedrouso, A., Gutiérrez-Pichel, A., Belmonte, M., Ruíz-Filippi, G., Jorquera, L., Jeison, D., Vergara, C., 2017. Energy and resources recovery in waste water treatment plants. In: Environmental Science and Engineering Volume 9 Environment and Energy Management: Ethics. Laws and Policies. Studium Press LLC, Houston, pp. 60–78.

Capson-Tojo, G., Rouez, M., Crest, M., Steyer, J.P., Delgenès, J.P., Escudié, R., 2016. Food waste valorization via anaerobic processes: a review. Rev. Environ. Sci. Biotechnol. 15, 499–547.

Eurostat, 2019. Electricity price statistics. https://ec.europa.eu/eurostat/statistics-explained/index.php/Electricity_price_statistics (accessed 30 September 2019).

Foladori, P., Andreottola, G., Ziglio, G., 2015. Current sludge disposal alternatives and costs in critical areas. In: Sludge Reduction Technologies in Wastewater Treatment Plants. IWA Publishing, London (UK), pp. 21–26.

Garcia-Heras, J.L., 2003. Reactor sizing, process kinetics and modelling of anaerobic digestion of complex waste. In: Mata-Alvarez, J. (Ed.), Biomethanization of the organic fraction of municipal solid wastes. IWA Publishing, London (UK), pp. 21–62.

Garrido-Baserba, M., Vinardell, S., Molinos-Senante, M., Rosso, D., Poch, M., 2018. The Economics of Wastewater Treatment Decentralization: A Techno-economic Evaluation. Environ. Sci. Technol. 52, 8965–8976.

Ghosh, S., Lobanov, S., Lo, V.K., 2019. An overview of technologies to recover phosphorus as struvite from wastewater: advantages and shortcomings. Environ. Sci. Pollut. Res. 26, 19063–19077.

Guest, J.S., Skerlos, S.J., Barnard, J.L., Beck, M.B., Daigger, G.T., Hilger, H., Jackson, S. J., Karvazy, K., Kelly, L., Macpherson, L., Mihelcic, J.R., Pramanik, A., Raskin, L., Van Loosdrecht, M.C.M., Yeh, D., Love, N.G., 2009. A new planning and design paradigm to achieve sustainable resource recovery from wastewater. Environ. Sci. Technol. 43, 6126–6130.

Guo, Y., Chen, Y., Webeck, E., Li, Y.Y., 2020. Towards more efficient nitrogen removal and phosphorus recovery from digestion effluent: Latest developments in the anammox-based process from the application perspective. Bioresour. Technol. 299, 122560.

Henze, M., van Loosdrecht, M.C.M., Ekama, G.A., Brdjanovic, D., 2008. Biological wastewater treatment : principles, modelling and design. IWA Publishing, London (UK).

Horstmeyer, N., Weißbach, M., Koch, K., Drewes, J.E., 2018. A novel concept to integrate energy recovery into potable water reuse treatment schemes. J. Water Reuse Desalin. 8, 455–467.

Koch, K., Plabst, M., Schmidt, A., Helmreich, B., Drewes, J.E., 2016. Co-digestion of food waste in a municipal wastewater treatment plant: Comparison of batch tests and full-scale experiences. Waste Manag. 47, 28–33.

Lackner, S., Gilbert, E.M., Vlaeminck, S.E., Joss, A., Horn, H., van Loosdrecht, M.C.M., 2014. Full-scale partial nitritation/anammox experiences - An application survey. Water Res. 55, 292–303.

Macintosh, C., Astals, S., Sembera, C., Ertl, A., Drewes, J.E., Jensen, P.D., Koch, K., 2019. Successful strategies for increasing energy self-sufficiency at Grüneck wastewater treatment plant in Germany by food waste co-digestion and improved aeration. Appl. Energy 242, 797–808.

Mata-Alvarez, J., Dosta, J., Romero-Güiza, M.S., Fonoll, X., Peces, M., Astals, S., 2014. A critical review on anaerobic co-digestion achievements between 2010 and 2013. Renew. Sustain. Energy Rev. 36, 412–427.

Molinos-Senante, M., Hernández-Sancho, F., Sala-Garrido, R., Garrido-Baserba, M., 2011. Economic feasibility study for phosphorus recovery processes. Ambio 40, 408–416.

Morelli, B., Cashman, S., Ma, X.C., Turgeon, J., Arden, S., Garland, J., 2020. Environmental and cost benefits of co-digesting food waste at wastewater treatment facilities. Water Sci. Technol. 82, 227–241.

Münch, E.V., Barr, K., 2001. Controlled struvite crystallisation for removing phosphorus from anaerobic digester sidestreams. Water Res. 35, 151–159.

Nghiem, L.D., Koch, K., Bolzonella, D., Drewes, J.E., 2017. Full scale co-digestion of wastewater sludge and food waste: Bottlenecks and possibilities. Renew. Sustain. Energy Rev. 72, 354–362.

Panos, E., Densing, M., 2019. The future developments of the electricity prices in view of the implementation of the Paris Agreements: Will the current trends prevail, or a reversal is ahead? Energy Econ. 84, 104476.

Peng, L., Dai, H., Wu, Y., Peng, Y., Lu, X., 2018. A comprehensive review of phosphorus recovery from wastewater by crystallization processes. Chemosphere 197, 768–781.

Pretel, R., Robles, A., Ruano, M.V., Seco, A., Ferrer, J., 2014. The operating cost of an anaerobic membrane bioreactor (AnMBR) treating sulphate-rich urban wastewater. Sep. Purif. Technol. 126, 30–38.

Riley, D.M., Tian, J., Güngör-Demirci, G., Phelan, P., Rene Villalobos, J., Milcarek, R.J., 2020. Techno-economic assessment of CHP systems in wastewater treatment plants. Environ. 7, 74.

Rodriguez-Garcia, G., Frison, N., Vázquez-Padín, J.R., Hospido, A., Garrido, J.M., Fatone, F., Bolzonella, D., Moreira, M.T., Feijoo, G., 2014. Life cycle assessment of nutrient removal technologies for the treatment of anaerobic digestion supernatant and its integration in a wastewater treatment plant. Sci. Total Environ. 490, 871–879.

Schaubroeck, T., De Clippeleir, H., Weissenbacher, N., Dewulf, J., Boeckx, P., Vlaeminck, S.E., Wett, B., 2015. Environmental sustainability of an energy self-sufficient sewage treatment plant: Improvements through DEMON and co-digestion. Water Res. 74, 166–179.

Sembera, C., Macintosh, C., Astals, S., Koch, K., 2019. Benefits and drawbacks of food and dairy waste co-digestion at a high organic loading rate: A Moosburg WWTP case study. Waste Manag. 95, 217–226.

Smith, A.L., Stadler, L.B., Cao, L., Love, N.G., Raskin, L., Skerlos, S.J., 2014. Navigating Wastewater Energy Recovery Strategies: A Life Cycle Comparison of Anaerobic Membrane Bioreactor and Conventional Treatment Systems with Anaerobic Digestion. Environ. Sci. Technol. 48, 5972–5981.

Stazi, V., Tomei, M.C., 2018. Enhancing anaerobic treatment of domestic wastewater: State of the art, innovative technologies and future perspectives. Sci. Total Environ. 635, 78–91.

Taboada-Santos, A., Rivadulla, E., Paredes, L., Carballa, M., Romalde, J., Lema, J.M., 2020. Comprehensive comparison of chemically enhanced primary treatment and high-rate activated sludge in novel wastewater treatment plant configurations. Water Res. 169, 115258.

Tian, X., Richardson, R.E., Tester, J.W., Lozano, J.L., You, F., 2020. Retrofitting Municipal Wastewater Treatment Facilities toward a Greener and Circular Economy by Virtue of Resource Recovery: Techno-Economic Analysis and Life Cycle Assessment. ACS Sustain. Chem. Eng. 8, 13823–13837.

Usack, J.G., Gerber Van Doren, L., Posmanik, R., Labatut, R.A., Tester, J.W., Angenent, L. T., 2018. An evaluation of anaerobic co-digestion implementation on New York State dairy farms using an environmental and economic life-cycle framework. Appl. Energy 211, 28–40.

Van Eekert, M., Weijma, J., Verdoes, N., De Buisonjé, F., Reitsma, B., Van den Bulk, J., Van Gastel, J., 2012. Explorative research on innovative nitrogen recovery. Amersfoort: STOWA. Available at: https://edepot.wur.nl/249715 (accessed 12 January 2021).

Van Loosdrecht, M.C.M., Brdjanovic, D., 2014. Anticipating the next century of wastewater treatment. Science 344, 1452–1453.

Vandekerckhove, T.G.L., Props, R., Carvajal-Arroyo, J.M., Boon, N., Vlaeminck, S.E., 2020. Adaptation and characterization of thermophilic anammox in bioreactors. Water Res. 172, 115462.

Vaneeckhaute, C., Lebuf, V., Michels, E., Belia, E., Vanrolleghem, P.A., Tack, F.M.G., Meers, E., 2017. Nutrient Recovery from Digestate: Systematic Technology Review and Product Classification. Waste and Biomass Valorization 8, 21–40.

Vázquez-Padín, J., Fernádez, I., Figueroa, M., Mosquera-Corral, A., Campos, J.L., Méndez, R., 2009. Applications of Anammox based processes to treat anaerobic digester supernatant at room temperature. Bioresour. Technol. 100, 2988–2994.

Vinardell, S., Astals, S., Peces, M., Cardete, M.A., Fernández, I., Mata-Alvarez, J., Dosta, J., 2020. Advances in anaerobic membrane bioreactor technology for municipal wastewater treatment: A 2020 updated review. Renew. Sustain. Energy Rev. 130, 109936.

Vinardell, S., Dosta, J., Mata-Alvarez, J., Astals, S., 2021. Unravelling the economics behind mainstream anaerobic membrane bioreactor application under different plant layouts. Bioresour. Technol. 319, 124170.

Wett, B., Omari, A., Podmirseg, S.M., Han, M., Akintayo, O., Gómez Brandón, M., Murthy, S., Bott, C., Hell, M., Takács, I., Nyhuis, G., O'Shaughnessy, M., 2013. Going for mainstream deammonification from bench to full scale for maximized resource efficiency. Water Sci. Technol. 68, 283–289.

Whiting, A., Azapagic, A., 2014. Life cycle environmental impacts of generating electricity and heat from biogas produced by anaerobic digestion. Energy 70, 181–193.

Xie, S., Higgins, M.J., Bustamante, H., Galway, B., Nghiem, L.D., 2018. Current status and perspectives on anaerobic co-digestion and associated downstream processes. Environ. Sci. Water Res. Technol. 4, 1759–1770.

SUPPLEMENTARY INFORMATION

Co-digestion of sewage sludge and food waste in a wastewater treatment plant based on mainstream anaerobic membrane bioreactor technology: A techno-economic evaluation

Sergi Vinardell[a,*], Sergi Astals[a], Konrad Koch[b], Joan Mata-Alvarez[a], Joan Dosta[a]

*Corresponding author (e-mail: svinardell@ub.edu)

Figure

Figure S1. (bottom) Schematic representation of the WWTP layout before retrofit; (top) schematic representation of the mainstream of the WWTP after retrofit.

Tables

Table S1. Composition of mixed sewage sludge and food waste.

Table S2. Equations used to calculate biological sludge production in the mainstream of the WWTP.

Table S3. Parameters used to model the AD sidestream as CSTR.

Table S4. Summary of the parameters used for the economic evaluation.

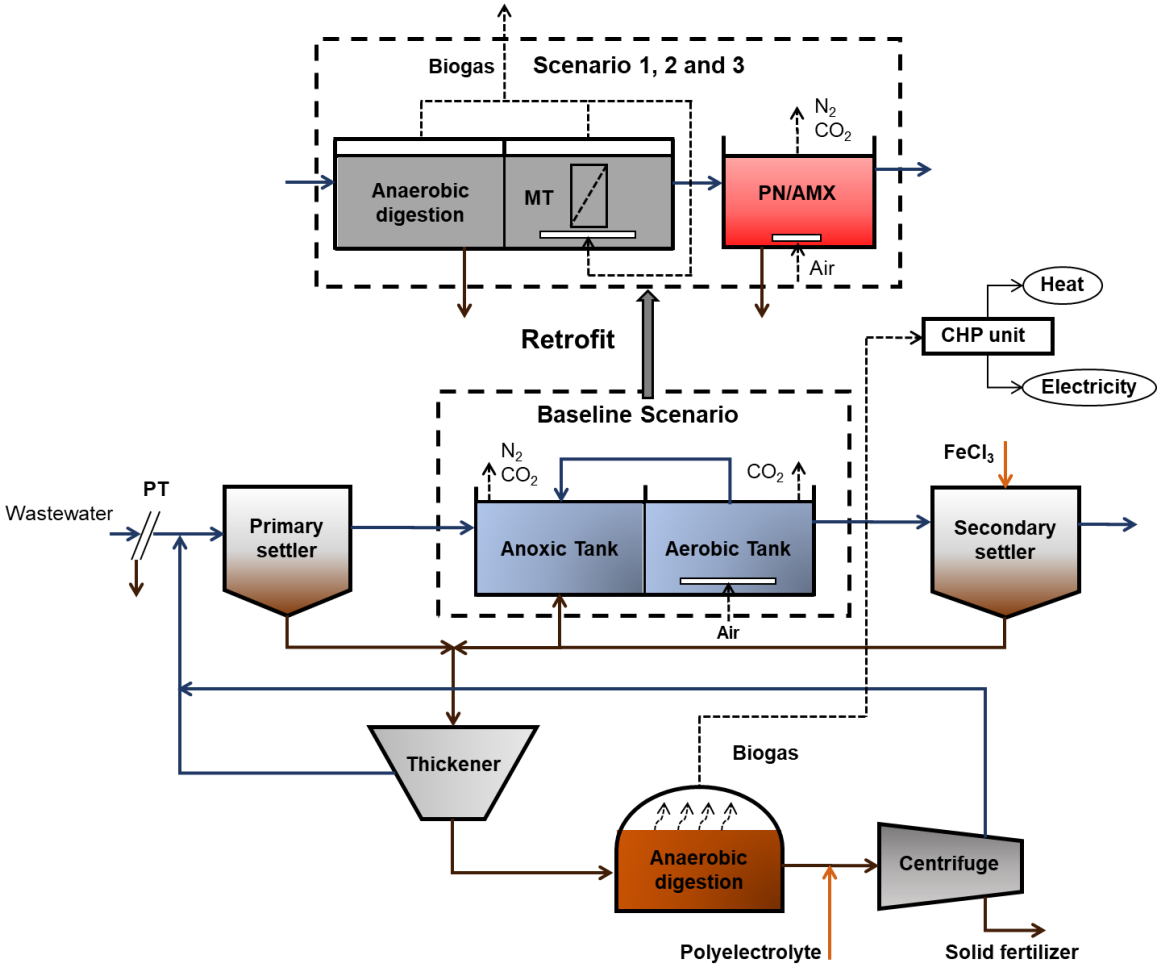

Figure S1. (bottom) Schematic representation of the WWTP layout before retrofitting; (top) schematic representation of the mainstream of the WWTP after retrofitting.

Table S1. Composition of mixed sewage sludge and food waste. The average was the value used in the techno-economic analysis.

	Sewage sludge							
	SS_1	**SS_2**	**SS_3**	**SS_4**	**SS_5**	**SS_6**	**SS_7**	**Average**
Total Solids (%)	3.83	1.84	3.27	3.52	4.84	3.99	3.13	3.50
VS/TS	0.73	0.78	0.79	0.75	0.84	0.74	0.65	0.75
TSS/TS	0.87	0.85	0.83	0.85	0.89	0.86	0.84	0.86
VSS/TSS	0.74	0.78	0.80	0.77	0.86	0.75	0.80	0.79
COD/VS	1.80	1.77	1.81	1.76	1.75	1.72	1.63	1.76
TS/TKN	20.26	16.00	15.00	15.11	20.86	17.20	19.32	17.68
TS/TP [a]	-	-	-	-	-	-	-	-
TKN/NH_4^+-N	8.25	7.14	15.35	12.07	15.26	15.36	4.95	11.20
TS:PO_4^{3-}-P	170.21	440.81	115.26	122.80	188.58	221.25	352.87	230.25
	Food Waste							
	FW_1	**FW_2**	**FW_3**	**FW_4**	**FW_5**	**FW_6**	**FW_7**	**Average**
Total Solids (%)	21.60	30.90	18.20	28.0	18.10	24.75	22.1	23.38
VS/TS	0.96	0.85	0.89	0.86	0.94	0.93	0.92	0.91
COD/VS	1.42	-	1.37	-	1.39	-	1.23	1.35
TS/TKN	36.93	31.65	40.35	33.85	33.39	33.45	40.32	35.71
TS/TP	-	192.31	-	207.04	121.48	-	-	173.61
TKN/NH_4^+-N	-	-	-	18.23	33.88	23.13	-	25.08
TS:PO_4^{3-}-P [b]	-	-	-	-	-	-	-	-

[a] A TS/TP ratio of 72.14 was used from the data reported by Peces et al. (2020).

[b] A TP:PO_4^{3-}-P of 2.02 was used from unpublished data from our research group.

Table S2. Equations used to calculate biological sludge production in the mainstream of the WWTP.

Sludge Production	Equation	Parameters	Reference
AnMBR (kg TSS d^{-1})	$W_{AnMBR} = \frac{Q}{10^3} \cdot \left[X_{I,TSS} + \frac{(1 + f_D \cdot b_H \cdot SRT) \cdot Y_T \cdot (S_{S,0} - S_S)}{1 + b_H} \right]$	f_D=0.2 kg TSS kg^{-1} TSS b_H=0.02 d^{-1} Y_T=0.076 kg TSS kg^{-1} COD	Smith et al., 2014
PN-Anammox (kg VSS d^{-1})	$W_{PN/AMX} = L_N \cdot f_{N,AOB} \cdot Y_{AOB} \cdot x_N + L_N \cdot f_{N,AMX} \cdot Y_{AMX} \cdot x_N$	f_{N_AOB}=0.565 Y_{AOB}=0.12 kg VSS kg^{-1} N $f_{N,AMX}$=0.435 Y_{AMX}=0.13 kg VSS kg^{-1} N	Cogert et al., 2019
Activated sludge (kg VSS d^{-1})	$W_{AS} = \frac{Q \cdot X_{I,VSS}}{10^3} + L_N \cdot Y_{AOB} \cdot x_N + L_N \cdot Y_{NOB} \cdot x_N + L_N \cdot N_{COD/N} \cdot Y_{DEN} \cdot x_N + (L_{COD} - L_{COD,DEN} - L_{COD,eff}) \cdot Y_{HET}$	Y_{AOB}=0.12 kg VSS kg^{-1} N Y_{NOB}=0.05 kg VSS kg^{-1} N Y_{DEN}=0.3 kg VSS kg^{-1} COD Y_{HET}=0.45 kg VSS kg^{-1} COD $N_{COD/N}$=5 kg COD kg^{-1} N	Cogert et al., 2019

Q: influent flow rate (m^3 d^{-1}); $X_{I,TSS}$: influent inert solids (mg TSS L^{-1}); f_D: decay coefficient (kg TSS kg^{-1} TSS); b_H: decay rate (d^{-1}); SRT: solids retention time (d); Y_T: biomass yield anaerobic microorganisms (kg TSS kg^{-1} COD); $S_{S,0}$: influent biodegradable organic matter (mg COD L^{-1}); S_S: effluent biodegradable organic matter(mg COD L^{-1}); L_N: nitrogen load (kg N d^{-1}); $f_{N,AOB}$: fraction of influent nitrogen undergoing partial nitritation (-); Y_{AOB}: biomass yield of ammonium oxidising bacteria (kg VSS kg^{-1} N); x_N: nitrogen removal efficiency; $f_{N,AMX}$: fraction of influent nitrogen undergoing anammox (-); Y_{AMX}: biomass yield anammox bacteria (kg VSS kg^{-1} N); $X_{I,VSS}$: influent inert solids (mg VSS L^{-1}); $N_{COD/N}$: stoichiometric coefficient COD to nitrogen (kg COD kg^{-1} N); Y_{NOB}: biomass yield of nitrite oxidising bacteria (kg VSS kg^{-1} N); Y_{DEN}: biomass yield of heterotrophs denitrifiers (kg VSS kg^{-1} COD); L_{COD}: COD load (kg COD d^{-1}); $L_{COD,DEN}$: COD used for denitrification (kg COD d^{-1}); $L_{COD,eff}$: effluent COD (kg COD d^{-1}); Y_{HET}: biomass yield of heterotrophs (kg VSS kg^{-1} COD).

Table S3. Parameters used to model the AD sidestream as CSTR. The average was the value used in the techno-economic analysis. Equations can be found in Section 2.3.

	Primary sludge					
	PSk_1	PSk_2	PSk_3	PSk_4	PSk_5	Average
k (d^{-1}) [a]	0.23	0.23	0.31	0.29	0.25	0.26
	PSf_1	PSf_2	PSf_3	PSf_4	PSf_5	Average
f_i (-) [b]	0.61	0.58	0.63	0.60	0.60	0.61
	Secondary sludge					
	SSk_1	SSk_2	SSk_3	SSk_4	SSk_5	Average
k (d^{-1}) [a]	0.22	0.18	0.16	0.20	0.24	0.20
	SSf_1	SSf_2	SSf_3	SSf_4	SSf_5	Average
f_i (-) [b]	0.36	0.29	0.40	0.33	0.48	0.37
	Food Waste					
	FWk_1	FWk_2	FWk_3	FWk_4	FWk_5	Average
k (d^{-1}) [a]	0.5	0.71	0.55	0.27	0.14	0.43
	FWf_1	FWf_2	FWf_3	FWf_4	FWf_5	Average
f_i (-) [b]	0.84	0.91	0.82	0.81	0.86	0.85

[a] First-order kinetic constant

[b] Substrate biodegradability. When data was not directly available, substrate biodegradability was calculated as: $fi=B_0/B_{0,max}$.

Table S4. Summary of the parameters used for the economic evaluation.

	Value	Reference
Capital cost food waste acceptance facility (€/(t/year))	71.4	Macintosh et al., 2019
Food waste delivery fee (€ t^{-1})	3	Macintosh et al., 2019
Polyelectrolyte cost (€ kg^{-1})	2.35	Pretel et al., 2015
Centrifuge energy consumption (kWh kg^{-1} TSS)	0.045	Pretel et al., 2014
Biosolids disposal cost (including transport) (€ t^{-1} TS)	147	Foladori et al., 2015
Energy consumption mainstream nitrogen removal (kWh kg^{-1} N)	2.38	Horstmeyer et al., 2018
Ferric chloride (€ t^{-1})	220	Taboada-Santos et al., 2020
Nitrogen removal efficiency (%)	89	Schaubroeck et al., 2015; Campos et al., 2017
Capital cost partial nitritation/anammox (€/(kg N/day))	1,600	Vandekerckhove et al., 2020; Van Eekert et al., 2012
Energy consumption sidestream nitrogen removal (kWh kg^{-1} N)	1.5	Lackner et al., 2014; Schaubroeck et al., 2015
Total operating costs partial nitritation/anammox process (€ kg^{-1} N)	0.8	Vandekerckhove et al., 2020; Van Eekert et al., 2012
Phosphate removal efficiencies (%)	90	Peng et al., 2018; Kumar and Pal., 2015
Capital cost struvite reactor (€/(kg P/day))	10,000	Vaneeckhaute et al., 2017
Energy consumption struvite crystallisation (kWh kg^{-1} P)	5.9	Ghosh et al., 2019
Magnesium chloride hexahydrate cost (€ t^{-1})	370	Bouzas et al., 2019
Sodium hydroxide cost (€ t^{-1})	620	Bouzas et al., 2019
Electrical efficiency CHP unit (%)	33	Riley et al., 2020; Vinardell et al., 2021
Methane calorific value (MJ kg^{-1})	55.5	Batstone et al., 2015
Electricity cost (€ kWh^{-1})	0.1149	Eurostat., 2019
Capital cost CHP unit upgrading (€ kW_{el}^{-1})	712	Riley et al., 2020; Smith et al., 2014
Operating cost CHP unit (€ kWh_{el}^{-1})	0.0119	Riley et al., 2020; Smith et al., 2014

3.5 Results and discussion

This section summarises the main findings of Publication V, VI and VII regarding the plant-wide impact of implementing an AnMBR in a WWTP.

3.5.1 Impact of flux and gas sparging rate on granular AnMBRs

SGD and permeate flux substantially affected membrane fouling extent during anaerobic granular sludge filtration. At fluxes below 10 LMH, the membrane filtration resistance (R_F) noticeably decreased as the SGD increased from 0.25 to 0.5 m^3 m^{-2} h^{-1} (Figure 2 in Publication V). However, increasing the SGD above 0.5 m^3 m^{-2} h^{-1} only led to a small reductions in R_F. At fluxes above 10 LMH, the R_F noticeably decreased for all SGD steps. However, the reduction in R_F was particularly less pronounced at SGDs above 1.0 m^3 m^{-2} h^{-1} (Figure 2 in Publication V). These results suggest that operating the membrane at 0.5 m^3 m^{-2} h^{-1} was the most favourable condition at fluxes below 10 LMH, whereas operating the membrane at 1.0 m^3 m^{-2} h^{-1} was the most favourable condition at fluxes above 10 LMH.

The soluble COD rejection was between 31 and 44% for the SGD and flux conditions under study (Figure 3 in Publication V). The results showed that soluble COD rejection was not affected by SGD and flux conditions. The rejection values were similar for all SGD conditions (33-38%) with no statistically significant differences between them

($p>0.05$). Concerning membrane flux, statistically significant differences ($p<0.05$) were observed between $Flux_4$ (J_{20}=16.8 LMH) and the other flux conditions. The difference between $Flux_4$ and the other conditions was attributed to changes in the concentration of DCOM compounds between filtration tests (Figure S2 of the supplementary material in Publication V). The three-dimensional excitation-emission matrix fluorescence (3DEEM) spectra indicated that the DCOM fluorophores of Region I+II, which corresponded to protein-like substances, were predominant (Table S5 of the supplementary material of Publication V) and were more retained by the membrane (39-50%) in comparison to the other regions (Table 2 in Publication V). These results indicate that these fluorophores could be important foulants in granular AnMBR systems.

The economic analysis was conducted for the four most favourable SGD conditions for each membrane flux and for three chemical cleaning strategies. The results showed that energy consumption for gas sparging represented the largest fraction of the discounted lifetime costs (DLC) for the different scenarios (Figure 4 in Publication V). Membrane purchasing cost also had a high impact on DLC although its importance was reduced at higher fluxes due to the lower membrane area required. Membrane replacement and chemical cost increased their contribution at higher fluxes since higher amounts of chemicals are necessary as membrane fouling increases (Figure 4 in Publication V). Scenario 2 (J_{20}=7.8 LMH and SGD=0.5 m^3 m^{-2} h^{-1}) was the most competitive scenario for more intensive chemical cleaning conditions (Condition A and C), which are likely to occur in AnMBR systems [46]. Accordingly, these results showed that the most economically competitive strategy for membrane fouling control in granular AnMBR systems could be associated with operating the membrane at moderate J_{20} and SGDs of 7.8 LMH and 0.5 m^3 m^{-2} h^{-1}, respectively.

3.5.2 Economics of mainstream AnMBR implementation under different plant layouts

Five different plant layout scenarios were evaluated combining AnMBR with different pre- and post-treatments technologies. All the scenarios included preliminary treatment, AnMBR, degassing membrane for methane recovery, sludge thickener and centrifuge (Table 1 in Publication VI).

Scenario 1 (without primary settler, sidestream anaerobic digester and nutrients treatment) featured a net treatment cost between 0.35 and 0.42 € m^{-3} (Figure 2 in Publication VI). These results are in agreement with other studies evaluating the economic feasibility of AnMBR-WWTPs [38]. The net treatment cost decreased as the sewage COD concentration increased from 100 to 1100 mg COD L^{-1} due to the higher methane production achieved at higher COD concentrations. However, the net treatment cost increased at sewage COD concentrations above 1100 mg COD L^{-1} since the higher methane production did not offset the higher energy required to control membrane fouling (Figure 2 in Publication VI). In Scenario 1, energy self-sufficiency was achieved at COD concentrations above 550 mg COD L^{-1}, with a maximum net energy production of 0.32 kWh m^{-3} achieved at 1100 mg COD L^{-1} (Figure 2 in Publication VI).

Scenario 2 included three scenarios combining primary settler and sidestream anaerobic digester. The net treatment cost of Scenario 2 ranged between 0.33 and 0.43 € m^{-3} (Figure 3A in Publication VI). Scenario 2C (including sidestream anaerobic digester and without primary settler) was the most competitive scenario for sewage COD concentrations between 100 and 1100 mg COD L^{-1}. This scenario featured a net treatment cost very similar to Scenario 1. Scenario 2A (including primary settler and sidestream anaerobic digester) was the most competitive scenario when the sewage COD concentration exceeded 1100 mg COD L^{-1} (Figure 3A in Publication VI). This was attributed to the reduction of the mixed liquor suspended solids (MLSS) concentration when implementing a primary settler in a WWTP, which reduced the costs associated with membrane fouling control. In addition, implementing a primary settler was particularly interesting for low sewage COD:SO_4^{2-}-S ratios (<8) since the implementation of a primary settler reduced the amount of organic matter converted into hydrogen sulfide in the mainstream AnMBR (Figure 3B in Publication VI). However, it is worth mentioning that, even after implementing a primary settler, the use of mainstream AnMBR appears questionable for the treatment of sewage containing high sulphate concentrations (COD:SO_4^{2-}-S<15). Scenario 2B (including primary settler and without sidestream anaerobic digester) was not economically competitive under any condition since this scenario produced a limited amount of methane and failed to stabilise primary sludge with a direct impact on the environment (Figure 3A in Publication VI).

Scenario 3 (including sidestream anaerobic digester, partial nitritation (PN)-Anammox and chemical phosphorus precipitation, and without primary settler) featured a net treatment cost between 0.51 and 0.56 € m^{-3} (discount rate of 5%) (Figure 5 in Publication VI). This treatment cost is within the range reported in the literature for other technologies used for wastewater treatment such as AS and aerobic MBR processes [36], which elucidates that mainstream AnMBR could be competitive for municipal sewage treatment. Scenario 3 achieved energy self-sufficiency for high-strength (1000 mg COD L^{-1}) sewage treatment containing a low concentration of sulphate (COD:SO_4^{2-}-S>40) (Figure 4 in Publication VI). In this scenario, AnMBR and PN-Anammox were the most important cost contributors and represented 58 and 30% of the cost, respectively (Figure 6 in Publication VI). These results showed that reducing the costs of these two technologies is important to further improve the economic prospect of AnMBR-WWTPs.

3.5.3 Economic evaluation of co-digesting sewage sludge and food waste in an AnMBR-WWTP

Four different scenarios were evaluated focusing on the sludge line of a WWTP: (i) Baseline Scenario, which represented an AS-WWTP, (ii) Scenario 1, which represented an AnMBR-WWTP without co-digestion, (ii) Scenario 2, which represented an AnMBR-WWTP implementing food waste co-digestion and treating the nutrients backload in the mainstream, and (iv) Scenario 3, which represented an AnMBR-WWTP implementing food waste co-digestion and treating the nutrients backload in the sidestream. Scenario 2 and 3 included three OLR strategies for food waste co-digestion (Table 1 in Publication VII).

Retrofitting an AS-WWTP to an AnMBR-WWTP decreases the sludge treatment costs as a result of the lower amount of secondary sludge produced under anaerobic conditions than under aerobic conditions. For this reason, the Baseline Scenario was costlier than all the scenarios that implemented mainstream AnMBR (Figure 2 in Publication VII). In an AnMBR-WWTP, co-digesting sewage sludge and food waste reduced the net cost of sludge line when the nutrients backload was treated in the mainstream (Scenario 2). The lower net cost of Scenario 2 is primarily attributed to the higher electricity revenue achieved in the sidestream anaerobic digester, which offsets the associated costs of food waste co-digestion. In Scenario 2, the net cost decreased as the OLR increased since

higher OLRs increased methane production with a direct impact on electricity revenue (Figure 2 in Publication VII). However, the costs associated with food waste co-digestion were not offset when the nutrients backload was treated in the sidestream rather than in the mainstream (Scenario 3). The higher net cost of Scenario 3 can be attributed to the implementation of PN-Anammox and struvite crystallisation to treat N and P backload, which increased capital and operating costs of the AnMBR-WWTP sludge line. In Scenario 3, the net cost increased as the OLR increased since higher OLRs increased the concentration of nutrients in the centrate with a direct impact on the costs of PN-Anammox and struvite crystallisation (Figure 2 in Publication VII). However, the treatment of nutrients in the sidestream can provide conceivable advantages in the WWTP beyond economic considerations, such as reducing disturbance in the mainstream [47], reducing uncontrolled struvite precipitation [48] or improving the overall removal of nutrients [49].

Biosolids disposal cost represented the highest contribution to the gross cost for all the scenarios followed by nutrients backload treatment and food waste acceptance installation (Figure 3 in Publication VII). High differences were observed between treating the nutrients backload in the mainstream or in the sidestream. Specifically, nutrients backload treatment in the mainstream represented between 13 and 18% of the gross cost, whereas nutrients backload treatment in the sidestream represented between 33 and 36% gross cost (Figure 3B in Publication VII). The higher contribution of sidestream nutrients treatment can be attributed to the costs associated with installing and operating PN-Anammox and struvite crystallisation technologies. The gross cost distribution of struvite crystallisation was slightly higher than PN-Anammox since struvite crystallisation required high quantities of chemicals (NaOH and $MgCl_2$) to adjust the pH and provide the Mg^{2+} for struvite crystallisation.

The sensitivity analysis showed that implementing food waste co-digestion in an AnMBR-WWTP should be particularly considered for disposal costs (including transport) below 200 € t^{-1} (Figure 4A in Publication VII). However, Scenario 1 (AnMBR-WWTP without food waste co-digestion) was the most economically favourable option at disposal costs above 200 € t^{-1} since Scenario 1 produced a lower amount of solids and minimised the impact of high disposal costs on net cost. Electricity prices above 0.10 €

kWh^{-1} were particularly advantageous for co-digestion scenarios since higher electricity prices led to higher electricity revenues, especially in those scenarios with higher electricity productions (Figure 4B in Publication VII). Struvite price also had an important impact on the net cost of Scenario 3. Specifically, increasing the struvite price from 0 to 1000 € t^{-1} decreased the net cost of Scenario 3 from 921,000-1,161,000 € y^{-1} to 54,000-340,000 € y^{-1}, respectively (Figure 4C in Publication VII). Finally, the results of the sensitivity analysis also showed that food waste delivery/gate fee is an economic driver since the economics of co-digestion scenarios were substantially affected by this parameter (Figure 4D in Publication VII).

Conclusions and recommendations

Conclusions

The conclusions of the state-of-the art review presented in Publication I are:

- Membrane fouling is a main barrier for AnMBR application. Gel layer could play an important role in membrane fouling, whose formation has been linked to the foulants' size and morphology.
- The operation of AnMBR under low psychrophilic temperatures and under high sulphate concentrations needs to be particularly considered to achieve a widespread application of the technology.
- Forward osmosis pre-concentration can overcome the limitations associated with the low organic matter concentration contained in municipal sewage.

The conclusions of Chapter 2 regarding FO pre-concentration before an AnMBR obtained from Publication II, III and IV are:

Publication II

- The AnMBR achieved stable COD removal efficiencies above 90% at pre-concentration factors of 1, 2, 5 and 10. The methane yield progressively increased from 214 to 322 mL g^{-1} COD due to the lower fraction of dissolved methane at higher pre-concentration factors.
- Membrane biofilm contributed to COD removal efficiency, particularly at the highest pre-concentration factor (6.5 g COD L^{-1} and 2.3 g Na^{+} L^{-1}).
- Economic self-sufficiency and temperature increments of 10 °C could be achieved in AnMBRs treating ten-fold pre-concentrated sewage.

Publication III

- The water production cost of the FO-RO system ranged between 0.80 and 1.30 € per m^3 of water produced. The minimum water production cost was estimated at 0.80 € m^{-3} for an open-loop scheme maximising water production and at 1.16 € m^{-3} for a closed-loop scheme.
- The wastewater treatment cost of the FO-RO+AnMBR system ranged between 0.80 and 1.40 € per m^3 of wastewater treated. The minimum wastewater treatment cost was estimated at 0.81 € m^{-3} for a closed-loop scheme operated at an FO recovery of 50%.
- The economic prospect of the FO-RO+AnMBR system could be substantially improved if an FO recovery of 10 LMH was achieved.

Publication IV

- The economic balance of combining FO and AnMBR technologies is clearly influenced by the FO membrane material since the net cost of using CTA membrane is noticeably higher than using TFC membrane.

- The influence of draw solute on the economic balance was low. CH_3COONa and $CaCl_2$ for CTA and $MgCl_2$ for TFC were the most economically favourable draw solutes.

- Membrane material and draw solute did not have a high impact on the AnMBR COD removal efficiency.

The conclusions of Chapter 3 regarding the plant-wide impact of AnMBR implementation obtained from Publication V, VI and VII are:

Publication V

- Membrane flux and SGD had a direct impact on membrane fouling control. On the one hand, operating the membrane at SGD of 0.5 $m^3\ m^{-2}\ h^{-1}$ was the most favourable condition at J_{20} of 8.7 and 4.4 LMH. On the other hand, operating the membrane at 1.0 $m^3\ m^{-2}\ h^{-1}$ was the most favourable condition at J_{20} of 16.7 and 13.0 LMH.

- DCOM rejection was not substantially effected neither by flux nor SGD. The 3DDEM analysis illustrated that DCOM compounds present in Region I+II of the spectra (protein fluorophores) could be important foulants in granular AnMBRs.

- Operating the system at J_{20} and SGDs of 7.8 LMH and 0.5 $m^3\ m^{-2}\ h^{-1}$, respectively, could be the most advantageous strategy for membrane fouling control in granular AnMBRs.

Publication VI

- The wastewater treatment cost ranged between 0.35 and 0.42 € m^{-3} (100-1200 mg COD L^{-1}) for an AnMBR-WWTP including mainstream AnMBR and degassing membrane for dissolved methane recovery. In this AnMBR-WWTP, energy self-sufficiency was reached at COD concentrations above 550 mg COD L^{-1} and at a COD:SO_4^{2-} ratio of 57.

- The wastewater treatment cost ranged between 0.51 and 0.56 € m^{-3} (100-1200 mg COD L^{-1}) for an AnMBR-WWTP including mainstream AnMBR, degassing membrane for dissolved methane recovery, PN-Anammox, phosphorus precipitation and sidestream anaerobic digester. In this AnMBR-WWTP, energy self-sufficiency

was reached at COD concentrations of 1000 mg COD L^{-1} and at a COD:SO_4^{2-} ratio above 40.

- AnMBR and PN-Anammox were the costliest processes of the AnMBR-WWTP, representing 58 and 30% of the cost, respectively. This shows that it is necessary to further improve the economic prospect of these technologies to reduce the wastewater treatment cost in AnMBR-WWTPs.

Publication VII

- Implementing co-digestion of sewage sludge and food waste in an AnMBR-WWTP decreased the net cost of the sludge line as a result of the higher electricity revenue achieved in the sidestream anaerobic digester. Biosolids disposal cost was the most important cost contributor followed by nutrients backload treatment and food waste acceptance installation.

- Treating the nutrients backload in the sidestream was costlier than in the mainstream because of the high costs associated with PN-Anammox and struvite crystallisation processes, which represented 15-17 and 18-19% of the gross cost, respectively.

- The sensitivity analysis illustrated that biosolids disposal cost, electricity price, struvite price and gate/delivery fee are key economic drivers determining the economics of co-digesting sewage sludge and food waste in an AnMBR-WWTP.

Recommendations

From the work reported in this thesis, the following recommendations for further research are proposed:

- To explore the evolution of the microbial community in the mixed liquor and membrane biofilm of an AnMBR operated under different organic and salinity conditions. Unravelling the different microbial communities present in the system is important to understand the relative impact of membrane biofilm on the performance of the AnMBR

- To test the combination of FO and AnMBR technologies at pilot- and/or demonstration-scale to understand the long-term implications of combining both

technologies. In this regard, the LIFE Green Sewer project (LIFE17 ENV/ES/000341) can help in its understanding.

- To evaluate the impact of the draw solute used in the FO stage on AnMBR performance under both batch and steady-state conditions.
- To explore the long-term performance of granular AnMBR systems operated under different SGD and permeate flux conditions.
- To further understand the impact of sulphate, and the underlying production of hydrogen sulphide, on AnMBR performance and process economics.
- To carry out further economic studies to evaluate the potential to implement biogas upgrading technologies for biomethane production in an AnMBR-WWTP.
- To evaluate alternative co-substrates to increase biogas production in the sidestream anaerobic digester of an AnMBR-WWTP.

Contributions by the author

List of publications

Publications derived from this thesis

Vinardell, S, Astals, S, Koch, K, Mata-Alvarez, J, Dosta, J. (2021). Co-digestion of sewage sludge and food waste in a wastewater treatment plant based on mainstream anaerobic membrane bioreactor technology: A techno-economic evaluation. Bioresour. Technol. 330, 124978.

Vinardell S, Dosta J, Mata-Alvarez J, Astals S. (2021). Unravelling the economics behind mainstream anaerobic membrane bioreactor application under different plant layouts. Bioresour. Technol. 297. 122395.

Vinardell S, Astals S, Jaramillo M, Mata-Alvarez J, Dosta J. (2021). Anaerobic membrane bioreactor performance at different wastewater pre-concentration factors: An experimental and economic study. Sci. Total Environ. 750, 141625.

Vinardell S, Astals S, Peces M, Cardete M.A, Fernández I, Mata-Alvarez J, Dosta J. (2020). Advances in anaerobic membrane bioreactor technology for municipal wastewater treatment: A 2020 updated review. Renew. Sustain. Energy Rev. 130, 109936.

Vinardell S, Astals S, Mata-Alvarez J, Dosta J. (2020). Techno-economic analysis of combining forward osmosis-reverse osmosis and anaerobic membrane bioreactor technologies for municipal wastewater treatment and water production. Bioresour Technol, 297, 122395

Vinardell, S., Sanchez, L., Astals, S., Mata-Alvarez, J., Dosta, J., Heran, M., Lesage, G. Impact of permeate flux and gas sparging rate on membrane performance and process economics of granular anaerobic membrane bioreactors. Accepted for publication in Science of the Total Environment.

Vinardell, S., Blandin, G., Ferrari, F., Lesage, G., Mata-Alvarez, J., Dosta, J., Astals, S. Techno-economic analysis of forward osmosis pre-concentration before an anaerobic membrane bioreactor: Impact of draw solute and membrane material. Submitted for publication.

Other publications of the author of this thesis:

Ruiz-Hernando M, **Vinardell S**, Labanda J, Llorens J. (2022). Effect of ultrasonication on waste activated sludge rheological properties and process economics. Water Research. 208, 117855.

Perez-Esteban, N., **Vinardell, S**., Vidal-Antich, C., Peña-Picola, S., Chimenos, J.M., Peces, M., Dosta, J., Astals, S. (2022) Potential of anaerobic co-fermentation in wastewater treatments plants: A review. Science of the Total Environment. 813, 152498.

Robles A, **Vinardell S**, Serralta J, Bernet N, Lens P.N.L, Steyer J.P, Astals S. (2020). Anaerobic treatment of sulfate-rich wastewaters: process modeling and control, in: Lens, P.N.L. (Ed.), Environmental Technologies to Treat Sulphur Pollution: Principles and Engineering, Second ed. IWA Publishing, London (UK), pp 277-317.

Garrido-Baserba M, **Vinardell S**, Molinos-Senante M, Rosso D, Poch M. (2018). The Economics of Wastewater Treatment Decentralization: A Techno-economic Evaluation. Environmental Science & Technology, 52, 8965-8976

Congresses and Technical conferences

Oral communications derived from this thesis

Vinardell S, Astals S, Mata-Alvarez J, Dosta J. Understanding the impact of implementing forward osmosis to pre-concentrate municipal sewage before an anaerobic membrane bioreactor. *Forward osmosis (FO) in the water sector: Return of experiences and new applications*. 07/09/2021 (On line Webinar).

Vinardell S, Astals S, Mata-Alvarez J, Dosta J. The Economics behind the combination of AnMBR and FO technologies for municipal wastewater treatment. *3rd IWA Resource Recovery Conference (IWARR2019)*. Venice, Italy. 8-12/09/2019.

Vinardell S. Tractament d'aigües residuals municipals mitjançant bioreactors de membrana anaeròbics: en el camí d'un canvi de paradigma en el sector de l'aigua? *4th IdRA Young Researchers Seminar*. Barcelona, Spain. 03/06/2019.

Vinardell S, Cardete M.A, Fernández I, Dosta J, Mata-Alvarez J. Estado del arte de los AnMBRs para el tratamiento de aguas residuales urbanas (State of the art of AnMBRs for urban wastewater treatment). *VII Jornada sobre Bioreactores de Membrana*. Barcelona, Spain. 16/05/2019.

Other oral communications of the author of this thesis

Astals S, Fernández D, Perez N, **Vinardell S**, Dosta J, Mata-Alvarez J. De Ecoparque a Biorefinería: la fermentación como etapa clave. Jornadas sobre biometanización de residuos sólidos urbanos. *XIV Jornada sobre Biometanización de Residuos Sólidos Urbanos*. Barcelona, Spain. 26/11/2020

Garrido-Baserba M, **Vinardell S**, Molinos-Senante M, Poch M, Rosso D. The price of the technological inertia: understanding the economics behind wastewater treatment

decentralisation. 4th IWA Specialist International Conference "Ecotechnologies for Wastewater Treatment (IWA ecoSTP18)". London, Ontario, Canada. 25-27/06/2018.

Other poster presentations of the author of this thesis

Pérez-Esteban N, Vidal-Antich C, **Vinardell S**, Fernández-Domínguez D, Mata-Álvarez J, Dosta J. Start-up of a sequencing batch reactor for the selection of polyhydroxyalkanoates accumulating cultures by means of a carbon and nitrogen decoupling strategy. *8th International Conference on Sustainable Solid Waste Management*. Thessaloniki, Greece. 23-26/06/2021.

Research stays

02/2021-07/2021: Six-month research stay at *Institut Européen des Membranes*, University of Montpellier (France).

10/2021-11/2021: One-month research stay at the *Chair of Urban Water Systems Engineering*, Technical University of Munich (Germany).

References

[1] E.R. Jones, M.T.H. Van Vliet, M. Qadir, M.F.P. Bierkens, Country-level and gridded estimates of wastewater production, collection, treatment and reuse, Earth Syst. Sci. Data. 13 (2021) 237–254.

[2] M.C.M. Van Loosdrecht, D. Brdjanovic, Anticipating the next century of wastewater treatment, Science. 344 (2014) 1452–1453.

[3] A.R. Sheik, E.E.L. Muller, P. Wilmes, K.B. Clark, X. Zhang, A hundred years of activated sludge: time for a rethink, Frointiers Microbiol. 5 (2014) 1–7.

[4] E.S. Heidrich, T.P. Curtis, J. Dolfing, Determination of the internal chemical energy of wastewater, Environ. Sci. Technol. 45 (2011) 827–832.

[5] P.L. McCarty, J. Bae, J. Kim, Domestic wastewater treatment as a net energy producer - can this be achieved?, Environ. Sci. Technol. 45 (2011) 7100–6.

[6] L. Seghezzo, G. Zeeman, J.B. Van Liel, H.V.M. Hamelers, G. Lettinga, A review: The anaerobic treatment of sewage in UASB and EGSB reactors, Bioresour. Technol. 65 (1998) 175–190.

[7] C.A.L. Chernicharo, J.B. van Lier, A. Noyola, T. Bressani Ribeiro, Anaerobic sewage treatment: state of the art, constraints and challenges, Rev. Environ. Sci. Biotechnol. 14 (2015) 649–679.

[8] G. Lettinga, L.W. Hulshoff Pol, UASB-Process Design for Various Types of Wastewaters, Water Sci. Technol. 24 (1991) 87–107.

[9] J.B. Van Lier, A. Vashi, J. Van Der Lubbe, B. Heffernan, Anaerobic sewage treatment using UASB reactors: Engineering and operational aspects, in: H.H.P. Fang (Ed.), Environ. Anaerob. Technol. Appl. New Dev., Imperial College Press, 2010: pp. 59–89.

[10] M.A. Latif, R. Ghufran, Z.A. Wahid, A. Ahmad, Integrated application of upflow anaerobic sludge blanket reactor for the treatment of wastewaters, Water Res. 45 (2011) 4683–4699.

[11] B. Heffernan, J.B. Van Lier, J. Van Der Lubbe, Performance review of large scale up-flow anaerobic sludge blanket sewage treatment plants, Wat Sci. Tech. 63 (2011) 100–107..

[12] A.C. Trego, B. Conall Holohan, C. Keating, A. Graham, S. O'Connor, M. Gerardo, D. Hughes, U.Z. Ijaz, V. O'Flaherty, First proof of concept for full-scale, direct, low-temperature anaerobic treatment of municipal wastewater, Bioresour. Technol. 341 (2021) 125786.

[13] D.J. Batstone, T. Hülsen, C.M. Mehta, J. Keller, Platforms for energy and nutrient recovery from domestic wastewater: A review, Chemosphere. 140 (2015) 2–11.

[14] A.L. Smith, L.B. Stadler, N.G. Love, S.J. Skerlos, L. Raskin, Perspectives on anaerobic membrane bioreactor treatment of domestic wastewater: A critical review, Bioresour. Technol. 122 (2012) 149–159.

[15] Á. Robles, M.V. Ruano, A. Charfi, G. Lesage, M. Heran, J. Harmand, A. Seco, J.P. Steyer, D.J. Batstone, J. Kim, J. Ferrer, A review on anaerobic membrane bioreactors (AnMBRs) focused on modelling and control aspects, Bioresour. Technol. 270 (2018) 612–626.

[16] D.C. Stuckey, Recent developments in anaerobic membrane reactors, Bioresour. Technol. 122 (2012) 137–148.

[17] R.K. Dereli, M.E. Ersahin, H. Ozgun, I. Ozturk, D. Jeison, F. van der Zee, J.B. van Lier, Potentials of anaerobic membrane bioreactors to overcome treatment limitations induced by industrial wastewaters, Bioresour. Technol. 122 (2012) 160–170.

[18] C. Shin, J. Bae, Current status of the pilot-scale anaerobic membrane bioreactor treatments of domestic wastewaters: A critical review, Bioresour. Technol. 247 (2018) 1038–1046.

[19] A. Robles, M. V Ruano, J. Ribes, J. Ferrer, Factors that affect the permeability of commercial hollow-fibre membranes in a submerged anaerobic MBR (HF-SAnMBR) system, Water Res. 47 (2013) 1277–1288.

[20] B.Q. Liao, J.T. Kraemer, D.M. Bagley, Anaerobic membrane bioreactors: Applications and research directions, Crit. Rev. Environ. Sci. Technol. 36 (2006) 489–530.

[21] H. Lin, W. Peng, M. Zhang, J. Chen, H. Hong, Y. Zhang, A review on anaerobic membrane bioreactors: Applications, membrane fouling and future perspectives, Desalination. 314 (2013) 169–188.

[22] Á. Robles, F. Durán, J.B. Giménez, E. Jiménez, J. Ribes, J. Serralta, A. Seco, J. Ferrer, F. Rogalla, Anaerobic membrane bioreactors (AnMBR) treating urban wastewater in mild climates, Bioresour. Technol. 314 (2020) 123763.

[23] K. Lim, P.J. Evans, P. Parameswaran, Long-Term Performance of a Pilot-Scale Gas-Sparged Anaerobic Membrane Bioreactor under Ambient Temperatures for Holistic Wastewater Treatment, Environ. Sci. Technol. 53 (2019) 7347–7354.

[24] G. Blandin, F. Ferrari, G. Lesage, P. Le-Clech, M. Héran, X. Martinez-Lladó, Forward osmosis as concentration process: Review of opportunities and challenges, Membranes. 10 (2020) 1–40.

[25] A.J. Ansari, F.I. Hai, W.E. Price, H.H. Ngo, W. Guo, L.D. Nghiem, Assessing the

integration of forward osmosis and anaerobic digestion for simultaneous wastewater treatment and resource recovery, Bioresour. Technol. 260 (2018) 221–226.

[26] A.J. Ansari, F.I. Hai, W. Guo, H.H. Ngo, W.E. Price, L.D. Nghiem, Selection of forward osmosis draw solutes for subsequent integration with anaerobic treatment to facilitate resource recovery from wastewater, Bioresour. Technol. 191 (2015) 30–36.

[27] A.M. Bacaksiz, Y. Kaya, C. Aydiner, Techno-economic preferability of cost-performance effective draw solutions for forward osmosis and osmotic anaerobic bioreactor applications, Chem. Eng. J. 410 (2021) 127535.

[28] F. Ferrari, J.L. Balcazar, I. Rodriguez-Roda, M. Pijuan, Anaerobic membrane bioreactor for biogas production from concentrated sewage produced during sewer mining, Sci. Total Environ. 670 (2019) 993–1000.

[29] G. Blandin, A.R.D. Verliefde, C.Y. Tang, P. Le-Clech, Opportunities to reach economic sustainability in forward osmosis–reverse osmosis hybrids for seawater desalination, Desalination. 363 (2015) 26–36.

[30] E.H. Cabrera-Castillo, I. Castillo, G. Ciudad, D. Jeison, J.C. Ortega-Bravo, FO-MD setup analysis for acid mine drainage treatment in Chile: An experimental-theoretical economic assessment compared with FO-RO and single RO, Desalination. 514 (2021) 115164.

[31] R. Valladares Linares, Z. Li, V. Yangali-Quintanilla, N. Ghaffour, G. Amy, T. Leiknes, J.S. Vrouwenvelder, Life cycle cost of a hybrid forward osmosis – low pressure reverse osmosis system for seawater desalination and wastewater recovery, Water Res. 88 (2016) 225–234.

[32] CEC, Council Directive of 21 May 1991 concerning waste water treatment (91/271/EEC), Off. J. Eur. Communities. (1991) No. L 135/40-52.

[33] L. Chen, Y. Gu, C. Cao, J. Zhang, J.W. Ng, C. Tang, Performance of a submerged anaerobic membrane bioreactor with forward osmosis membrane for low-strength

wastewater treatment, Water Res. 50 (2014) 114–123.

[34] W. Luo, H. V. Phan, F.I. Hai, W.E. Price, W. Guo, H.H. Ngo, K. Yamamoto, L.D. Nghiem, Effects of salinity build-up on the performance and bacterial community structure of a membrane bioreactor, Bioresour. Technol. 200 (2016) 305–310.

[35] H. Yeo, J. An, R. Reid, B.E. Rittmann, H.S. Lee, Contribution of Liquid/Gas Mass-Transfer Limitations to Dissolved Methane Oversaturation in Anaerobic Treatment of Dilute Wastewater, Environ. Sci. Technol. 49 (2015) 10366–10372.

[36] W. Verstraete, P. Van de Caveye, V. Diamantis, Maximum use of resources present in domestic "used water," Bioresour. Technol. 100 (2009) 5537–5545.

[37] V. Sanahuja-Embuena, G. Khensir, M. Yusuf, M.F. Andersen, X.T. Nguyen, K. Trzaskus, M. Pinelo, C. Helix-Nielsen, Role of operating conditions in a pilot scale investigation of hollow fiber forward osmosis membrane modules, Membranes. 9 (2019) 66.

[38] A.L. Smith, L.B. Stadler, L. Cao, N.G. Love, L. Raskin, S.J. Skerlos, Navigating Wastewater Energy Recovery Strategies: A Life Cycle Comparison of Anaerobic Membrane Bioreactor and Conventional Treatment Systems with Anaerobic Digestion, Environ. Sci. Technol. 48 (2014) 5972–5981.

[39] R. Pretel, A. Robles, M. V. Ruano, A. Seco, J. Ferrer, The operating cost of an anaerobic membrane bioreactor (AnMBR) treating sulphate-rich urban wastewater, Sep. Purif. Technol. 126 (2014) 30–38.

[40] A.L. Smith, S.J. Skerlos, L. Raskin, Psychrophilic anaerobic membrane bioreactor treatment of domestic wastewater, Water Res. 47 (2013) 1655–1665.

[41] K.M. Wang, D. Cingolani, A.L. Eusebi, A. Soares, B. Jefferson, E.J. McAdam, Identification of gas sparging regimes for granular anaerobic membrane bioreactor to enable energy neutral municipal wastewater treatment, J. Memb. Sci. 555 (2018) 125–133.

[42] K.I. Cogert, R.M. Ziels, M.K.H. Winkler, Reducing Cost and Environmental Impact of Wastewater Treatment with Denitrifying Methanotrophs, Anammox, and

Mainstream Anaerobic Treatment, Environ. Sci. Technol. 53 (2019) 12935–12944.

[43] R. Pretel, B.D. Shoener, J. Ferrer, J.S. Guest, Navigating environmental, economic, and technological trade-offs in the design and operation of submerged anaerobic membrane bioreactors (AnMBRs), Water Res. 87 (2015) 531–541.

[44] B. Morelli, S. Cashman, X.C. Ma, J. Turgeon, S. Arden, J. Garland, Environmental and cost benefits of co-digesting food waste at wastewater treatment facilities, Water Sci. Technol. 82 (2020) 227–241.

[45] M. Wehner, T. Lichtmannegger, S. Robra, A. do Carmo Precci Lopes, C. Ebner, A. Bockreis, The economic efficiency of the co-digestion at WWTPs: A full-scale study, Waste Manag. 133 (2021) 110–118.

[46] Y. Yao, Z. Zhou, D.C. Stuckey, F. Meng, Micro-particles-A Neglected but Critical Cause of Different Membrane Fouling between Aerobic and Anaerobic Membrane Bioreactors, ACS Sustain. Chem. Eng. 8 (2020) 16680–16690.

[47] C. Sembera, C. Macintosh, S. Astals, K. Koch, Benefits and drawbacks of food and dairy waste co-digestion at a high organic loading rate: A Moosburg WWTP case study, Waste Manag. 95 (2019) 217–226.

[48] A. Bouzas, N. Martí, S. Grau, R. Barat, D. Mangin, L. Pastor, Implementation of a global P-recovery system in urban wastewater treatment plants, J. Clean. Prod. 227 (2019) 130–140.

[49] G. Rodriguez-Garcia, N. Frison, J.R. Vázquez-Padín, A. Hospido, J.M. Garrido, F. Fatone, D. Bolzonella, M.T. Moreira, G. Feijoo, Life cycle assessment of nutrient removal technologies for the treatment of anaerobic digestion supernatant and its integration in a wastewater treatment plant, Sci. Total Environ. 490 (2014) 871–879.